EANDC (E) 127 "U"
INDC-355
INDC(EUR)-4/G

PROGRESS REPORT ON NUCLEAR DATA RESEARCH IN THE EURATOM COMMUNITY

for the period January 1 to December 31, 1969

Submitted by the Joint European Nuclear Data and Reactor Physics Committee

(Secretariat: Central Bureau for Nuclear Measurements, Euratom, Geel, Belgium)

March 1970

EUROPEAN AMERICAN NUCLEAR DATA COMMITTEE

LEGAL NOTICE :

The information contained in this progress report has a preliminary character.

No data contained in this report may be used without the permission of the responsible authorities.

It is suggested that experimentators should be contacted in this respect.

EANDC(E) 127 "U"

PROGRESS REPORT
ON NUCLEAR DATA RESEARCH IN THE EURATOM COMMUNITY
for the period January 1 to December 31, 1969

Submitted by the Joint Euratom Nuclear Data
and Reactor Physics Committee

(Secretariat: Central Bureau for Nuclear
Measurements, Euratom, Geel, Belgium)

March 1970

EUROPEAN AMERICAN NUCLEAR DATA COMMITTEE

I N D E X

I. REACTOR CENTRUM NEDERLAND (PETTEN)

1. RCN activities

1.1. Circular polarization of gamma radiation after capture of polarized thermal neutrons (K. Abrahams)

By means of an earlier mentioned system of 74 magnetized cobalt-iron mirrors [1) 2) 5)], a 90% polarized beam of thermal neutrons can be extracted from the High Flux Reactor at Petten. With the reactor running at 30 MW a flux of 3.10^7 $cm^{-2}s^{-1}$ has been measured at the target position.
One may assign spins to nuclear states, excited by the (n,γ) reaction, by a measurement of the polarization of the gamma radiation resulting from the capture of polarized neutrons.

Last year the ^{40}A (n,γ) and the $^{59}Co(n,\gamma)$ have been extensively studied [3) 4) 5)]. The first reaction was leading to unambiguous results because the sign of the polarization determines the spin of levels with $l_n(d,p) = 1$, in case of an even-even target nucleus. The interpretation of our results on the $^{59}Co(n,\gamma)$ reaction was more difficult, due to an incoherent mixture of the spins 3 and 4 in the capturing state of ^{60}Co.
By means of a careful analysis of our measurements and of measurements on radiative capture in and between resonances [6)], it is, however, possible to estimate the spin admixture for several primary γ-transitions, and to assign spins to excited states of ^{60}Co (fig. 1).

A new development is the study of the angular correlation of positon-electron pairs created by circularly polarized γ radiation. A preliminary set-up of two Si(Li) detectors in coincidence yielded promising results. These measurements can test some quantum electrodynamical calculations [7)] and are of interest for the study of systematical errors in measurements on parity admixture in nuclear states [8)].

References

1) K. Abrahams and W. Ratynski, Nucl.Phys. A124 (1969) 34.
2) K. Abrahams, "Experiments with Polarized Thermal Neutrons" Thesis (1969).
3) J. Kopecký, F. Stecher-Rasmussen and K. Abrahams, Proceedings of the "International Conference on Properties of Nuclear States", Montreal 1969.

4) F. Stecher-Rasmussen, J. Kopecký and K. Abrahams, "International Symposium on Neutron Capture Gamma-Ray Spectroscopy", Studsvik 1969.
5) K. Abrahams, Atoomenergie 11 (1969) 308.
6) O.A. Wasson, R.E. Chrien, M.R. Bhat, M.A. Lone and M. Beer, Phys. Rev. 136 (1968) 1314.
7) H. Kolbenstvedt and H. Olsen, Il Nuovo Cimento XXII (1961) 610.
8) K. Abrahams, W. Ratynski, F. Stecher-Rasmussen and E. Warming, Proceedings of the 2nd International Symposium on Polarization of Nucleons (Birkhäuser Verlag Basel-Stuttgart 1965).

1.2. Integral measurements of cross sections of fission products

(M. Bustraan)

The fast-thermal coupled critical reactor facility STEK, referred to in the report over 1968, came into operation in 1969.
The actual measurements will start in early 1970.
The fissile material in the central, fast, zone is highly enriched ^{235}U, in the form of platelets. The neutron spectrum is softened by graphite, also in the form of platelets.
In order to be able to predict the neutron spectra correctly an evaluation was made of the ^{235}U fission and absorption cross section [1].
These evaluated data were condensed to a 26 group set. The resonance integrals derived from this set are 281 b (fission), 143 b (capture) compared to the experimental values of 274 b and 144 b; the α value derived from this set is 0.51, the experimental value being 0.525 (BNL 325 latest ed.).
The critical masses observed during the loading of STEK are supporting this group set.

---

1) R. Kuiken, Private communication.

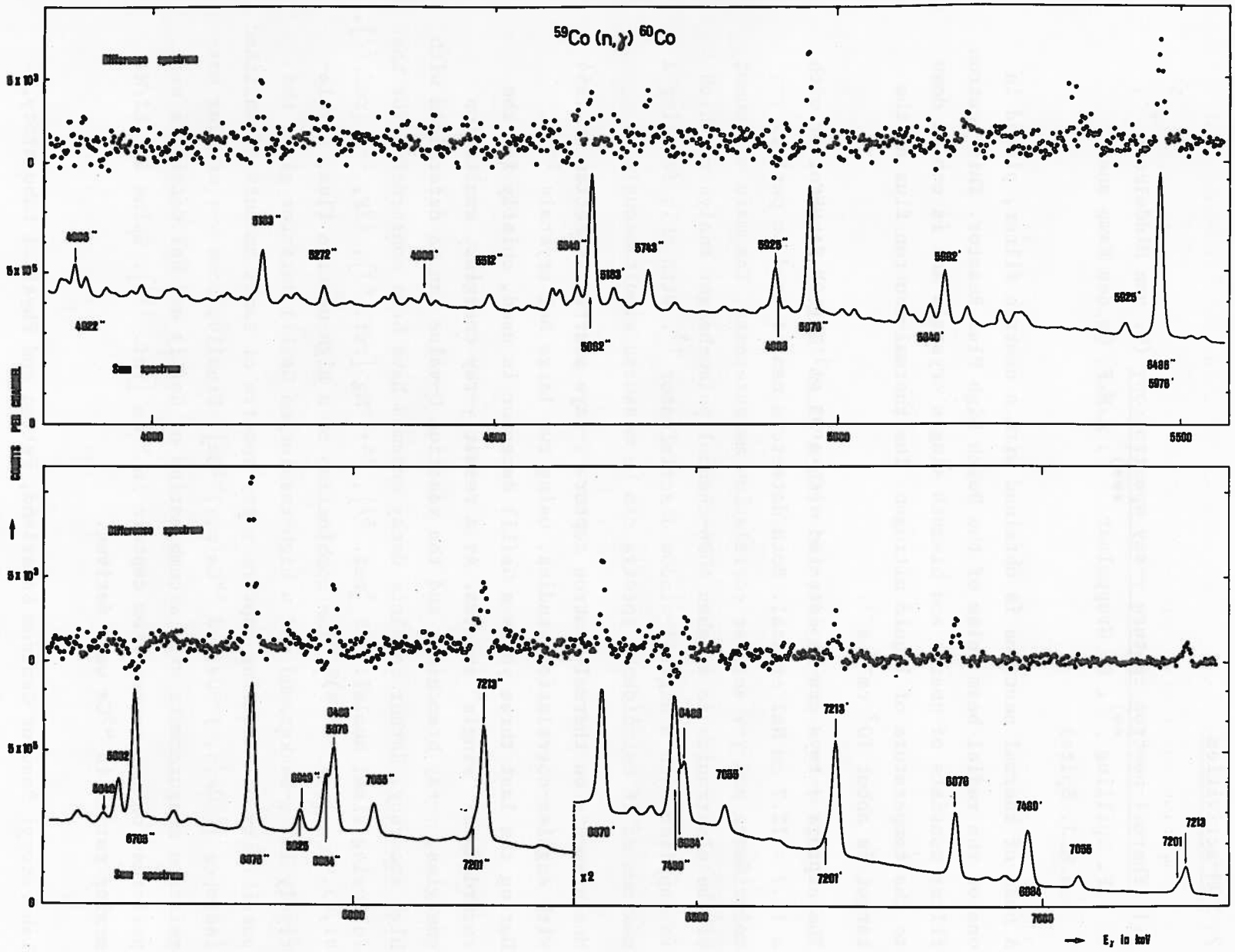
^{59}Co (n,γ) ^{60}Co
Difference spectrum
Sum spectrum
COUNTS PER CHANNEL
x2
E$_\gamma$ in keV

Figure 1

2. FOM-activities

2.1. Thermal-neutron capture γ-ray spectroscopy (G. van Middelkoop *), P. Spilling **), H. Gruppelaar ***), A.M.F. Op den Kamp and A.M.J. Spits)

A beam of thermal neutrons is obtained with a neutron filter, placed in one of the radial beam holes of the Dutch High Flux Reactor. This neutron filter consists of quartz and bismuth single crystals and is cooled down to the temperature of liquid nitrogen. The thermal-neutron flux at the target is about 10^7 cm^{-2} s^{-1}.

The capture γ-rays can be detected with a 23 cm^3 Ge(Li) detector or with a 12.7 × 12.7 cm NaI crystal. Both detectors can be used to perform γ-γ coincidence and γ-γ angular correlation measurements. The main component of the electronics is a Laben 4096-channel pulse-height analyser, which is supplied with a digital-window discriminator [1]. With this facility a maximum of 16 coincidence spectra can be measured simultaneously.

Measurements on thermal-neutron capture γ-rays started in Petten in 1964 with angular-correlation studies, using two large NaI crystals [2-4]. During the last three years a Ge(Li) detector is used, chiefly for the recording of "single" spectra. As a result γ-ray energies, excitation energies, γ-ray branchings and the reaction Q-value can be determined with high accuracy. Rather complete decay schemes have been constructed for the following final nuclei: ^{32}P [ref. 5)], $^{25,26}Mg$ [ref. 6)], ^{20}F, ^{13}C [ref. 7)], $^{41,43,45}Ca$ [ref. 8-10)]. The combination of a high neutron flux, a relatively low γ-background and a high-resolution Ge(Li) detector gives the possibility of measuring capture γ-ray spectra of samll amounts of enriched isotopes [$^{42}Ca(n,\gamma)^{43}Ca$ and $^{44}Ca(n,\gamma)^{45}Ca$]. Finally, some γ-γ angular correlation measurements with a combination of Ge(Li) and NaI detectors were performed on the γ-rays from capture in ^{44}Ca [ref. 11)]. Spins and E2/M1 mixing ratios in ^{45}Ca were derived.

Laboratory: Reactor Centrum Nederland, Petten and Physical Laboratory, State University, Utrecht.

*) Present address: Physical Laboratory, State University, Utrecht.

**) Present address: Technical University, Eindhoven.

***) Present address: Physical Laboratory, State University, Groningen.

References:

1) P. Spilling, H. Gruppelaar and P.C. van den Berg, Int. Symp. on Nucl. Electronics, Versailles, 1968, Part II, Contr. 140.
2) G. van Middelkoop and P. Spilling, Nucl. Phys. 72 (1965) 1.
3) G. van Middelkoop and P. Spilling, Nucl. Phys. 77 (1966) 267.
4) G. van Middelkoop and H. Gruppelaar, Nucl. Phys. 80 (1966) 321.
5) G. van Middelkoop, Nucl. Phys. A97 (1967) 209.
6) P. Spilling, H. Gruppelaar and A.M.F. Op den Kamp, Nucl. Phys. A102 (1967) 209.
7) P. Spilling, H. Gruppelaar, H.F. de Vries and A.M.J. Spits, Nucl. Phys. A113 (1968) 395.
8) H. Gruppelaar and P. Spilling, Nucl. Phys. A102 (1967) 226.
9) H. Gruppelaar, A.M.F. Op den Kamp and A.M.J. Spits, Nucl. Phys. A131 (1969) 180.
10) H. Gruppelaar, P. Spilling and A.M.J. Spits, Nucl. Phys. A114 (1968) 463.
11) H. Gruppelaar, Nucl. Phys. A133 (1969) 545.

2.2. Neutron capture experiments with oriented nuclei (H. Postma, E.R. Reddingius, J. Mellema and R.Kuiken, F.O.M. - Petten, Physical Laboratory State University, Leiden).

The anisotropy of the directional distribution of neutron-capture gamma rays from ^{55}Mn oriented in single crystals of $La_2Mn_3(NO_3)_{12}.24D_2O$ and $MnSiF_6.6H_2O$ has been measured with a thermal neutron beam of the high flux reactor in Petten. The necessary low temperature of 0.05 - 0.06 K has been obtained with the aid of a ^3He - ^4He dilution refrigerator. The analysis of the results is complicated since the neutron capture is related to various resonances with spins 2 and 3. Nevertheless it was possible to limit the spins of many levels of ^{56}Mn to two values. For a few levels of ^{56}Mn it was possible to arrive at a definite assignment. A similar experiment has been started with the $^{141}Pr(n,\gamma)$ reaction. The ^{141}Pr nuclei are oriented in $Pr_2Mg_3(NO_3)_{12}.D_2O$.

In a joint English-Dutch project the directional distribution of fragments from neutron-induced fission of ^{235}U has been studied, while similar experiments with ^{233}U and ^{237}Np have been started. These experiments are mainly carried out at the electron linear accelerator in Harwell.

References:

J. Mellema and H. Postma, Spin Investigation of Excited States of ^{60}Co by Means of Nuclear Orientation, Nucl. Phys. A130 (1969) 161.

E.R. Reddingius and H. Postma, Directional Anisotropy of Capture Gamma Rays from Aligned ^{149}Sm Nuclei, Proc. Int. Symp. on Neutron Capture Gamma Ray Spectroscopy, Studsvik (1969) 359 and Nucl. Phys. A137 (1969) 389.

H. Postma and J.F.M. Potters, The Change of Nuclear Orientation Parameters Related to Pseudo-continuous Neutron Capture Gamma Ray Spectra, Physica 45 (1969) 559.

II. INSTITUTE FOR NUCLEAR PHYSICS RESEARCH (AMSTERDAM)

Neutron cross-section data (E_n > 20 keV)

(W. Pauw)

$\sigma_{^{197}Au(n,\gamma)^{198}Au}$ $\sigma_{^{115}In(n,\gamma)^{116}In^m}$ (54 minute activity)

For these reactions all literature values have been carefully studied and renormalized in such a way that they can be represented by a smooth curve. The result of an absolute measurement of the activation cross-section of gold (σ = 692 ± 14 mb) for SbBe neutrons (22.4 keV) agrees well with this cross-section curve.
Below 100 keV the indium cross-section curve has been extrapolated through the value of σ = 577 ± 20 mb for SbBe neutrons, obtained by an absolute measurement for the 54 minutes' period.

$^{115}In(n,n')^{115}In^m$

The literature cross-section values have been renormalized. On the basis of the renormalized values the calculated average cross-section for the ^{252}Cf-neutron spectrum $\phi(E) \sim \sqrt{E} \exp\left(\frac{-E}{1.39}\right)$ (σ = 179 ± 18 mb).

(The data given in the table I will be discussed more fully in a thesis, to be submitted to the University of Amsterdam).

Table I

keV	$\sigma_{^{197}Au(n,\gamma)^{198}Au}$ (+5%, except at 22 keV)	$\sigma_{^{115}In(n,\gamma)^{116}In^m}$ (+10%, except at 22 keV)	$\sigma_{^{115}In(n,n')^{115}In^m}$ (+10%)
22.4	692 ± 14* (mb)	577 ± 20* (mb)	-
30	596	(500)	-
40	490	(435)	-
50	435	(390)	-
60	400	(360)	-
70	370	(330)	-
80	350	(310)	-
90	330	(295)	-
100	315	(280)	-
150	275	230	-
200	255	200	-
250	230	185	-
300	200	170	-
400	162	154	-
500	136	149	2
600	120	160	4.6
700	108	173	12
800	98	182	22.5
900	92	190	40.5
1000	88	194	62
1200	80	192	115
1400	74	180	160
1600	68	166	200
1800	58	150	250
2000	49	135	300
2500	31	100	310
3000	19.5	64	310
4000	14	29	310
5000	12.8	16	310
6000	-	11.3	305
7000	-	9	290
8000	-	7.4	280
9000	-	6.4	240
10.000	-	5.8	190

* values measured at I.K.O.

III. PHYSICAL LABORATORY OF THE FREE UNIVERSITY (AMSTERDAM)

1. Cockroft-Walton accelerator of 0.7 MeV

1.1. Neutron scattering from Bi, Sr and Na at 14.8 MeV
(P. Kuijper and C.C. Jonker)

Absolute differential cross sections for the elastic and inelastic scattering of 14.8 MeV neutrons from Bi, Sr and Na were measured with four neutron detectors placed at the same scattering angle. The associated particle time-of-flight technique with a flight parth of 2.40 m was used. The overall time resolution was 1.4 ns. The energy dependence of the detector efficiency was calculated and measured.
An optical model fit to the elastic scattering results was made.
The inelastic scattering from collective levels in Bi and Sr were compared with DWBA-calculations and the deformation parameters which are dependent on real or complex coupling were determined.

1.2. Angular correlations in the $^{12}C(n,n'\gamma)^{12}C$ reaction at 15.0 MeV
(D. Spaargaren and C.C. Jonker)

The angular correlation between neutrons inelastically scattered from the 4.44 MeV level of ^{12}C and the deexcitation gamma radiation was investigated with the gamma detector in and perpendicular to the reaction plane. The neutron spin-flip probability could be determined. By the use of two separate time-of-flight spectrometers, one coupled to the neutron detector, the other to the gamma detector, an accurate determination of the contributions of the chance coincidences was possible. Moreover the differential cross sections of the elastically and inelastically scattered neutrons and of the gamma rays could be obtained simultaneously.
The results were compared with the predictions of DWBA calculations.
The anisotropy and symmetry angle of the angular correlation in the reaction plane are in good agreement with corresponding proton data.

1.3. Scattering of 3 MeV polarized neutrons

(P.J. van Hall*, E. Zijp, C.C. Jonker)

The polarization of 3 MeV neutrons scattered elastically by Fe, Ni, Zr, Sn, Pb and Bi has been measured at 9 angles ranging from 30 deg. to 150 deg. The measured asymmetries were corrected for finite geometry and multiple scattering.
The results are compared with the optical model in which compound elastic scattering has been included. Discrepancies are found at forward angles in general and at other angles in the case of Ni and Zr.

2. A.V.F. Cyclotron (protons 33 MeV, deutons 7 MeV, alpha's 33 MeV ^{3}He 45 MeV)

2.1. Total cross section measurements

(J. Rethmeier, C. Hoekstra, C.C. Jonker)

Total neutron cross sections of C, Mg, Al, Si, Ti, Fe, Co, Ni, Cu, Zr, Nb, Ag, In, Sn, Bi, Sb and Ta were measured from 20- 30 MeV with steps of 1 MeV and an energy resolution of 0.3%.
A time-of-flight technique, based on a burstlength of the cyclotron of about 1 ns, enabled a good background subtraction. The short burstlength is obtained by a special tuning of the cyclotron. The results are in good agreement with the scarce available data. An optical model description is made.

2.2. Elastic scattering of 25 MeV neutrons

(J.G. Nijenhuis and J. Blok)

Attempts are made to measure the elastic scattering of 25 MeV neutrons from Zr with a time-of-flight technique. The time resolution is 1 ns determined by the burstlength of the cyclotron. The flight path is 2.50 m. The detector has a 40 cm collimator for γ-background reduction.
The results will be used in an optical model analysis. A determination of the symmetry term in the potential seems possible.

---

* Present adress:
Eindhoven, University of Technology.

3. New instrumentation

3.1. A CDC1700 computer will shortly be working coupled on line with the cyclotron instrumentation.

3.2. A split-pole magnetic spectrograph has been installed and will be used for the investigation of pick-up reactions with the analysed beam of the cyclotron.

3.3. An isotope separator coupled with the cyclotron by a rabbit system is in use for the spectroscopy of short living isotopes (life-times longer than one second).

IV. INTERUNIVERSITAIR REACTOR INSTITUUT (DELFT)

Summary of activities in the field of neutron physics
(covering the period 1968 and 1969)

Using a 5 meV (4 Å) incident neutron beam incoherent inelastic neutron scattering experiments covering a range of momentum transfers between 0.6 and 2.2 $Å^{-1}$ have been carried out in globular compounds, cyclohexane (C_6H_{12}) and cyclopentane (C_5H_{10}) in the liquid and solid phase. A study is made of the molecular motions in these compounds based on line-width and intensity measurements of the quasi-elastic peaks in the time-of-flight spectra (L.A. de Graaf, Physica 40, 497-516 (1969)). In addition rotational motions of neopentane molecules (C_5H_{12}) in the plastic-crystalline phase have been studied both at Delft and in Dubna, the results of which will be published in Physica (L.A. de Graaf and J. Sciensinski).

Similar experiments have been performed in 1,1 dimethyl-, cis-1,2 dimethyl- and trans-1,4 dimethylcyclohexane in the liquid, the plastic and the solid phase. The time-of-flight spectra are analysed with a Fortran computer program (IBM 360-65) using fast fourier transforms to deconvolute the resolution function from the measured spectra. Width functions are obtained which can be interpreted in terms of various types of motions of the molecules.

Total cross sections of various organic compounds containing methyl-groups have been measured for neutrons with wavelength in the range 4.3 - 7.7 Å. The scattering cross sections per H atom for aceton (at 100 K) was found to be 11.6 ± 0.3 barn/Å H; for dimethylpolysiloxane (viscosity 1000 c stokes) 12.9 ± 0.3 barn/Å H.

Incoherent inelastic scattering of 5 meV neutrons has also been studied in strontiumdicalciumpropionate ($SrCa_2(C_2H_5(00)_6)$, in order to investigate the width of the quasi-elastic peak above and below the ferro-electric curie point at 281 K. Contrary to results reported in the literature (Physics Letters 25A, 123, 1967), no significant line-broadening has been found at the ferro-electric transition.

Scattering experiments of 5 meV neutrons by an isotopically pure sample of ^{36}Ar led to a scattering cross section of 74 ± 2 barn (C.D. Andriesse and co-authors, Physics Letters 28A, 642 (1969)). From the neutron spectra obtained from gaseous ^{36}Ar in five different states close to condensation (at temperatures between 141.5 and 147 K and pressures between 26.5 and 38 atm respectively), intermediate scattering functions are derived and tabulated in a publication submitted by C.D. Andriesse to Physica. Deviations from the ideal gas behaviour of these functions are specified.

The diffraction of 0.91 Å neutrons has been studied in various tetragonal chlorides in the liquid state (CCl_4, $TiCl_4$, $SnCl_4$) in order to determine the structure factor and the radial density distribution function. For CCl_4 at room temperature the results are consistent with those reported in the literature (J. of Chem. Physics 48, 2395 (1968)).

A polarized neutron beam of 1.18 Å wavelength has been used to measure the spontaneous magnetization in nickel near the Curietemperature (H.K. Bakker, M.Th. Rekveldt and J.J. van Loef, Physics Letters 27A, 69(1968)). Further experiments have been carried out to study the domain structure in nickel foils under stress.

V. PHYSIK-DEPARTMENT DER TECHNISCHEN HOCHSCHULE MÜNCHEN

E 14

1. Measurement of Neutron Capture Conversion Electrons

T.v.Egidy, W.Kaiser, W.Mampe, B.Olma

1.1. ^{152}Eu

The conversion electron spectrum of ^{151}Eu(n,e)^{152}Eu was measured between o keV and 700 keV. 500 lines were detected and 36 multipolarities determined. A level scheme with states at 0 keV (3^-), 77.258 keV ($3,4^-$), 89.849 keV (4^+), 108.115 keV (5^+), 141.826 keV (4^-), 147.87 keV (8^-) and 150.687 keV (4^-) was developed. A strong transition (19.663 keV) to the 9.3 h isomeric state was observed.

1.2. ^{158}Gd and ^{200}Hg

Conversion electrons of the ^{157}Gd (n,e)^{158}Gd reaction and of the ^{199}Hg (n,e)^{200}Hg reaction were measured between 1 MeV and 8 MeV. It was tried to determine high energy conversion coefficients with very good accuracy. The evaluation of the data is not yet finished.

1.3. ^{208}Pb

It was looked for E0 transitions in the ^{207}Pb(n,e)^{208}Pb reaction between 2 MeV and 8 MeV. No such transion was found.

2. The Spin of the 1029 keV Level in ^{200}Hg

K.E.G.Löbner, D.Rabenstein, O.W.B.Schult

The spin of the 1029 keV level in ^{200}Hg has been determined to be 0 through measurements of the γ-γ-angular correlation of the 661 keV and 368 keV γ-rays following slow neutron capture in

^{199}Hg. The upper limit for the γ-intensity ratio Iγ(1029 keV)/ Iγ(661 keV) obtained from the curved crystal spectrometer (n,γ)-data is much lower than the ratio found during the ^{200}Tl → ^{200}Hg decay studies. This implies that the 1029 keV γ-line seen in the decay work does not lead from the 1029 keV level to the ground state in ^{200}Hg, but that it depopulates a level which is only weakly fed through the (n,γ)-process.

---

published in Z.f.Physik 226 (1969) 13

3. Measurement of Gamma-Ray Spectra Following the Capture of Thermal Neutrons with Ge(Li)-Detectors

D.Rabenstein, H.K.Vonach, I.Winkelmann

An external beam of thermal neutrons has been used to measure gamma-ray spectra following the capture in various targets:

- low energy spectra (0 - 2 MeV) with a resolution of 2.7 eV at 1 MeV (single Ge(Li)-Detector) from capture in natural Se and In and in targets enriched in ^{80}Se, ^{76}Se, and ^{113}In;
- high energy spectra (1.5 - 10 MeV) with a resolution of 8 keV at 6 MeV (3-crystal-pair-spectrometer) from capture in natural Se and In and in enriched ^{80}Se.

γ-spectra from the decay of ^{114}In, ^{116}In and ^{81}Se have been measured as well.

γ-energies and -intensities have been determined and are used to extend the according level schemes.

In ^{81}Se the following levels have been found:

0 ($1/2^-$), 103.3 keV ($7/2^+$), 294.5 keV ($9/2^+$), 467.7 keV ($(1/2, 3/2)^-$), 624.5 keV ($5/2^-$), 1052.9 keV ($5/2^+$), 1232.8 keV ($1/2^+$),

1302.5 keV ($5/2^+$), 1406.7 keV ($(1/2,3/2)^-$), 1702.4 keV ($(3/2,5/2)^+$), 1725.0 keV ($(1/2,3/2)^-$), 1827.9 keV ($(3/2,5/2)^+$). The levels at 467.7 keV and 1725.0 keV are populated very strongly from the capture state, which gives an explanation for the unsystematically low value of the isomeric cross section ratio in this nucleus /1/.

/1/ W.Mannhart, H.K.Vonach, Z.f.Physik 210 (1968) 13

4.1. Eu 151 (n,γ) Studies

K.Mühlbauer, H.R.Koch, H.A.Baader, D.Breitig and O.W.B.Schult

A high-resolution study of the low-energy γ-spectrum from slow neutron capture in Eu 151 has been performed with the curved crystal spectrometer at Risø. About 2500 γ-lines with energies from 20 keV to 1 MeV have been observed. Their intensities were measured and precise transition energies were obtained. These data have lead to a modification of the level scheme of Eu 152 given in the literature.

4.2. Levels of Eu 153 observed through slow neutron capture in Eu 152 (12.4a)

K.Mühlbauer, H.R.Koch, H.A.Baader, D.Breitig and O.W.B.Schult

The Eu 152 (12.4a) (n,γ) Eu 153 spectrum was recorded simultaneously with the Eu 151 (n,γ) spectrum. Most of the observed Eu 153 lines were located in a level scheme which includes several new states /1/ of the [523↑] and the [411↑] bands. Numerous interband transtions have been disclosed. The [532↑] band was found to be strongly distorted.

/1/ K. Mühlbauer, Z.f.Physik 230 (1970) 18

4.3. The measurement of low energy (n,γ)-rays of Ag 108 and Ag 110

D.Breitig, H.R.Koch, H.A.Baader and O.W.B.Schult

The low energy (n,γ)-spectra from slow neutron capture in Ag 107 and Ag 109 have been measured with the Risø spectrometer. The resolution was $\Delta E/E \approx 3.3$ E/n GeV with n = 2 for weak transitions and n = 3 or 5 for strong lines. The spectra are very complex. The data are being analysed at the present time.

4.4. Low energy (n,γ)-spectra of Au 198 and Au 199

D.Breitig, H.R.Koch, H.A.Baader and O.W.B.Schult

The automatised curved crystal spectrometer at Risø has been used for the investigation of low energy γ-rays from slow neutron capture in Au 197 and - through double capture - in Au 198. The resolution during these measurements was $\Delta E/E \approx 2.5$ E/n GeV with n = 2, 3 or 5, depending on the intensity of the (n,γ)-lines. The γ-energies cover the region from 30 keV to 1 MeV.

4.5. Low-energy (n,γ)-spectrum of Tb 160

H.R.Koch, H.A.Baader, D.Breitig and O.W.B.Schult

The low energy γ-spectrum from slow neutron capture in Tb 160 has been measured with the automatised curved crystal spectrometer at Risø. The line width obtained was ΔE (FWHM) = 3.3 E^2/n GeV. The symbol n stands for the order of reflection. Strong γ-lines are observed in the 5th order and weak transitions in the 2nd order. The data will be analysed in the near future.

4.6. Low-energy γ-spectra from the irradiation of Ta 181 with slow neutrons

P.van Assche, J.M. van den Cruyce, H.R.Koch, H.A.Baader, D.Breitig and O.W.B.Schult

The Ta 181 (n,γ)-spectrum and - through double capture- the Ta 182 (n,γ)-spectrum have been measured with the diffractometer at Risø. The resolution obtained during these studies was $\Delta E/E \approx 4\ E/n$ GeV, where n stands for the order of reflection (n = 2 for weak γ-lines, and n = 3 or 5 for strong transitions).

4.7. High-resolution studies of the Gd 157 (n,γ) spectrum

H.A.Baader, H.R.Koch, D.Breitig and O.W.B.Schult

The preliminary analysis of the previously measured /1/ spectrum from slow neutron capture in Gd 157 has shown that the density of lines in the 1 MeV region is very large. These transitions are, however, important for the construction of the Gd 158 level sheme. For this reason, a high-resolution run has been taken in order to resolve as many as possible of the complex structures. The line width during this measurement was $\Delta E \approx 2.3\ E^2/n$ GeV. About 100 additional transitions have been disclosed in the energy region up to 2.2 MeV.

/1/ H.A.Baader, H.R.Koch, D.Breitig, O.W.B.Schult, R.C.Greenwood, C.W.Reich, A.Bäcklin and B.Fogelberg: "Neutron Capture Gamma-Ray Spectroscopy", Vienna 1967, p.363

4.8. Slow neutron capture γ-ray spectra of Yb 172 and Yb 175

D.Breitig, H.R.Koch, H.A.Baader and O.W.B.Schult

The low energy Yb 171 (n,γ) spectrum has been measured has been measured with the automatised /1/ curved crystal spectrometer

at Risø. The resolution obtained was $\Delta E/E \approx 7$ E/n GeV with n = 2 for weak and 3 or 5 for strong intensities. Numerous γ-lines were recorded during the Yb 174 (n,γ)-measurement, where the resolution was $\Delta E/E \approx 4.5$ E/n GeV. Many of the observed transitions with a γ-intensity sum of 90% of the total γ-intensity of all measured Yb 174 (n,γ)-lines were located in the level scheme of Yb 175. The level scheme is in good agreement with that proposed by Burke et al on the basis of dp and dt data /2/.

/1/ H.R.Koch, H.A.Baader, D.Breitig, K.Mühlbauer, U.Gruber, B.P.K.Maier, O.W.B.Schult: "Neutron Capture Gamma-Ray Spectroscopy", IAEA,Vienna 1969

/2/ D.G.Burke and B.Elbek, Dan.Mat.Fys.Medd. 36 (1967) No.6

5. Precise Measurement of the Total Cross Sections of Bi,Pb,Si, C with 130 eV-Neutrons (Resonance of Co 59)

W. Dilg, H.K. Vonach

At the present time transmission measurements are being carried out with single- and polycrystalline samples of Bi, Pb, Si, C at the Munich Research Reactor (FRM). A precision of about 0,05% (including systematic errors) is aimed at for the total cross sections at E_n = 130 eV.

A resonance method is applied, which consists of a transmission measurement with reactor neutrons, which have been scattered twice from Co-foils.

The preliminary results are:

$\sigma_{tot}(E_n = 130\ \text{eV})$ Bi (9.18 ± 0.01) b

C (4.72 ± 0.02) b

6. Coherent scattering length measured by total reflection of slow neutrons

L. Koester, N. Nücker, W. Nistler, D.Trüstedt

Measurement of some new substances and determinations of impurities in the measured organic substances result in more precise scattering length values which are listed below.

Hydrogen : $a = -(3.718 \pm 0.008)\ 10^{-13}$ cm

Carbon : $a = +(6.622 \pm 0.005)\ 10^{-13}$ cm

Oxygen : $a = +(5.75 \pm 0.02)\ 10^{-13}$ cm

Fluorine : $a = +(5.74 \pm 0.02)\ 10^{-13}$ cm

Sulfur : $a = +(2.847 \pm 0.001)\ 10^{-13}$ cm

Chlorine : $a = +(9.588 \pm 0.003)\ 10^{-13}$ cm

Lead : $a = +(9.42 \pm 0.01)\ 10^{-13}$ cm++

++ preliminary value

7. Measurement of Total Cross Sections for Very Cold Neutrons

A. Steyerl, H.K. Vonach

The total cross sections of aluminum and gold for very slow neutrons from 0.1 μeV to 60 μeV (5 m/s to 100 m/s) were measured at 298 °K , 80 °K and 30 °K by a transmission experiment /1/. If plotted versus neutron velocity v corrected for its reduction due to the index of refraction, the total cross sections show a 1/v behaviour and agree with 1/v extrapolations of earlier measurements in the meV region. At v = 10 m/s (0.526 μeV, 395 Å) the following values were obtained: 61 ± 1 b, 50 ± 1 b, and 50 ± 1 b for aluminum at 298 °K, 80 °K, and 30 °K, respectively, and 21600 ± 500 b for gold at 298 °K and 80 °K. The values for Al at 80°K and 30°K

and for Au agree with 1/v extrapolations of the pure absorption cross-sections.

/1/ A. Steyerl, Phys.Lett. 29B (1969) 33

8. Measurement of the gamma radiation from inelastic scattering of 2.8 MeV in ^{93}Nb

H.Göbel, E.Feicht, H.K.Vonach

Energies and intensities of the gamma rays produced in the (n,n'γ) reaction on ^{93}Nb by 2.8 MeV (DD) neutrons were measured with a Ge(Li) detector. The energies and production cross-sections determined in this way are given in Table I. The cross-sections are measured relativ to the (n,n'γ) cross-section for the production of the 846 keV gamma ray in ^{56}Fe using a value of 950 mb for this cross-section. The errors given in Table I include all sources of systematic errors including that of the reference cross-section.
An extended level scheme of ^{93}Nb including almost all observed gamma transitions was constructed from the data. Using this level scheme a value of 2.0 ± 0.2 b was obtained for the total (n,n'γ) cross-section of ^{93}Nb at 2.8 MeV.

Table I. γ-Transitions of $^{93}Nb(n,n'\gamma)^{93}Nb$

Observed energies and production cross-sections for 2.8 MeV neutrons

E_γ (keV)	$\sigma_{n,n'\gamma}$ (mb)		
318.4	94	±	24
338.8	162	±	34
365.1	21	±	12
385.2	100	±	27
477.7	74	±	17
541.5	146	±	23
553.2	35	±	9
571.7	48	±	10
585.1	50	±	12
625.5	18	±	8
655.7	82	±	15
733.3	30	±	9
743.9	459	±	60
779.7	183	±	31
808.5	167	±	27
833.7	32	±	9
921.0	25	±	9
934.5	16	±	7
939.2	36	±	11
949.9	490	±	64
979.1	291	±	42
1053.1	23	±	8
1082.5	30	±	9
1141.5	18	±	7
1184.7	9	±	5
1193.7	13	±	6
1206.8	12	±	6
(1209)	8.5	±	6
1212.5	15	±	7
1221.6	10	±	6
1253.8	8.5	±	4
1297.8	55	±	9
1484.7	50	±	13
1500.5	86	±	14

Table I. γ-Transitions of $^{93}Nb(n,n'\gamma)^{93}Nb$

continuation:

E_γ (keV)	$\sigma_{n,n'\gamma}$ (mb)
1537.1	7 ± 4
1604.8	15 ± 5
1683.2	25 ± 8
1687.2	33 ± 10
1910.7	51 ± 10
1951	12 ± 4
1970	31 ± 7
2125	8.5 ± 4
2203	13 ± 5
(2505)	

The errors of the energy lies between 0.5 and 1 keV.

9. Precision-measurement of $^{27}Al(n,\alpha)$-cross-section for 14.4 MeV-neutrons

H.K.Vonach, M.Hille, G.Stengl, W.Breunlich, E.Werner

A precision measurement of the $^{27}Al(n,\alpha)^{24}Na$ cross-section for 14.4 MeV neutrons was performed in cooperation with the Institut für Radiumforschung, Vienna and IAEA Laboratory, Seibersdorf.

Aluminum samples were irradiated in an accurately known neutron flux determined by the associated particle method. The induced ^{24}Na activity was measured with a scintillation detector accurately calibrated by means of ^{24}Na standards which had been calibrated themselves by β-γ coincidence method. By means of careful minimizing all sources of systematic errors an overall accuracy of 1.5% on a 99.5 (3 σ) confidence level was obtained.

The measurements result in a cross-section of 117.3 mb for the $^{27}Al(n,\alpha)^{24}Na$ reaction for neutrons of an average energy of 14.4 MeV and an energy width of approximately 0.2 MeV.

VI. INSTITUT FÜR FESTKÖRPER- UND NEUTRONENPHYSIK, KFA JÜLICH

1. Search for delayed prompt γ-rays in ^{235}U-thermal fission in the time range (1 - 100) μsec

(J.W. Grüter, K. Sistemich, J. Eidens, H. Lawin, P. Armbruster)

The gas-filled mass separator for fission products at the reactor FRJ-2 has been used to search for γ-emission from primary fission products in the time range (1 - 100) usec (1), (2), (3). The separator allows a rough mass determination of the emitting nuclides. Moreover, delayed X-ray emission from the investigated isomers detected by solid state X-ray detectors gives an unambigous isotope identification. Fig. 1.1 gives the experimental set-up. A coincidence between fission fragments leaving the separator and γ- or X-ray quanta emitted from these fragments after having been stopped in a stopping foil allows to detect delayed radiation. The quanta are detected by Ge(Li)- or Si(Li)-diodes, the fission fragments by a transmission counter as proposed by Muga (4). A time to pulse height converter triggered by the fission fragment, and stopped by the quantum registered is used to determine the half-life of the emitting isomeric state. The data are stored by a 2-parameter 4096 channel analyzer.

The intensity of the isomeric γ-lines has been measured as a function of the magnetic field, as shown in fig. 1.2. The mass assignment is uncertain within certain limits, as the nuclear charge dispersion of the separator leads for small values of the mass dispersion constant $\Gamma = \Delta(\ln B\cdot\rho)/\Delta(\ln A)$ to an ambiguity in the mass assignment. Table 1 gives a compilation of the γ-lines, their relative intensities, half-lives, energies, and the mass region, they have been found in. X-rays have been observed from Br, Rb, Y, Zr, Nb, Mo. The following isotopes have isomeric states in the time range investigated: ^{88}Br, $^{92-93}$Rb, ^{98}Y, ^{99}Zr, ^{100}Nb, ^{101}Mo.

(1) R.E. Sund and R.B. Walton, Phys. Rev. 146 (1966) 824

(2) R.B. Walton and R.E. Sund, Phys. Rev. 178 (1969) 1894

(3) J.J. Wesolowski, W. John, F. Guy, and R. Jewell, Bull. Am. Phys. Soc. Ser. II. 14 (1969) 536

(4) M.E. Muga, and H.E. Taylor, Report ORO-2843-12 (1967)

2. Mass dependence of anisotropy and yield of prompt γ-rays in ^{235}U thermal fission

(H. Labus, P. Armbruster, F. Hossfeld, K. Reichelt)

The yield of prompt γ-rays and the anisotropy of the angular correlation, γ-ray versus fission product, has been measured (1), (2).

An external neutron beam of the reactor FRJ-2 has been used to produce fission fragments from an uranyl acetate target electrosprayed on a plastic scintillator. The energy of the fragments has been measured with 4 Si-detectors giving in addition stop signals for a time-of-flight analysis. Start signals are obtained from a photomultiplier viewing via a light guide system the scintillating target. Energy and time-of-flight give the fragment mass.

The prompt γ-rays are detected by 4 plastic scintillators observing the fragments at the angles of emission 30°, 90°, 150° referred to the direction of flight of the fragment. A precision collimator between target and γ-detector separates the radiation of the two complementary fragments. The high symmetry of the experimental set-up eliminates small differences in detection of the different combinations of γ- and fragment detectors. A time-of-flight discrimination between prompt γ-rays and prompt neutrons is applied.

An average emission time of the radiation observed through the collimator of (11 $\pm$ 3) psec has been found. A method to determine emission times comparable to the stopping time of fission fragments from the $0^{\circ}/180^{\circ}$ aberration has been discussed and applied to determine a lower limit for the emission time of the prompt radiation to 2.6 psec.

The yield and anisotropy depending on fragment mass and mass ratio is given in fig. 2.1. In the mass range (90 - 101) and (133 - 144) the yield increases for both the groups within increasing mass of the fragments. Within the accuracy of our measurement the anisotropy is constant and depends

neither on the mass ratio nor on the fragment mass. The data obtained have been used to reconstruct the mass dependence of the angular momenta of the primary fission fragments. Using different models to calculate from yield and anisotropy data primary angular momenta an increase of the latter within both fission product groups has been obtained.

(1) P. Armbruster, F. Hossfeld, H. Labus, K. Reichelt, Physics and Chemistry of Fission (Proc. Symp. Vienna 1969) IAEA Vienna, 545

(2) H. Labus, thesis Technische Hochschule Aachen (1970)

Figure captions

Fig. 1.1 Experimental set-up used to detect isomeric states in the (1 - 100) μsec time range among fission products

Fig. 1.2 Intensity distribution of a 9-μsec 165 keV gamma-line

Fig. 2.1 Yield and anisotropy of prompt gamma-rays in ^{235}U fission

a) fission yields η_{ex}
b) relative anisotropy depending on the mass ration of the fragment
c) relative anisotropy depending on the fragment mass
d) relative gamma-yield depending on the mass ratio of the fragment
e) relative gamma-yield depending on the fragment mass

all quantities are referred to the average values for all fragments

Table 1 Compilation of data on isomeric prompt gamma-quanta

SET-UP FOR PROMPT γ-ISOMERS

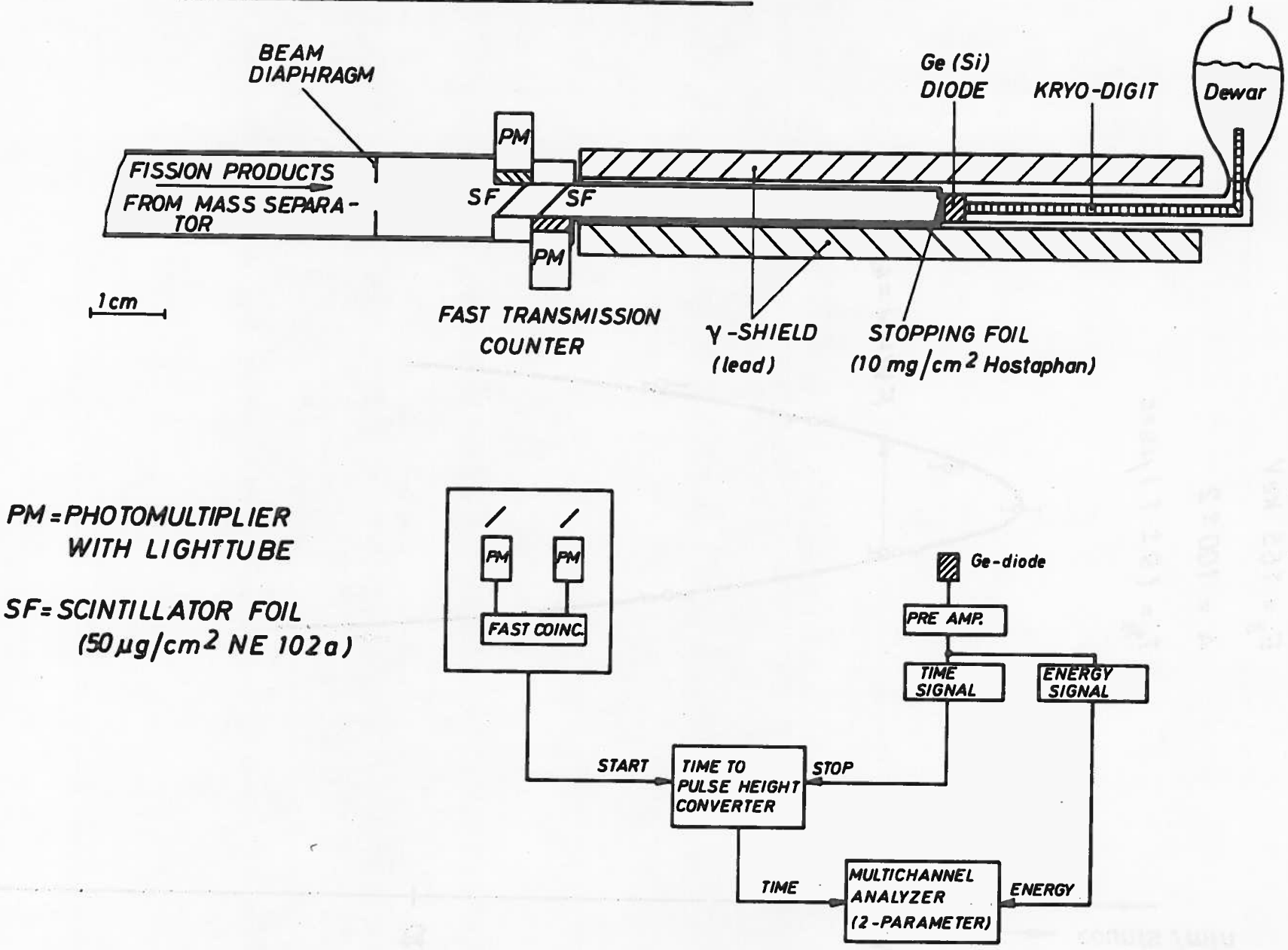

Fig. 1.1

Fig. 1.2

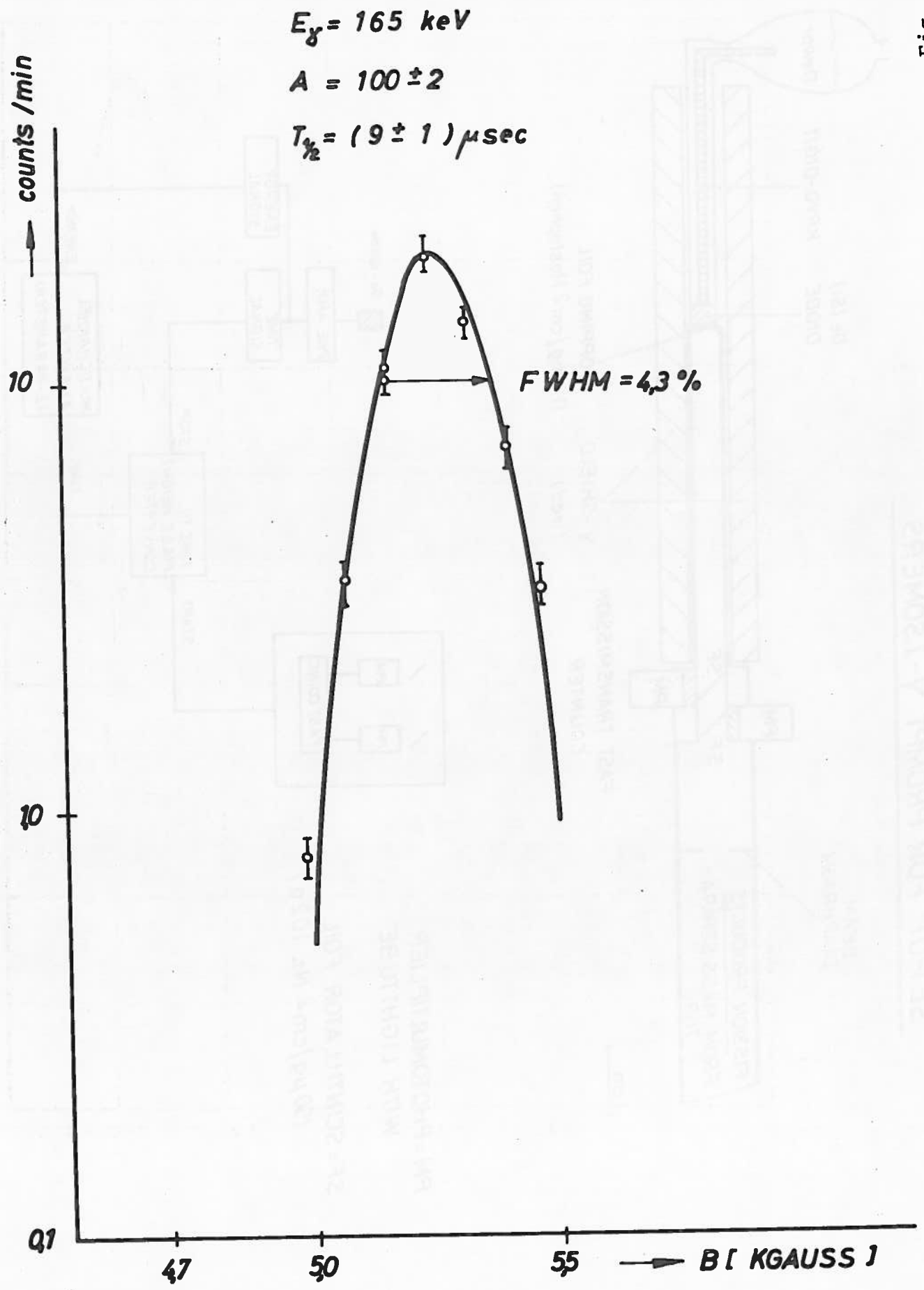
E_γ = 165 keV
A = 100 ± 2
$T_{1/2}$ = (9 ± 1) μsec
counts /min
10
1,0
0,1
FWHM = 4,3 %
4,7
5,0
5,5
B [KGAUSS]

Fig. 2.1

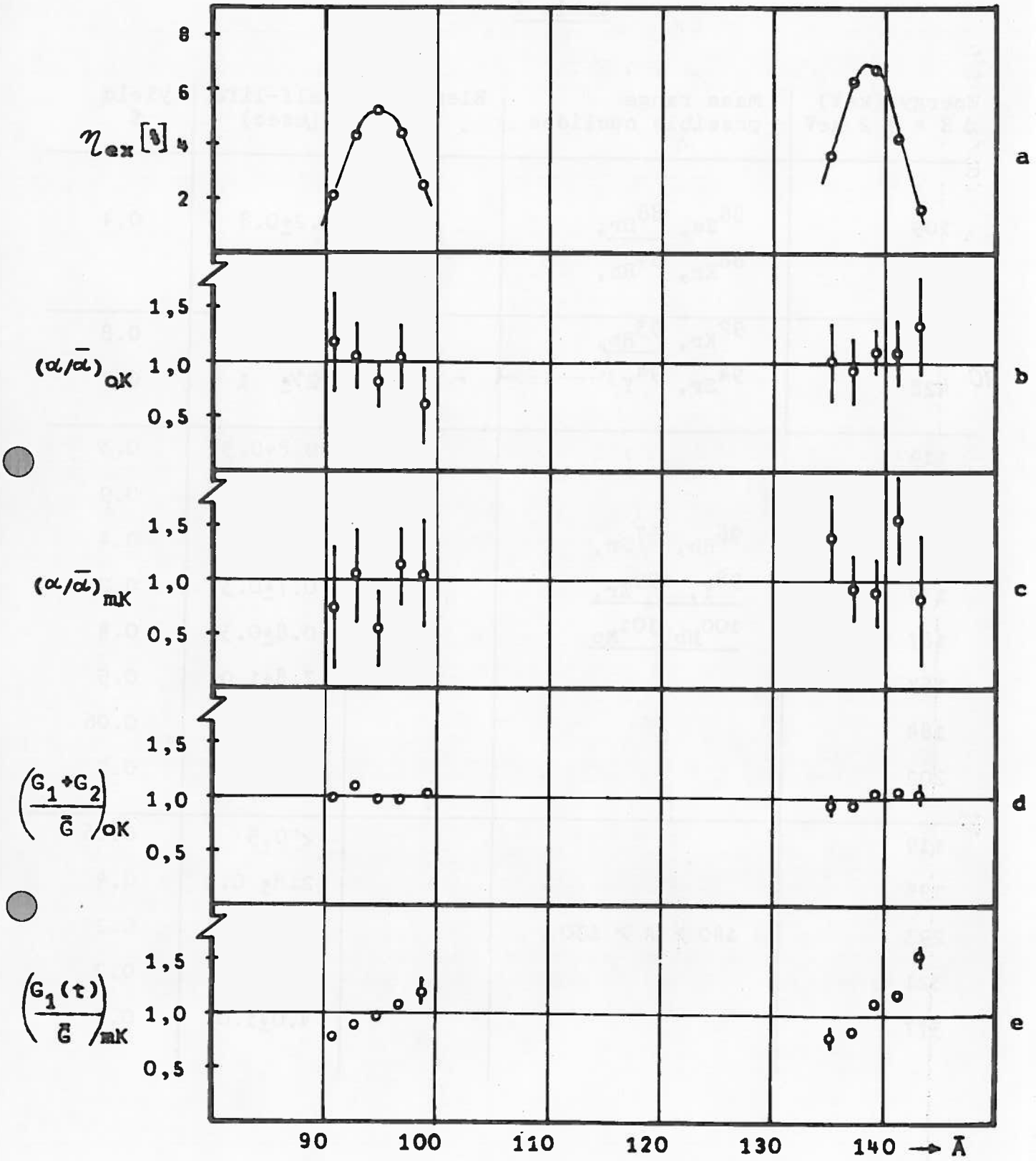
8
6
η_{ex} [%]
4
2
a
1,5
$(\alpha/\bar{\alpha})_{oK}$
1,0
0,5
b
1,5
$(\alpha/\bar{\alpha})_{mK}$
1,0
0,5
c
1,5
$\left(\frac{G_1+G_2}{\bar{G}}\right)_{oK}$
1,0
0,5
d
1,5
$\left(\frac{G_1(t)}{\bar{G}}\right)_{mK}$
1,0
0,5
e
90
100
110
120
130
140 → $\bar{A}$

Table I

Energy (keV) $\Delta E = \pm 2$ keV	Mass range possible nuclides	Elements	Half-life (μsec)	yield %
109	^{88}Se, ^{88}Br,	Br	6.2±0.8	0.4
156	^{88}Kr, ^{89}Rb,			
257	^{92}Kr, ^{93}Rb,	Rb	57 ± 15	0.8
428	^{94}Sr, ^{94}Y		2 ± 1	0.2
119			0.8±0.3	0.3
119		Y	7.5±1.0	0.9
128	^{96}Rb, ^{97}Sr,	Zr	< 0.7	0.4
139	^{98}Y, ^{99}Zr,	Nb	0.7±0.3	0.2
167	^{100}Nb, ^{101}Mo	Mo	0.8±0.3	0.4
167			7.8±1.0	0.5
184			1.3±0.6	0.06
202			7.4±1.0	0.7
119			< 0.5	0.06
195			2.8± 0.5	0.4
293	140 > A > 130		< 0.5	0.2
321			0.7±0.3	0.2
377			4.0±1.0	0.7

VII. INSTITUT FÜR REAKTORENTWICKLUNG, KFA, JÜLICH (GERMANY)

The Fast Fission Factor ε of Be and BeO

M. Demmeler, R. Hecker, N. Kirch, R. Schulten

Experiments for the determination of the fast fission factor ε of Be and BeO resulting from the σ(n, 2n)process are carried out at our Institute for Reactor Development. The following results are averaged over the fission spectrum:

	ε	Method	Reference
BeO	1.048 ± 0.004	$MnSO_4$ bath	N. Kirch, R. Hecker Nukleonik 12,1969
	1.048 ± 0.004	Liquid scintillator	
	1.051 ± 0.004	Pulsed neutron source	
Be	1.078 ± 0.004	Pulsed neutron source	M. Demmeler (to be published)

VIII. I. INSTITUT FÜR EXPERIMENTALPHYSIK, UNIVERSITÄT HAMBURG, HAMBURG (Germany)

1. Angular Distributions of the Alpha-Particles from the Reactions $^{63}Cu(n,\alpha)^{60}Co$ and $^{14}N(n,\alpha)^{11}B$ at 14.2 MeV.

(M. Bormann, V. Schröder, U. Seebeck)

In these investigations α-particles were detected with a thin CsI-crystal. Particle discrimination was achieved by applying the method of pulse shape analysis. For ^{63}Cu differential cross sections for the total α-particle spectrum, for ^{14}N those for the groups α_0, α_1, $\alpha_{2,3}$ and $\alpha_{4,5,6}$ were measured. The results for ^{63}Cu have been analysed on the background of the statistical theory from which for ^{60}Co a level density parameter $a = 7.8 \pm 0.4$ MeV^{-1} and a spin-cutoff parameter $\sigma = 2.80 \pm 0.30\,\hbar$ were obtained.
The results are given in the Tables I and II.

Table I. Differential cross sections in mb for $^{14}N(n,\alpha)^{11}B$ at 14.2 MeV

θ_{CM}	$\frac{d\sigma}{d\Omega}(\alpha_0)$	$\frac{d\sigma}{d\Omega}(\alpha_1)$	$\frac{d\sigma}{d\Omega}(\alpha_{2,3})$	$\frac{d\sigma}{d\Omega}(\alpha_{4,5,6})$
20.9°	1.43 ± 0.33	0.49 ± 0.35		
42.5°	1.52 ± 0.21	1.01 ± 0.24	3.56 ± 0.32	1.14 ± 0.27
45.3°	1.17 ± 0.31	0.64 ± 0.28	1.58 ± 0.19	0.55 ± 0.18
64.0°	0.43 ± 0.09	0.25 ± 0.09	0.43 ± 0.13	0.17 ± 0.10
89.5°	0.23 ± 0.06	0.14 ± 0.06	0.77 ± 0.15	0.60 ± 0.18
109.0°	0.40 ± 0.07	0.33 ± 0.08	1.40 ± 0.15	
132.0°	0.67 ± 0.19	0.70 ± 0.25	2.30 ± 0.39	
149.0°	1.51 ± 0.33	1.15 ± 0.29	2.27 ± 0.52	
157.0°	2.23 ± 1.05	1.19 ± 0.71	3.52 ± 0.81	

Table II. Differential cross sections in mb for $^{63}Cu(n,\alpha)^{60}Co$ at 14.2 MeV

θ_{CM}	$\frac{d\sigma}{d\Omega}(n,\alpha + n,n'\alpha)$ 1)	$\frac{d\sigma}{d\Omega}(n,\alpha)$ 2)
19°	4.40 ± 1.46	4.10 ± 1.36
38°	3.29 ± 0.37	2.86 ± 0.32
58°	3.64 ± 0.21	3.02 ± 0.17
83°	2.43 ± 0.13	1.92 ± 0.10
101°	2.65 ± 0.12	1.99 ± 0.09
125°	4.36 ± 0.29	3.28 ± 0.22
145°	3.42 ± 0.57	2.82 ± 0.47

1) From total experimental α-particle spectrum

2) From the experimental total α-particle spectrum the $(n,n'\alpha)$ contribution has been subtracted by statistical theory analysis

2. $^{11}B(n,\alpha)^{8}Li(\beta^{-})^{8}Be^{*}(2\alpha)$ and $^{9}Be(n,d)^{8}Li(\beta^{-})^{8}Be^{*}(2\alpha)$ Cross Sections.

W. Scobel, M. Bormann

The excitation functions of these two reactions have been measured for neutron energies between 15.5 and 19 MeV. The neutrons were produced using deuterons from a 2.5 MV Van de Graaff generator impinging on a thin tritium-titanium target. The neutron flux was measured with a stilbene recoil proton spectrometer.

The measurements were performed with a modified activation technique. The ^{11}B or ^{9}Be target was placed in the cathode of a gridded back-to-back ionization chamber. Alternately the chamber was irridiated with neutrons and the induced α-decays $^{8}Be^{*}(2\alpha)$ appearing with a 0.853 $\pm$ 0.017 sec half life of the ^{8}Li-β-decay, were counted.

The results of the ^{11}B-reaction are given in table 1, those for $^{9}Be(n,d)^{8}Li$ in table 2.

The first excited state of ^{8}Be was found at 2.95 $\pm$ 0.07 MeV with a full width at half maximum of 1.42 $\pm$ 0.15 MeV in the center of mass system.

Table 1: Cross Sections for $^{11}B(n,\alpha)^{8}Li(\beta^{-})^{8}Be^{*}(2\alpha)$

$E_n \pm \Delta E_n$(MeV)	$\sigma \pm \Delta\sigma$ (mb)	$E_n \pm \Delta E_n$(MeV)	$\sigma \pm \Delta\sigma$(mb)
15.63 ± 0.24	28.5 ± 2.6	17.33 ± 0.12	22.6 ± 2.0
15.80 ± 0.21	28.9 ± 2.6	17.52 ± 0.12	21.6 ± 1.9
15.99 ± 0.19	25.8 ± 2.3	17.71 ± 0.11	20.6 ± 1.8
16.18 ± 0.18	24.7 ± 2.2	17.90 ± 0.11	18.6 ± 1.7
16.37 ± 0.16	25.1 ± 2.3	18.09 ± 0.11	18.4 ± 1.6
16.56 ± 0.15	25.0 ± 2.2	18.28 ± 0.10	17.8 ± 1.6
16.75 ± 0.14	24.8 ± 2.2	18.47 ± 0.10	18.4 ± 1.7
16.94 ± 0.13	24.1 ± 2.2	18.67 ± 0.10	18.8 ± 1.7
17.13 ± 0.13	23.3 ± 2.1	18.86 ± 0.10	19.4 ± 1.7

Table 2: Cross Sections for $^{9}Be(n,d)^{8}Li$

$E_n \pm \Delta E_n$(MeV)	$\sigma \pm \Delta\sigma$(mb)	$E_n \pm \Delta E_n$(MeV)	$\sigma \pm \Delta\sigma$ (mb)
16.42 ± 0.16	<0.04	17.68 ± 0.13	7.8 ± 0.7
16.56 ± 0.16	0.10 ± 0.04	17.82 ± 0.12	8.2 ± 0.8
16.70 ± 0.15	0.56 ± 0.07	17.96 ± 0.12	8.9 ± 0.8
16.84 ± 0.14	1.38 ± 0.15	18.10 ± 0.12	9.2 ± 0.8
16.98 ± 0.14	2.73 ± 0.25	18.24 ± 0.12	9.8 ± 0.8
17.12 ± 0.14	4.06 ± 0.35	18.38 ± 0.13	9.9 ± 0.8
17.26 ± 0.13	5.88 ± 0.50	18.52 ± 0.13	10.0 ± 0.8
17.40 ± 0.13	6.5 ± 0.5	18.66 ± 0.13	10.5 ± 0.9
17.54 ± 0.13	7.0 ± 0.6	18.80 ± 0.13	10.9 ± 0.9

3. Excitation Functions of (n,2n) Reactions.

(H. Bissem, M. Bormann, E. Magiera, R. Warnemünde)

The activation method was used for measuring (n,2n) excitation functions in the neutron energy region 12 - 18 MeV for medium and heavy target nuclei. Neutrons were produced by the reaction $^{3}H(d,n)^{4}He$ in thin titanium-tritium targets with the 2 MeV deuteron beam of a Van de Graaff accelerator. For detecting β^{+}-, β^{-}- and γ-activities a NaI $\gamma\gamma$-coincidence spectrometer, a Methane-flow proportional counter and a NaI well-crystal spectrometer, respectively, were used. Counting efficiencies were calculated and checked by means of calibrated probes. The neutron flux was measured with a Stilbene recoil proton spectrometer. The results are given in Table I. Those half-lives which have been remeasured in the investigations are stated in the Table I with error indications. The results agree reasonably well in most cases with statistical theory calculations.

Table I (n,2n) Cross Sections in mb

$^{93}Nb(n,2n)\ ^{92}Nb^{m}$		$^{96}Ru(n,2n)\ ^{95}Ru$		$^{104}Ru(n,2n)\ ^{103}Ru$	
T 1/2 = 10.16d		T 1/2 = 97.89±1.27m		T 1/2 = 39.6d	
E_n (MeV)	σ (mb)	E_n (MeV)	σ (mb)	E_n (MeV)	σ (mb)
12.66±0.10	556±34.4	12.62±0.06	459±41	12.66±0.10	1510±140
13.39±0.13	524±31.4	13.32±0.08	627±55	13.39±0.13	1480±140
14.82±0.15	491±29.5	13.90±0.09	774±66	14.09±0.14	1460±145
15.64±0.15	468±28.1	14.82±0.10	879±75	15.09±0.15	1530±135
16.95±0.14	428±25.7	15.42±0.10	892±77	16.19±0.14	1595±160
17.96±0.13	402±24.1	16.12±0.11	969±83	16.95±0.14	1510+135
		16.79±0.11	990±85	17.58±0.13	1450±140
		17.48±0.11	982±84	18.13±0.14	1350±130
		18.17±0.11	913±79		

Table I (continued)

$^{103}Rh(n,2n)\ ^{102}Rh$		$^{102}Pd(n,2n)\ ^{101}Pd$		$^{142}Nd(n,2n)\ ^{141}Nd$	
T 1/2 = 206d		T 1/2 = 510±31m		T 1/2 = 150.0±4.5m	
E_n (MeV)	σ (mb)	E_n (MeV)	σ (mb)	E_n (MeV)	σ (mb)
12.96±0.10	729±65	12.62±0.06	581±68	12.92±0.10	1230±119
13.61±0.13	756±70	13.32±0.07	741±86	13.42±0.12	1340±130
14.60±0.15	692±67	13.81±0.08	942±109	14.10±0.14	1540±150
15.37±0.15	680±70	14.82±0.09	1030±105	14.66±0.15	1525±148
16.13±0.14	661±65	15.42±0.10	1195±115	15.19±0.16	1570±155
16.85±0.14	628±55	16.12±0.10	1080±95	15.79±0.16	1695±165
17.55±0.13	581±50	16.79±0.10	1042±94	16.36±0.16	1785±172
18.03±0.14	568±50	17.48±0.11	1148±98	17.04±0.16	1740±167
		18.17±0.11	1040±79	17.56±0.14	1710±162
				18.02±0.13	1740±165

Table II (continued)

Target Nucleus	^{110}Pd	^{110}Pd	^{128}Te	^{128}Te	^{130}Te	^{130}Te
Residnal. Nucl.	^{109}Pd	^{109m}Pd	^{127g}Te	^{127m}Te	^{129g}Te	^{129m}Te
E_n (MeV) \ T1/2	13.67±0.07h	4.6±0.4m	9.48±0.13h	109d	70.2±0.3m	33.2±0.5d
12.65±0.06	1341±124	417±46	660±48	791±108	731±44	875±54
13.01±0.07	1403±100	438±48	788±58	807±107	794±48	939±53
13.53±0.08	1430±101	450±50	809±60	885±105	819±49	968±55
14.30±0.09	1539±107	486±53	841±63	936±107	812±50	1000±61
15.31±0.09	1527±107	489±54	831±60	937±110	839±55	1009±58
15.85±0.10	1581±147	505±55	839±60	933±105	846±53	994±65
16.33±0.10	1589±149	512±149	810±59	906±100	835±53	950±62
16.97±0.10	1594±146	516±55	817±58	881±98	834±53	931±58
17.59±0.10	1490±133	482±53	794±56	847±94	791±49	875±57
18.23±0.11	1285±90	419±45	735±53	818±89	584±38	510±32

Table I (continued)

Target Nucleus	^{192}Os		^{191}Ir		^{198}Pt	^{198}Pt
Residual Nucl.	^{191}Os		$^{190m_2}Ir$		^{197}Pt	^{197m}Pt
E_n(MeV) \ T1/2	15d	E_n(MeV) \ T1/2	195±12m	E_n(MeV) \ T1/2	18.32±0.33h	83.2±4.1m
12.64±0.07	2131±192	12.62±0.06	117±13	12.65±0.05	2163±143	1004±73
13.00±0.08	2259±218	12.96±0.07	152± 8	13.01±0.06	2223±145	1089±92
13.53±0.09	2284±205	13.32±0.07	143±13	13.54±0.06	2265±155	1108±82
14.29±0.10	2233±199	13.61±0.08	179±10	14.30±0.06	2275±144	1147±82
15.25±0.11	2145±178	13.90±0.08	164±14	15.04±0.06	2207±142	1138±96
15.69±0.11	2031±168	14.82±0.09	188±15	15.69±0.07	2240±154	1100±79
16.34±0.11	1851±148	15.42±0.10	203±15	16.33±0.08	1900±127	965±62
16.99±0.11	1472±124	16.12±0.10	273±16	16.97±0.08	1465± 98	749±69
17.61±0.11	1328±111	16.79±0.10	212±16	17.59±0.09	1229±83	642±45
18.25±0.10	1059± 92	17.48±0.11	198±15	18.23±0.11	1058±67	505±41
		18.17±0.11	203±15			

IX. INSTITUT FÜR REINE UND ANGEWANDTE KERNPHYSIK UNIVERSITÄT KIEL (IKK), GEESTHACHT

1. Fast Chopper

H.H. JUNG, H.G. PRIESMEYER

1.1 Resonance Parameters of Cs 133/135/137

Total neutron cross section measurements on stable Cs 133 and fission product Cs 133 - Cs 135 - Cs 137 have been completed.

For the measurements on stable Cs 133, samples of powdered CsCl of high purity with thicknesses between 0.02 and 0.000075 Cs-atoms/barns were run at 2250, 6000, and 12000 rpm chopper speed which correspond to 163, 62, and 31 nsec/m resolution, respectively.

Up to 600 ev, parameters of 21 resonances in Cs 133 have been determined by area analysis. They are given in Table I which supersedes Table III on p.78 of the last progress report (EANDC (E) 115). From these values an average level spacing per spin state of D = (40 ± 2) ev, a Strength Function of $S_o = (1.15 \pm 0.1) \cdot 10^{-4}$, and an average partial radiation width of $\overline{\Gamma_\gamma} = (120 \pm 10)$ mev are calculated.

Two runs (at 6000 and 12000 rpm) were done on a sample of fission product cesium (in the chemical form of its chloride). The total sample thickness was 0.00703 Cs-atoms/barns. The abundances of the three cesium isotopes 133, 135, and 137 were 0.488, 0.171, and 0.341, respectively.

Two resonances in the cross section of this sample at (42.3 ± 0.1) ev and (880 ± 20) ev belong to either Cs 135

or Cs 137. Their neutron widths are (7 ± 2) and (700 ± 300) mev, respectively. These values are based on Γ_γ = 120 mev; the large errors result from the unknown isotopic assignment.

From the fact, that only two resonances of the two isotopes Cs 135 and Cs 137 have been found up to 900 ev, a lower limit for the average level spacing per spin state of the two isotopes can be estimated: 1400 ev. This value seems to be much to high compared with comparable values of neighbouring nuclei. It is concluded, therefore, that some resonances above about 200 ev were not detected, due to the lack of sample thickness and/or resolution.

1.2 Total Cross Section Measurements on Ruthenium

Total neutron cross sections of the stable isotopes Ru 100 and Ru 104 have been measured in the energy range from 1 ev to 3 kev.

In Ru 100 one new resonance has been found at 231.5 ev. In Ru 104 three new resonances have been found at 227 ev, 637 ev and 1072 ev.

Two other isotopes, Ru 101 and Ru 102, are measured at present in the energy range from 1 ev to 135 ev. In Ru 101 we found the seven known resonances, whereas in Ru 102 no resonances appeared so far. The measurements in the high energy range will begin soon. To determine the resonance parameters of the identified resonances, further measurements on natural Ruthenium will be done.

The resonances in Ru 100 at 231.5 ev and in Ru 104 at 227 ev are considerably close to the resonance at 227 ev in Ru 99 (cf(1)). The isotopic assignment for the latter was estimated from total width determination, so that its existence

seems to be doubtful now. This question will be investigated. We shall try to resolve both resonances in natural Ruthenium.

(1) Bolotin, Chrien : Nuclear Physics 42 (1963) 676 - 692

1.3 Total Neutron Cross Sections of Gross Fission Products

A first measurement of total neutron cross sections of gross fission products has been prepared. A special fuel element containing U 235 samples with tight cannings has been inserted into the FRG-2 in July 1969 and will be irradiated till March 1970. At this time, a burn up of about 40 % is expected.

The U235 samples will then be brought into the sample changer of the chopper. The beginning of these measurements is scheduled for April 1970. The activity of the total sample will be several 1000 Ci at this time; the shielding of the sample changer will be increased to 175 mm of lead for this measurements.

1.4 Publications

H.H. JUNG, H.G. PRIESMEYER: A Lithium Glass Detector Bank for Neutron Time-of-Flight Measurements (Nucl. Inst. Meth. 68 (1969) 353)

H.H. JUNG, H.G. PRIESMEYER: Determination of Resonance Parameters for Cs 133 (ATKE 14 (1969) 271)

H.H. JUNG: Das Flugzeitspektrometer am Forschungsreaktor FRG-1 in Geesthacht (Askaniawarte, home journal of Askania-Werke, Berlin , 26, Heft 73 (1969) 6)

H.H. JUNG: Totale Neutronenwirkungsquerschnitte der Caesium-Isotope 133, 135 und 137 im Resonanzbereich (Dissertation, Kiel 1969)

Table I: Resonance Parameters of Cs 133

E_o (ev)	Γ_n (mev)	Γ (mev)	Γ_γ (1) (mev)
5,90 ± 0,02	5,5 ± 0,4	115 ± 10	110 ± 10
22,7 ± 0,2	7,5 ± 0,5	120 ± 10	110 ± 10
48,0 ± 0,2	20 ± 2	150 ± 20	130 ± 20
83,6 ± 0,3	7,5 ± 1,0	130 ± 20	120 ± 20
95,2 ± 0,3	24 ± 3	150 ± 25	125 ± 25
127,6 ± 0,4	125 ± 15	240 ± 30	115 ± 30
144 ± 1	6,5 ± 0,5		(120)
148 ± 1	28 ± 3	130 ± 20	110 ± 20
183 ± 2	2,5 ± 0,2		(120)
(193) (2)	-		-
203 ± 2	25 ± 3	135 ± 20	110 ± 20
210 ± 2	6 ± 1,5		(120)
223 ± 2	33 ± 3	150 ± 20	120 ± 20
237 ± 2	470 ± 50		(120)
299 ± 3	115 ± 10		(120)
363 ± 3	22 ± 3		(120)
380 ± 4	7 ± 1		(120)
404 ± 4 (3)	-		-
417 ± 4 (3)	-		-
436 ± 5	50 ± 10		(120)
474 ± 5	105 ± 15		(120)
520 ± 6	320 ± 40		(120)
566 ± 6	180 ± 25		(12o)
591 ± 6	180 ± 25		(120)

(1) values in parentheses are assumed

(2) doubtful resonance

(3) not analyzed, as these resonances were superposed by the 405 ev-resonance in Cl 35.

2. Crystal Spectrometer

K. BRAND, M. SAAD

2.1 The Effect of Chemical Binding on Neutron Cross Sections of Metalhydrides, -deuterides and Uranium Carbide.

All the total neutron cross section measurements had been done with the crystal spectrometer at the FRG I.

2.1.1 $VH_{o.6}$ and $VH_{o.39}$

The cross sections per proton had been measured in the energy range 0,07 to 0,7 ev. The cross sections show no clear excited niveaus of hydrogen vibration. There is only a small indication of optical niveaus between 0,12 - 0,18 and 0,24 - 0,34 ev (broad shoulders).

2.1.2 $VD_{o.61}$

The cross section per deuteron in $VD_{o.61}$ shows no excited deuteron states.

2.1.3 $TaH_{o.62}$ and $TaH_{o.52}$

The cross sections per proton in the energy range 0,07 - 0,7 ev show as in the case of $NbH_{o.9}$ two well seperated optical niveaus at 0,126 and 0,158 ev for $TaH_{o.52}$. Both niveaus are attributed to the 0 - 1 transition of hydrogen atoms in the metal lattice. The cross section curves also show the double excited proton-states. The cross section curve for $TaH_{o.52}$ has been published in ATKE 14, 449 (1969).

2.1.4 $TaD_{o.63}$

The cross section per deuteron in $TaD_{o.63}$ shows only one broad deuteron vibration around 0,136 ev.

2.1.5 UC

The total neutron cross section for polycrystalline UC was measured at 24 , 250 and 510°C between 0,034 and 0,140 eV. The measurement showed that there is only one isolated harmonic oscillation at 0,044 ev. Other minimum-maximum-structures may be due to various sets of crystal planes (Bragg-reflections).

X. KERNFORSCHUNGSZENTRUM KARLSRUHE (GERMANY)

INSTITUT FÜR NEUTRONENPHYSIK UND REAKTORTECHNIK

Neutron Nuclear Data Evaluation

B. Hinkelmann, R. Meyer, J.J. Schmidt

The evaluation of recent discrepant absorption and fission cross section measurements for U235, U238 und Pu239 has been continued [1] and its results incorporated in various special group sets. The results of their feedback on reactor physics calculations concerning several fast facilities were reported at the International Conference on the Physics of Fast Reactor Operation and Design, London, June 1969 [2].

The revision of the neutron nuclear data for Pu239 in particular σ_f, $\bar{\nu}$, α on the KEDAK file has been started.

Microscopic and 5-group averaged values for σ_γ, σ_f, σ_{2n} and $\bar{\nu}$ have been determined in the entire energy range from thermal up to 10 MeV for the following actinides: Pa231, U232, U234, U236, U237, Np237, Np238, Pu236, Pu238, Am241, Cm242. The data have been requested for fast and thermal reactor burnup calculations within the framework of the Karlsruhe safeguard project. For the completion of the only sparse available experimental data information simple systematic methods have been used. The documentation will be finished in the beginning of 1970 [3].

In the framework of an extention of the upper energy limit of 10 MeV up to 15 MeV on the KEDAK file the neutron cross section measurements for reactions of Cr, Fe, Ni in this energy range have been evaluated. Because of the lack of enough experimental data information the (n,γ) cross sections have

been calculated in the MeV range by means of a computer program developed on the basis of the direct and collective nuclear model. A description of the data recently, i.e. after edition of KFK 750, incorporated in the KEDAK file will be published in 1970 [4].

Further efforts for the creation of an advanced international neutron data storage and retrieval system (CSISRS) were undertaken [5].

Table of Literature

1. J.J. Schmidt, "Aktueller Stand der physikalischen Kenntnis der wichtigsten Reaktorkerndaten", KFK 966 (EANDC(E)-117"U", EUR 4172d), 1969.

2. E. Kiefhaber, J.J. Schmidt et al., to be published as KFK 969 (EANDC(E)-118"U).

3. B. Hinkelmann, to be published as KFK-report.

4. B. Hinkelmann, R. Meyer, J.J. Schmidt et al., to be published as KFK-report.

5. J.J. Schmidt, "Basic Requirements of Advanced Neutron Data Storage and Retrieval Systems (CSISRS)", KFK 941 (EANDC(E)-114"U", EUR 4163e), 1969.

XI. KERNFORSCHUNGSZENTRUM KARLSRUHE (GERMANY)

INSTITUT FÜR ANGEWANDTE KERNPHYSIK

1. 3 MeV Van de Graaff

1.1 High-Resolution Transmission Work

K.-N. Müller, M.A. Kazerouni, F.H. Fröhner

Transmission measurements on Sc^{45} between 20 and 300 keV were completed. A newly developped automatic least-squares fit programme was used to extract s-wave resonance parameters by shape analysis of the data (see fig. 1). It was found that most resonance spins could be determined from a careful study of level-level interference effects. In this way the spins of 50 Sc^{45} resonances could be assigned. A similar treatment of Ti^{49} and Cr^{53} transmission data yielded resonance parameters including spins for 27 (30) resonances of Ti^{49} (Cr^{53}, resp.). With these resonance parameters the spin-dependent strength function values shown in table I could be determined.

1.2 Temperature-dependent Average Transmission

F.H. Fröhner, E. Schneider

The average transmission of moderately thick Au and W samples is measured between 5 and 50 keV at various temperatures. The results are compared to computer calculations in order to understand the relative importance of Doppler broadening of unresolved resonances, multilevel effects, and temperature expansion of the sample.

In this connection resonance scattering from bound atoms was studied theoretically. It is found that the conventional scattering-law formalism must be modified if narrow resonances are involved.

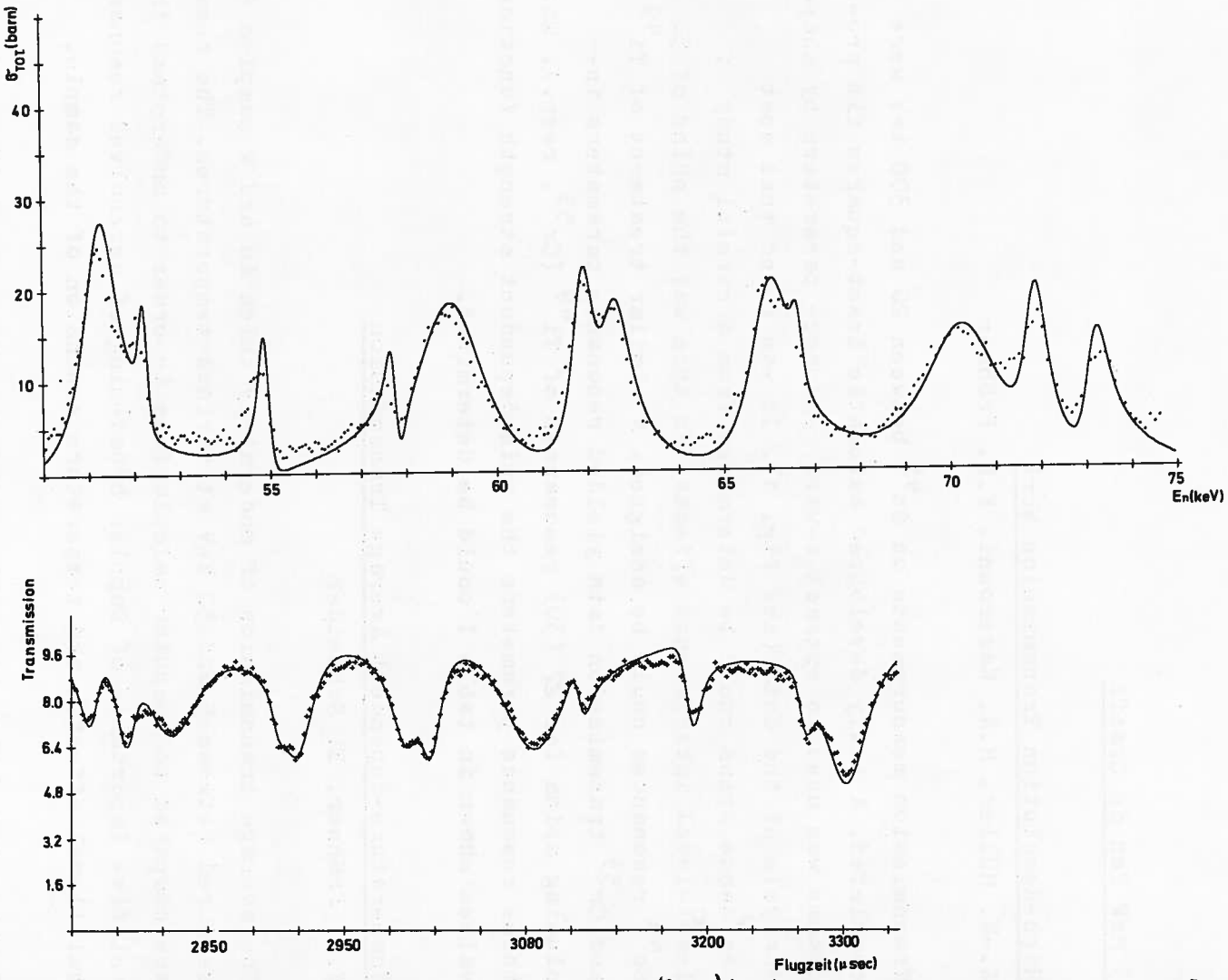

Fig.1 Sc^{45} neutron transmission data. Upper part: $\sigma_{tot} \equiv -(\ln T)/n$ (T = transmission, n = sample thickness in nuclei/b). Lower part: transmission versus flight time. Solid line: R matrix multi-level fit.

Table I

Compound System	Compound Spin	Strength Function
Sc^{45} + n	3	$7.6 \begin{smallmatrix} +1.5 \\ -1.2 \end{smallmatrix} \; 10^{-4}$
	4	$3.1 \begin{smallmatrix} +0.7 \\ -0.6 \end{smallmatrix} \; 10^{-4}$
Ti^{49} + n	3	$3.1 \begin{smallmatrix} +1.1 \\ -0.8 \end{smallmatrix} \; 10^{-4}$
	4	$3.3 \begin{smallmatrix} +1.0 \\ -0.8 \end{smallmatrix} \; 10^{-4}$
Cr^{53} + n	1	$5.7 \begin{smallmatrix} +2.8 \\ -1.5 \end{smallmatrix} \; 10^{-4}$
	2	$3.0 \begin{smallmatrix} +0.7 \\ -0.5 \end{smallmatrix} \; 10^{-4}$

1.3 High-resolution Capture Measurements

A. Ernst, F.H. Fröhner

Resonance capture of Fe^{56}, Fe^{57}, Ni^{58}, Ni^{60} and Ni^{61} was measured with enriched isotopes between 7 and 200 keV with a resolution of 1.5 ns/m (fig. 2). An 800 l scintillator tank served as detector. The capture cross section of gold was used as standard. Transmission data will be combined with the capture data to extract resonance parameters including spins and radiation widths. The necessary shape analysis programmes are being developped.

1.4 Average Capture Cross Sections /1/

D. Kompe, A. Ernst and F.H. Fröhner

The average capture cross sections of natural Ce and Tl were measured relative to gold between 10 and 200 keV. Maxwellian averages were calculated for kT values between 15 and 100 keV. These averages are needed for calculations of s-process nucleosynthesis. The cross sections of these near-magic elements were found to be extremely low (see figs. 3 and 4).

1.5 High-precision Measurements of Pu^{239} and U^{233} Fission Cross Sections Relative to U^{235} between 5 keV and 1 MeV

E. Pfletschinger and F. Käppeler

The final results of the measurements described in /2/ are shown in fig. 5 and 6 together with previously published data. The accuracy of the ratio values is 2 ... 3 %, see /3/. Similar measurements are planned on Pu^{241}.

/1/ Kompe et al., Nucl. Phys., to be published
/2/ E. Pfletschinger and F. Käppeler, EANDC Rept. 1968
/3/ E. Pfletschinger and F. Käppeler, Nucl. Phys. (1970)

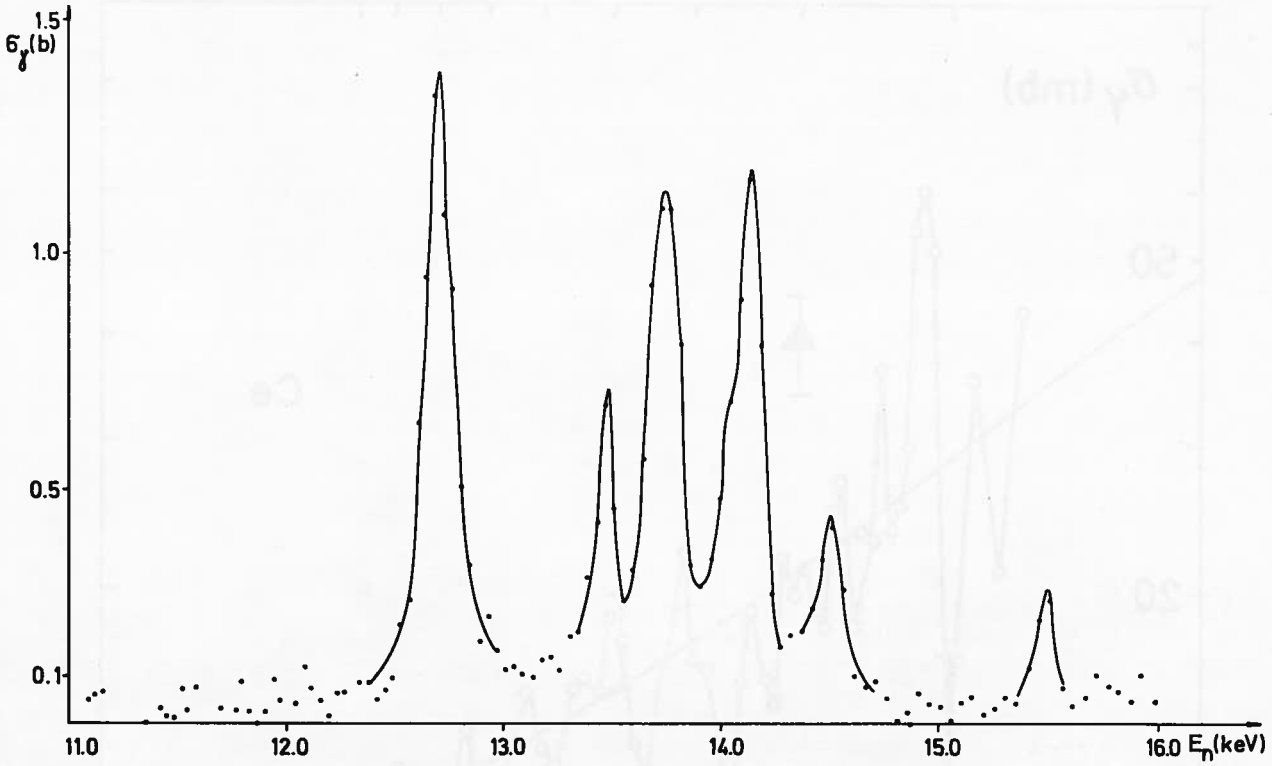

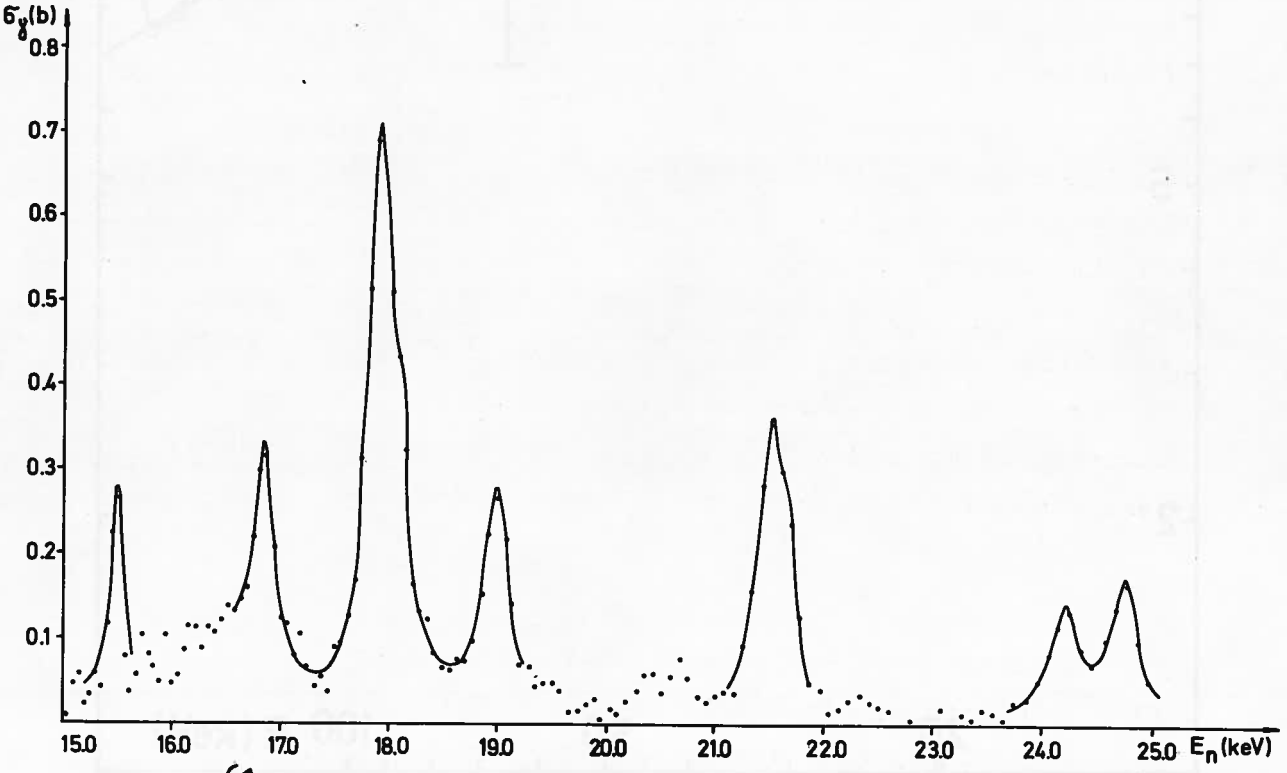

Fig.2 Ni^{61} neutron capture cross section, still uncorrected for resolution effects and multiple scattering. The solid lines are mere eye guides.

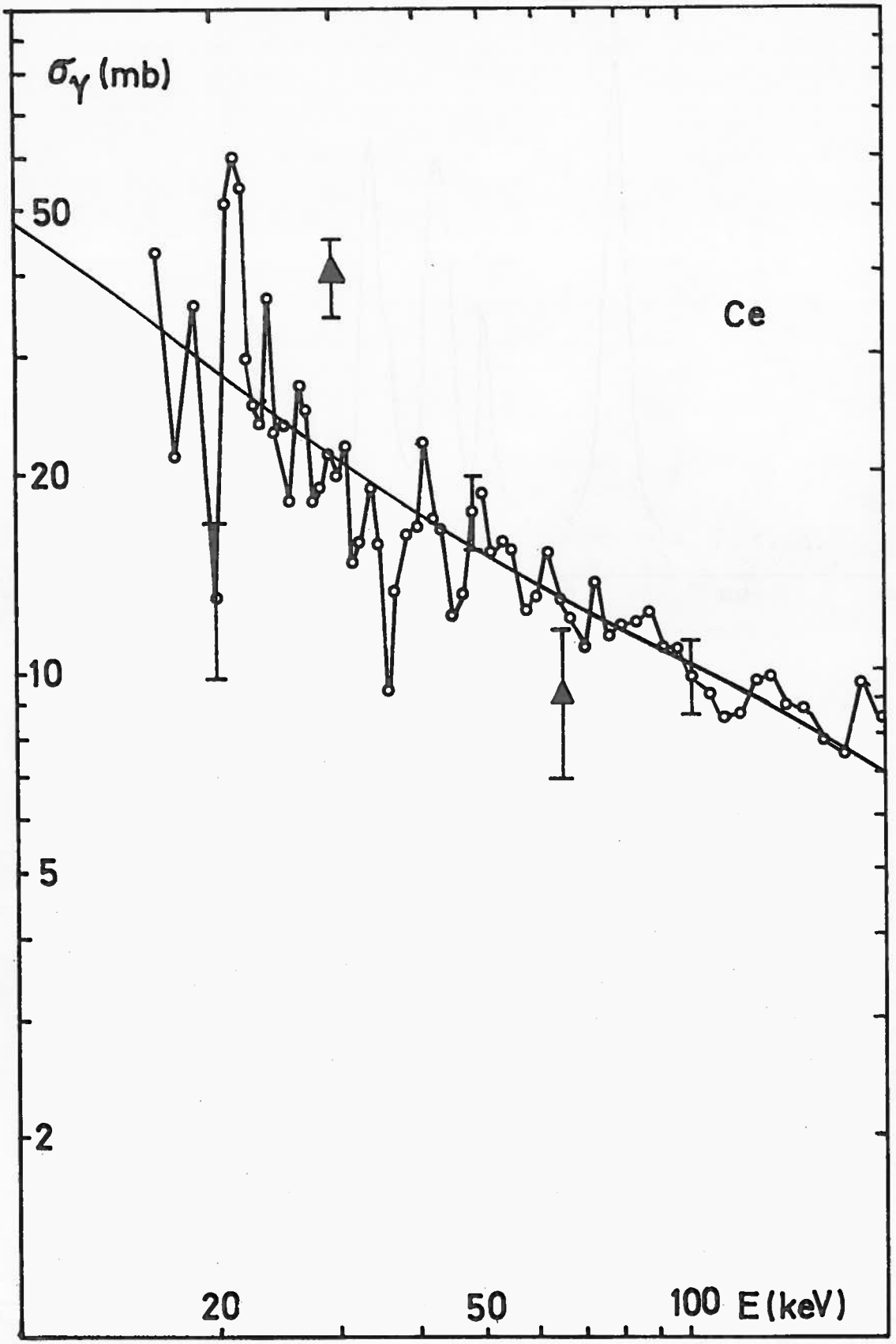

Fig.3 Ce neutron capture cross section. Open circles: present work. Smooth curve: level-statistical fit. Triangles: Data of Gibbons et al., Phys.Rev. 122 (1961) 182, renormalized to the gold standard cross section used in this work.

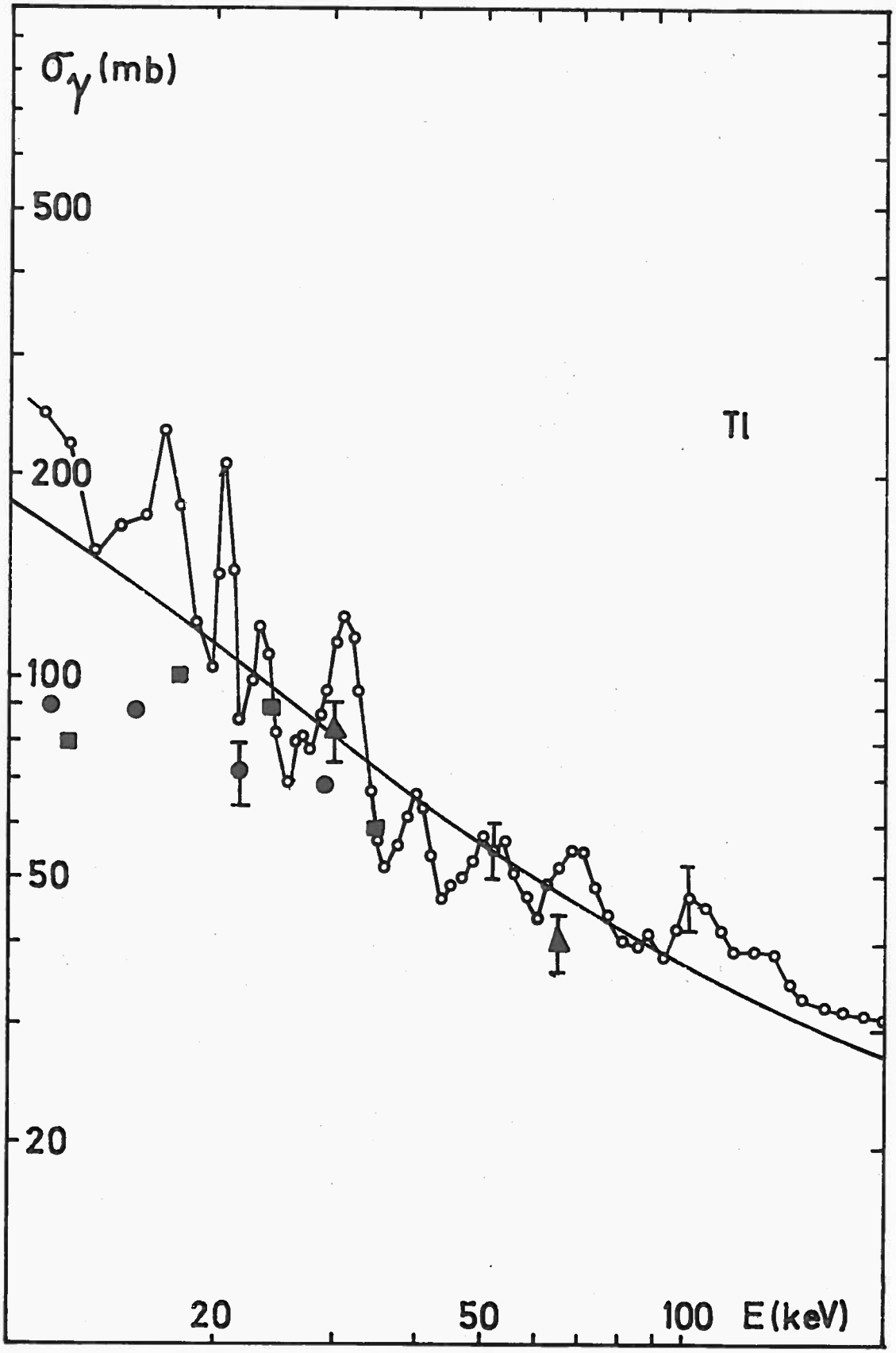

Fig.4 Tl neutron capture cross section. Open circles: present work. Smooth curve: level-statistical fit. Triangles: Gibbons et al., Phys.Rev. 122 (1961) 182. Solid circles and squares: Konks and Shapiro, ZhETF 47 (1964) 795, sov.Phys. JETP 20 (1965) 531. All data are referred to the same standard gold cross section.

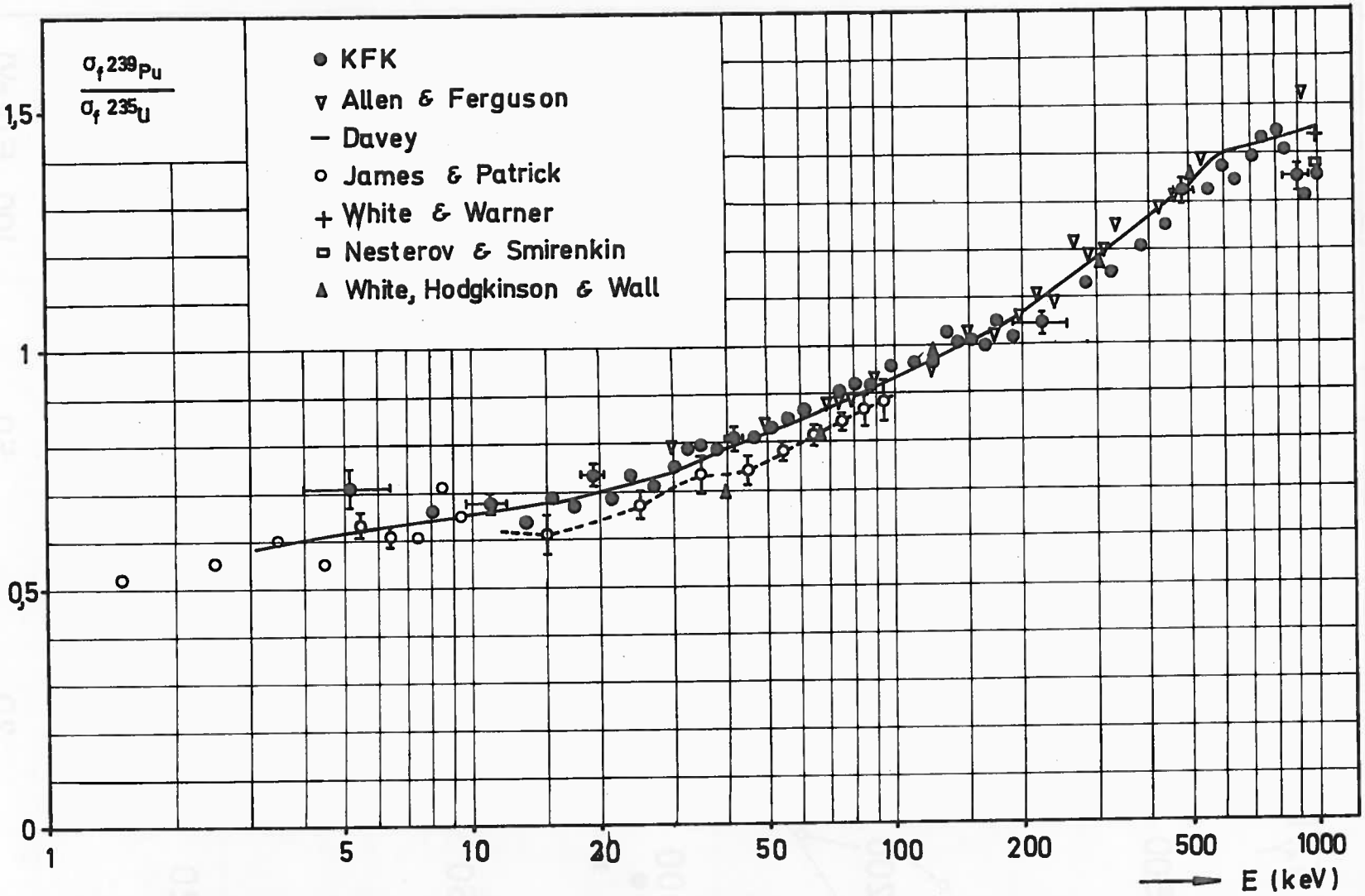

Fig.5 Pu^{239} : U^{235} fission cross section ratio.

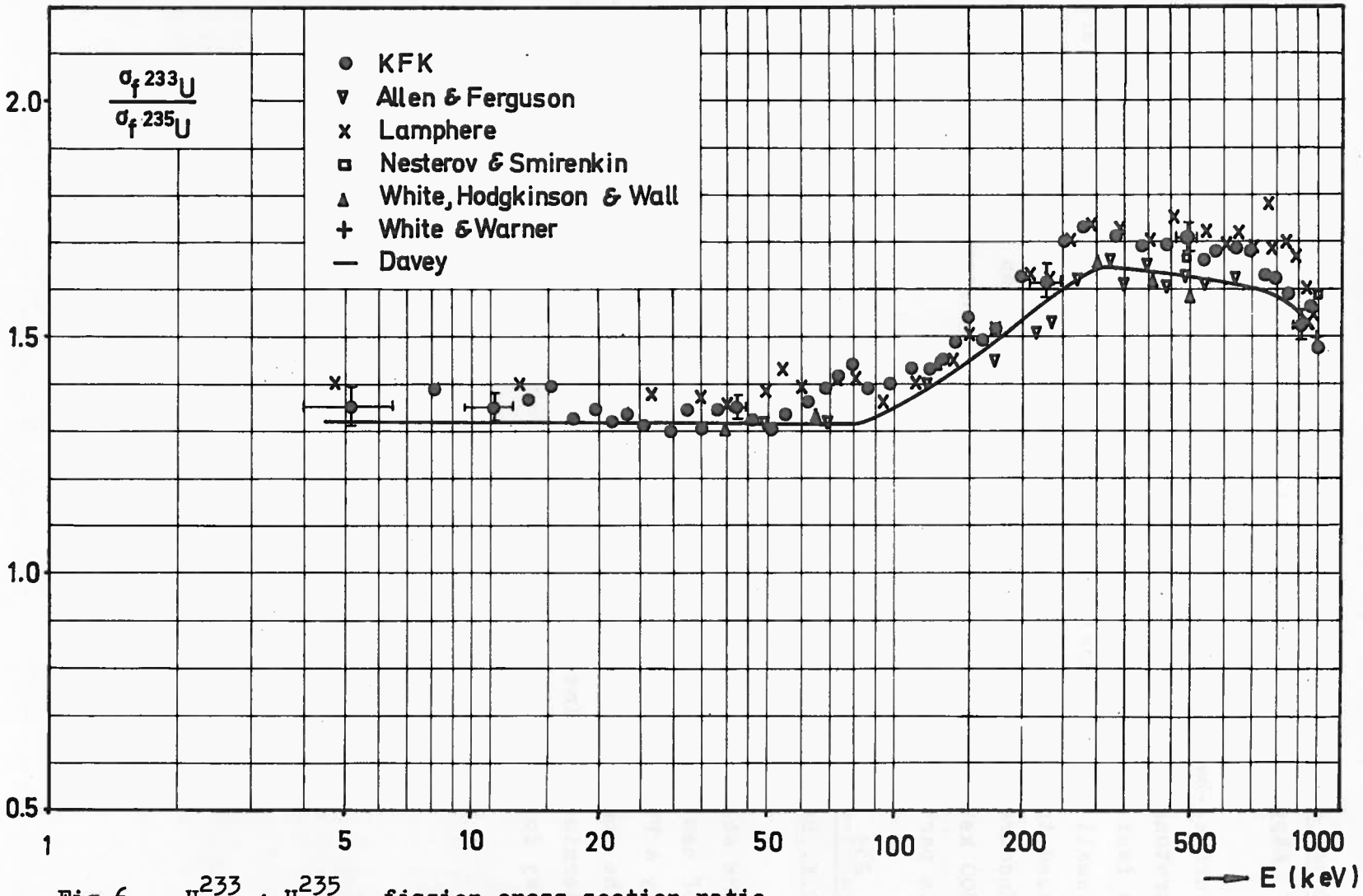

Fig.6 U^{233} : U^{235} fission cross section ratio.

1.6 Cross Section Measurements Relative to the (n,p)-Cross Section

F. Käppeler, F. Fröhner and E. Pfletschinger

Surface-barrier silicon detectors are used to count recoil protons from a thin layer of hydrogenous material. In this way a fast, compact detector system useful for fast-neutron work (small flight paths) can be built. Monte Carlo calculations are used to convert proton count rates to absolute neutron fluxes. Encouraging results were obtained for neutron energies as low as 300 keV. These detectors will be used to measure neutron fluxes in partial cross section experiments.

1.7 Pu^{239}-α-Measurement

R.E. Bandl, H. Mießner

The absorption of Pu^{239} can be measured by comparing the number of neutrons scattered by a Pu-sample with the number scattered by a Pb-sample of equal transmission. By simultaniously measuring the number of fission neutrons the value of η and α can be determined. A time-of-flight experiment along these lines is underway for energies between 10 and 70 keV.

2. Isochronous Cyclotron

S. Cierjacks, G. J. Kirouac, D. Kopsch, L. Kropp, J. Nebe

2.1 Development of the Time-of-Flight spectrometer

In 1969 the first measurements with the new flight path with a total length of 190 m had been performed. The newly developed 25 cm dia. neutron detector was used for these measurements and an overall time resolution of 2,5 ns was achieved. Using the new isotope collimator system a first measurement of the total cross section of the seperated isotope N^{15} had been performed with a 3 cm^2 sample area.

By the spring of 1969 new outer deflector plates with 100 Ω impedance and a reflectivity of less than 2 % had been put into operation. Repetition rates up to 200 kc were obtained. Further development of the 200 kc inner deflector bunching system is in progress. This work is closely connected with the use of an ion source pulser which will increase the lifetime of the inner deflector system. The cooling system for the outer deflector system is also beeing improved.
The purpose of these reconstructions is to increase the repetition rate from 20 kc to 200 kc thus obtaining an increase of the beam current from the present value $\sim$ 2,5 μA to $\sim$25 μA at the neutron producing target.

2.2 Total Cross Section Measurements

In the period covered by this report the total cross sections of H, Na, O, Ca and U and of the seperated isotope N^{15} were measured between $\sim$0.3 and 32 MeV. In the total n-p scattering cross

section measurement (fig. 1) which was performed with a statistical precision varying from 0.2 to 1 % it was intended to search for the recently reported oscillations. No evidence for such oscillations was found.
The measurement of the total cross section of sodium was carried out in the energy range between 300 and 900 keV with an energy resolution of 0.2 keV at 300 keV and 0.9 keV at 800 keV, respectively (fig. 2). The statistical uncertainty in the measurement was $\leq$0,3 % between 600 and 900 keV and $\leq$1 % from 420 keV to 600 keV. Below 420 keV the statistical accuracy was between 2 and 3 %. A total number of only 16 resonances was found which leads to the conclusion that the total level density is lower by about an order of magnitude than that reported in the literature. The measurements of the total cross sections of oxygen between 0.5 and 32 MeV and of calcium between 0.5and 4.496 MeV were performed with the long 190 m flight path. These measurements were performed with a resolution of 0.02 ns/m. In several energy regions these new data exhibit more structure than was observed in earlier studies.
Also the total cross section measurements on natural U were performed with the enlarged flight path to search for individual resonances in the cross section. This cross section was measured with a statistical accuracy of $<$1 % and a time resolution of $\sim$ 4 ns. No structure with large amplitude was found in this cross section.

For the first time a high resolution total cross section measurement of the seperated isotope N^{15} was performed at the KIC time-of-flight spectrometer in the energy range 0.9 - 30 MeV.

/1/ S. Cierjacks, P. Forti, G. J. Kirouac, D. Kopsch, L.Kropp, J. Nebe
KFK-Report 1027, July 1969

/2/ S. Cierjacks, P. Forti, G. J. Kirouac, D. Kopsch, L. Kropp, J. Nebe
Phys. Rev. Letters 23 (1969), 866

/3/ S. Cierjacks, P. Forti, D. Kopsch, L. Kropp, J. Nebe
KFK-Report 1060, June 1969

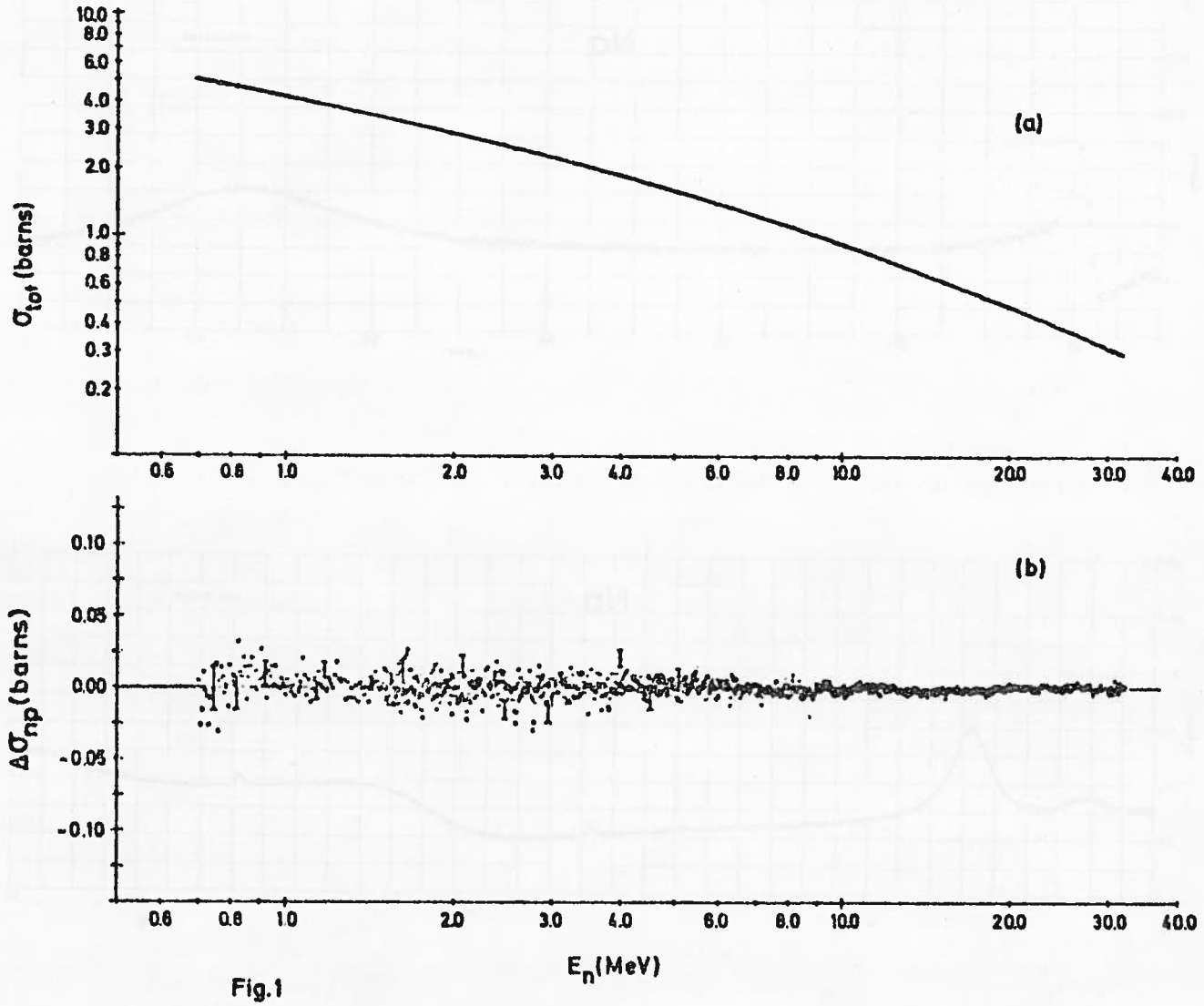
(a)
σ_{tot} (barns)
10.0
8.0
6.0
4.0
3.0
2.0
1.0
0.8
0.6
0.4
0.3
0.2
0.6
0.8
1.0
2.0
3.0
4.0
6.0
8.0
10.0
20.0
30.0
40.0
(b)
$\Delta\sigma_{np}$ (barns)
0.10
0.05
0.00
-0.05
-0.10
E_n(MeV)

Fig.1

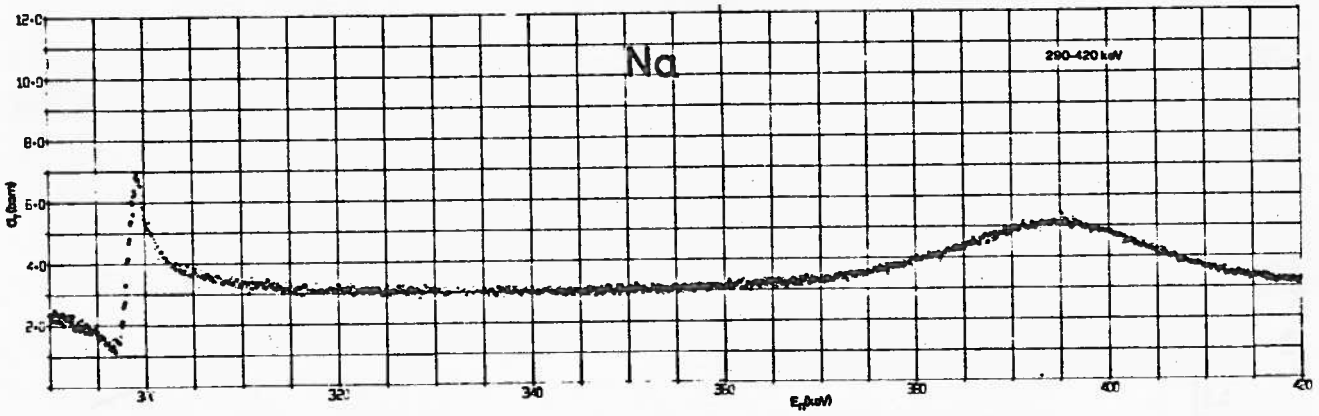
Na
290-420 keV
12·0
10·0
8·0
6·0
4·0
2·0
σ_t (barn)
320
340
360
380
400
420
E_n (keV)

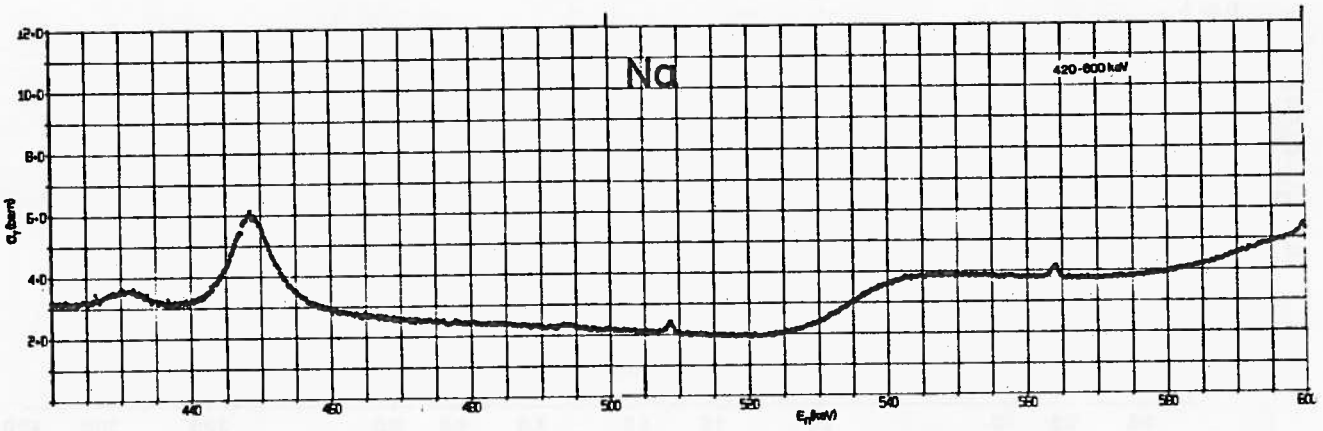
Na
420-600 keV
12·0
10·0
8·0
6·0
4·0
2·0
σ_t (barn)
440
460
480
500
520
540
560
580
600
E_n (keV)

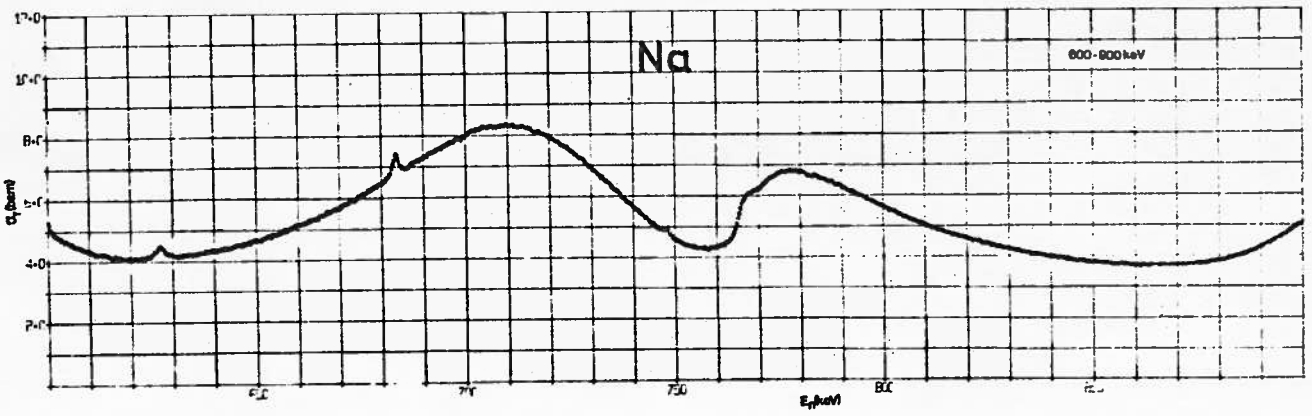
Na
600-900 keV
4·0
σ_t (barn)
750
800
E_n (keV)

Fig. 2

/4/ S. Cierjacks, P. Forti, D. Kopsch, L. Kropp, J. Nebe
Phys. Lett. Vol 29 B, No. 7, June 1969

/5/ S. Cierjacks, G. J. Kirouac, D. Kopsch, L. Kropp, J. Nebe
KFK-Report 1000
EANDC (E) - "U"- 111
EUR 3963 e
III. Supplement, to be published

2.3 Partial Cross Section Measurements

The evaluation of the neutron induced reactions on Be^9 in the energy range 10 to 30 MeV with the KIC had been continued. The charged particle seperation between α-particles and He^6 could be achieved completely, while protons, deuterons and tritons were resolved by about 97 %. In the analysis performed up to now only α-particles and He^6 nuclei have been investigated. The determination of the energy and angular distributions of the α's for different angles between 20° and 160° (in 20° steps) for the ground state, the first and the second excited level of He^6 had been completed. An analysis of the angular distributions using a plane wave approximation gave riseto the assumption that the backward part of these distributions is due to a heavy particle mechanism , while the position of the maxima at forward angles can be explained by knock-on or pick-up processes. For the ground state and the first and second excited state of He^6, the excitation functions have been evaluated.
For the first time, few-angle high resolution neutron resonance scattering measurements have been performed in the energy range 0.54 to 5.9 MeV on C^{12} and Ca^{40}. The energy resolution obtained was 0.6 keV at 0.6 MeV and 16 keV at 5.0 MeV respectively. The purpose of these measurements is to assign the angular momenta for observed neutron resonances. The method of assignment utilizes the Wigner formalism and the Blatt-Biedenhorn expressions for the differential cross section. The resonance shapes are very sensitive to the l value of the resonant state but the method has heretofore not been extensively used due to the lack of sufficiently intense neutron sources with high energy resolution. Interference effects between resonances with same or different spin and parity has not been neglected in the analysis. The evaluation of data is underway.

/1/ L. Kropp, Physikertagung Freudenstadt, März 1969
/2/ G. J. Kirouac, J. Nebe, KFK-Report 1069

2.4 Subthreshold fission cross section measurements

Further investigations in this field were deferred because an increase of neutron intensity was insight. Fission cross section measurements on U^{238}, U^{234} and U^{236} will be performed with an improved set-up of 8 gas scintillation detectors and an overall resolution of 0.04 ns/m. The behaviour of the fission cross section below $\sim$ 1 MeV is of special interest in connection with the microscopic theory of fission processes.

25 Resonance Spectroscopy and Fluctuation Analysis

Microscopic resonance analysis of ^{40}Ca for s-, p- and d-waves has been continued. The analysis uses a least squares method in connection with the multilevel R-matrix formalism for the data in the energy range 0.5 - 1 MeV. Because of some ambignities in the results, the few-angle high resolution neutron resonance scattering measurement on calcium was performed. First results will be presented in the spring 1970.

From the new high resolution total cross section data for N^{15} in the energy range 0.9 - 10 MeV, resonance energies, total widths, spins and parities have been determined up to 4.5 MeV neutron energy by multilevel cross section fitting. These assignments are discussed with respect to previous analysis and single particle levels of N^{16}; the results will be presented in the spring of 1970.

To investigate the broad structure in the cross sections as well as the fine structure in the energy region of overlapping levels, a fluctuation analysis of the total neutron cross sections of 13 elements from F to Co is in progress. The analysis of the measured fluctuations has been executed using an autocorrelation function. First results show that in most cases these fluctuations could be accounted for as statistical fluctuations in the widths

and the spacings of compound nucleus levels or at higher energies as fluctuations of the Ericson type. Values of average level widths between 2.5 and 50 keV which were in good agreement with values reported by other authors could be deduced for the various elements. For some nuclei, for instance F, Na, Al, S, Ca, V, Cr and Ni in certain energy regions, a superposition of the fluctuations mentioned above yielded a broader structure. For this broader structure widths between 50 and some hunded keV were obtained.

/1/ J. Nebe, G. J. Kirouac,
KFK Report 1069

/2/ D. Kopsch, S. Cierjacks, J. Nebe
Physikertagung Freudenstadt, März 1969

3. Neutron Capture Gamma-Ray Spectroscopy

U. Fanger, D. Heck, W. Michaelis, H. Ottmar, H. Schmidt,
C. Weitkamp, F. Weller

The system of gamma-ray spectrometers installed at the Karlsruhe research reactor FR 2 has been considerably improved. A resolution of 1.62 keV FWHM for the ^{137}Cs 662 keV γ-ray and a peak-to-Compton ratio of 150 : 1 has been achieved for the anti-Compton spectrometer [1]. The Ge(Li) five-detector pair spectrometer arrived at an energy resolution of 4.5 keV FWHM at 6 MeV [2]. The multiple coincidence apparatus [3] was modified for measuring both Ge(Li)-Ge(Li) and Ge(Li)-NaI(Tl) coincidences. By introducing disk memories for the multiple input on-line computer the storage capabilities for both the coincidence and the angular correlation experiments [4] have been largely extended. The memory capacity for these experiments is now 72 K and 68 K channels at 21 bits, respectively. A new spectrometer has been constructed and installed which allows to extend the (n,γ) method to fissionable target nuclei [5]. The prompt γ radiation from fission is suppressed by detecting the fast fission neutrons in anti-coincidence and 4π geometry. First promising measurements have been performed on ^{235}U. The results are of particular interest in view of the application of the (n,γ) reaction to instrumented non-destructive nuclear safeguards techniques [6, 7, 8]. For the near future, a spectrometer is designed utilizing the internal pair formation for the determination of transition multipolarities in neutron capture spectroscopy [9]. It consists of a silicon detector telescope, two NaI(Tl) scintillation detectors and a superconducting magnet.

A new investigation of the very complex capture γ-ray spectra of the isotopes ^{152}Eu and ^{154}Eu with the anti-Compton device proved to be successful [10]. About 300 γ-ray lines in the energy range

from 130 keV to 880 keV were resolved in the spectra of either isotope, corresponding to a mean line spacing of 2.5 keV. Furthermore, measurements of the gamma radiation induced by thermal neutrons completed the studies on the nuclei ^{68}Zn, ^{96}Mo, ^{98}Mo, ^{168}Er, ^{169}Yb and ^{190}Os, taking advantage of the improved spectrometers. The results on natural and enriched zinc made possible to determine relative isotopic capture cross sections [11].

The combined effort of these spectrometers yields very detailed and complete information on the structure of nuclei up to high excitation energies. Level spins and multipole character of γ-ray transitions as determined by the γ-γ angular correlations [12] allow interesting comparisons with shell model calculations. The agreement may be regarded as satisfactory for ^{58}Fe [13] and ^{62}Ni [14], fairly well for ^{96}Mo and bad for ^{98}Mo [15]. The validity of the collective vibration picture for even spherical nuclei seems to be restricted to the very first levels. A particular role is played by the first 0^+ state, as demonstrated for ^{68}Zn [11] in comparison with even nuclei around A = 68. - As to the strongly deformed nuclei studied in Karlsruhe, detailed analysis of the ^{167}Er data suggests considerable mixing between Nilsson states and the quadrupole vibrations Q_{22}, Q_{2-2} and Q_{20} [16]. Own theoretical calculations have been performed yielding surprisingly good agreement with the experimental results. In ^{168}Er [17] a large number of new levels has been assigned to specific two-quasiparticle configurations and their superimposed rotational bands.

[1] W. Michaelis and F. Horsch, Proc.Int.Symp. on Neutron Capture Gamma-Ray Spectroscopy, Studsvik, August 1969

[2] D. Heck, U. Fanger, W. Michaelis, H. Ottmar and H. Schmidt, Nucl. Phys. (to be published)

[3] U. Fanger, KFK 887 (1969)

[4] H. Schmidt and D. Heck, Proc.Int.Symp. on Neutron Capture Gamma-Ray Spectroscopy, Studsvik, August 1969

[5] W. Michaelis, H. Leuschner and P. Matussek, Proc.Int.Symp. on Neutron Capture Gamma-Ray Spectroscopy, Studsvik, August 1969

[6] W. Michaelis, F. Horsch, H. Leuschner and C. Weitkamp, Paper presented at the Winter Meeting of the American Nuclear Society, Washington, D.C., November 11 - 15, 1968

[7] W. Michaelis, Atomkernenergie 14 (1969) 347

[8] W. Michaelis, F. Horsch, H. Leuschner and C. Weitkamp, USAEC Publication (in press)

[9] W. Michaelis, D. Lange and G. Wilhelmi, Proc.Int.Symp. on Neutron Capture Gamma-Ray Spectroscopy, Studsvik, August 1969

[10] W. Michaelis, Nucl. Phys. (in press)

[11] H. Ottmar, N.M. Ahmed, U. Fanger, D. Heck, W. Michaelis and H. Schmidt, Proc.Int.Symp. on Neutron Capture Gamma-Ray Spectroscopy, Studsvik, August 1969; Nucl. Phys. (to be published)

[12] H. Schmidt, W. Michaelis and U. Fanger, Nucl. Phys. A136 (1969) 122

[13] U. Fanger, W. Michaelis, H. Schmidt and H. Ottmar, Nucl. Phys. A128 (1969) 641 - 667

[14] U. Fanger, D. Heck, W. Michaelis, H. Ottmar, H. Schmidt and R. Gaeta, Proc.Int.Symp. on Neutron Capture Gamma-Ray Spectroscopy, Studsvik, August 1969; Int.Conf. on Properties of Nuclear States, Montreal, August 1969; Nucl. Phys. (in press)

[15] D. Heck, W. Michaelis and H. Ottmar, Proc.Int.Symp. on Neutron Capture Gamma-Ray Spectroscopy, Studsvik, August 1969; Int.Conf. on Properties of Nuclear States, Montreal, Aug.1969; Nucl. Phys. (to be published)

[16] W. Michaelis, F. Weller, U. Fanger, R. Gaeta, G. Markus, H. Ottmar and H. Schmidt, Proc.Int.Symp. on Neutron Capture Gamma-Ray Spectroscopy, Studsvik, August 1969; Int.Conf. on Properties of Nuclear States, Montreal, August 1969; Nucl. Phys. (in press)

[17] W. Michaelis, H. Ottmar and F. Weller, Nucl. Phys. (in press)

XII. GRUPPO DI RICERCA INFN-ISTITUTO DI FISICA DELL'UNIVERSITA', PADOVA (ITALY)

1. Analysis of the Proton-^{12}C Low-Energy Interaction in Terms of Collective Doorway States

(A. Pascolini, G. Pisent, F. Zardi - Lettere al Nuovo Cimento 1 (1969) 643)

The phase shifts relative to the p-^{12}C elastic scattering between 0 and ~7 MeV are analyzed in terms of the coupled channel phenomenological model [1], [2] by considering the virtual and real excitation of the 2^+ target level (4.43 MeV).

The best fit with experiments has been obtained in correspondence with the following potential parameters (the radial dependence of the potential is of the usual Woods-Saxon form):

Central potential strength: V_o = (55.73-0.133E)MeV, E being the laboratory energy in MeV.

Spin orbit strength: V_{is} = 7 MeV.

Mean radius: $R = r_o A^{1/3}$, r_o = 1.2 fm.

Diffuseness: a = 0.73 fm.

Coupling constant: $\beta = -0.4$

The results are summarized in figures 1, 2, 3 and in table I. It is seen that the general trend of the phase shifts and four resonances are well reproduced by the model.

The fifth experimental resonance ($J^\pi = 5/2^+$; E = 4.80 MeV) is wrongly accounted for. This point is widely discussed in the paper.

It is worthwhile noting that the value of the deformation parameter obtained ($\beta = -0.4$) is of the correct magnitude, as expected from Coulomb excitation experiments and mean life measurements. This is an important point, because earlier calculations led to exceedingly small deformations [3].

With the same potential parameters the n-^{12}C process has been tentatively analyzed between 0 and ~4 MeV. The results are shown in the paper.

The agreement between theory and experiment is satisfactory if one considers that no improvements have been introduced with respect to the p-^{12}C parameters.

2. <u>(^{3}He,α) Reactions on Silicon Isotopes</u>(*)

(F. Pellegrini, I. Filosofo, F. Gentilin, I. Scotoni)

Angular distributions for ^{29}Si(^{3}He,α)^{28}Si and ^{30}Si(^{3}He,α)^{29}Si reactions induced by 10 MeV ^{3}He particles have been measured. We have found experimental evidence that the Silicon isotopes contain large core excited components in their ground states. Neutron occupation numbers for $d_{5/2}$, $d_{3/2}$, $s_{1/2}$ and $f_{7/2}$ orbits are obtained for the ground state of the Silicon isotopes and compared with the shell model prediction.

3. <u>The ^{31}P(^{3}He,α)^{30}P Reaction</u>(*)

(F. Pellegrini, I. Filosofo, F. Gentilin)

Angular distributions for the ^{31}P(^{3}He,α)^{30}P reaction induced by 10 MeV ^{3}He particles have been measured. We have found experimental evidence that the 3^+(T=0) states at 2.54 and 1.98 MeV excitation energy and the 2^+(T=0) 1.46 MeV states, arise from the excitation of the ^{28}Si core. The other states up to an excitation energy of 3 MeV are well described by the $2s_{1/2}$-$1d_{3/2}$ configuration.

4. <u>(^{3}He,α) Reactions on Even Calcium Isotopes</u>(*)

(F. Pellegrini, R.A. Ricci)

The ^{44}Ca(^{3}He,α)^{43}Ca and ^{48}Ca(^{3}He,α)^{47}Ca reactions have been investigated in order to confirm the presence of core excitation

---

(*) Work performed as a part of the NU2 programme of the Istituto Nazionale di Fisica Nucleare.

components in the ground state of the even Calcium isotopes. The angular distribution of the outgoing α particles and absolute cross sections for different l-transitions have been measured.

5. <u>The Mean-Lives of the First Two Excited States in ^{34}S</u>

(F. Brandolini, C. Signorini - Submitted to "Il Nuovo Cimento")

The mean-lives of the excited states in ^{34}S at 2.13 and 3.30 MeV have been found to be 460±95 and 190±40 fs, respectively from D.S.A.M. on the $^{31}P(\alpha,p\gamma)^{34}S$ reaction. The usual method of attenuation coefficient and a new method, that does not need to take into account nuclear scattering, have both been applied in order to deduce mean-lives from experimental data. Experimental results are compared with the predictions of the M.S.D.I. calculations; an effective charge $e_{eff} \simeq 0.5$ is necessary to reproduce experimental results.

6. <u>Spins and Mean-Lives of ^{34}Cl Levels</u>(*)

(F. Brandolini, I. Filosofo, C. Signorini, M. Morando(**) - Submitted to Nuclear Physics)

The spins of the 0.46 , 0.66 , 1.23 and 1.89 MeV states in ^{34}Cl have been established as J = 1,1,2 and 2, respectively, from angular correlation measurements in the $^{32}S(\tau,p\gamma)^{34}Cl$ reaction. The branching ratios of these states were also obtained, in addition to the mixing ratios of some transitions.

(*) Work partly performed under the NU2 research programme of the Istituto Nazionale di Fisica Nucleare.

(**) Present address: Max-Planck Institut für Kernphysik, Heidelberg (Germany).

The mean lives of the ^{34}Cl levels at 0.46 , 0.66 and 1.23 MeV, $\tau_m = 9\pm4$, 14^{+11}_{-6} and >14 ps, respectively, were found from DSA measurements in the reaction $^{31}P(\alpha,n\gamma)^{34}Cl$.
The $1^+ \rightarrow 0^+$, $\Delta T = 1$, M1 transitions are quite slow as compared with similar transitions in other self-conjugated nuclei, which can be understood from shell model arguments.

7. <u>Determination of the Mean Lives of Some Excited States of ^{33}S through Doppler-Shift Attenuation Measurements</u>(*)
(F. Brandolini, J. Benuzzi-Martins(**), R.A. Ricci, C. Signorini - Lettere al Nuovo Cimento)

With the Doppler-shift attenuation method the mean lives of the ^{33}S excited states at 0.84 MeV, 1.97 MeV, 2.31 MeV, 2.87 MeV, 2.97 MeV excitation energies have been determined to be (1730±300)fs, (125±37)fs, (178±53)fs, (33±13)fs, (90±31)fs, respectively; the ^{33}S recoiling nuclei have been slowed down in solid stoppers. The excited levels of ^{33}S have been populated with the reaction $^{30}Si(\alpha,n)^{33}S$ at energies between 5.5 and 7.8 MeV; each single level has been studied at an energy of few hundred keV higher than its threshold for (α,n) reaction. For all levels the measurements have been performed with recoil in SiO_2; in the case of the 0.84 MeV level a measurement has been done slowing down excited nuclei in metallic calcium; this material has a very small stopping power and therefore it is well suited for determining mean lives of some ps. In this case a good agreement has been obtained with SiO_2 results. The enhancement of E2 transitions in this nucleus may suggest collective effects. Anyhow these effects can also be taken into account

(*) Work performed as a part of the NU2 programme of the Istituto Nazionale di Fisica Nucleare.

(**) On leave of absence from Centro Brazileiro de Pesquisas Fisicas (Rio de Janeiro).

in the frame of shell-model calculations [4], with the residual interaction acting in the whole s-d shell, if one introduces an effective charge for each single subshell. Such calculations are quite reliable because many spectroscopic characteristics are reproduced with very few parameters.

8. The Lifetime of the First $7/2^-$ State in ^{33}S

(F. Brandolini, C. Signorini - Physics Letters, 30B (1969) 342)

The levels in ^{33}S at 2937 keV and 2970 keV excitation energy are an interesting doublet. The first has spin $7/2^-$, probably a rather pure $1f_{7/2}$ configuration, and only a lower limit of its mean life has been established (τ>10 ps) from DSA measurements with solid stoppers [5] while in the second only the mean life is known [5] (τ=(90±31)fs) and the spin has not yet been measured; for this level the model foresees [6] $J=7/2^+$. The mean life of the 2934 keV level has been determined from DSA measurements slowing down ^{33}S ion gas. Krypton has been used at 3.0 , 5.0 , 7.0 and 9.0 atm pressure; measurements have been done with a gas cell with a 1.8 mg cm^{-2} Ni window which could stand up to 10 atm pressure. The resulting mean life of (38±10) ps is in qualitative agreement with theoretical [7] values obtained assuming the $7/2^-$ state wave function built up from the coupling of a neutron in a pure $1f_{7/2}$ state to a ^{33}S core described by published wave functions [6].

9. Polarization of neutrons from the D'd,n) Reaction [8,9]

(L. Drigo, C. Manduchi, G. Moschini, M.T. Russo-Manduchi, G. Tornielli, G. Zannoni)(*)

An investigation of the polarization of neutrons produced by the D(d,n) reaction has been performed, at reaction angles of

---

(*) Laboratori Nazionali dell'Istituto Nazionale di Fisica Nucleare, Legnaro - Istituto di Fisica dell'Università, Padova.

35° and 55°, for deuteron energies 1.1 to 3.1 MeV. The polarization measurements [8] allowed a determination in this energy range of the coefficients a_n in the series expansion of the differential polarization

$$P(E,\theta)\,\sigma(E,\theta) = \sum_n a_n(E)\ \mathrm{sen}2n\theta$$

where $P(E,\theta)$ and $\sigma(E,\theta)$ are the polarization of neutrons and the differential cross section of the D(d,n) reaction at deuteron energy E and reaction angle θ (centre of mass), respectively.

The polarization of neutrons has been determined by measuring the left-right asymmetry by means of a helium polarimeter.

The results are summarized in Table II.

10. Polarization of Neutrons Elastically Scattered from Carbon

(L. Drigo, C. Manduchi, G. Moschini, M.T. Russo-Manduchi, G. Tornielli, G. Zannoni)(*)

A systematic measurement of the polarization of neutrons elastically scattered from ^{12}C was carried out in the energy range between 1.2 and 5.2 MeV at angles 25°, 45°, 65°, 90°, 115°, 135°, 155°, making use of a suitable polarimeter [10] and using the reactions $^{7}Li(p,n)$ and D(d,n) as sources of polarized neutrons.

The analysis of data is in progress.

11. Elastic and Inelastic Scattering of Fast Neutrons from ^{12}C in the Energy Range 2.2÷8.5 MeV [11-14]

(U. Fasoli, D. Toniolo, G. Zago)

The analysis of the results of the measurement of the angular

---

(*) Laboratori Nazionali dell'Istituto Nazionale di Fisica Nucleare, Legnaro - Istituto di Fisica dell'Università, Padova).

distributions of the neutrons elastically and inelastically scattered by ^{12}C in the energy range 2.2÷8.5 MeV, has been carried on (EANDC(E)115"U").
Preliminary values of the Legendre polynomial coefficients of the elastic scattering in the energy interval 2.2÷4.7 MeV are given in Fig. 4. The calculations of the corresponding phase shifts are in progress.
The works of Refs. [11-14], quoted in previous annual reports, have recently been published or have been submitted for publication.

12. Gamma Rays Produced in (n; n'γ) Reactions

(F. Demanins, G. Nardelli)(*)

Cross sections for the productions of gamma rays by inelastic neutron scattering from Na, Cr, Fe, Ni and Cu have been measured for incident neutron energies 1 MeV to 4 MeV.
Relative angular distributions for 30 gamma rays produced by the (n; n'γ) reaction in Na^{23}, Cr^{50}, Cr^{52}, Cr^{53}, Cr^{54}, Fe^{56}, Ni^{58}, Ni^{60}, Cu^{63} and Cu^{65} were measured over the same energy range and compared with the theoretical predictions of the Satchler formalism using the neutron penetrabilities of Perey-Buck and Bjorklund-Fernbach. The calculated relative angular distributions are in agreement with the experimental values.
For incident neutron energies 1 MeV to 2,5 MeV the calculated cross sections are larger than the experimental values.
In most cases the calculated cross sections based on the Moldauer theory are in better agreement with the experimental ones than those of the Hauser-Feshbach calculations.

(*) Work performed under the CNEN - University of Padua Contract.

References

[1] T. Tamura - Rev. Mod. Phys. 37 (1965) 679.

[2] G. Pisent and A.M. Saruis - Nucl. Phys. 91 (1967) 561.

[3] J.T. Reynolds, C.J. Slavik, C.R. Lubitz and N.C. Francis - Phys. Rev. 176 (1968) 1213.

[4] P. Glaudemans - private communication.

[5] F. Brandolini, J. Benuzzi-Martins, R.A. Ricci and C. Signorini - Determination of the Mean Lives of Some Excited States of ^{33}S through Doppler-Shift Attenuation Measurement.

[6] P. Glaudemans, G. Wiechers and P. Brussaard - Nucl. Phys. 56 (1964) 548.

[7] G. Harris and S. Maripuu - private communication.

[8] L. Drigo, C. Manduchi, G. Moschini, M.T. Russo-Manduchi, G. Tornielli and G. Zannoni - Lettere al Nuovo Cimento 1 (1969) 237.

[9] C. Manduchi, G. Moschini, G. Tornielli and G. Zannoni - Nucl. Instr. and Meth. 67 (1969) 267.

[10] L. Drigo, C. Manduchi, G. Moschini, M.T. Russo-Manduchi, G. Tornielli and G. Zannoni - BE/INFN, to be published.

[11] U. Fasoli, D. Toniolo, G. Zago and V. Benzi - Elastic and Inelastic Scattering of Neutrons by ^{23}Na at 1.51, 2.47, 4.04 and 6.40 MeV - Nucl. Phys. A125 (1969) 227.

[12] U. Fasoli, P. Sambo, D. Toniolo, G. Zago and L. Zuffi - Interaction of Fast Neutrons with ^{165}Ho - Nucl. Phys. A133 (1969) 572.

[13] U. Fasoli, I. Scotoni, D. Toniolo and G. Zago - Asymmetries from Double Scattering of Fast Neutrons by ^{12}C - Rendiconti della Accademia Nazionale dei Lincei, Serie VIII, Vol. XLVI, pag. 725 (1969).

[14] U. Fasoli, D. Toniolo, G. Zago and L. Zuffi - Total Neutron Cross Section of Th^{232} in the Energy Interval 1.5÷8.5 MeV - CNEN Report, in press.

TABLE I

Resonance Parameters in the p-^{12}C Scattering Process

Dominant configuration (j,I;J)(*)	Resonance energy in the laboratory frame (MeV)		Γ(keV)	
	Experimental	Calculated	Experimental	Calculated
$1/2^+, 0^+, 1/2^+$	0.46	0.54	32	87
$5/2^+, 0^+, 5/2^+$	1.70	1.76	61	76
$3/2^+, 0^+, 3/2^+$	6.70	6.70	1720	2300
$1/2^+, 2^+, 5/2^+$	4.80	5.34	12	40
$1/2^+, 2^+, 3/2^+$	5.30	5.41	50÷100	100

(*) The single-particle spin j is coupled with the target spin I, to give the channel spin J .

TABLE II

Polarization P_1 and a_1, a_2 Coefficients

E_d (MeV)	θ_n	θ	P_1 %	(θ) (mb/sr)	a_1	a_2
1.09	35°	42.20°	−12.6 ± 1.8	9.7	−1.18 ± 0.15	−0.23 ± 0.14
	55°	65.30°	−12.0 ± 1.7	5.5		
2.12	35°	44.44°	−11.3 ± 1.0	7.8	−0.87 ± 0.07	−0.10 ± 0.09
	55°	68.55°	− 9.4 ± 1.4	5.2		
3.14	35°	45.88°	− 9.1 ± 1.1	5.7	−0.52 ± 0.07	+0.09 ± 0.09
	55°	70.63°	− 8.1 ± 1.5	5.1		

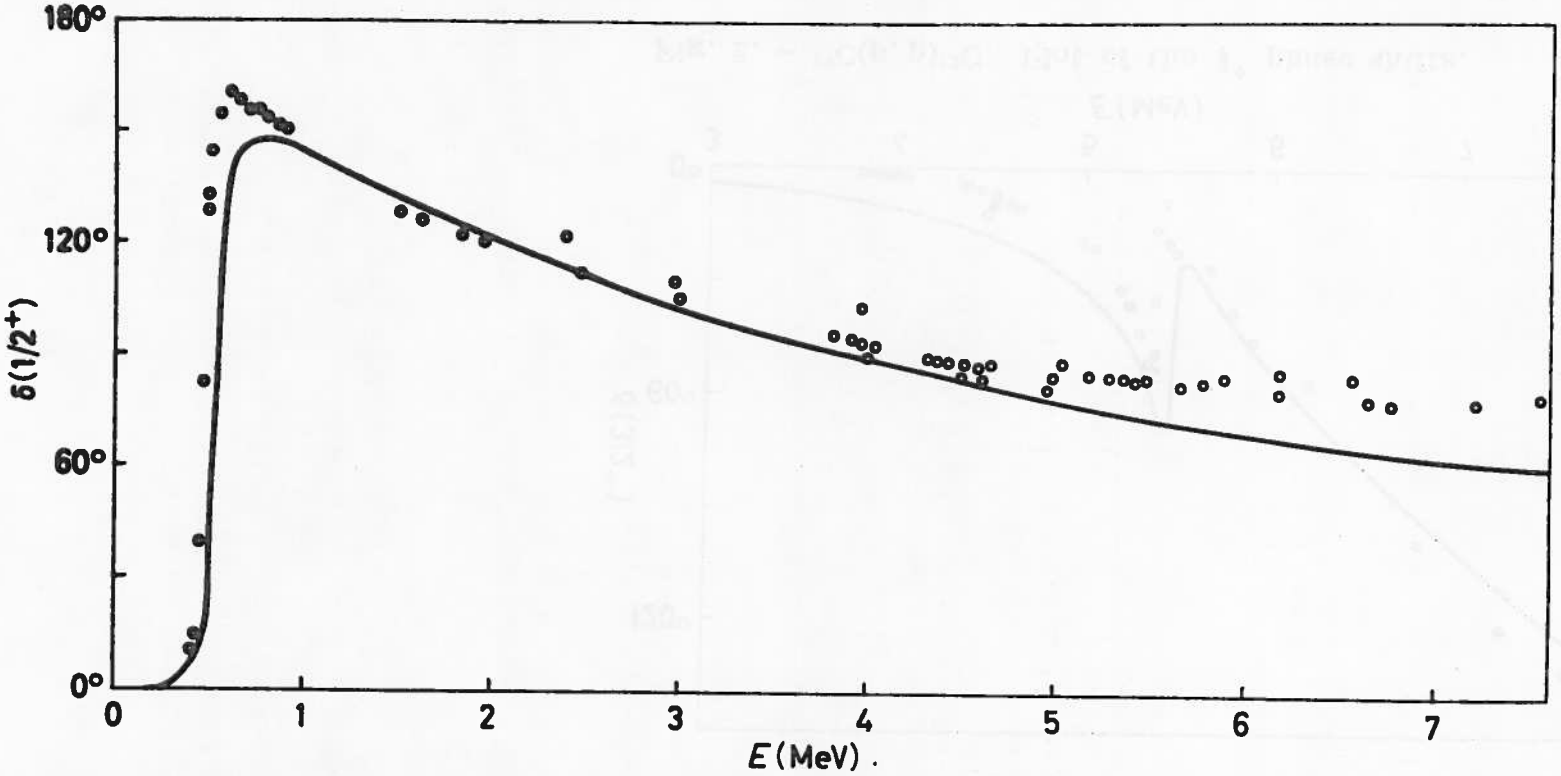

Fig. 1. – $^{12}C(p, p)^{12}C$. Comparison between experimental (dots) and calculated (lines) $\frac{1}{2}^+$ phase shifts.

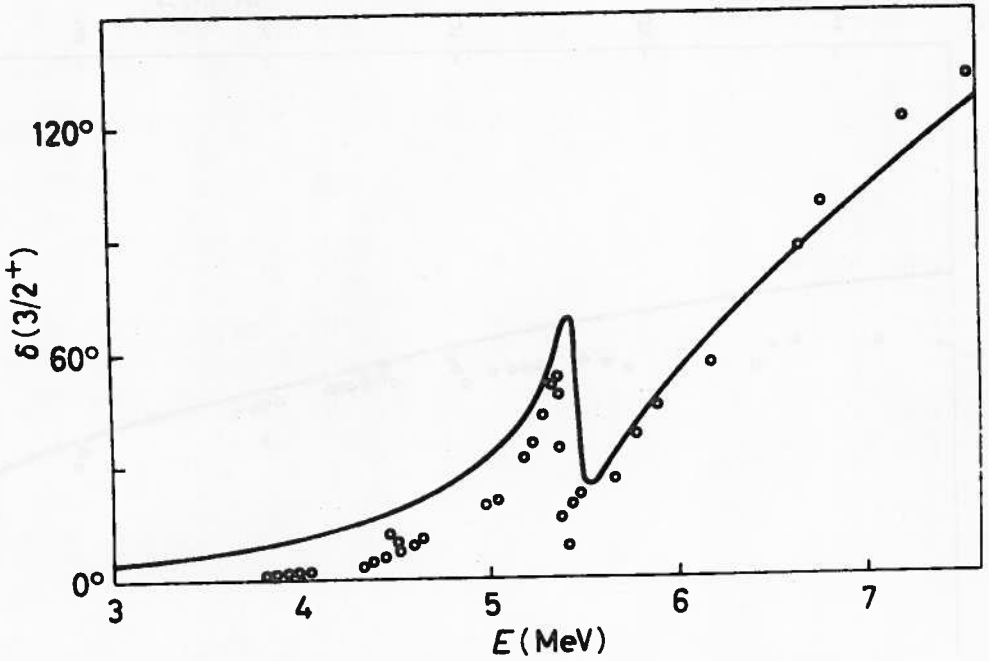

Fig. 2. – $^{12}C(p, p)^{12}C$. Plot of the $\frac{3}{2}^+$ phase shifts.

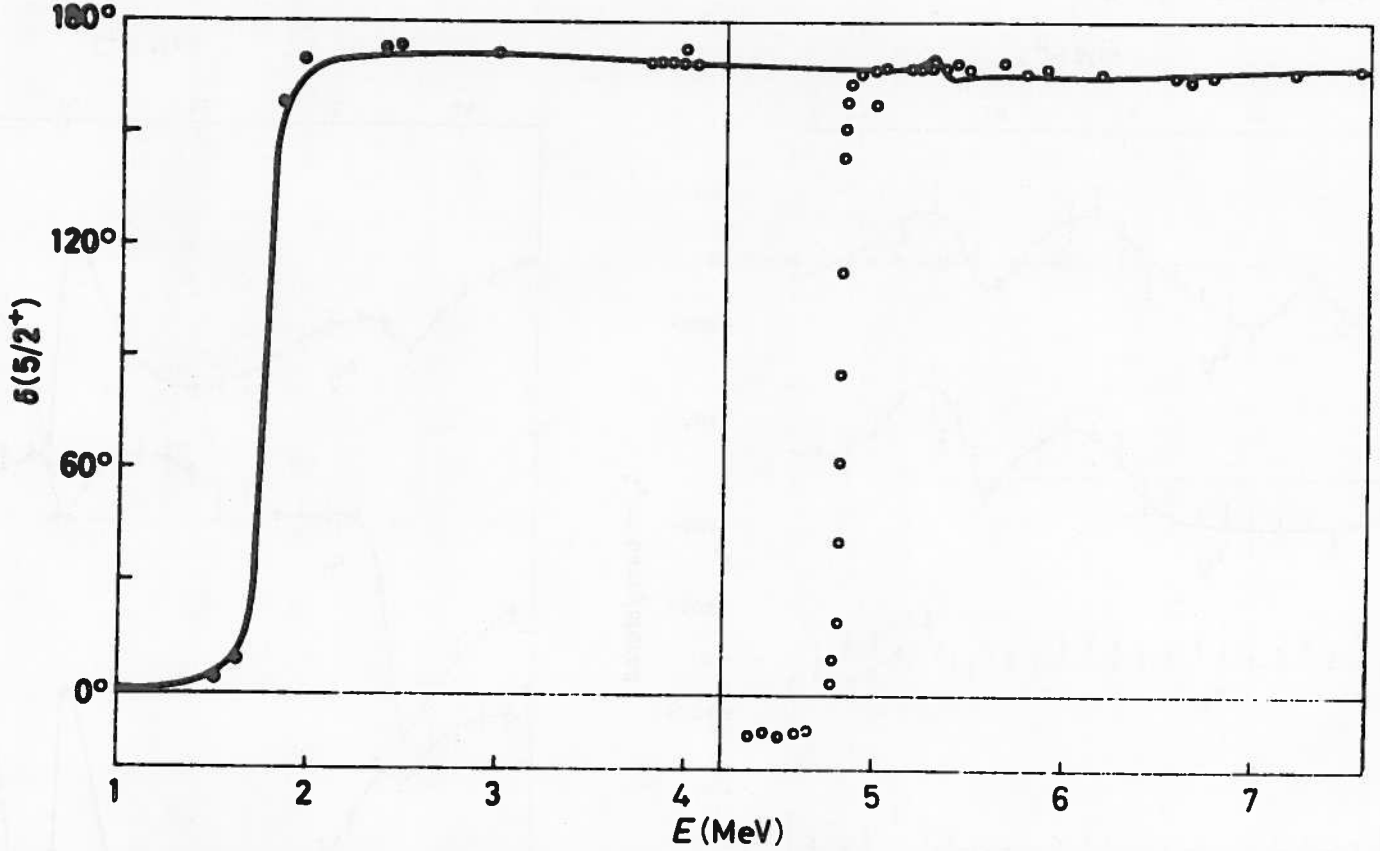

Fig. 3. – $^{12}C(p, p)^{12}C$. Plot of the $\frac{5}{2}^+$ phase shifts. For a better comparison the experimental points have been lowered by 180° at 4.2 MeV.

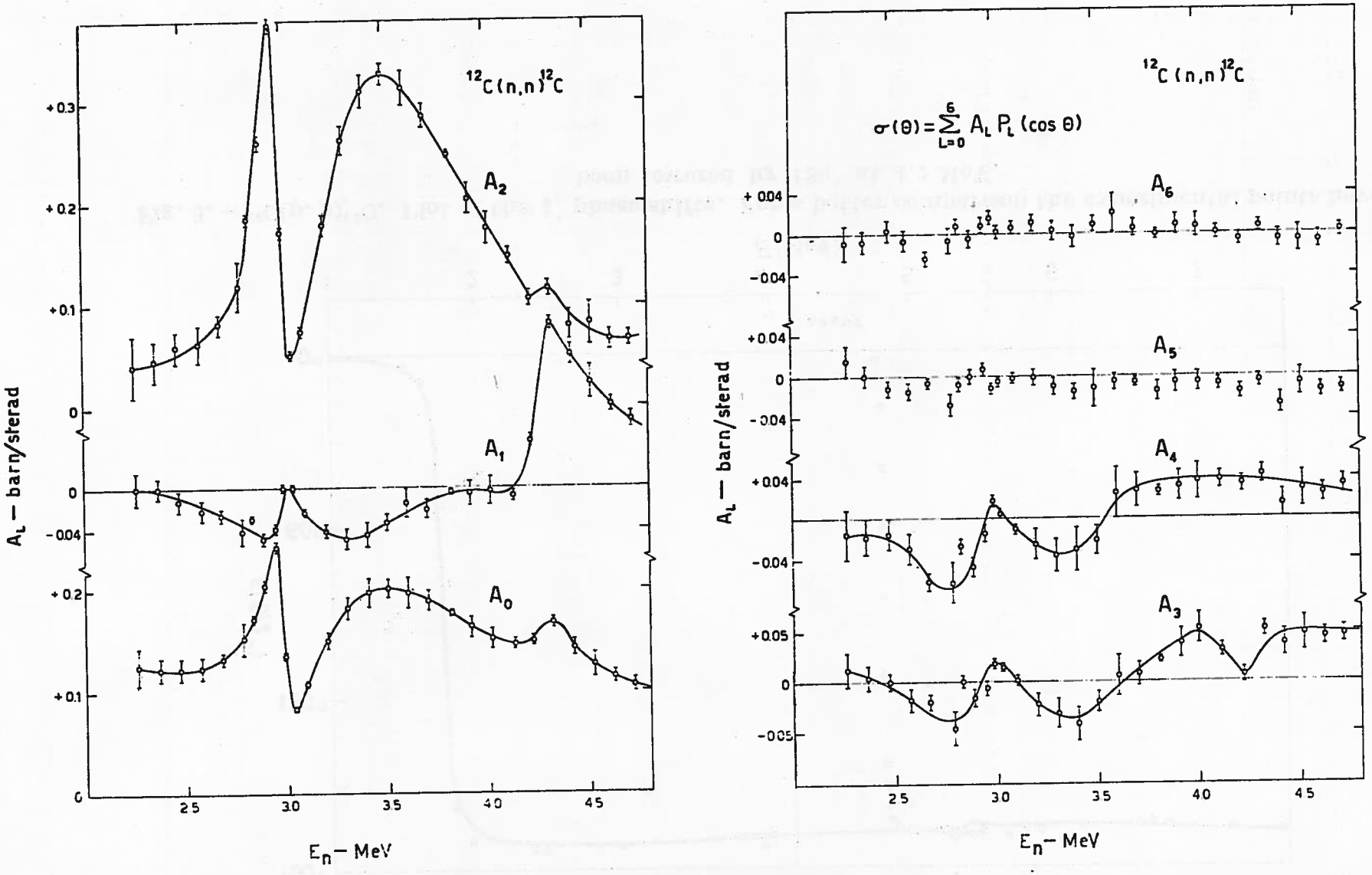

Fig. 4 - Preliminary values, <u>not corrected for the multiple scattering</u>, of the Legendre polynomial coefficients A_L of the expansion:

$$\sigma(\theta)\ ^{12}C(n,n)^{12}C = \sum_{L=0}^{6} A_L P_L(\cos\theta)$$

plotted as a function of neutron energy. The vertical bars are the statistical errors.

XIII. SOTTOSEZIONE DI TRIESTE DELL'ISTITUTO NAZIONALE DI FISICA NUCLEARE - ISTITUTO DI FISICA DELL'UNIVERSITA' - TRIESTE (ITALY)

Gamma rays following the inelastic scattering of 14.2 MeV neutron from ^{24}Mg, ^{28}Si and ^{56}Fe

(U. Abbondanno, R. Giacomich, L. Granata, M. Lagonegro and G. Pauli)

In this experiment the differential cross-sections $\sigma(E_\gamma,\theta)$ for the production of the γ-rays of 1.37 MeV from ^{24}Mg, 1.78 MeV from ^{28}Si, 0.845 MeV and 1.24 MeV from ^{56}Fe have been measured for an incident neutron energy of 14.2 MeV, and the absolute yields of these gamma rays have been deduced. The nuclei used are all even-A. The γ-rays observed, with the exception of the 1.24 MeV γ-ray from ^{56}Fe, correspond to transitions from 2^+ first excited levels to 0^+ ground levels; the 1.24 MeV γ-ray corresponds to the transition of ^{56}Fe from the second 4^+ to the first 2^+ excited level.

The measurements have been performed using the neutrons of the $T(d,n)^4He$ reaction, produced by bombarding a titanium-tritium target by 200 keV deuterons. A beam of neutrons of 14.2 MeV energy was defined by means of the associated-particle technique [1], by detecting the alpha particles which were emitted within a cone of 5°35'. The neutron energy was defined within $\pm$ 0.16 MeV.

All the samples used for the measurements were of the natural isotopic mixture, and were placed at a distance of 40 cm from the tritium target.

The γ-rays were detected by means of a 3"x3" NaI(Tl) crystal coupled with a 56 AVP photomultiplier and placed at a distance of 90 cm from the scattering sample.

A time-of-flight technique has been used to distinguish between γ-rays and scattered neutrons produced in the sample by the $(n,n'\gamma)$ reaction.

The errors quoted on the experimental data include (i) the sta-

tistical error (2 to 3 percent), (ii) the error in the determination of the photopeak efficiency of the detector (3 percent), (iii) the error involved in the evaluation of the photopeak area (4 to 5 percent). The magnitude of the overall error has been estimated to be ± 10 percent.

No corrections have been made to take the absorption and the multiple scattering of neutrons in the sample into account, since the sizes of the samples were chosen so that this correction was smaller than the error involved in the determination of the photo peak area. This point has been checked by making measurements with a number of samples of different sizes and shapes. The γ-ray attenuation in the samples was taken into account and a correction for this effect gave an appreciable result only in the case of the iron sample.

The γ-ray production has been measured at nine angles between 30° and 150° in the laboratory frame of reference.

The total cross-sections for the production of the γ-rays have been deduced by integrating the angular distributions after having extrapolated the experimental data to 0° and to 180°. The error assigned to the values obtained in this way includes both the experimental error previously mentioned and the error due to the extrapolation to the extreme angles. This last error has been taken equal to the difference between the integrated cross-section deduced by extrapolating the experimental data down to zero at 0° and 180°, and the one obtained by assuming that the angular distribution goes parallel to the horizontal axis beyond the extreme measured angles.

The differential cross-section values for the 1.37 MeV γ-ray from ^{24}Mg are plotted in Fig. 1. For the sake of comparison, the data of Martin and Stewart [2] are displayed in the same figure. The value of the integrated cross-section $\sigma(E_\gamma = 1.37$ MeV), derived in the manner above described, is reported in Table I.

The differential cross-section values for the 1.78 MeV γ-ray from ^{28}Si are shown in Fig. 2, and the value of the total cross-

-section $\sigma(E_\gamma = 1.78$ MeV) is reported in Table I. In Fig. 3 are instead shown the differential cross-sections for the 0.847 MeV γ-ray and for the 1.24 MeV γ-ray from ^{56}Fe. The values of the total cross-sections $\sigma(E_\gamma = 0.845$ MeV) and $\sigma(E_\gamma = 1.24$ MeV) are also reported in Table I.

Measurements are in progress on similar neutron inelastic scattering from other nuclei.

References

[1] L. Granata and M. Lagonegro - Nucl. Instr. and Meth. 70(1969) 93

[2] D.T. Stewart and P.W. Martin - Nucl. Phys. 60(1964)349

Table I

Total cross-sections for γ-ray production

Element	E_γ (MeV)	$\sigma_{n,n'}(E_\gamma)$ (mb)
^{24}Mg	1.37	605 ± 60
^{28}Si	1.78	360 ± 40
^{56}Fe	0.84	733 ± 70
	1.24	420 ± 40

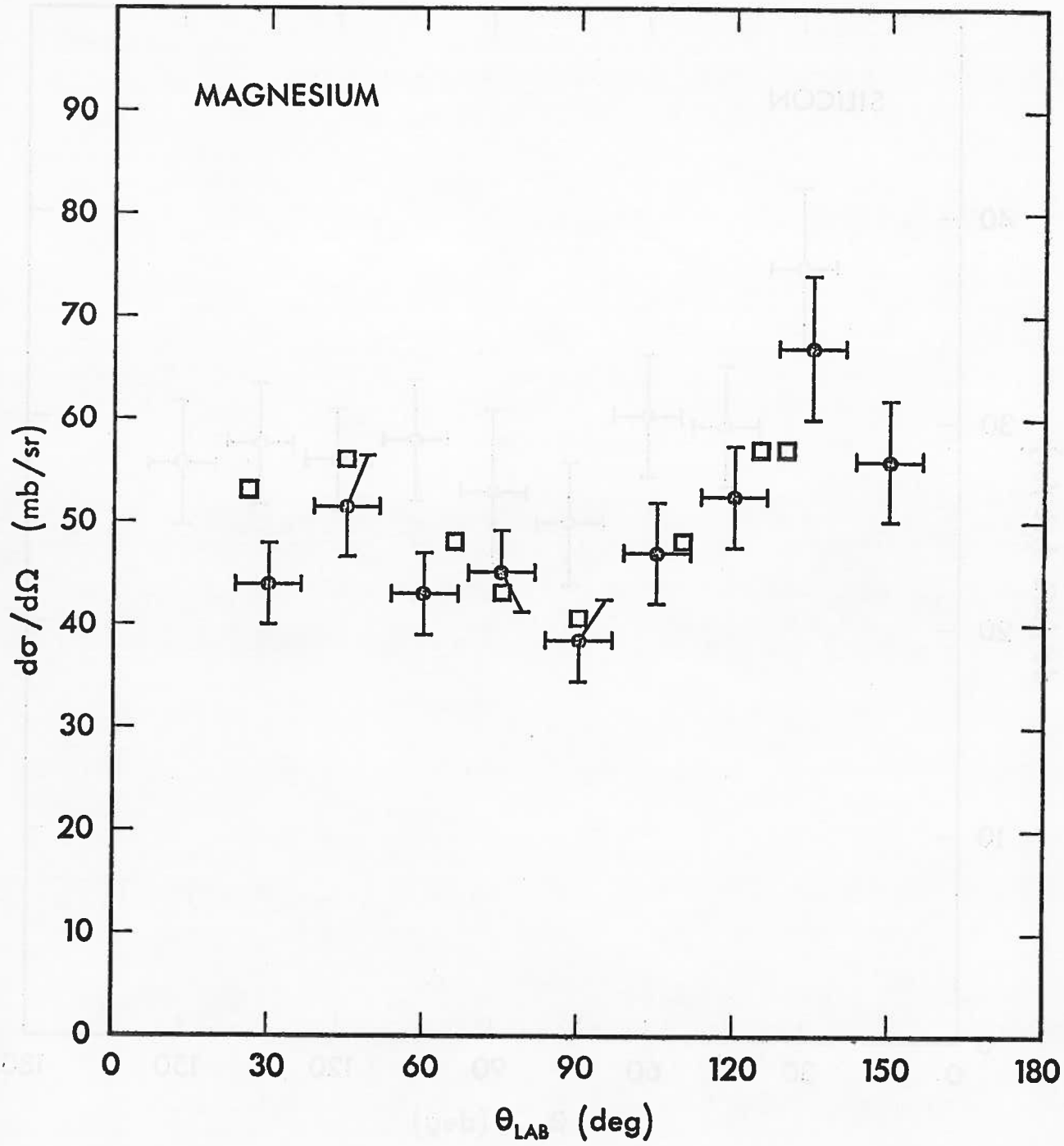

Fig. 1 - The differential cross sections for the 1.37 MeV gamma ray from ^{24}Mg: ● present work, □ data of Stewart and Martin [2].

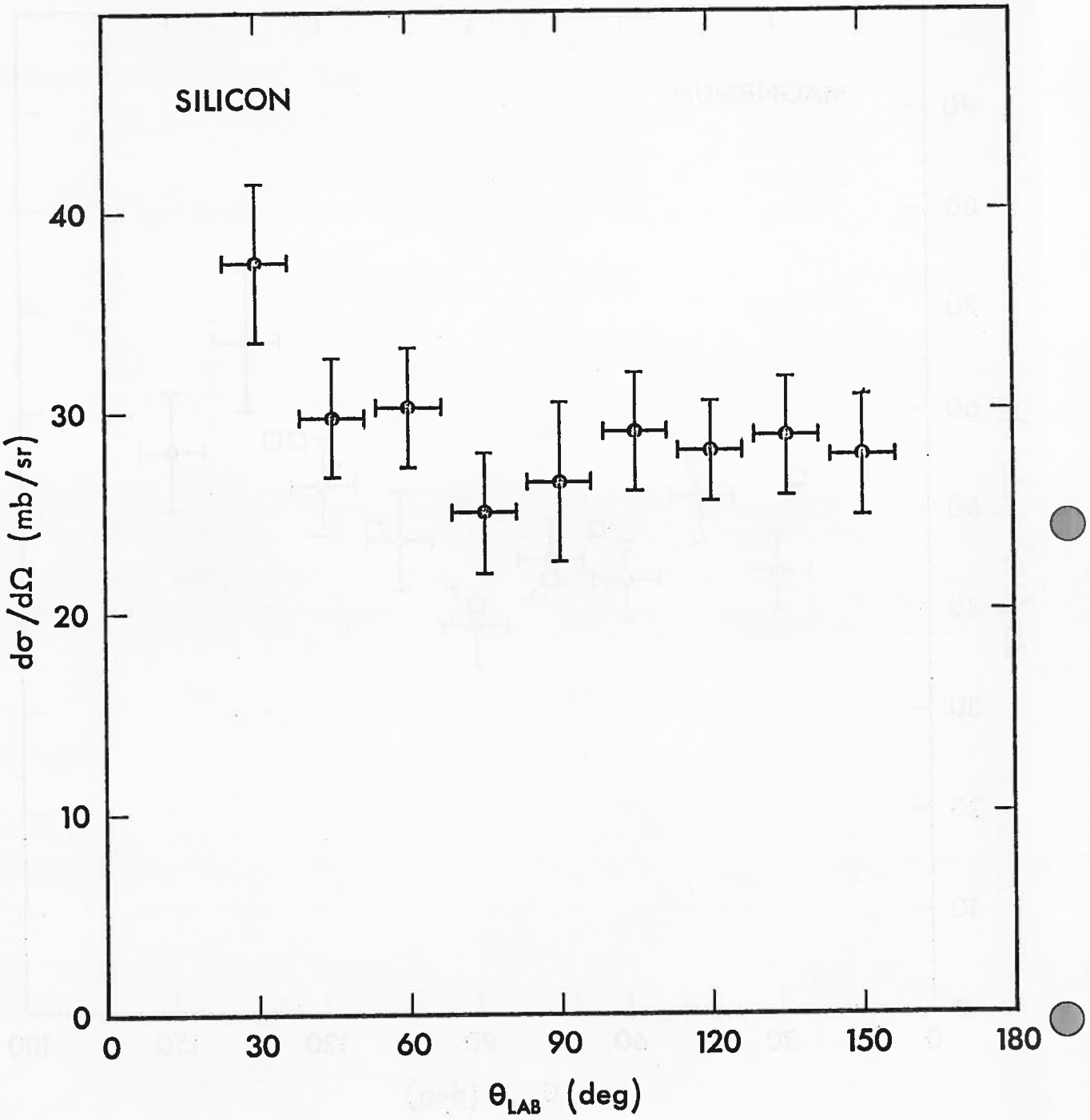

Fig. 2 – The differential cross sections for the 1.78 MeV gamma ray from ^{28}Si.

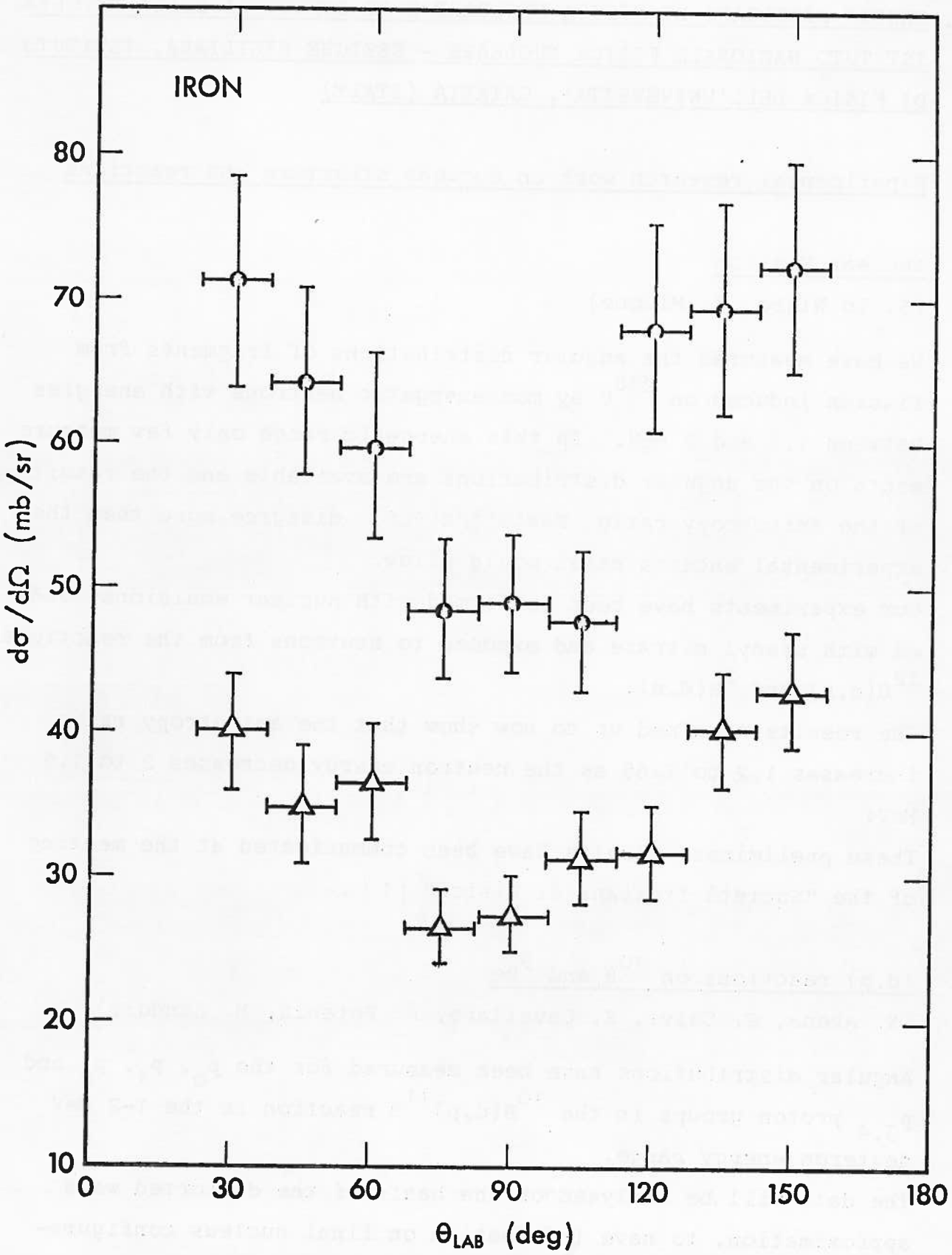

Fig. 3 - The differential cross sections for the 0.845 MeV (●) and 1.24 MeV (▲) gamma rays from ^{56}Fe.

XIV. CENTRO SICILIANO DI FISICA NUCLEARE E DI STRUTTURA DELLA MATERIA, ISTITUTO NAZIONALE FISICA NUCLEARE - SEZIONE SICILIANA, ISTITUTO DI FISICA DELL'UNIVERSITA', CATANIA (ITALY)

1. Experimental research work on nuclear structure and reactions

Nuclear Fission

(S. Lo Nigro, C. Milone)

We have measured the angular distributions of fragments from fission induced on ^{238}U by monoenergetic neutrons with energies between 1.4 and 2 MeV. In this energetic range only few measurements on the angular distributions are available and the results of the anisotropy ratio $R=N(0°)/N(90°)$ disagree more than the experimental uncertainties would allow.

Our experiments have been performed with nuclear emulsions loaded with uranyl nitrate and exposed to neutrons from the reactions $^{12}C(d,n)$ and $^{2}H(d,n)$.

The results obtained up to now show that the anisotropy ratio increases 1.2 to 1.65 as the neutron energy decreases 2 to 1.6 MeV.

These preliminary results have been communicated at the meeting of the "Società Italiana di Fisica" [1].

(d,p) reactions on ^{10}B and ^{9}Be

(N. Arena, G. Calvi, S. Cavallaro, R. Potenza, M. Sandoli)

Angular distributions have been measured for the p_0, p_1, p_2 and $p_{3,4}$ proton groups in the $^{10}B(d,p)^{11}B$ reaction in the 1-2 MeV deuteron energy range.

The data will be analysed on the basis of the distorted wave approximation, to have information on final nucleus configurations [2].

$^7Li+d \rightarrow \alpha + \alpha + n$ reaction

(C. Milone, R. Potenza)

The angular correlations of the α particles from the reaction $^7Li+d \rightarrow (^9Be^*) \rightarrow \alpha + ^5He \rightarrow \alpha + \alpha + n$ have been measured at E_d=0.8 MeV and 1 MeV.

The analysis of the bidimensional spectra of α particles is in progress.

Experimental and calculated energy spectra of standard neutron sources

(S. Notarrigo, F. Porto, A. Rubbino, S. Sambataro)

The measurements on the neutron energy spectrum of the Am-Be source have been completed, confirming the good agreement with the calculations made by taking into account the anisotropy in the angular distributions of the $^9Be(\alpha,n)$ reaction.

The results were already published [3].

Angular distributions of the $^{25}Mg(^3He,\alpha)$ reaction

(S. Notarrigo, A. Rubbino, S. Sambataro, D. Zubke)

The measurements on the angular distributions of the $^{26}Mg(^3He,\alpha)$ reaction [4] have been extended at the incident energy of 10 MeV. The results are being analysed by means of the diffractional model previously used and by DWBA calculations, in order to find out the relation between the two models [5].

$^{16}O(d,d)$, $^{16}O(d,p)$, $^{16}O(d,\alpha)$ reactions

(Cavallaro Salv., A. Cunsolo, R. Potenza, A. Rubbino)

Angular distributions for the reactions $^{16}O(d,d)$, $^{16}O(d,p)$, $^{16}O(d,\alpha)$ from E_d=1.5 to 2.0 MeV, at 50 keV energy intervals, were measured using a differentially pumped gas scattering chamber.

The preliminar data agree with other Authors' results.

The theoretical analysis is in progress.

2. Theoretical research work on nuclear structure and reactions

The extended Tamm-Dancoff (ETD) approximation in nuclear physics

(F. Catara, M. Di Toro, R. Parisi)

The compilation of a code to compute in a microscopic way (ETD approximation) the cross sections for the reactions (n,n'), (p,p'), (n,p), (n,γ) and (p,γ) on a quasi-magic nucleus, has been performed. Through a more careful analysis of the range parameter of the single particle bound wave functions it is possible to reproduce the "potential" resonances just via an "orthogonality scattering" description.

A comparison of the results among themselves and with the experimental data will allow to test the reliability of the particle--hole scheme.

The analysis of the importance of ground state particle correlations is in progress.

A new approximation in the theory of nuclear structure and reactions

(A. Agodi, M. Baldo, F. Catara)

A method has been developed [6] allowing the analysis of nuclear structure and reactions in the framework of a new approximation [7] in which ground state particle correlations are taken into account. This approximation contains (in a sense) R.P.A. but does not violate Pauli's principle.

Some preliminary calculations have been performed showing the importance of g.s. correlations to explain the fine structure of the giant resonance and the positions of the most collective levels (0^+, 2^+, etc..) of magic nuclei.

On the structure of isobaric analog resonances (IAR)

(M. Di Toro in coll. with the Center for Theoretical Physics, MIT, Cambridge)

The effects on the elastic and inelastic scattering of an analog

state acting as a "doorway state" have been studied within a unified theory of nuclear reactions [8].
A method to extract the IAR parameters from the analysis of the fine structure experiments of proton elastic scattering has been performed [9]. The results have been compared with a theoretical investigation allowing a study of the effects of the anti-analog state on the proton escape width. Spectroscopic factors of the parent states have been evaluated.

On the effect of short-range correlations and charge-dependent nuclear forces on the energy of the analog state [10]
(M. Di Toro in coll. with the Center for Theoretical Physics, MIT, Cambridge, Mass.- USA)

The effect of short-range correlations on the displacement energy (energy difference between the analog and the parent state) has been computed to first order in perturbation theory, using the plane-wave approximation for intermediate states. This allows to get a quantitative analysis of the correlation radius.
Both the contributions of the Coulomb interaction and of a charge dependent component of the nuclear two-body interaction have been taken into account.
A realistic nucleon-nucleon interaction (the Kerman-Ronben-Riihimäki one) has been used in the calculations.

Inverse problem for a class of non local interactions
(D. Gutkowski, A. Scalia)

The study of the inverse problem for a class of nonlocal interaction is in progress [11]. Interactions are factorable and of finite rank as those considered in previous papers [12,13], but in general non-hermitian.
The method is that of transformation operators as defined in L.D. Faddeyev, Journ. Math. Phys. 4 (1963) 72.

Low-energy level distributions of light nuclei

(E. Gadioli, E. Recami, L. Zetta)

By following a procedure suggested by Ericson, the cumulative number of low-energy levels of residual nuclei in statistical reactions has been analysed. The analysis showed that the Lang and Le Couteur level density, based on the Fermi gas-model of the nucleus, with a fixed set of average parameters (obtained by considering slow neutron resonance spacings, level widths at high excitation energy, and energy spectra of particles emitted in statistical reactions), fits with a good accuracy the real level density of light nuclei ($A \leq 70$) also for very low excitation energies [14].

Four-particle system ground state

(V.S. Olkhovsky, E. Recami)

Calculations have been developed on the bound states of four particle systems, and particularly the fundamental one, by considering a rather general expression for the binary central attractive potential. First, a Hamiltonian expansion in the strong-coupling-constant approximation has been used; and then, afterwards, it was made recourse to the harmonic polynomial method. In the practical case, the first method was useful, but did not reveal itself to be a very precise one; on the contrary, the second method confirmed its value, as - under reasonable simplifications - the influence on the ground level of all the "partial waves" following the first ones was shown to be quite negligible. In the particular case of the Yukawa potentials and α-particle ground energy, for instance, the value obtained is very near to the one of previous Authors and not far from experimental values [15].

Applications to nuclear (and elementary particle) physics of (relativistic) triangle-diagram cross-sections

(M. Baldo, E. Recami)

The total cross-section for relativistic processes, with three

final particles, proceeding through triangle-diagrams has been explicitly evaluated. The aim was to evidentiate possible anomalous behaviour produced purely by "kinematics" in some cross-sections.

It has been suggested that the considered final-state-interactions may contribute in explaining (partially, at least) some enhancements in the effective-mass distributions as due to kinematical (nondynamical) effects. The general formulae were for example applied to the $pn\pi$ system, and seemed to allow reproducing the known peaking (in the $d\pi$ distribution) at 2.2 GeV/c^2 ; the model, in particular, can give a possible justification for the appreciable deuteron survival in some collisions of mesons and deuterons, even at high projectile-energies. The triangle-graph peaks appear asymmetric.

In the proper Nuclear Physics field, the kinematical peaks are expected in the range about 1÷10 MeV.

For instance the following reactions appeared interesting:

1) $d+\alpha \to {}^5He+p \to n+p+\alpha$; 2) $d+d \to {}^5Li+p \to n+p+\alpha$; 3) $\gamma + {}^6Li \to {}^5Li+n \to p+n+\alpha$; 4) $n+d \to \alpha^* + n \to p+n+{}^3H$; and so on.

The theory and the first results appeared in Ref. [16].

References

[1] S. Lo Nigro and C. Milone - Boll. SIF 71 (1969)25

[2] N. Arena, G. Calvi, S. Cavallaro, R. Potenza and M. Sandoli - Boll. SIF 71 (1969) 10

[3] S. Notarrigo, F. Porto, A. Rubbino and S. Sambataro - N.P. A125 (1969) 28

[4] S. Notarrigo, A. Rubbino, S. Sambataro and D. Zubke - N.C. 64B (1969) 7

[5] S. Notarrigo, F. Porto, A. Rubbino and S. Sambataro - Boll. SIF 71 (1969) 8

[6] A. Agodi, M. Baldo and F. Catara - Boll. SIF 71 (1969)

[7] A. Agodi - Seminar delivered at the "Enrico Fermi" Summer School - Varenna 1965

[8] A.K. Kerman, M. Di Toro and others - Contrib. 1969 Spring Meeting of American Physical Society - Washington D.C.

[9] M. Di Toro - Contrib. International Conference on Properties of Nuclear States - Montreal, August 1969

[10] M. Di Toro, P. Nunberg and E. Riihimäki, MIT-CTP Preprint No. 111(1969) - Paper accepted for the publication on Physical Review

[11] D. Gutkowski and A. Scalia - Boll. SIF 71 (1969) 82

[12] D. Gutkowski and A. Scalia - Journ. Math. Phys. 9 (1968) 588

[13] D. Gutkowski and A. Scalia - "Analytic properties of a class of nonlocal interactions. II", to be published on Journ. Math. Phys.

[14] E. Gadioli, E. Recami and L. Zetta - Nucl. Phys. A128 (1969) 339

[15] V.S. Olkhovsky and E. Recami - N. Cim. 63B (1969) 593

[16] M. Baldo and E. Recami - Report INFN/AE-69/4, Frascati 1969

XV. LABORATORIO DI FISICA E CALCOLO DEI REATTORI, CENTRO DI STUDI NUCLEARI DELLA CASACCIA (C.N.E.N.) - ROMA (ITALY)

1. Cross-section of the reaction $^{151}Eu(n,\gamma)^{152m}Eu$ in the energy range 0.0 eV to 0.63 eV

(F.V. Orestano, F. Pistella)

Discrepancies are present in the available evaluations of the energy dependence of the cross-section for the production of ^{152m}Eu(9.2 h): significant information are reported by Wood [1] and by Keisch [2]. The curve of the activation cross-section $\sigma_{act}(E)$, measured in arbitrary units by Wood in the range $0.08\ eV \leq E \leq 10\ eV$, compared with the absorption cross-section trend indicates that the ratio α between activation and absorption cross-section significantly decreases as neutron energy E increases. On the other hand, Keisch performed integral measurements of the ratio α in two different spectra: he found that the ratio in the thermal-neutron spectrum was equal to the ratio in the epicadium-neutron spectrum.

Two different sets of the activation cross-section in the thermal-energy range were deduced from these two sets of measurements. If the ratio α is supposed to be a constant, as suggested by Keisch, the activation cross section may easily be evaluated by assuming for α the value at 2200 m/sec,

$$\alpha = \sigma_{act}(2200) / \sigma_{abs}(2200) .$$

In the opposite assumption - that the ratio α changes with energy, as suggested by Wood - an evaluation of the activation cross-section $\sigma_{act}(E)$ is needed in the energy range which was not investigated by Wood (below 0.08 eV). The $\sigma_{act}(E)$ may be obtained over the whole range by evaluating the contributions of each different resonance and by multiplying them by the corresponding α_k value (α_k is the population fraction of the isomeric state of ^{152}Eu for the k'th resonance). The α_k values given by Wood were obtained by means of the resonance parameters then available

[3]; these parameters are now considered to be of doubtful quality. To obtain a more reliable evaluation of $\sigma_{act}(E)$ of ^{151}Eu over the whole range, the first step was the analysis of the absorption cross-section $\sigma_{abs}(E)$ of ^{151}Eu to determine the different contributions due to each resonance, with particular regard to the contribution given by the negative energy level. Then the α_k values were determined by fitting the Wood $\sigma_{act}(E)$ curve in terms of the different absorption contributions just evaluated. The values obtained (as reported in [4]) for the resonance at negative energy of ^{151}Eu are:

$E_{res} = -0.045$ eV; $2g\Gamma_n = 0.06$ mV; $\Gamma_\gamma = 92.2$ mV.

The corresponding cross-section $\sigma_{abs}(E)$, at the resonance energy E_{res}, is 18700 barns.

The determination of the $\sigma_{act}(E)$ is based on the curve given by Wood in arbitrary units above 0.08 eV. The values of Wood were fitted in terms of a linear combination of the different contributions to the absorption cross-section which were evaluated for each resonance. The coefficients of the combination are proportional to the α_k ratios. The trend of $\sigma_{act}(E)$ may be obtained also in the energy range below 0.08 eV by applying the linear combination to the coefficients determined as above explained.

The resulting trend was normalized to the 2200 m/sec value (3100 barns) recommended in BNL-325, 2nd edition, suppl. 2 (1966), thus obtaining the normalized α_k values. These are compared in Table I with the values by Wood for the resonance investigated. The values of the resonance parameters for the activation cross section $\sigma_{act}(E)$ are given in Table II. The $\sigma_{act}(E)$ obtained from these parameters is plotted in fig. 1 as curve 1, and compared with the $\sigma_{act}(E)$ obtained according to Keisch's results, plotted as curve 2.

Tests were performed [6], by comparing calculated and measured spectral indexes involving ^{151}Eu, to choose between the sets obtained from the two hypotheses. The assumption that α is dependent on energy (with α_k values reported in Table II) gave a much better

agreement.

2. Evaluation of the activation resonance integral for ^{151}Eu and ^{175}Lu by cadmium ratio measurements

(A. Gibello, F.V. Orestano, F. Pistella)

Experiments performed in order to test a correlation method [6] gave indications that the activation resonance integral of ^{151}Eu by Jacks [7] might be inadequate. The same opinion has also been expressed independently by Damle et al. [8].
A new evaluation of the resonance integral was obtained [4], [9] from cadmium ratio measurements (1.0 mm Cd thickness) in a known spectrum (central water filled cavity of the RANA reactor). By using the activation thermal cross-section of ^{151}Eu previously described (Sec. 1), the value 1230 ± 30 barns was obtained for the RI of ^{151}Eu (activation), with a cut off energy of 0.63 eV. Analogous considerations held also for ^{175}Lu; the value of the resonance integral by Schmid [10] seemed to be inadequate. Cadmium ratio measurements, performed as above described, analyzed adopting for ^{175}Lu a 1/v law in the thermal range (σ (E_o) = 13.26 barns), gave a resonance activation integral (cut off energy 0.63 eV) of 405 ± 15 barns ($\sim$15% lower than the experimental value by Schmid).

Evaluation of the reliability of the cross-section for ^{235}U (fission), ^{239}Pu(fission), ^{197}Au, ^{176}Lu, ^{175}Lu, ^{55}Mn, ^{63}Cu, ^{151}Eu (activ.), and natural Eu(absorption)

(A. Gibello, F.V. Orestano, F. Pistella, E. Santandrea)

Spectral index measurements have been performed in a set of equilibrium neutron spectra, similar to reactor spectra, produced in water solutions of boron and europium, irradiated in the RITMO reactor. In the europium solutions the thermal resonance absorption by ^{151}Eu (0.46 eV) mocked-up the resonance absorption by plutonium isotopes in plutonium fuelled lattices.
From the calculational standpoint after discussing the cross-section

data available for the detectors, two independent approaches have been adopted. 1) The activation rates calculated by means of the neutron energy distributions, obtained from standard theoretical methods, have been compared with the experimental reaction rates. 2) The reaction rates have been directly evaluated from the measured spectral indexes according to a correlation method [11]. From both approaches information about detector cross-sections were obtained [6].

The sources of the cross-section data which resulted to be reliable for the interpretation of spectral index measurements are listed in Table III. The cross-section sets generated from such data are reported in ref. [6].

In addition to the sources reported in Table III, the thermal cross-section sets were taken from ref. [19] for ^{235}U(fission) and natural Eu(absorption) and from ref. [21] for ^{239}Pu(fission); the epithermal fission cross-section sets were taken from ref. [22] for both fissile isotopes and from ref. [23] for natural Eu(absorption).

The good agreement found in the europium solutions, between experimental results and calculated spectral indexes and cadmium ratios, has shown the reliability of the absorption cross-section set used for the natural europium.

4. Deposition of thin films

(G. Balducci, A.M. Biancifiori, M. Martini)

Techniques of thin film deposition are widely employed when ionization or fission chambers and activation detectors are used to detect the neutron flux.

The coating method is chosen on the basis of the use foreseen for the coated film [24].. The "vacuum evaporation by heated resistor" technique was used to prepare thin films of fissionable materials for neutron detectors (50 ÷ 150 μgr/cm^2) as well as for mass spectroscopy (∼10 μgr/cm^2); on the other side "electron beam" technique was used for thorium oxides and ^{10}B films. The "cathodic sput

tering" technique was used to obtain thin films of materials having high melting point (W,Mo) and to coat plastic sheets with a metallic film (*). To prepare large thick films (200 ÷ 400 $\mu gr/cm^2$) of fissile materials, the "electro-chemical deposition" technique was used by the molecular plating method [25]; this technique allows to obtain thin and uniform films of inorganic materials, with a large and reproducible yield (∼98%) and a short operation time (∼40'); moreover it is possible to determine the weights of the coated film by counting the alpha activity of the solution left after the deposition.

We developed also a miniaturized device (set-up in a glove-box, in order to avoid contamination) evaporating fissionable alpha emitting materials, such as ^{239}Pu, ^{237}Np, ^{233}U. Several methods were also developed to check thickness and uniformity of the films. The thickness of the layer is checked during the evaporization by a quartz oscillator system.

Two different methods are employed to determine the uniformity of the film thickness: the "autoradiography method", where the alpha tracks from fissionable materials are recorded by photographic slides, the "interferometric and gravimetric method" for conventional materials [24]. The coated disks are plugged into a vacuum chamber in a fixed and reproducible position, and counted by a solid state detector; the relative masses of the fissionable materials may be evaluated if the alpha decay rate of the sample and the half life of the nuclide are known. In the case that it is not possible to detect the impurities among the main constituent, because the energies of the alpha particles are similar (as for ^{235}U

(*) Till now we obtained films of conductive materials by the diode sputtering technique; in next future we shall be able to make films of plastic and ceramic materials by radio-frequency diode sputtering system.

and ^{239}Pu), the irradiation in a thermal neutron flux of both bare and cadmium covered detectors, may give a relative calibration. To correlate the two calibration methods, natural uranium detectors may give a relative calibration. To correlate the two calibration methods, natural uranium detectors are used because both calibration techniques can be employed and the percentages of different alpha emitting nuclides are exactly known.

References

[1] R.E. Wood - Phys. Rev. 95 (1954) 453

[2] B. Keisch - Phys. Rev. 129 (1963) 769

[3] V.L. Sailor, H.H. Landon, L.H. Foote - Phys. Rev. 93 (1954) 1292

[4] F.V. Orestano, F. Pistella - Nucl. Sci. Engng. 37 (1969) 478

[5] P.J. Sturm - Phys. Rev. 71 (1947) 757

[6] A. Gibello, F.V. Orestano, F. Pistella, E. Santandrea "Evaluation of neutron spectral effects in systems with thermal resonance absorbers by applying a correlation method to measured spectral indexes" Nucl. Sci. Engng. 39 (March 1970)

[7] G.M. Jacks DP-608 E.I. Dupont de Nemours & Co. Savannah River Laboratory (1961)

[8] P.P.Damle, A. Fabry, H. Van Den Broeck BLG-421 C.E.N./S.C.K. (1967)

[9] F.V. Orestano, F. Pistella - RT/FI(68)52 C.N.E.N. (1968)

[10] L.C. Schmid HW-69475 Hanford Atomic Products Operation (1961)

[11] F. Pistella - Nucl. Sci. Engng. 34 (1968) 329

[12] A.H. Baston et al. J. Nucl. Energy,Part A 13 (1960) 35

[13] J. Brunner, F. Widder - Nuclear Data for Reactors,Vol.I pp. 61-70 IAEA, Vienna (1967)

[14] C.H. Westcott AECL-1101 Atomic Energy of Canada Ltd. Chalk River (1960)

[15] BNL - 325 2nd Edit., Suppl. 1 (1960)

[16] J.W. Meadows, J.F. Whalen - Nucl. Sci. Engng. 9 (1961) 132

[17] A.F. Henry - WAPD-TM-224 Bettis Atomic Power Laboratory (1960)

[18] L.L. Anderson - Health Physics 10 (1964) 315

[19] R.H. Shudde, J. Dyer - NAA (Dec N° 3W-354) Atomics International (1960)

[20] BNL - 325, 2nd Edit., Suppl. 2 (1966)

[21] J.J. Schmidt - KFK-120 Kernforschungszentrum, Karlsruhe (1962)

[22] L.P. Abagjan et al. Gruppovye konstanty dlja raŝceta jadernik reactorov M. Gosatomizdat URSS (1964)

[23] J.J. Schmidt, I. Siep - KFK-352 Kernforschungszentrum Karlsruhe (1965)

[24] G. Balducci, M.A. Biancifiori, M. Martini "Deposition of thin films" (to be published in RT/FI series by CNEN)

[25] W. Parker, H. Bildstein, N. Getoff - Nucl. Instr. Meth. 26 (1964) 55.

Table I

Values of the population ratios α_k, for each resonance of ^{151}Eu significant in the thermal-energy range, compared with the values by Wood.

k	E_{res}(eV)	α_k	
		Present work	Wood
1	-0.045[a]	0.38	0.24
2	0.321	0.22	0.19
3	0.461	0.13	0.11
4	1.055	0.13	0.08

[a] The value -0.045 eV for the bound level has been obained in the present work; Wood used the value -0.011 eV given by Sturm [5].

Table II

Resonance parameters for activation cross-section of ^{151}Eu

k	Ref. for Γ_n, Γ_γ values	Γ_n (mV)	Γ_γ (mV)	α_k Γ_γ (mV)	σ_{act} (E_{res}) (barns)
1	Pres. Work	0.06	92.2	35.0	7095
2	BNL325(66)	0.073	79.5	17.6	960
3	BNL325(66)	0.67	89.0	11.6	3216
4	BNL325(66)	0.201	90.0	11.7	419

Table III

Selected sources of nuclear data for detectors

Data / Isotopes	$\sigma(E_o)$	Resonance integral	Resonance parameters for $\sigma(E)$ in thermal range	Differential epithermal cross-section
^{176}Lu	12	10	13	-
^{175}Lu	10	Pres.Work Sec. 2	1/v	-
^{197}Au	14	15	15	15
^{55}Mn	16	17	1/v	17
^{63}Cu	15	18	1/v	-
^{151}Eu	20	Pres.Work Sec. 2	Pres.Work Sec. 1	-

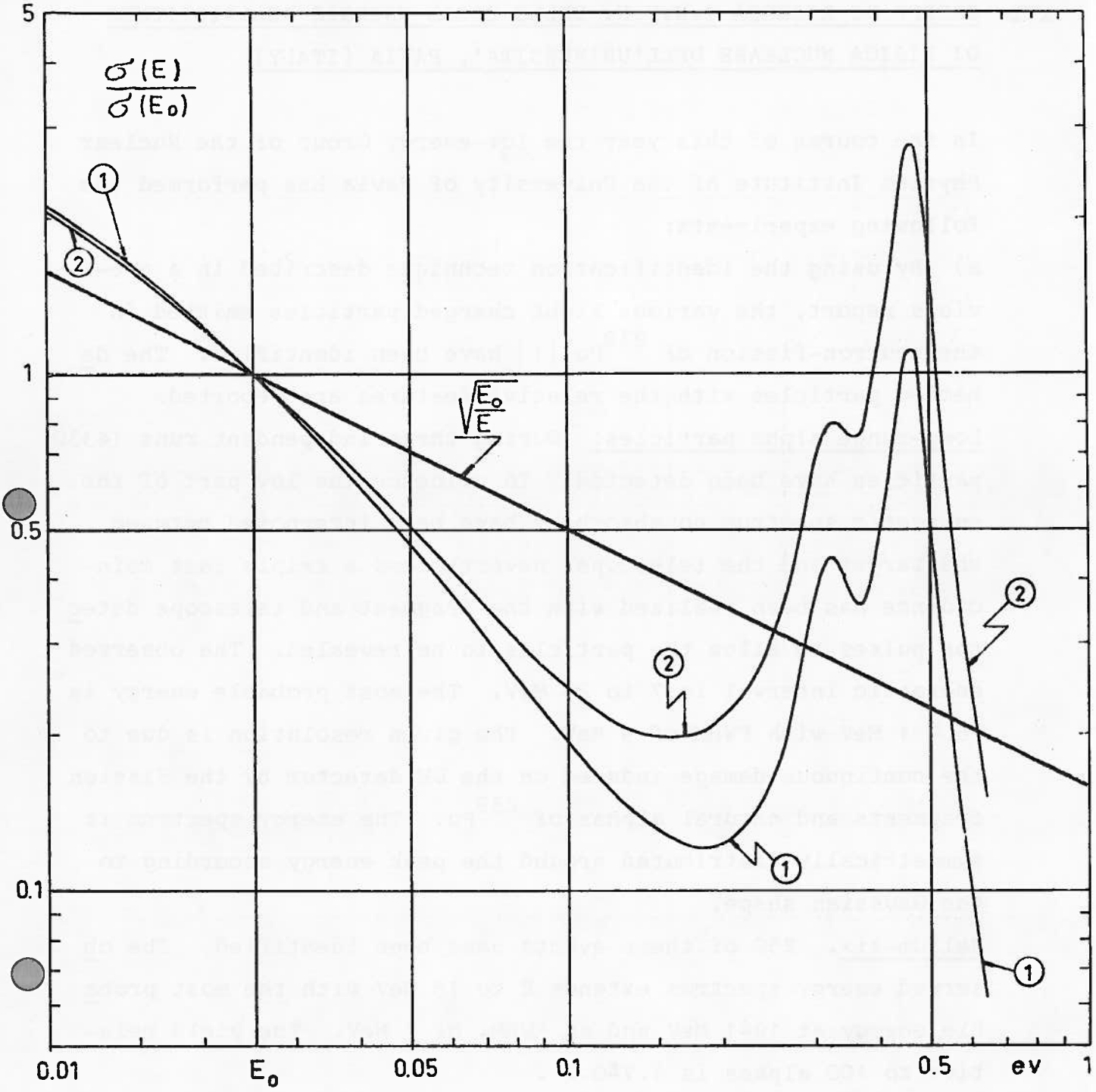

Fig.1 - Comparison between the $\sigma_{act}(E)$ curves calculated assuming either an energy dependent α (curve 1) or a constant α (curve 2). The curves are plotted normalizing to unity the 2200 m/sec value.

XVI. GRUPPO DI RICERCA I.N.F.N. DELLE BASSE ENERGIE DELL'ISTITUTO DI FISICA NUCLEARE DELL'UNIVERSITA', PAVIA (ITALY)

In the course of this year the low-energy Group of the Nuclear Physics Institute of the University of Pavia has performed the following experiments:

a) By using the identification technique described in a previous report, the various light charged particles emitted in the neutron-fission of ^{239}Pu [1] have been identified. The detected particles with the relative features are reported:

Long-range alpha particles. During three independent runs 14330 particles have been detected. To evidence the low part of the energetic spectrum no absorbers have been interposed between the target and the telescope: nevertheless a triple fast coincidence has been realized with the fragment and telescope detector pulses to allow the particles to be revealed. The observed energetic interval is 7 to 28 MeV. The most probable energy is 16 ± 1 MeV with FWHM of 9 MeV. The given resolution is due to the continuous damage induced on the DE detector by the fission fragments and natural alphas of ^{239}Pu. The energy spectrum is symmetrically distributed around the peak energy according to the Gaussian shape.

Helium-six. 250 of these events have been identified. The observed energy spectrum extends 8 to 18 MeV with the most probable energy at 12±1 MeV and an FWHM. of 7 MeV. The yield relative to 100 alphas is 1.7±0.2 .

Helium-three. These particles have been detected during two runs with a Ni absorber interposed between the telescope and the target. The yield relative to 100 alphas is 0.9 . Owing to overlapping of the alpha-particle tail, this yield is to be considered as an upper limit. The peak energy is 16±1 MeV but probably the energy spectrum is influenced by the alpha tail.

Tritons. The observed energy interval is 5.5 to 11 MeV. The peak energy is 8.2±0.7 MeV with an FWHM of 6±1 MeV. The yield

relative to 100 alphas is 5.5 ± 0.5 .

Deuterons. Evidence has been obtained of such particles in the energy range 4 to 7 MeV. The lower limit of the yield relative to 100 alphas is 0.3 .

(F. Cavallari, M. Cambiaghi, F. Fossati, T. Pinelli).

b) A neutron spectrometer [2], based both on the identification and the energy measurement of recoiling protons from a hydrogenous radiator, has been developed. The performance of such an apparatus is characterized by a large energy range (100 keV to 25 MeV), a satisfactory energy resolution (about 100 keV), and an effective discrimination of the background, whose frequency can reach an order magnitude higher than that relative to the events to be considered.

(M. Cambiaghi, F. Fossati, T. Pinelli).

References

[1] F. Cavallari, M. Cambiaghi, F. Fossati, T. Pinelli - Proceedings on the Second IAEA Symposium on Physics and Chemistry of Fission - Vienna 1969 - SM - 122/16 pag. 891.

[2] M. Cambiaghi, F. Fossati, T. Pinelli - to be published in Nuclear Instruments and Methods.

XVII. GRUPPO DI ISPRA PER LE MISURE DI SEZIONI D'URTO DEL C.N.E.N., ISPRA (VARESE), (ITALY)

The works of this Group were performed in the frame of a CNEN-EURATOM cooperation programme for nuclear data measurements, and are reported in the chapter of CBNM-Geel activities.

XVIII. GRUPPO DI RICERCA INFN-ISTITUTO DI FISICA DELL'UNIVERSITA', GENOVA (ITALY)

The Genova Group for Nuclear Research consists of 6 researchers and 3 technicians.
During 1969 the many activities of the Group were divided as follows.

1. Study of the mechanism for the reactions (γ,p) on light nuclei

Using a telescope of scintillation counters the yield of photoprotons by bremstrahlung γ rays is measured for different maximum energies E_o of the bremstrahlung beams of the Turin syncrotron.
The range of E_o is between 45 and 90 MeV. The analysis of the yield curves gives the cross section for the process of photoproton emission.
This process may be due to an interaction of the photon with one or two nucleons: in the first case it is usually called a direct interaction, while in the second case it is called an interaction with a quasi deuteron.
It was clearly shown by our measurements on the nucleus C^{12} that the process is mainly due to the direct interaction mechanism. [1].
Further evidence is expected from the present measurements on the nucleus Li^7.

2. Cooperation with the Universities of Pavia and Torino for the design of a racetrack microtron electron accelerator giving a final energy of about 500 MeV

This is a new type of machine that seems very suitable for the nuclear research because it gives a high current final beam (20 KW average) of very precisely defined energy (10^{-3} at least) with a duty cycle of about 3%.

It consists of a linac section in which the electron beam is recycled many times ($\simeq 25$) with the aid of two 180° ending magnets.

The work of the Genova Group was mainly on the design of the focusing system that insures a beam of limited spatial dimensions. Many quadrupoles are used to control the beam dimension and divergence, together with a particular shape of the magnet edges particularly studied to avoid the well known "fringing field defocusing effect".

The project of the optical system for the microtron is now completed [2] and we are performing final test with a ray tracing computer programme able to simulate completely the behaviour of a particle in the microtron.

References

[1] G. Manuzio, G. Ricco, M. Sanzone - High Energy Photoproton from ^{12}C - Nucl. Phys. A133 (1969) 225.

[2] M. De Mutti, E. Mancini, G. Manuzio - Microtron Optics III - LIRFA Report No. 18 (1969). (Much of the work on the microtron is published on internal LIRFA Report).

XIX. LABORATORIO DATI NUCLEARI, CENTRO DI CALCOLO DEL C.N.E.N., BOLOGNA (ITALY)

1. Radiative Capture Cross-Sections for Stable Nuclei with $32 \leq Z \leq 66$ in the Energy Range 1 keV - 10 MeV

(V. Benzi, G. Reffo)

The evaluation of the radiative capture cross-sections of all stable nuclei with $32 \leq Z \leq 66$ in the energy range 1 keV÷10 MeV has been completely revised. The results of the evaluation will soon be published in the CCDN-Newsletter Bulletin NW/10. In addition, graphs showing the comparison between the evaluated cross-sections and experimental data available have been compared, and will be published in the first months of 1970. The evaluated data have been put in the UKAEA and ENDF/B format, and are available through the CCDN-ENEA (Saclay).

2. Coupled-Channel Calculations of the Giant Dipole Resonance in the One Particle-One Hole Continuum Approximation - II. ^{28}Si

(M. Marangoni, A.M. Saruis)

The electric dipole photoreaction cross-sections of ^{28}Si have been calculated in the frame of the shell-model approach to nuclear reactions. The model and the method of solution are identical to those described in ref. [1], where the giant dipole resonance of ^{12}C and ^{40}Ca is computed. Isospin mixing is included, since the single-particle potential for protons has a central Coulomb part. A fair agreement is reached with the experimental data as far as the gross structure of the excitation curve is concerned (Figs. 1,2,3) [2-4]. The peculiar property exhibited by the angular distribution of the $^{27}A(p,\gamma_o)Si^{28}$ reaction, which essentially remains the same when the energy is varied, despite the fact that the excitation curve is strongly energy dependent (Fig.4), can be understood in the frame of the present model as a doorway state phenomenon [5].

3. Microscopic Model for the Description of the Giant Dipole Resonance of Even-Even Nuclei with a Valence Nucleon

(M. Marangoni, A.M. Saruis)

The electric dipole matrix element of even-even nuclei plus a valence nucleon has been calculated.
The dipole wave function has been computed in the approximation where the valence nucleon motion is coupled to the core excitations in the giant resonance region. The valence nucleon has been described by a spherical Woods-Saxon potential and the core energetic spectrum is given in the shell model Tamm-Dancoff or RPA approximation [6].

4. Coupled Channel Calculation of Elastic and Inelastic Scattering of 17.5 MeV Protons by ^{23}Na (*)

(P.L. Ottaviani, L. Zuffi)

We analyze elastic and inelastic differential cross sections of 17.5 MeV protons scattered from ^{23}Na [7]. The scattering cross sections of nucleons for the first excited levels (0. , 0.439 , 2.078 MeV) can be satisfactorily analyzed in the framework of the simple collective model describing the nucleus like an axially symmetric rigid rotor [8]. However, the energy spacing of such levels and the presence at higher energies of other levels which cannot be considered as belonging to the ground state band, show that ^{23}Na cannot be considered a pure axially symmetric rotor.
Experimental and theoretical results indicate indeed a mixing of different bands based on different proton orbits [9-11].
For this reason, we describe the nucleon target interaction with a macroscopic non central optical potential plus a residual

(*) Contribution to International Conference on Properties of Nuclear States - Montreal, Canada - August 25-30, 1969.

term which allows the single particle (proton) excitations. The macroscopic nuclear potential is obtained as Legendre polynomial expansion to the second order of the following expression [12]

$$V(r,\theta,\varphi) = -(V+iW)\frac{1}{1+\exp[(r-R)/a]} - 4iW_D \frac{\exp[(r-\bar{R})/a]}{\{1+\exp[(r-\bar{R})/a]\}^2} -$$

$$- V_{so}(\underline{\sigma}\cdot\underline{l})\,\lambda\!\!\!^{-}_{\pi}{}^2 \frac{1}{ar}\frac{\exp[(r-R)/a]}{\{1+\exp[(r-R)/a]\}^2}$$

with

$$R=R_o(1+\sum_\lambda \beta_\lambda Y_{\lambda o}(\theta')) \qquad \bar{R}=\bar{R}_o(1+\sum_\lambda \beta_\lambda Y_{\lambda o}(\theta')) \qquad R_o=r_o A^{1/3} \qquad \bar{R}_o=\bar{r}_o A^{1/3}$$

The effective nucleon-nucleon interaction used is $(V_o+V_1\,\underline{\sigma}_1\cdot\underline{\sigma}_2)$ $\exp(-r_{12}^2/b^2)$.

The results shown in Fig. 5 have been obtained by means of a coupled channel calculation [12] using the following parameter values

V=49. MeV $\quad W$=0. MeV $\quad V_{so}$=3.0 MeV $\quad a$=0.65 F $\quad W_D$ = 6.5 MeV

$\bar{a}$=0.5 F $\quad r_o=\bar{r}_o$=1.2 F $\quad \beta_2$=0.488 $\quad V_o$=-24.4 MeV $\quad V_1$=+5.12 MeV

b=1.85 F.

Coulomb potential for a uniformly charged sphere of radius $1.2 \times A^{1/3}$F has been added. Space-exchange process has been neglected dealing with the microscopic part of interaction [13] and the wave functions used for ^{23}Na are taken from ref. [11]. The angular distribution calculations to the inelastic scattering from the 2.391-MeV $\frac{1}{2}^+$ level are the more sensitive to the characters of the microscopic interaction. The agreement with experiment is reasonable even if for $\frac{1}{2}^+$ level the details of cross-section are not always well described. Calculations are in progress with different sets of target wave functions.

5. Total Neutron Cross Section for ^{232}Th in the Energy Region 1.5-8.5 MeV (*)

(U. Fasoli(**), D. Toniolo(**), G. Zago(**), L. Zuffi)

The neutron total cross section has been measured in the energy range 1.5÷8.5 MeV with a statistical error less than 2%. The results have been analyzed in terms of a non-spherical optical model because ^{232}Th is a strongly deformed nucleus. Various forms of the optical potential and several coupling schemes of the lowest levels were tried in order to obtain the best agreement with the experimental results. Differential elastic scattering cross-sections were also calculated using the optical model parameters obtained from the analysis, and compared with the experimental results obtained by other authors. The work was published as Doc.CEC(70)1.

6. Direct and collective radiative capture

(G. Longo, F. Saporetti)

For each transition of the $^{208}Pb(p,\gamma)$ and $^{208}Pb(n,\gamma)$ reactions the partial direct and collective cross-sections have been obtained for (6÷30)MeV nucleon energies. The radial, energy and angular momentum dependence of matrix elements has been investigated and explained by means of considerations on the Coulomb and the centrifugal repulsion influences. It has been found that in the (10÷20)MeV energy region the direct capture of protons is favoured with respect to that of neutrons, while the opposite is true for collective capture. The theoretical predictions of direct and collective models for the two kinds of nucleons are in qualitative agreement with the available (n,γ) and (p,γ) experimental data [14].

(*) Work performed under the CNEN-University of Padua Contract.

(**) INFN Group, Institute of Physics, University of Padua.

The trend of nucleon radiative capture cross-sections in the giant resonance region have been studied. Suggestions have been made for measurements to throw light on this trend [15]. The influence of the form and radius of the nuclear charge distribution on the predicted direct and collective cross-sections for proton radiative capture in ^{82}Se and ^{100}Mo has been investigated. Calculations have shown that this influence is a rather small one [16].

References

[1] M. Marangoni and A.M. Saruis - Nucl. Phys. A132 (1969) 649.

[2] N. Bezic, D. Janmik, G. Kernel, J. Krajnik and J. Snaider - Nucl. Phys. A117 (1968) 124.

[3] J.M. Wyckoff, B. Ziegler, H.W. Koch and R. Uhlig - Phys. Rev. 137 (1965) B576.

[4] P.P. Singh, R.E. Segel, L. Meyer - Schützmeister, S.S. Hanna and R.G. Allas - Nucl. Phys. 65 (1965) 577.

[5] M. Marangoni and A.M. Saruis - submitted to Nucl. Phys.-

[6] M. Marangoni and A.M. Saruis - Comm. at the SIF Annual Meeting, Bari, 1969.

[7] G.M. Crawley and G.T. Garvey - Phys. Rev. 167 (1968) 1070.

[8] U. Fasoli, D. Toniolo, G. Zago and V. Benzi - Nucl. Phys. A125 (1969) 227.

[9] J.L. Durell et al. - Phys. Letters 29B (1969) 100.

[10] J. Dubois - Nucl. Phys. A104 (1967) 657.

[11] I. Kelson and C.A. Levinson - Phys. Rev. 134 (1964) 269.

[12] T. Tamura - Rev. Mod. Phys. 37 (1965) 679.

[13] N.K. Glendenning and M. Veneroni - Phys. Rev. 144 (1966) 839; G.R. Satchler - Nucl. Phys. A95 (1966) 1.

[14] G. Longo and F. Saporetti - LV Congresso S.I.F., Bari, ottobre 1969, Boll. 71, pag. 24. Submitted for publication to "Il Nuovo Cimento".

[15] G. Longo and F. Saporetti - "Neutron Capture Gamma Ray Spectroscopy", I.A.E.A., Vienna, 1969, pag. 575.

[16] G. Longo and F. Saporetti -"Contributions and Communications" Int. Conf. on Prop. of Nucl. States, Montreal, August 25-30, 1969, Session 2, pag. 70.

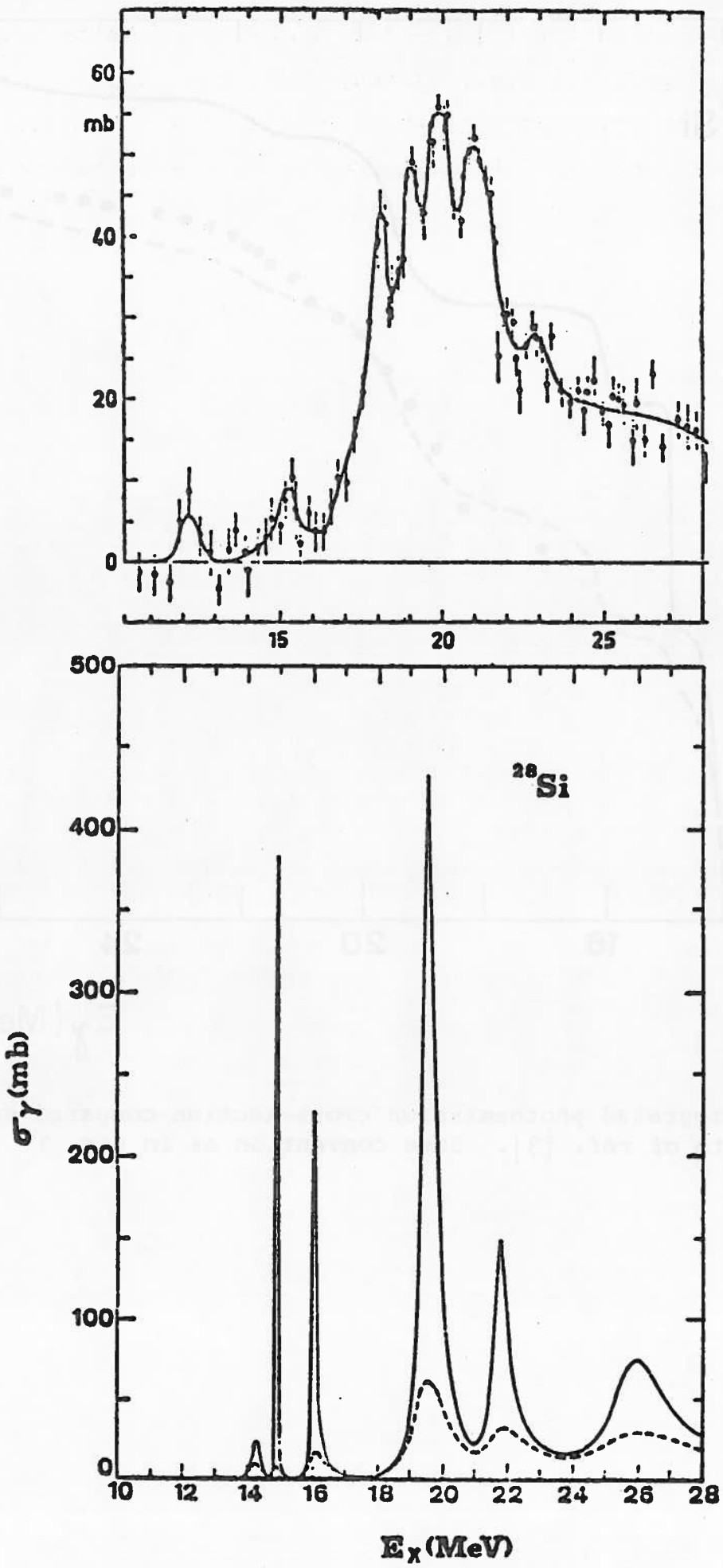

Fig. 1 - Total dipole photoemission cross-section of ^{28}Si compared with the date of ref. [2].
In the dashed curve, the absorptive potential: W(MeV)=0.08E (MeV) - 0.93 has been assumed.
The full curve corresponds to W=0.

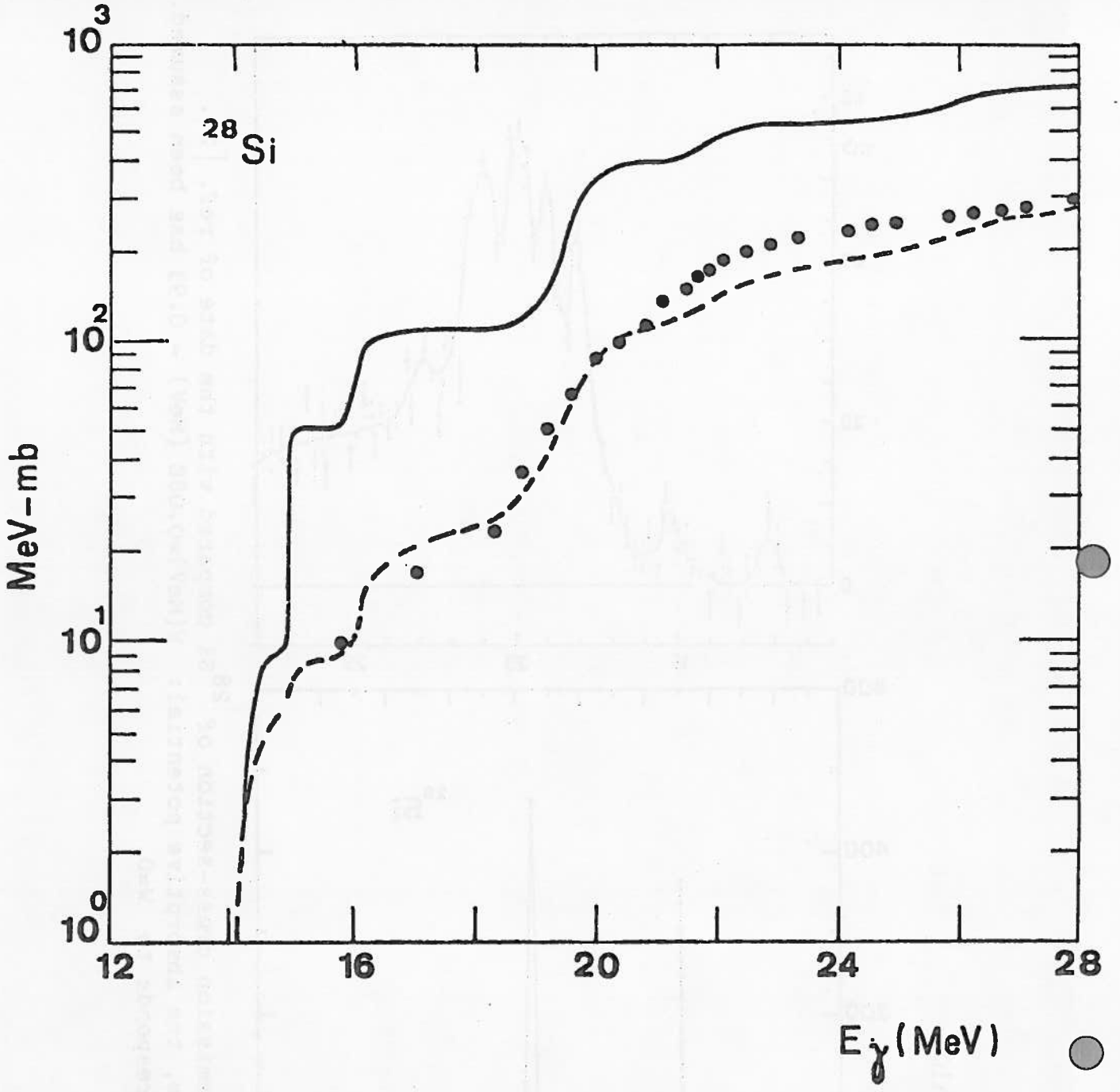

Fig. 2 - Integrated photoemission cross-section compared with the data of ref. [3]. Some convention as in Fig. 1.

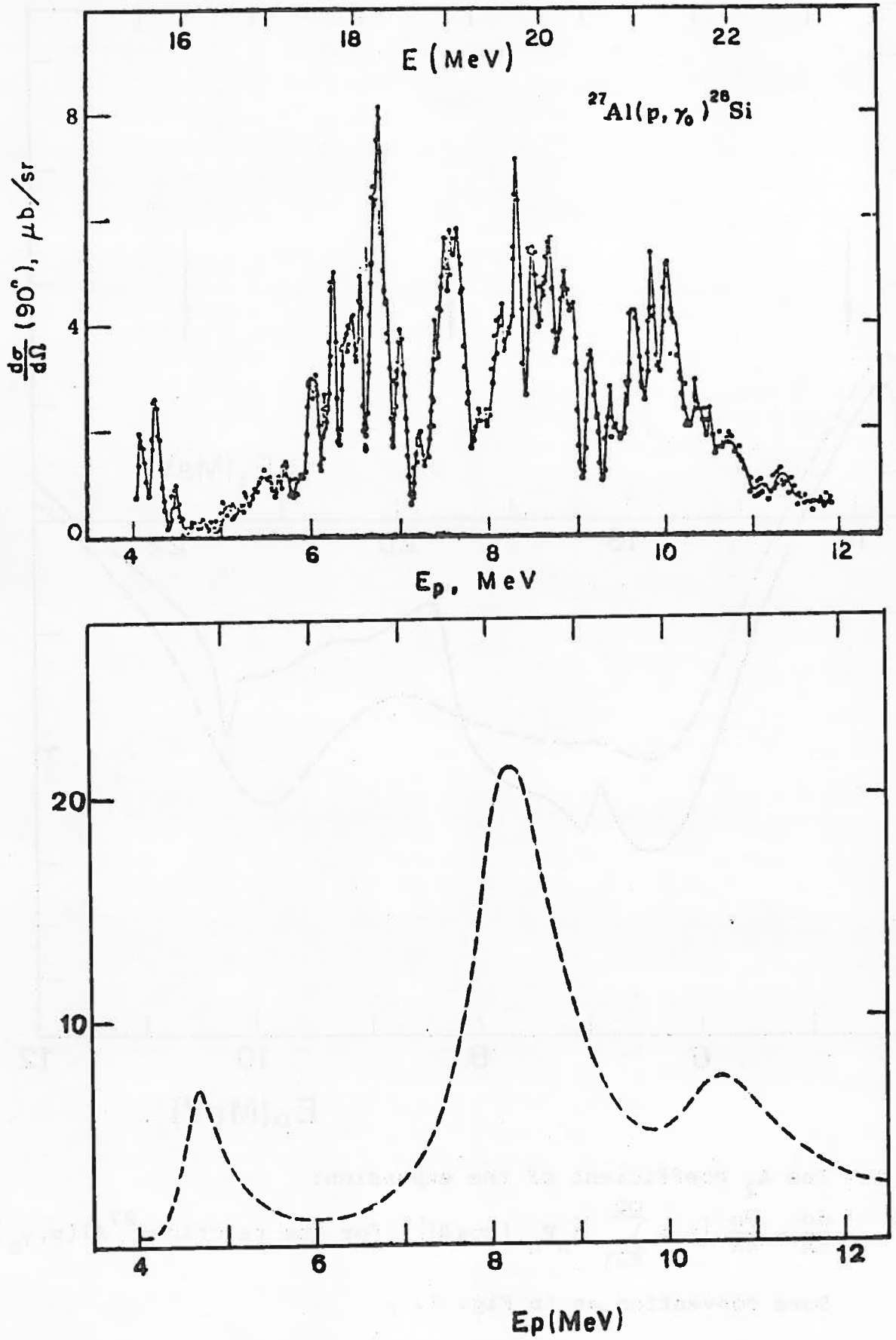

Fig. 3 - The $^{27}Al(p,\gamma_0)^{28}Si$ at 90° cross-section compared with the data of ref. [4].

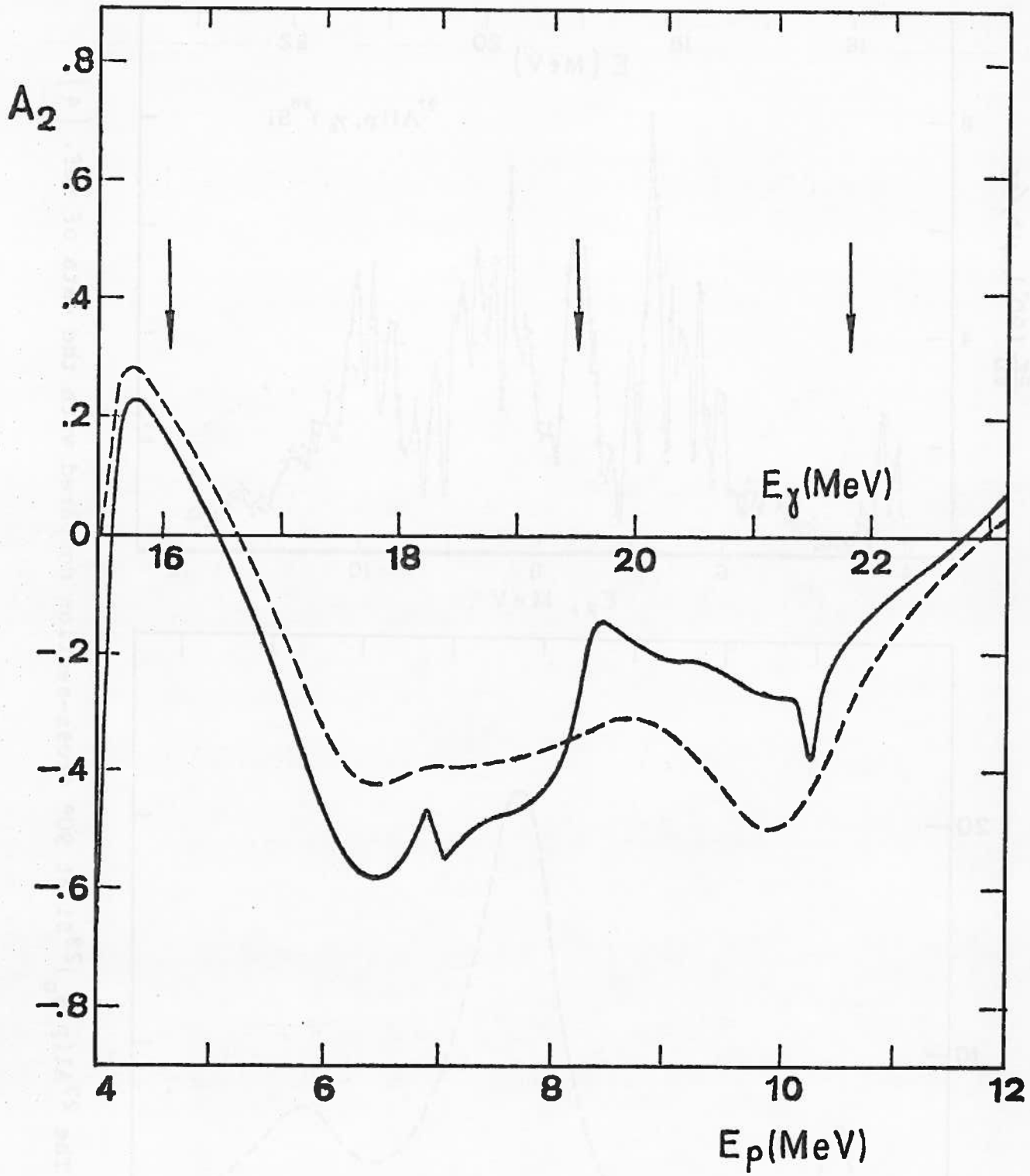

Fig. 4 - The A_2 coefficient of the expansion:

$$\frac{d\sigma}{d\Omega} = \frac{\sigma_o}{4\pi}\left[1 + \sum_{n=1}^{\infty} A_n P_n(\cos\theta)\right]$$ for the reaction $^{27}Al(p,\gamma_o)^{28}Si$

Some convention as in Fig. 1.

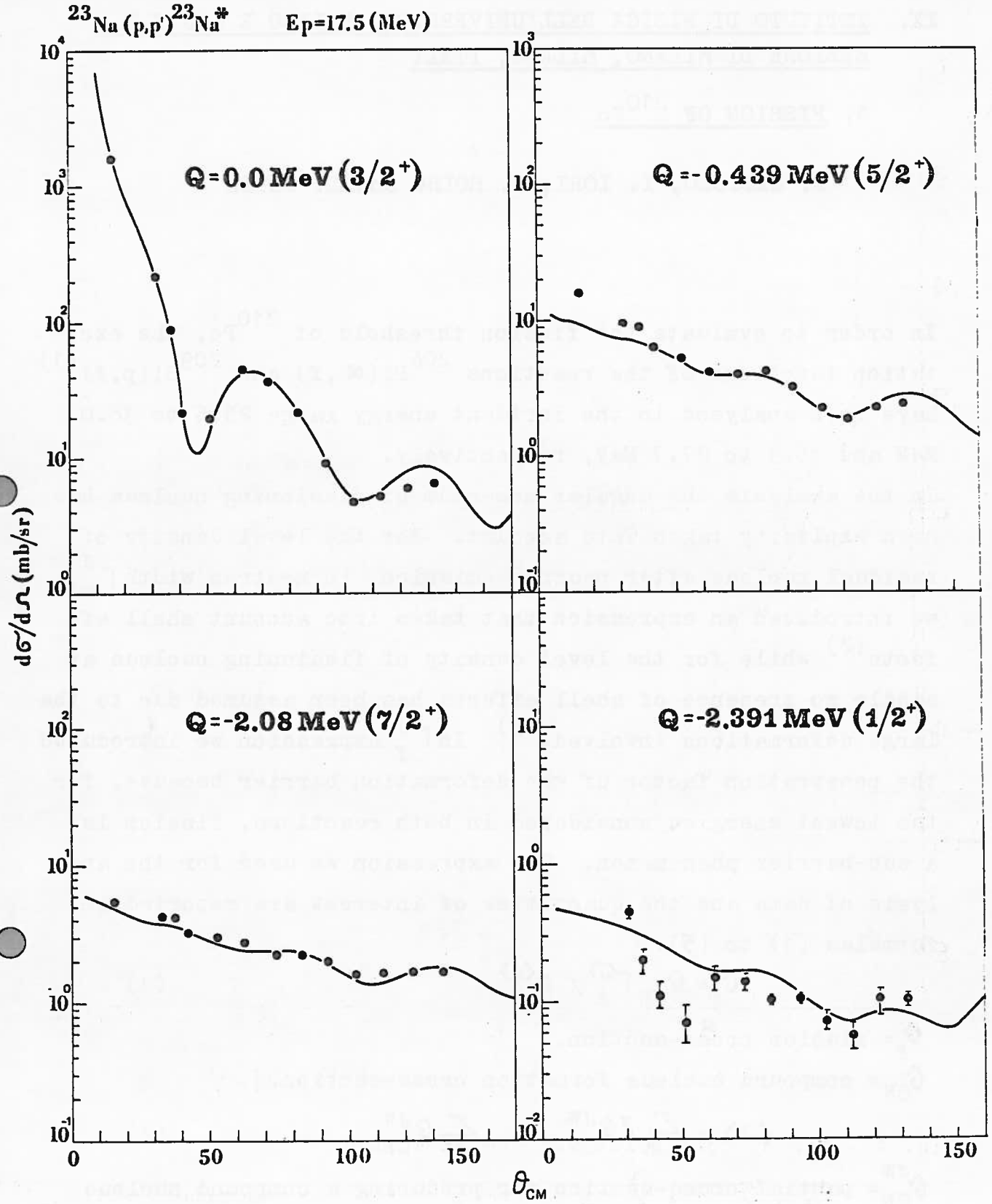

Fig. 5 - The experimental data are taken from G.M. Crawley and G.T. Garvey [7]. The solid curves are the results of coupled channel calculations with the potential parameter values shown in the text.

XX. ISTITUTO DI FISICA DELL'UNIVERSITA, MILANO E I.N.F.N., SEZIONE DI MILANO, MILANO, ITALY

1. FISSION OF ^{210}Po

E. GADIOLO, I. IORI, N. MOLHO and L. ZETTA

In order to evaluate the fission threshold of ^{210}Po, the excitation functions of the reactions $^{206}Pb(\alpha,f)$ and $^{209}Bi(p,f)$[1] have been analysed in the incident energy range 25.6 to 38.0 MeV and 15.3 to 27.7 MeV, respectively.

In the analysis the angular momentum of fissioning nucleus has been explicity taken into account. For the level density of residual nucleus after neutron emission, in neutron width Γ_n^J, we introduced an expression that takes into account shell effects[2] while for the level density of fissioning nucleus at saddle no presence of shell effects has been assumed due to the large deformations involved.[3] In Γ_f^J expression we introduced the penetration factor of the deformation barrier because, for the lowest energies considered in both reactions, fission is a sub-barrier phenomenon. The expression we used for the analysis of data and the quantities of interest are reported in formulas (1) to (5):

$$\sigma_f = \sigma_{CN}\,\Gamma_f^{\langle J\rangle} / \Gamma_n^{\langle J\rangle} \qquad (1)$$

σ_f = fission cross-section,

σ_{CN} = compound nucleus formation cross-section.

$$\langle J\rangle = \sum_{J\pi} J\,\sigma_{CN}^{J\pi} \Big/ \sum_{J\pi} \sigma_{CN}^{J\pi} \qquad (2)$$

$\sigma_{CN}^{J\pi}$ = partial cross-section for producing a compound nucleus of spin J and parity π.

$$\Gamma_n^J(E) = (1/(2\pi\,\rho_{CN}(E^*,J)))\int_0^{\varepsilon_{max}} \left\{\sum_j \rho_R(\varepsilon_{max}-\varepsilon,j)\sum_s\sum_{l,T_l}(\varepsilon)\right\} d\varepsilon \,. \qquad (3)$$

$\rho_R(\varepsilon_{max}-\varepsilon, j)$ = residual nucleus level density defined as in paper (2).

$$\Gamma_f^J=(1/(2\pi\,\rho_{CN}(E^*,J)))\int_0^{E-\Delta_s}\rho(\varepsilon,J)\,d\varepsilon/(1+\exp(-2\pi(E-\Delta_s-B-\varepsilon)/\hbar\omega)) \tag{4}$$

$$\rho(\varepsilon,J)=(1/(24\sqrt{8}))\,\hbar^3\mathcal{J}^{*-3/2}\,a_s^{1/2}\,(\varepsilon+t_s)^{-2}\,\exp(2\sqrt{a_s\varepsilon})\cdot$$
$$\cdot(2J+1)\,\exp(-J(J+1)\hbar^2/(2\mathcal{J}^*\,t_s))$$
$$\mathcal{J}^*=\mathcal{J}_{\parallel}^{1/3}\,\mathcal{J}_{\perp}^{2/3}. \tag{5}$$

Figg. 1 and 2 report the best fits to the considered excitation functions and Table I the best fit parameters.
The expressions utilised for Γ_f^J and Γ_n^J allowed to calculate the ratio $\Gamma_f^J/\Gamma_n^J=f(J)$ for various CN excitation energies.
Fig 3 reports f(J) vs. J at various excitation energies of ^{210}Po.
For the lowest excitation energies f(J) is decreasing with J while usually one assumes that an high CN angular momentum should always favour fission against neutron emission.
The value of the "effective fission threshold" B_{eff} $(=B+\Delta_s)$ has been used to predict the energy behaviour of the anisotropy parameter $K_0^2(E)$ (1),(4) that characterises the angular distributions of fission fragments. The fit is shown in fig 4.
The quantity k^* characterising the two reported curves is defined through the relation:

$$K_0^2(E)=k^*\,A^{5/3}\,10^{-2}\,\langle t\rangle \tag{6}$$

where $\langle t\rangle$, the average thermodinamic temperature of fissioning nucleus at saddle is calculated with Fermi Gas Model.
This value for k^* implies either a quite low value for the nuclear radius ($\simeq 1.1\,A^{1/3}$ fm) or that the value $\mathcal{J}_{sp.rig.}/\mathcal{J}_{eff}$ (being $\mathcal{J}_{sp.rig.}=(2/5)MR^2$ and $1/\mathcal{J}_{eff}=1/\mathcal{J}_{\parallel}-1/\mathcal{J}_{\perp}$) is underestimated, by conventional liquid drop model calculations, by about 15%.(5) However this point requires further study before definite conclusions can be drawn. From the effective fission threshold the value of the fissility parameter x is estimated

to be ~ 0.72 a value about 2% higher than the one recently proposed by Myers and Swiatecki.[6]
A detailed account of this work has been exposed in a paper submitted for publication to Nuclear Physics.

REFERENCES

(1) A. KHODAI-JOOPARI, Ph.D. Thesis, Lawrence Radiation Laboratory Report, UCRL 16489 (1966), unpublished.

(2) E. GADIOLI, I. IORI, N. MOLHO and L. ZETTA, Lettere al Nuovo Cimento, 2 (1969) 904.

(3) V.M. STRUTINSKI, Nuclear Physics A95 (1967) 420.

(4) E. GADIOLI, I. IORI, N. MOLHO and L. ZETTA, Nuclear Physics A 138 (1969) 321.

(5) S. COHEN and W.J. SWIATECKI, Ann. of Phys. 22 (1963) 406.

(6) W.D. MYERS and W.J. SWIATECKI, Arkiv för Fysik 36 (1966) 343.

TABLE I

Reaction	a_s (MeV)	B_{eff} (MeV)	$\hbar\omega$ (MeV)	$\mathcal{J}^*/\mathcal{J}_{sp.rig.}$
$^{206}Pb(\alpha,f)$	27.485	21.95	1.625	1.599
$^{209}Bi(p,f)$	28.485	21.98	1.81	1.599

Best fit parameters obtained from the analysis of $^{206}Pb(\alpha,f)$ and $^{209}Bi(p,f)$ excitation functions.

FIGURE CAPTIONS

Fig. 1
Comparison between calculated (solid line) and experimental values (open circles) of Γ_f^J in the case of the reaction ^{206}Pb (α,f).

Fig. 2
Comparison between calculated (solid line) and experimental values (open circles) of Γ_f^J in the case of the reaction $^{209}Bi(p,f)$.

Fig. 3
J dependence of f(J) for different compound nucleus excitation energies.

Fig. 4
Fit to the experimental values of the anisotropy parameter K_o^2 of the Fermi Gas Model predictions.

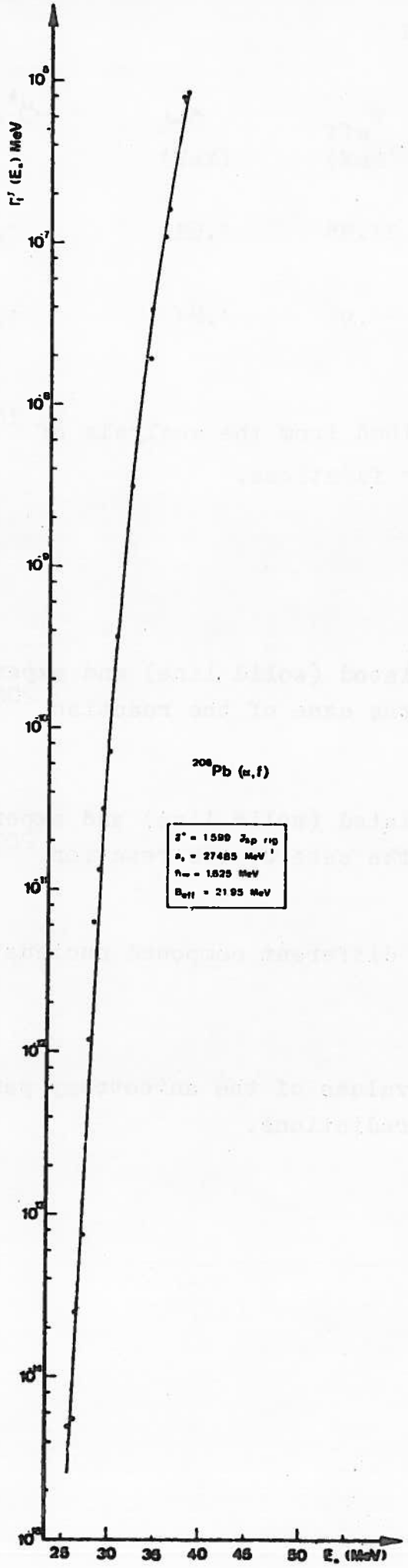
$\Gamma_f^{\prime}$ (E$_n$) MeV
10^8
10^7
10^6
10^5
10^4
10^3
10^2
10^1
10^0
10^{-1}
10^{-2}
^{208}Pb (n,f)
S° = 1.599 $J_{3/2}$ rip
a_f = 27.485 MeV^{-1}
η_m = 1.625 MeV
B_{eff} = 21.95 MeV
25
30
35
40
45
50
E$_n$ (MeV)

Fig. 1

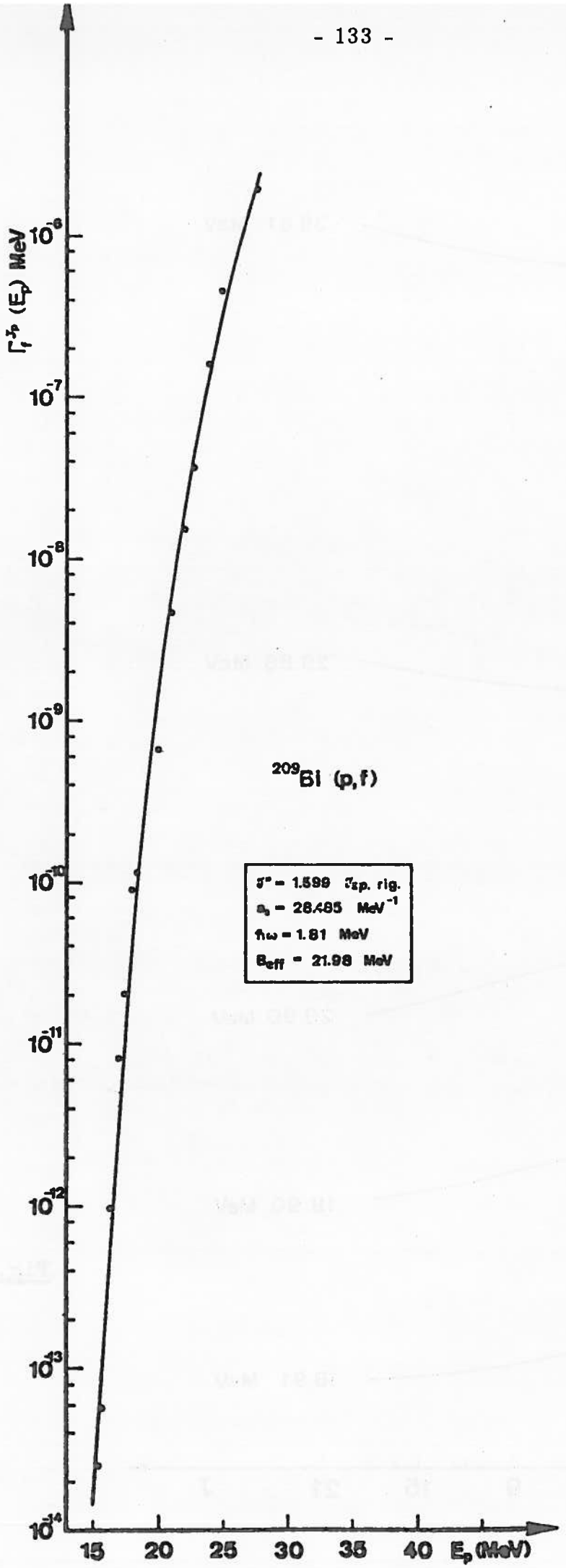
$\Gamma_f^{\lambda\nu}(E_p)$ MeV
10^{-6}
10^{-7}
10^{-8}
10^{-9}
10^{-10}
10^{-11}
10^{-12}
10^{-13}
10^{-14}
15
20
25
30
35
40
E_p (MeV)
^{209}Bi (p,f)
$\sigma^* = 1.599$ $\sigma_{sp.\ rig.}$
$a_0 = 28.485$ MeV^{-1}
$\hbar\omega = 1.81$ MeV
$B_{eff} = 21.98$ MeV

Fig. 2

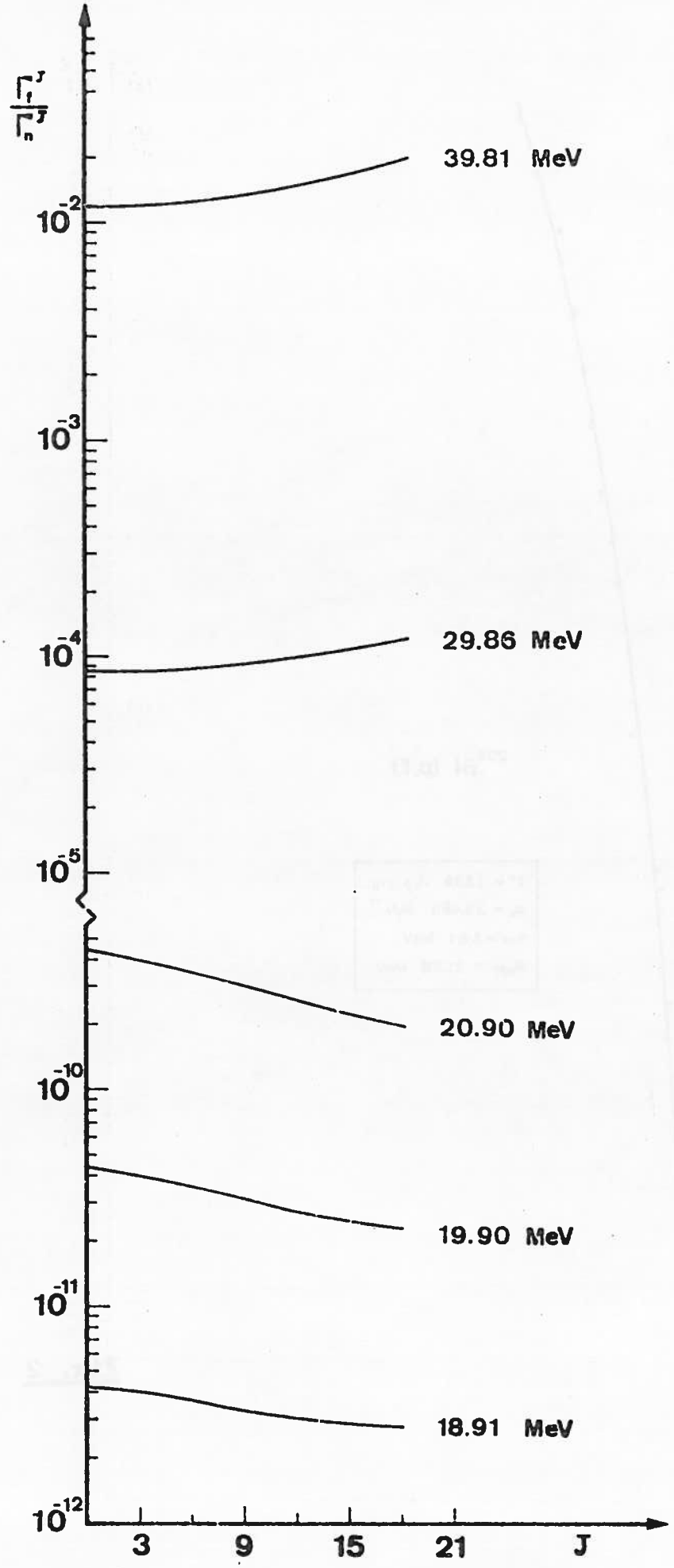
$\frac{\Gamma_\gamma^J}{\Gamma_n^J}$
39.81 MeV
29.86 MeV
20.90 MeV
19.90 MeV
18.91 MeV
10^{-2}
10^{-3}
10^{-4}
10^{-5}
10^{-10}
10^{-11}
10^{-12}
3
9
15
21
J

Fig. 3

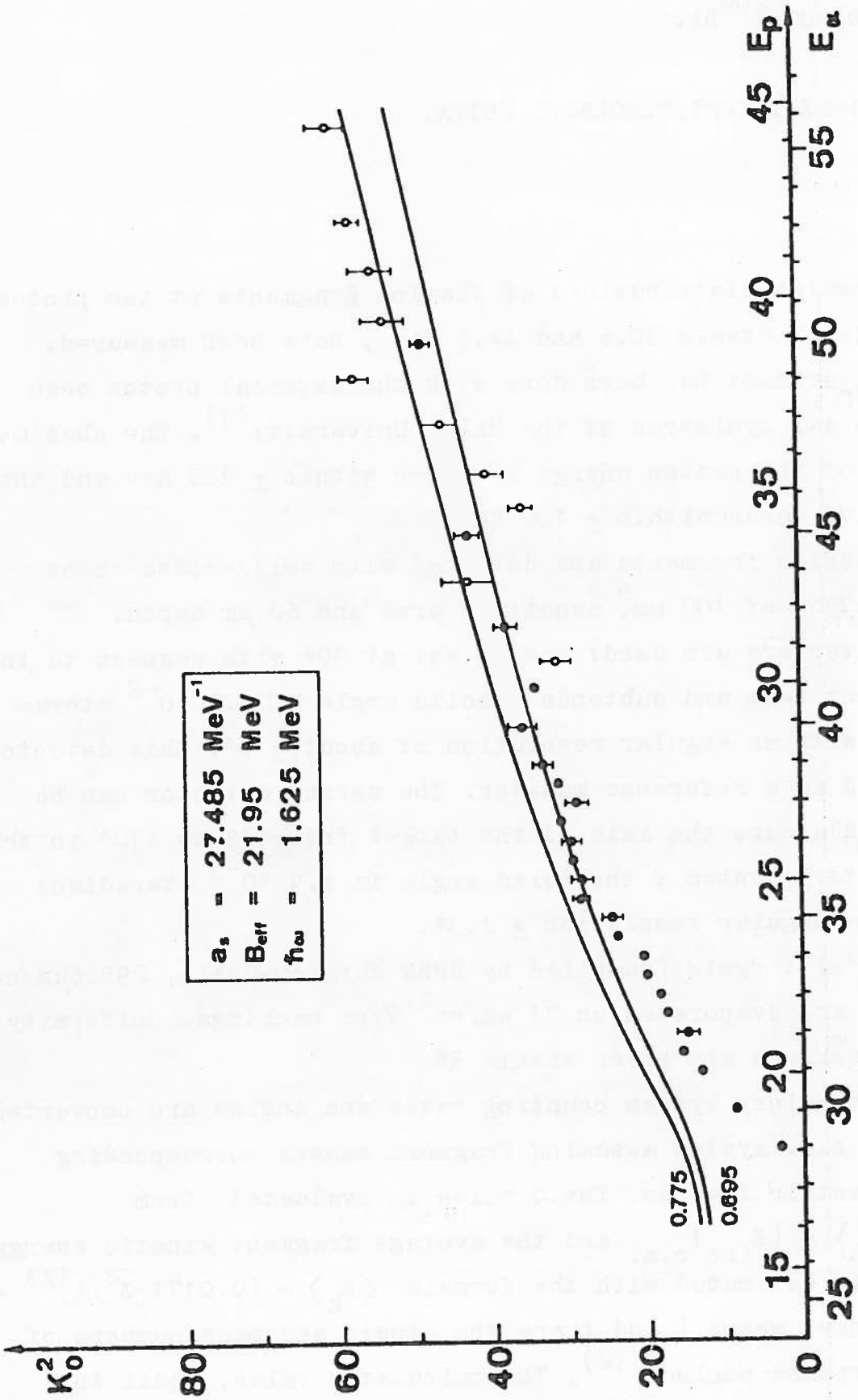
K_0^2
80
60
40
20
0
15
25
20
30
25
35
30
40
35
45
40
50
45
55
E_p
E_α
0.775
0.895
a_s = 27.485 MeV^{-1}
B_{eff} = 21.95 MeV
$\hbar\omega$ = 1.625 MeV

Fig. 4

2. FISSION FRAGMENT ANGULAR DISTRIBUTION IN PROTON-INDUCED FISSION OF ^{209}Bi.

E.GADIOLI, I.IORI, N.MOLHO, L.ZETTA.

The angular distributions of fission fragments at ten proton energies, between 30.6 and 44.5 Mev , have been measured. The experiment has been done with the external proton beam of the AVF cyclotron of the Milan University[1]. The absolute value of the proton energy is given within ± 200 Kev and the relative value within ± 100 Kev.

The fission fragments are detected with solid-state counters Ortec 7901 of 100 mm^2 sensitive area and 60 μm depth.

Two detectors are used: one is set at 90° with respect to the incident beam and subtends a solid angle of 1.5 10^{-2} steradians with an angular resolution of about ± 4°. This detector is used as a reference monitor. The second detector can be rotated around the axis of the target from 15° to 170° in the laboratory system : the solid angle is 4.9 10^{-3} steradians and the angular resolution ± 2.3°.

The ^{209}Bi targets (supplied by CBNM Euratom-Geel), 295.6μm/cm^2 thick, are evaporated on 22 μm/cm^2 Vyns backings. Uniformity and thickness are given within 5%.

The laboratory system counting rates and angles are converted to the c.m. system assuming fragment masses corresponding to symmetric fission. The Q value is evaluated from $Q = \langle E_k \rangle - (E_{inc})_{c.m.}$ and the average fragment kinetic energy $\langle E_k \rangle$ is estimated with the formula $\langle E_k \rangle = (0.0171\ Z^2/A^{1/3} + 22.2)$ Mev, where Z and A are the atomic and mass numbers of the compound nucleus [2]. The calculated value, equal to

149.3 Mev , is in rather good agreement with the measured one of 147 Mev obtained calibrating the detector energy scale with a ^{252}Cf source [3].

In Fig.1 the measured anisotropy $W_{exp}(\theta) = \sigma(\theta)/\sigma(90°)$ is shown as a function of $\theta_{c.m.}$. Due to the symmetry of the angular distributions with respect to 90°, the data at forward angles are reported at the corresponding backward angles. The given errors are purely statistical. In Fig.2 are reported, as a function of tha proton energy, the cross-sections evaluated integrating the best-fit theoretical anisotropies $W(\theta)$. The agreement with the values measured by Joopari[4], with the mica technique, is quite good.

The fissioning nucleus ,at saddle point[5], is characterized by the quantum numbers I (total angular momentum), M (projection of I on a quantization axis assumed coincident with the direction of the incident beam) and K (projection of I on the nuclear symmetry axis). For a Gaussian K distribution $f(K) \propto \exp(-K^2/2K_0^2)$, the exact expression of the angular distribution is given by the following formula[6]:

$$W(\theta) \propto \sum_I \sum_M \left[\sum_L \sum_S \sum_\mu \left(\frac{(2L+1)T_L |\langle SLM0|IM\rangle|^2}{\sum_L (2L+1)T_L} \cdot \frac{|\langle I_0 i \mu (M-\mu)|SM\rangle|^2}{\sum_L (2L+1)T_L} \right) \right] \sum_K \left[(2I+1) |d^I_{MK}(\theta)|^2 \cdot \exp\left[\frac{-K^2}{2K_0^2}\right] \Big/ \sum_K \exp\left[\frac{-K^2}{2K_0^2}\right] \right]$$

where I_0 , i, S are target, projectile and channel spins respectively; $d^I_{MK}(\theta)$ is the symmetrical top wave function[7], T_L are transmission coefficients. The analysis of $W_{exp}(\theta)$

permits to evaluate the K_o^2 values; however, given the complexity of formula (1), that, when the number of contributing L values is large, requires very long computing time, approximate expressions are usually introduced. An expansion of (1) in powers of $\beta = 1/2K_o^2$ is possible when the anisotropy is small[8]. The optical model parameters used in the calculation of T_L, are reported in Tab.I.

In Fig.3 the values of K_o^2 are reported with those obtained from the reaction $^{206}Pb(\alpha,f)$ [9]. The good agreement between the various data shows that, to a good approximation, the angular distributions of fission fragments, for the same compound nucleus and the same excitation energy, are characterized by the same K_o^2 independent of the entrance channel of the fission process.

REFERENCES

1) M.Castiglioni,G.Dutto,M.Fois,F.Resmini,G.Strini,C.Succi and G.Tagliaferri:Nuovo Cimento 41B (1966) 244
2) N.E.Viola jr.:Nucl.Data 1 (1966) 391
3) H.W.Schmitt,W.M.Gibson,J.H.Neiler,F.J.Walter,T.D.Thomas: Physics and Chemistry of Fission I (1965) 331
4) A.Khodai-Joopari:Thesis URCL 16489 (1966)
5) A.Bohr: Proceedings of the International Conference on the Peaceful Uses of Atomic Energy Geneva 1955 2 (1956)151
6) J.R.Huizenga,A.N.Bekhami and L.G.Moretto:Phys.Rev.177 (1969) 1826
7) J.A.Wheeler: Channel analysis of fission in Fast neutron physics 2 (1963) 2051
8) J.J.Griffin: Phys.Rev. 127 (1962) 1248
9) L.G.Moratto,R.C.Gatti,S.G.Thompson,J.R.Huizenga and J.O.Rasmussen: Phys.Rev. 178 (1969) 1845

TABLE I

Optical model parameters for p+^{209}Bi.

V (Mev)	W (Mev)	V_s (Mev)	c	c'	r_o (fm)	r_o' (fm)	a (fm)	a' (fm)	R_c (fm)
-59	-9	-6.6	0.2	0.05	1.2	1.428	0.65	0.704	1.2

The optical model potential is

$$U(r) = V_c(r)+(V+cE)(1+\exp x)^{-1}+i(W+c'E)(1+\exp x')^{-1}+$$
$$+ \lambda\!\!\!^{-2}_{\pi} V_s(1/r)(d/dr)(1+\exp x)^{-1} \quad \vec{\sigma} \times \vec{l}$$

E is the proton energy, $V_c(r)$ is the Coulomb potential due to an uniformly charged sphere of radius R_c and

$x = (r-r_o A^{1/3})/a$, $x' = (r-r_o' A^{1/3})/a'$.

FIGURE CAPTIONS

Fig. 1 - Center of mass angular distributions of fission fragments in proton induced fission of ^{209}Bi for the following proton energies: a) 30.6 Mev. b) 32.7 Mev. c) 34.6 Mev. d) 35.5 Mev. e) 36.8 Mev. f) 38.1 Mev. g) 39.5 Mev. h) 40.8 Mev. i) 42.05 Mev. j) 44.5 Mev.

° backward angles, ● forward angles

Fig. 2 - Proton induced fission cross-sections of ^{209}Bi as a function of proton energy; ° Kodhai-Joopari, ● our data

Fig. 3 - Energy dependence of the anisotropy parameter K_o^2 for the fission nucleus ^{210}Po : ° α + ^{206}Pb, ● p + ^{209}Bi.

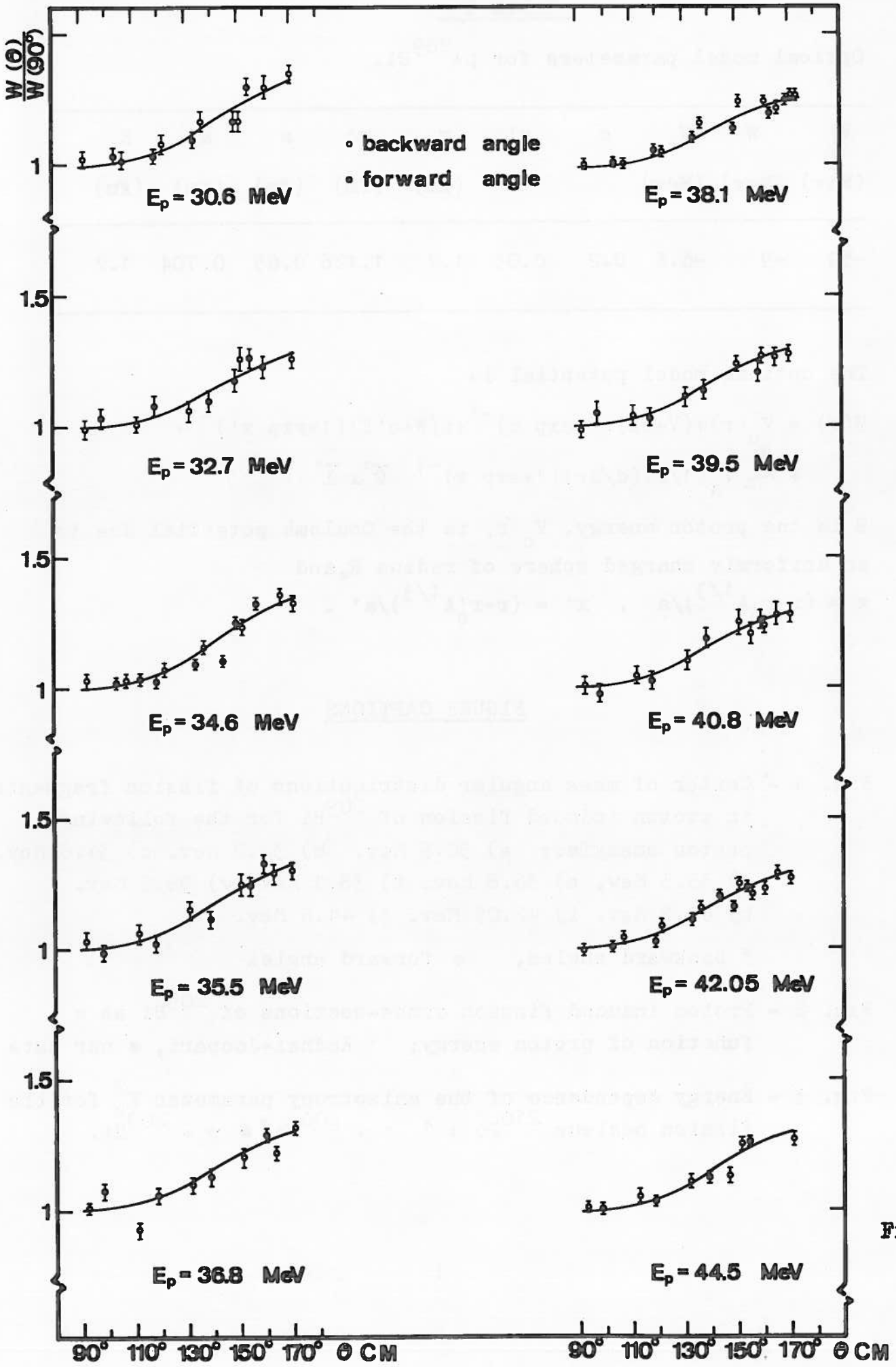
W (θ) / W (90°)
1
1.5
∘ backward angle
• forward angle
Ep = 30.6 MeV
Ep = 38.1 MeV
Ep = 32.7 MeV
Ep = 39.5 MeV
Ep = 34.6 MeV
Ep = 40.8 MeV
Ep = 35.5 MeV
Ep = 42.05 MeV
Ep = 36.8 MeV
Ep = 44.5 MeV
90° 110° 130° 150° 170° θ CM

Fig. 1

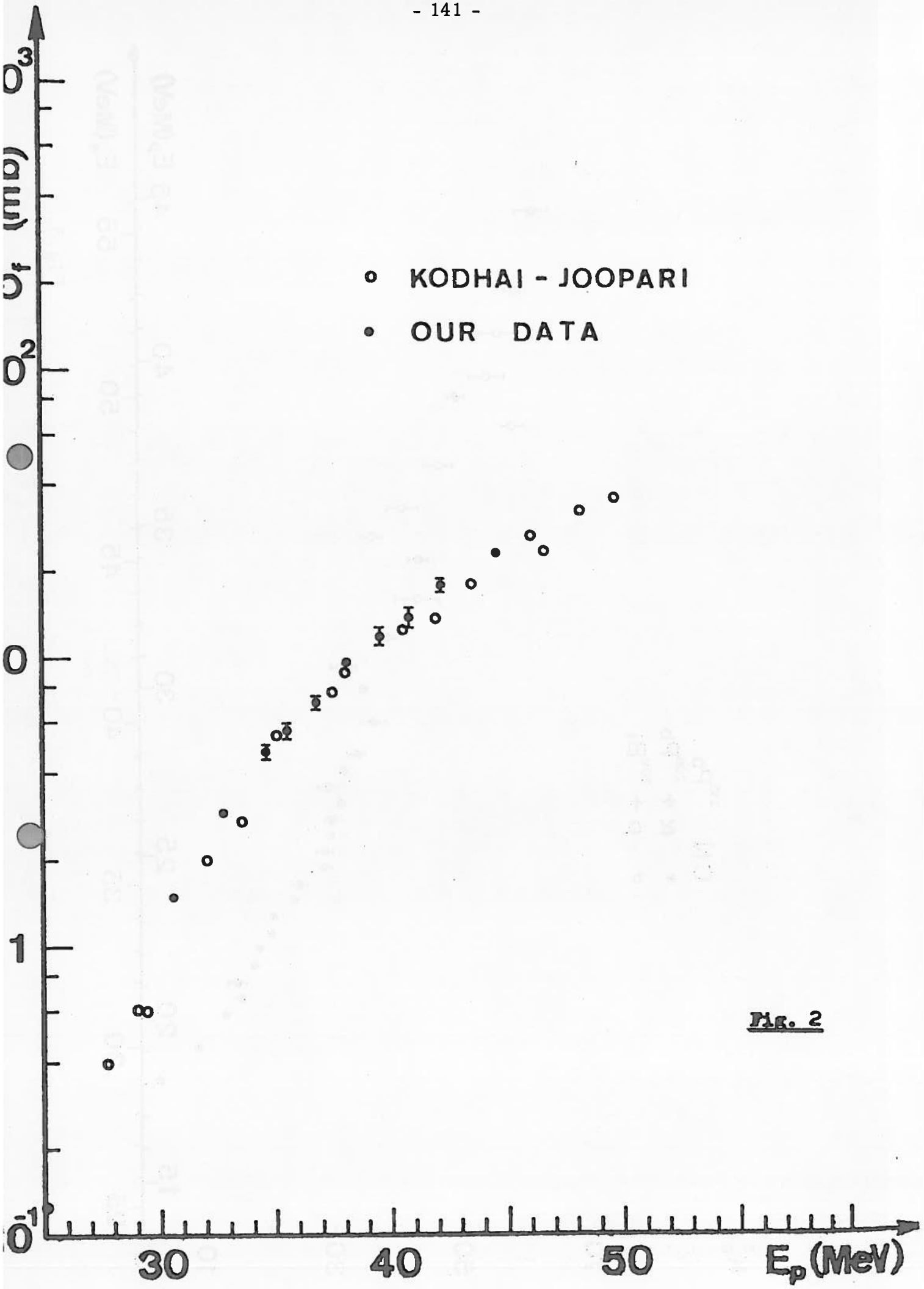
KODHAI - JOOPARI
OUR DATA
10^3
10^2
10
1
10^{-1}
σ_t (mb)
30
40
50
E_p (MeV)

Fig. 2

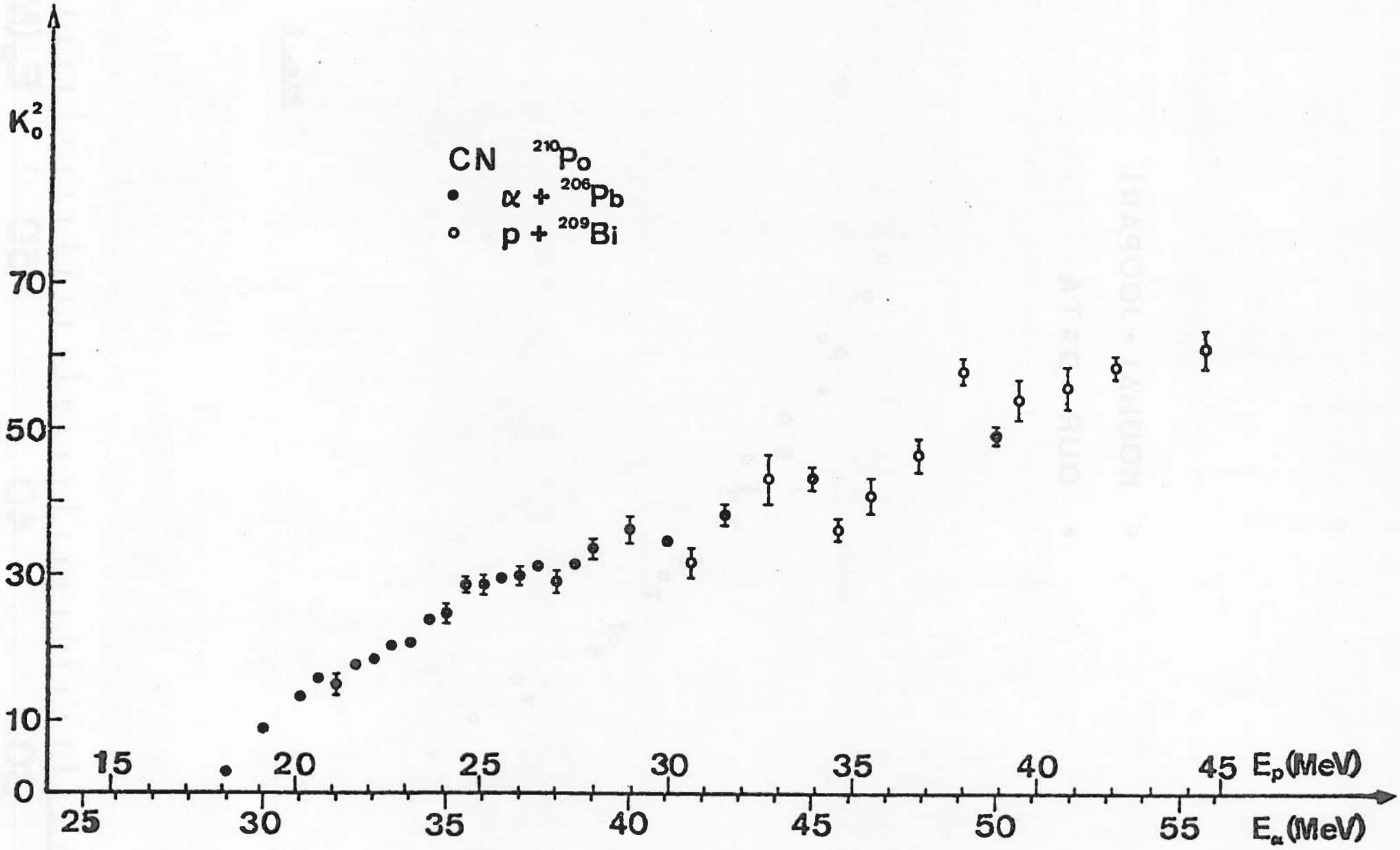
K_o^2
CN ^{210}Po
• $\alpha + {}^{206}Pb$
○ $p + {}^{209}Bi$
70
50
30
10
0
15
20
25
30
35
40
45
E_p(MeV)
25
30
35
40
45
50
55
E_α(MeV)

Fig.3

XXI. SERVICE DE LA METROLOGIE ET DE LA PHYSIQUE NEUTRONIQUES FONDAMENTALES - CEA - SACLAY (FRANCE)

R. JOLY

1. GROUPE DES NEUTRONS THERMIQUES (H. NIFENECKER)

1.1. Etude sur la fission (C. Signarbieux, M. Ribrag, J. Poitou, J. Matuszek)

1.1.1. Mode symétrique dans le cas de la fission à basse énergie

On a mesuré sur la fission thermique de l'^{235}U et de l'^{233}U la distribution de probabilité P (M, EK) - M est la masse de l'un des deux fragments, EK est l'énergie cinétique totale des deux fragments - en éliminant systématiquement les évènements aberrants qui contaminent particulièrement les données dans la région symétrique (voir rapport EANDC (E) - 89). Un résultat nouveau est la variation de la largeur σ_{EK} en fonction de M : contrairement aux données de la littérature (voir Fig. 1) la valeur de σ_{EK} dans la région symétrique diminue significativement à partir de la masse 130 pour l'^{235}U (128 pour l'^{233}U), puis accuse une structure prononcée avant une valeur minimum pour le mode exactement symétrique. On essaie de vérifier que cette structure n'est pas d'origine expérimentale.

1.1.2. Etudes sur la tripartition (en collaboration avec l'Université de Bordeaux)

La technique des émulsions nucléaires a été utilisée pour mesurer avec précision la corrélation énergie cinétique - angle (par rapport à la direction des fragments) des particules alpha de long parcours émises lors de la tripartition de l'^{235}U par neutrons thermiques [1].

Une expérience multiparamétrique a été réalisée pour étudier la probabilité de tripartition en fonction du rapport des masses des gros fragments en faisant un effort expérimental particulier pour étendre les mesures dans les régions symétriques et très asymétriques où il n'existe pas de données dans la littérature. Les résultats sont montrés sur la figure 2 : exaltation de la probabilité dans la région symétrique, diminution notable dans la région très asymétrique. Un essai d'interprétation est donné dans la publication citée en référence [2].

1.1.3. Etude de l'émission neutronique prompte par les fragments individuels

a) Méthodes d'analyse : un programme de Monte Carlo qui permet de simuler l'émission neutronique par les fragments de fission et la détection des neutrons dans un milieu scintillant de géométrie variable a été developpé [3]. Ce programme a permis de déterminer les dimensions optimum du détecteur : on a choisi deux demi-sphères de 1 m de diamètre. On peut ainsi obtenir la loi de probabilité P (ν_1, ν_2) pour qu'un fragment émette ν_1 neutrons et le fragment complémentaire ν_2 neutrons.

Les détecteurs ayant des efficacités finies il y avait lieu de mettre au point une méthode permettant d'obtenir P (ν_1, ν_2) à partir de l'histogramme Q (P_α, P_β) représentant la probabilité de détecter P_α neutrons dans un détecteur et P_β dans l'autre, lors d'un évènement de fission. La méthode de correction d'efficacité qui généralise celle utilisée par Diven et al. est décrite dans la référence [4]. Elle permet, entre autres, de relier les moments de P aux moments de Q.

b) Mesure de l'émission neutronique des fragments individuels du ^{252}Cf en fonction de leur charge (en collaboration avec le CEN de Bruyères-le-Châtel) : des résultats partiels [5] [6] ont été publiés : ils sont relatifs aux valeurs des moments d'ordre 1 et 2 de la distribution des neutrons émis en fonction de la charge des fragments, ainsi qu'aux valeurs des pentes $\langle \frac{dN_1}{dE_T} \rangle$, et $\langle \frac{dN_T}{dE_T} \rangle$ de la variation du nombre de neutrons émis en fonction de l'énergie cinétique totale des fragments. Des résultats complémentaires sont donnés par le tableau I. Il apparaît que le fragment léger absorbe environ 2/3 de l'énergie d'excitation supplémentaire apportée au système des deux fragments. Cette constatation est en accord avec l'hypothèse qui veut que le fragment lourd soit plus rigide que le fragment léger. Par ailleurs l'énergie nécessaire pour émettre un neutron est beaucoup plus grande pour le fragment léger que pour le fragment lourd. La valeur élevée de cette énergie pour le fragment léger ne s'explique que par l'existence d'une compétition entre l'émission de neutrons et l'émission gamma. Cette compétition est particulièrement forte si le noyau excité est très déformé, conformément aux calculs de Sperber.

c) Mesure du nombre total de neutrons émis par fission du ^{252}Cf en fonction de la masse des fragments : le détecteur décrit en a) a été utilisé dans une première expérience consistant à mesurer la distribution P (ν_T, m, E_T^c) ou m est la masse d'un fragment (le fragment léger par exemple), E_T^c l'énergie cinétique totale des fragments. Il apparaît dès maintenant que la variance σ^2 (ν_T : m) de l'émission neutronique varie peu en fonction de la masse des fragments. Ce résultat justifie à priori le traitement des données pour l'expérience décrite en b). De même la valeur moyennée sur E_T de $\langle \sigma^2$ (ν_T : E_T, m) $\rangle$, variance de l'émission neutronique pour E_T et m donné, varie peu en fonction de la masse et vaut environ 0,5 ; cette valeur est notablement inférieure à la valeur de σ^2 (ν_T : m) qui vaut environ 1,5. Ainsi la largeur de l'émission neutronique semble due essentiellement à la largeur de la distribution d'énergie d'excitation des fragments et non au processus d'évaporation. Cette remarque confirme également les résultats exposés en b).

d) Mise en évidence d'une source d'erreur systématique dans les mesures de $\bar{\nu}$ réalisées avec la technique du scintillateur liquide (en collaboration avec le CEN de Bruyères-le-Châtel) : les mesures de $\bar{\nu}$ faites avec un scintillateur liquide reposent généralement sur l'hypothèse que l'efficacité de détection pour le signal synchrone de la fission (γ prompts + protons de recul) est indépendante du nombre de neutrons émis.

Pour le scintillateur liquide de Bruyères-le-Châtel (Ø 75 cm), on a mis en évidence une variation d'efficacité, pratiquement linéaire, de 8 % entre l'efficacité pour 0 neutron et l'efficacité pour 7 neutrons. Cette variation si elle est négligée se traduit par une erreur systématique de 0,6 % sur la mesure de l'efficacité neutronique du détecteur (83 %).

Pour le scintillateur liquide de Saclay (deux hémisphères accolées de Ø 100 cm) la variation de même allure mais d'amplitude plus faible se traduit par une erreur de 0,3 % sur l'efficacité neutronique du détecteur (78 %).

Cet effet pourrait éventuellement expliquer les divergences actuelles existant entre les différentes mesures de $\bar{\nu}$ pour le ^{252}Cf.

e) Mesure simultanée de la distribution en charge, en énergie cinétique et en masse des fragments de fission de ^{235}U + n : on a réalisé une expérience dans laquelle on enregistrait simultanément l'énergie cinétique des deux fragments et l'énergie délivrée par un détecteur de rayons X. En même temps, pour comparaison, on enregistrait l'énergie des fragments sans condition de coïncidence sur le détecteur de rayons X.

Les dépouillements sont en cours. L'expérience b) nous ayant amenés à envisager que l'émission de rayons X soit favorisée pour les fissions d'énergie cinétique totale faible, nous avons comparé les variations de l'énergie cinétique totale moyenne en fonction de la masse pour des fissions donnant lieu à émission X et pour des fissions quelconques. Nous avons constaté que entre les masses légères 80 et 107 les énergies cinétiques totales moyennes étaient identiques dans les deux cas. Entre la masse 107 et la masse 112 l'énergie cinétique moyenne des fissions accompagnées d'émission de rayons X est inférieure d'environ 2 MeV à celle des fissions quelconques.

1.2. Spectrométrie nucléaire par γ de capture de neutrons thermiques (R. Samama, A. Audias, R. Babinet, J. Girard)

a) Spectrométrie directe : utilisant un détecteur Ge (Li) de 120 cm^3, l'étude des spectres directs des réactions suivantes a été faite : ^{138}Ba (n, γ) ^{139}Ba,

^{85}Rb (n, γ) ^{86}Rb ; ^{139}La (n, γ) ^{140}La, ^{140}Ce (n, γ) ^{141}Ce.

Un schéma de désexcitation à partir du niveau de capture a été établi pour chacun de ces corps [7] .

b) Spectrométrie de "paires" et "d'absorption totale" : ce spectromètre est constitué d'un détecteur au Ge (Li) placé au centre d'un gros cristal annulaire d'I Na.

Une unité de logique électronique permet l'acquisition simultanée sur bande magnétique 16 pistes des spectres de paires et d'anti-Compton pour le corps étudié.

Les réactions ^{62}Ni (n, γ) ^{63}Ni [8] et ^{60}Ni (n, γ) ^{61}Ni [9] ont été étudiées ; l'étude du ^{176}Lu a été entreprise.

La précision que nous permettent d'atteindre nos méthodes de dépouillement est limitée par celle des étalons, du moins en ce qui concerne les transitions les plus intenses.

c) Etude des coïncidences $\gamma - \gamma$ à l'aide de deux détecteurs Ge (Li) : un ensemble a été mis au point pour étudier les cascades γ, γ émises après capture neutronique. Les informations en coïncidence sont stockées à l'aide d'un enregistreur multiparamétrique sur bandes magnétiques traitées ensuite par le calculateur 360/9

Un enregistrement a été effectué portant sur 20.10^6 informations en coïncidence dans la réaction ^{175}Lu (n, γ) ^{176}Lu. Le dépouillement de cette expérience est en cours.

1.3. Etude du rayonnement de fluorescence des niveaux nucléaires (M. Schneeberger, R. Lucas, J. Fagot)

Un faisceau γ d'énergie variable a été réalisé auprès du réacteur Triton. Ce faisceau d'énergie variable est obtenu par la diffusion Compton des rayons γ d'une cible en Titane placée près du cœur de la pile. La figure 3 montre le dispositif expérimental et la réponse d'un ensemble scintillant placé dans le faisceau réfléchi. Le flux sortant à l'extrémité du canal de la pile est de $5,5.10^8$ photons de 6,75 MeV/cm^2/s. Une expérience préliminaire de fluorescence a été entreprise sur le niveau à 3,560 MeV du ^6Li. (Fig. 4)

1.4. Installations nouvelles

Un deuxième tube conducteur a été mis en fonctionnement. Il mesure 50 m et donne un flux de sortie de 7.10^7 n /cm^2/s. Ce flux doit être notablement augmenté par la mise en service d'une source froide.

. GROUPE DES NEUTRONS INTERMEDIAIRES (A. MICHAUDON)

L'accélérateur linéaire a été arrêté pendant une période de 4 mois (de juillet à octobre 1969) au cours de laquelle il a été profondément modifié. En particulier les sections ont été changées et leur nombre a été porté à 4, l'intensité de la source de neutrons se trouvant approximativement doublée.

Cet arrêt a été mis à profit pour effectuer un certain nombre de travaux (Ch. Eggermann), comportant notamment l'étude d'une nouvelle cible productrice de neutrons pouvant dissiper 6 à 8 kw.

2.1. Electronique - Calculateur CAE 510 - Programmes de dépouillement et d'analyse des données (B. Cauvin, M. Sanche)

2.1.1. Système d'acquisition de données

- Agrandissement du parc du matériel électronique : en particulier un codeur de temps de résolution 1ns par canal est disponible. Le développement des expériences a nécessité une extension des dispositifs particuliers (tels que l'utilisation en 8 K des blocs-mémoires BM 96) et des unités d'enregistrement sur bande magnétique 16 pistes.
- Développement des organes périphériques du calculateur CAE 510 ; des dispositifs d'affichage numérique (utilisant largement la technique des circuits intégrés) ont été associés à la visualisation du calculateur, qui améliorent la manipulation des réticules et du crayon sensible.

2.1.2. Programmation

- Programmation du calculateur CAE 510 en ligne sur l'acquisition des expériences. Les travaux ont porté sur l'organisation des programmes secondaires en vue d'une vérification de plus en plus précise et complète des résultats avant d'entreprendre leur dépouillement : visualisation, tracé, impression, perforation de séries brutes de la veille sont possibles en cours d'acquisition d'une expérience. Ces différents programmes secondaires seront, dans une étape ultérieure, automatiquement enchaînés en l'absence d'opérateur par lectures successives, pendant l'acquisition, d'un ruban perforé, préposé avant le départ en ligne du calculateur.
- Programmation du calculateur CAE 510 hors ligne. La bibliothèque des programmes hors-ligne s'est enrichie de programmes effectuant : la correction de spectres ayant subi des dérives par rapport à un spectre de référence ; la normalisation rapide d'une zone de l'expérience en cours dont on veut vérifier la bonne marche ; des traitements et vérifications divers de bande magnétique support de résultats expérimentaux ou support de programmes.

- Programmation des gros calculateurs du centre : les programmes de prédépouillement ont été complétés et améliorés par adjonction de modules s'insérant dans le système central fonctionnant sur 360-91.

Une visualisation conversationnelle IBM 2250 couplée au calculateur 360-91 est mise à la disposition des physiciens. Son utilisation a nécessité la réécriture des programmes d'analyse de forme des résonances et de convolution de fonctions de probabilité.

Un programme de dépouillement des expériences biparamétriques (4 K en temps et 4 K en amplitude) élabore une matrice de 16 millions de classes d'évènements représentant chaque jour la somme des expériences acquises à l'origine sur bandes 16 pistes. Cette matrice est supportée par une bande 9 pistes unique de densité 1 600 c/p. Les conditionnements sont ensuite facilités car tous les évènements sont gardés jusqu'à la fin du dépouillement.

2.2. Sections efficaces totales dans la région des résonances (H. Tellier)

2.2.1. Les mesures faites en 1968 sur les isotopes stables du Tellure ont été analysées [10] [11].

2.2.2. L'Holmium, refroidi à la température de l'azote liquide, a été étudié en utilisant des distances de vol de 53 et 103 mètres. La gamme d'énergie analysée s'étend jusqu'à 1,7 keV. Nous avons détecté 346 niveaux et déterminé la fonction densité pondérée sur les deux états de spin qui est : $\bar{S}_o = (1,77 \pm 0,15)\ 10^{-4}$

Les spins d'un certain nombre de résonances d'énergie inférieure à 645 eV ont été obtenus par la mesure de la multiplicité des rayons γ (voir 2.4.). La fonction densité est notablement différente suivant l'état de spin [12] (fig. 5) :

$S_o\ (J = 3) = (2.54 \pm 0.53)\ 10^{-4}$ et $S_o\ (J = 4) = (1.44 \pm 0,29)\ 10^{-4}$

2.2.3. La résonance à 4,9 eV de l'or a été étudiée à 17,9 mètres en utilisant quatre épaisseurs d'échantillon (3,8 à 101 μ). Les paramètres obtenus sont les suivants $E = 4,900 \pm 0,005$ eV ; $\Gamma = 137,5 \pm 2,0$ meV et $\Gamma_n = 15,0 + 0,2$ meV. [12 bis]

2.2.4. Une étude systématique de la fonction de résolution du ralentisseur a été entreprise en analysant certaines résonances très étroites de l'uranium naturel.

2.3. Sections efficaces totales moyennes (Ch. Newstead, B. Cauvin)

Le but de cette mesure est de déterminer les fonctions densité pour les neutrons "s", "p" et "d", grâce à l'analyse de la section efficace totale moyennée sur un grand nombre de résonances.

Des résultats préliminaires ont été obtenus de 10 keV à 2 MeV pour Te et H_o avec une base de vol de 200 mètres. Les premiers résultats ont également permis d'obtenir un certain nombre d'informations nécessaires à la construction d'un nouveau

détecteur au ^{10}B qui a été réalisé et installé à une distance de vol de 200 mètres. Ce nouveau détecteur sera utilisé en 1970 pour améliorer les résultats déjà obtenus sur H_o et Te et également pour étudier ^{239}Pu. La fonction densité pour les neutrons "p" de ces noyaux est intéressante pour les raisons suivantes :

- dans le cas de Te, elle peut permettre de préciser l'aile du côté des nombres de masse élevée, de la résonance 3 P.
- dans le cas de H_o et de ^{239}Pu, elle peut aider à vérifier le dédoublement possible de la résonance 4 P, par couplage rotationnel tel qu'il a été prédit par Buck et Peray.

2.4. Multiplicité des rayons γ de capture radiative (B.Cauvin, A.Katsanos, C.Newstead)

La technique de mesure des spins des résonances par la multiplicité des rayons γ de capture radiative a été utilisée pour plusieurs noyaux moyens et lourds : ^{121}Sb, ^{123}Sb, ^{127}I, ^{129}Xe, ^{131}Xe, ^{147}Sm, ^{149}Sm, ^{165}Ho. Les résultats ont été obtenus avec ces bases de vol de 20 mètres et de 50 mètres et une résolution qui, au mieux était de 1 ns/m. Tous les résultats expérimentaux ont été analysés sauf pour le Xe.

Pour Sb, aucune variation significative n'a été observée de résonance en résonance

Pour l'I, l'attribution du spin a pu être faite pour la plupart des résonances jusqu'à une énergie de 237 eV. Les résultats sont donnés sur la figure 6 où le rapport R des taux de comptage "simple" et "en coïncidence" est porté en fonction de l'énergie des résonances. Le groupe de résonances ayant la valeur la plus élevée de R correspond à J = 2, l'autre groupe (valeur la plus faible de R) à J = 3.

Pour le Sm, les mesures ont été faites avec un échantillon de Saramium naturel. Environ 80 résonances ont été analysées jusqu'à 180 eV : Les rapports R, correspondants sont portés sur les figures 7 et 8. Le spin était déjà connu pour 11 d'entre elles pour ^{147}Sm et pour 25 autres dans ^{149}Sm. Ces mesures ont en outre montré qu'il était possible de faire une attribution isotopique de certaines résonances en comparant leur rapport R aux valeurs moyennes de R pour les deux états de spin des deux isotopes impairs ; c'est ainsi que :

- les résonances à 107,1 - 163,8 - 171,8 eV appartiennent à ^{147}Sm (J = 4),
- la résonance à 44,3 eV appartient à ^{149}Sm (probablement J = 4)
- les résonances à 60,9 - 111,4 - 119,6 - 154,4 appartiennent à ^{149}Sm (J = 3)
- les résonances à 40,8 - 50,5 - 74,7 - 104,7 - 109,2 - 115,3 - 125,4 - 134,3 - 140,2 - 151,7 - 168,5 - 178,1 - 179,9 eV appartiennent soit à ^{147}Sm (J = 3) soit ^{149}Sm (J = 4)

- la résonance à 77 eV appartient à un isotope impair sans qu'il soit possible de préciser lequel.

Pour l'Ho, une centaine de résonances ont été analysées jusque vers 650 eV. Cette mesure conduit donc à un échantillonnage statistique suffisant pour étudier, d'une façon significative la variation de la fonction densité S_o en fonction de l'état de spin : une forte dépendance a été soulignée au paragraphe 2.2.2. ci-dessus.

2.5. Diffusion élastique (J. Trochon)

L'ensemble expérimental a été adapté à l'étude des noyaux fissiles : comme pour les corps non fissiles, la mesure utilise des scintillateurs liquides chargés en bore 10. Mais ces détecteurs étant sensibles aux neutrons de fission, nous faisons simultanément une mesure identique avec des scintillateurs liquides sans bore. La contribution de la fission peut ainsi être soustraite de la mesure de diffusion. Les conditions expérimentales sont les suivantes :

- détecteur de neutrons diffusés : 6 cellules indépendantes (Ø = 47 mm ; e = 15 mm chargées au NE 321 A, chacune étant couplée à un photomultiplicateur EMI 9514 SA la discrimination de forme neutrons-γ en l'absence de faisceau et en présence de l'échantillon de ^{239}Pu utilisé ($5{,}5.10^{-4}$ at/b) permet une atténuation de $\simeq 0{,}7.10^{5}$ du taux de comptage γ pour un taux de perte de $\simeq$40 % sur les neutrons lents.
- détecteur de fission : deux cellules identiques aux précédentes mais chargées au NE 213 et couplées à des photomultiplicateurs 56 AVP 03
- échantillons utilisés : $5{,}5.10^{-4}$ at/b et $4{,}0.10^{-4}$ at/b
- taux de comptage du détecteur de neutrons diffusés : $\simeq$250 c/mn sur la base de vol de 32 m utilisée (accélérateur : 500 c/s ; 50 ns).

Les spins d'environ 120 résonances, entre 10 eV et 650 eV, ont été déterminés il apparaît un léger excès de niveau 0^+ vis-à-vis de la loi en 2 J + 1 ; les fonction densité trouvées sont respectivement : $S_o^- = (1{,}77 \pm 0{,}34)\ 10^{-4}$

$$S_o^+ = (0{,}91 \pm 0{,}18)\ 10^{-4}$$

2.6. Sections efficaces de fission (J. Blons)

2.6.1. ^{239}Pu : les mesures effectuées en 1968 ont permis d'analyser 255 résonances jusqu'à une énergie de 660 eV.

La distribution des largeurs de fission par intervalle d'énergie de 110 eV a montré une variation relative très nette de $\langle \Gamma_f \rangle$ pour les résonances étroites (de spin 1^+) allant de 64 meV à 6 meV, ce qui n'est pas le cas pour les résonances larges (de spin 0^+).

Ceci est illustré par les figures 9 et 10 où sont tracées les distributions des largeurs de fission respectivement pour les gammes d'énergie 110 eV - 220 eV et 350 eV - 660 eV. D'une façon plus qualitative, la brusque diminution de la largeur de fission des résonances étroites situées au-dessus de 580 eV est visible à la comparaison des sections efficaces totale et de fission telles qu'elles sont tracées sur la figure 11. Les résonances étroites sont systématiquement d'amplitude plus faible dans σ_f au-delà de 580 eV.

Cette étude montre, dans le cas de ^{239}Pu, l'existence d'une structure intermédiaire dans la partie de la section efficace de fission qui est due à la voie 1^+ [13] [14].

2.6.2. ^{235}U : la mesure de la section efficace de fission de l'^{235}U a été effectuée dans des conditions de résolution analogues à celles du ^{239}Pu (scintillateur gazeux fonctionnant à la température de l'azote liquide et situé à 50 m ; l'accélérateur : 500 c/s, 50 ns). L'analyse est en cours et permettra d'obtenir un ensemble des paramètres des résonances jusqu'aux environs de 150 eV.

2.6.3. ^{241}Pu : une mesure de section efficace de fission du ^{241}Pu a été effectuée à basse énergie (entre 1 eV et 3 keV) à la température de l'azote liquide avec un scintillateur gazeux contenant 140 mg de ^{241}Pu (distance de vol : 11 m, accélérateur : 500 c/s, 100 ns).

Cette mesure avait deux buts :

- connaître les paramètres de résonances à basse énergie,
- préparer la mesure à haute énergie et haute résolution qui sera effectuée à 50 m en 1970.

L'analyse à un niveau des résonances de 1 à 70 eV est terminée et une analyse multiniveaux de 1 à 32 eV est en cours notamment pour quelques cas marquants d'interférence entre résonances vers 4 eV, 6 eV et 10 eV.

2.6.4. ^{237}Np (D. Paya)

- L'analyse de la section efficace de fission de ^{237}Np entre 54 eV et 95 eV a été reprise. Les largeurs de fission de 21 résonances appartenant à cette zone ont pu être déterminées avec une meilleure précision. Pour les autres résonances on ne peut encore donner qu'une limite supérieure de Γ_f. L'analyse se poursuit au-delà de 95 eV.

- Autour de 40 eV la section efficace de fission se présente comme un bouquet de résonances étroites plantées sur une petite butte dont la largeur est de l'ordre de 7 à 8 eV. L'étude des neutrons diffusés par les matériaux qui constituent le détecteur, montre que l'action de ces neutrons ne peut expliquer que la formation d'une

butte de hauteur moitié. Après soustraction de cet effet, il reste donc autour de 40 eV une section efficace résiduelle qui a la forme d'une résonance large dissymétrique et qui pourrait être la composante en classe I de l'état de classe II responsable de la structure intermédiaire. Un programme expérimental est en cours qui permettra de préciser cet effet.

- La section efficace de fission, après un "lissage" obtenu en faisant le produit de convolution de la section efficace mesurée par une gaussienne dont la largeur est très supérieure à l'espacement des résonances est formée de pics d'amplitudes très différentes. La distribution de ces amplitudes est incompatible avec une loi en χ^2 mais suggère très fortement une séparation en deux familles de populations comparables et dont les amplitudes moyennes sont dans le rapport 25. La distribution des espacements des pics de grande amplitude obéit à la loi de Wigner à une population. Ce résultat joint à la dissymétrie constatée dans la section efficace résiduelle (qui pourrait être due à l'interférence de niveaux de classe II) conduit à penser que ces pics appartiennent à la même famille de spin [13] [14].

2.7. <u>Analyse multiniveaux des sections efficaces des noyaux fissiles</u> (H. Derrien M. Sanche).

Le formaliseme utilisé est celui de Reich-Moore dont les caractéristiques essentielles sont les suivantes :

- on néglige les interférences dues aux voies capture,
- on tient compte des interférences dues à la voie diffusion et aux voies fission dont le nombre est faible,
- on travaille directement sur la relation matricielle entre les matrices U et R sans passer par la matrice des niveaux A.

2.7.1. Un programme a été écrit qui effectue les opérations suivantes :

- calcul des sections efficaces théoriques totales, de fission et de diffusion.
- produit de convolution des sections efficaces théoriques, de l'effet Doppler et de la résolution.
- comparaison des sections efficaces théoriques et expérimentales avec ajustement des paramètres de résonances par la méthode des moindres carrés ; les dérivées sont calculées par une méthode numérique, l'ajustement peut se faire : soit sur la section efficace totale seule ; soit sur la section efficace de fission seule ; soit simultanément sur ces deux sections efficaces.
- tracé des sections efficaces expérimentales et théoriques.

Les principales caractéristiques du programme sont : 3 000 points de calcul, au maximum ; 100 résonances, au maximum ; 15 paramètres variables simultanément ; 2 voies de fission ; calculateur CDC 6600 ; Fortran IV ; temps de calcul 1 minute pour 1 000 pts, 50 résonances et 1 paramètre variable.

2.7.2. Analyse des sections efficaces totale et de fission du ^{239}Pu

L'analyse est faite de 4 eV à 150 eV. En particulier :

- l'étude précise, des résonances larges, a conduit, dans certains cas, à des résultats totalement différents de ceux de l'analyse à 1 niveau ; par exemple à 11,5 eV, entre 50 et 66 eV, entre 79 et 86 eV ; des résonances introduites dans l'analyse à 1 niveau sont explicables par de forts effets d'interférences dans les voies 0^+ (2 voies 0^+ sont nécessaires);
- il y a, probablement, une seule voie de sortie dans l'état 1^+ ; les résultats de l'analyse multiniveaux ne sont pas différents des résultats de l'analyse à 1 niveau.
- les paramètres sont obtenus avec ce formalisme jusqu'à 150 eV ; les spins attribués sont généralement en accord avec ceux déduits d'autres mesures, en particulier avec ceux déterminés à partir de l'analyse de la section efficace de diffusion mesurée à Saclay (voir 2.5.).

2.8. Anisotropie d'émission des fragments de la fission induite par des neutrons de résonances dans des noyaux ^{135}U orientés (J.W. Dabbs*, B. Cauvin, Ch. Eggermann, M. Sanche, A. Michaudon)

La mesure faite à Saclay en 1968, a été analysée d'une façon plus complète en 1969 en utilisant le formaliseme multiniveaux de D.B. Adler et F.T. Adler. L'analyse qui a porté sur 46 résonances (ou groupes de résonances) confirme en les précisant, les résultats déjà obtenus en 1968, à savoir [15] :

- la très faible contribution de la bande K = 0 dans les résonances analysées,
- la valeur $K \simeq J$ pour les très petites résonances de fission.

2.9. Spectre des rayons γ de capture radiative dans les résonances (A. Lottin, D. Paya)

L'obtention des spectres d'un grand nombre de résonances (et des bruits de fond pris entre les résonances) a été rendue possible grâce à l'utilisation du calculateur CAE 510. Le programme de dépouillement d'expériences biparamétriques mis en service cette année fournit les spectres de rayons γ correspondant à différentes conditons imposées à l'énergie des neutrons. Jusqu'à dix conditions, peuvent être affichés simultanément et les dix spectres correspondants sont obtenus chaque jour sans manipulations fastidieuses de bandes magnétiques.

* Laboratoire National d'Oak Ridge

2.9.1. Antimoine (détecteur Ge Li de 8 cm^3) [16]

On a amélioré la précision statistique des résultats obtenus en 1968 pour la part à haute énergie des spectres γ ($E\gamma \geqslant 4,5$ MeV). On a analysé, au-dessous de 170 eV, 12 résonances de ^{121}Sb (35 raies de désexcitation observées) et quatre résonances de ^{125}Sb (9 raies de désexcitation observées). Cette étude a permis de mettre en évidence des transitions γ nouvelles et, pour d'autres, d'en précise l'attribution isotopique. L'analyse des transitions γ (énergie et intensité) est maintenant faite à l'aide du programme GRAP de ORNL, qui a été adapté .

L'analyse d'une étude complémentaire à basse énergie ($E\gamma \leqslant 2$ MeV) est en cours

2.9.2. ^{239}Pu

Une étude préliminaire a permis d'observer une trentaine de raies γ d'énergie supérieure à 450 KeV ; au-dessous de 900 KeV, toutes les raies γ observées ont été identifiées comme provenant de la fission (certaines avaient d'ailleurs été observées par Weigmann et als dans la réaction $^{235}U + n$), à l'exception d'une raie à 554 KeV (transition du niveau 1^- à 597 Kev au niveau 2^+ à 43 KeV).

Pour la résonance à 7,8 eV (J = 1), on a observé une transition d'énergie $E\gamma$ = 5 935 KeV. Cette transition conduisant vraisemblablement au niveau 1^- à 597 KeV, l'énergie de liaison du neutron dans ^{240}Pu serait égal à 6,532 MeV, sensiblement supérieure à la valeur admise (6,41 MeV). Aucune transition complémentaire vers le fondamental ou le premier niveau excité n'a cependant pu être observée.

Le tableau I donne une comparaison des résultats avec ceux obtenus par Greewoc (II TRI 1193-53, vol. 1 (1965) et ceux de Weigmann précités. Les valeurs entre parenthèses indiquent des raies probables.

3. GROUPE DES NEUTRONS RAPIDES (J.L. LEROY)

3.1. Développement des méthodes de mesure absolue de flux de neutrons rapides

Ce programme est poursuivi de façon continue depuis plusieurs années : au cours de l'année écoulée, la précision est passée de ± 4 % à ± 2 % dans la gamme d'énergie allant de 10 KeV à 1 MeV. Pour pouvoir garantir une précision de cet ordre, il est indispensable de mesurer le même flux par différentes méthodes absolues et de vérifier qu'elles sont en accord dans la limite des erreurs prévues pour chacune. De cette façon, on réduit fortement la probabilité d'une erreur systématique importante. Les méthodes suivantes ont été employées :

- la particule associée avec la réaction $T(p,n)^3He$,
- la cuve de sulfate de manganèse, calibrée au moyen d'une source de RaBe étalonnée par le BIPM,
- le compteur proportionnel à protons de recul.

Comme ce travail de comparaison a été échelonné sur un temps assez long, les différentes méthodes absolues ont été appliquées successivement à la calibration d'un même instrument de mesure dont la stabilité dans le temps a été soigneusement vérifiée. Cet instrument qui a déjà été décrit [17] était un assemblage de compteurs à BF^3 dans la paraffine. Nous l'appellerons par la suite "compteur directionnel".

.1.1. Méthode de la particule associée (E. Fort, J.L. Leroy)

La réaction T (p,n)^{3}He est utilisée pour produire des neutrons dans une gamme d'énergie comprise entre 100 KeV et 1,5 MeV. La détermination du flux de neutrons est obtenue en détectant les particules ^{3}He associées d'énergie supérieure à 0,8 MeV ; ces particules ^{3}He sont triés des p et T diffusés par la cible à l'aide d'un analyseur combinant un champ électrique et un champ magnétique [18 .

Deux techniques peuvent être utilisées :

- coïncidences neutrons - ^{3}He : le rapport du nombre de coïncidences n - ^{3}He au nombre de ^{3}He détectés donne l'efficacité du détecteur de neutrons ; pour le détecteur utilisé (verre au ^{6}Li en forme de disque), des corrections doivent être effectuées pour tenir compte des diffusions multiples des neutrons dans le verre: ces corrections ont été calculées par une méthode Monte-Carlo [19] [20]. La fig. 12 donne l'efficacité obtenue pour un scintillateur NE905 (Ø = 44 mm ; e = 9,5 mm).
- comptage absolu des ^{3}He dans un angle solide défini : cette méthode mise en œuvre pour la réaction T (p, n)^{3}He par Liskien et als (Nucl. Inst. and Meth. 69, 70, 1969) présente un certain nombre d'avantages sur la précédente : électronique plus simple, taux de comptage plus élevés, élimination des difficultés dues aux diffusions multiples des neutrons. Par contre, l'analyseur est soumis à des exigences plus sévères puisqu'il doit non seulement éliminer toutes les particules étrangères, mais encore ne perdre aucune des particules ^{3}He. Avec l'appareillage sous sa forme actuelle, nous pensons qu'il est possible d'atteindre la précision de ± 2 % en travaillant dans les gammes d'énergie 200 KeV - 1,5 MeV avec la réaction T (p,n) ^{3}He et 1,9 MeV - 2,1 MeV avec la réaction D (d,n) ^{3}He.

3.1.2. Méthode de la cuve de sulfate de manganèse (J.L. Huet, J.L. Leroy, I. Szabo, J. Gentil).

Cette méthode a été largement utilisée pour la calibration de sources radioactives : pour situer sa précision, la calibration d'une même source par 14 laboratoires a donné des résultats cohérents à 1 % près (V. Naggiar, B.I.P.M., 1967).

Nous l'avons adaptée à la mesure de flux neutroniques produits par une source quasi ponctuelle. L'expérience (fig. 13) consiste en fait à déterminer l'efficacité absolue du "compteur directionnel" en mesurant le flux des neutrons capturés dans la cuve de sulfate de manganèse. Cette mesure doit être corrigée pour tenir compte d'effets parasites, notamment la capture de neutrons par les parois métalliques du puits que comporte la cuve ainsi que la fuite des neutrons hors de la cuve ; ces corrections ont été calculées par une méthode de Monte-Carlo (fig. 14). La mesure du flux de neutrons capturés est effectuée en soutirant la solution, après irradiation, dans une cuve sphérique (Ø 90 cm) comportant un puits permettant de loger un scintillateur NaI destiné à déterminer la radioactivité de la solution. L'ensemble du détecteur (cuve, solution et scintillateur) a été étalonné à l'aide d'une source de Ra-Be de 100 mC calibrée par le "Bureau International des Poids et Mesures".

La précision sur la mesure de flux est estimée à ± 1,65 % (dont 1,1 % sur la calibration de la source de Ra-Be et 0,2 % représentant la reproductibilité des mesures d'activité). La méthode a été appliquée à plusieurs versions du "Compteur directionnel" ; les résultats (courbes en trait plein de la fig. 15) sont donnés pour deux valeurs (13 cm et 17 cm) de l'écartement des compteurs BF^3 constituant le "Compteur directionnel". Pour un écartement de 17 cm, on ne constate aucune variation systématique de l'efficacité en fonction de l'énergie pour 14 points de mesure entre 20 KeV et 1 MeV.

3.1.3. Compteur proportionnel à protons de recul (I. Szabo)

Grâce à la collaboration de MM. Liskien et Paulsen du B.C.M.N., on a pu utiliser un compteur construit par eux d'après les travaux de Skyrme et al. (Rev. Sc. Instr. 23, 204, 1952) et White (J. Nucl. Energ. 19, 325, 1965). Une première comparaison a été faite dans le domaine d'énergie allant de 100 KeV à 450 KeV auprès du Van de Graaff de Geel, entre le compteur proportionnel et le scintillateur de verre au ^6Li déjà étalonné par la méthode de la particule associée. Le résultat est représenté par la fig.12. Compte tenu des marges d'erreur, les deux méthodes sont en bon accord, principalement entre 180 et 300 KeV. En-dessous de 180 KeV et au-dessus de 350 KeV, le compteur proportionnel donne des valeurs légèrement supérieures, ce qui est peut être dû à une estimation imparfaite du bruit de fond du scintillateur dans l'expérience de comparaison. Une deuxième comparaison a été faite à Cadarache entre le compteur proportionnel et le compteur directionnel dans le domaine d'énergie allant de 800 KeV à 2 MeV.

Dans toutes ces mesures, le spectre expérimental des protons de recul n'avait pas exactement la même forme que le spectre théorique qui sert au calcul du flux. Ceci introduisait une erreur de ± 3 %. L'incertitude totale était de ± 4 %.

3.1.4. Calcul direct de l'efficacité du détecteur directionnel par la méthode de Monte-Carlo [21] (J.L. Leroy)

Cette méthode est particulièrement commode dans ce cas à cause des cavités importantes constituées par le puits d'arrivée des neutrons et les trous des compteurs. Le résultat de ce calcul est donné par la figure pour deux versions de l'appareil (écartement des BF 3 : 17 cm et 13 cm), l'accord avec les valeurs mesurées de l'efficacité est excellent.

3.1.5. Discussion sur l'ensemble des méthodes de mesures de flux

Dans l'état actuel, la méthode du bain de sulfate de manganèse est de loin la plus précise et elle donne de bons résultats à partir de 10 KeV jusqu'à 1,5 MeV. Pour appliquer la méthode à des énergies plus élevées, il faudrait sans doute augmenter le diamètre de la sphère. La méthode de la particule associée appliquée à un détecteur de verre au ^{6}Li souffre de difficultés d'interprétation et la variation très rapide de la section efficace de la réaction ^{6}Li (n, α) T en fonction de l'énergie, introduit une source d'erreur supplémentaire. L'utilisation du compteur proportionnel à protons de recul a fourni des résultats moins reproductibles que ce qu'on pouvait espérer d'après les travaux faits ailleurs (cf. par exemple White, J. Nucl. Energ. 19, 325 - 1965). Néanmoins, ces deux dernières méthodes sont en accord dans la limite des erreurs inventoriées, avec la méthode du bain de manganèse, ce qui laisse espérer qu'aucune erreur systématique importante n'est passée inaperçue. La méthode de la particule associée en version comptage absolu devrait connaître des développements intéressants dans un très proche avenir. Nous évaluons l'erreur globale de nos mesures de flux à ± 2 % (écart standard) dans le domaine allant de 10 KeV à 1 MeV.

3.2. Mesure de la section efficace de fission de ^{235}U et ^{239}Pu (I. Szabo, E. Fort, R. Sher - Stanford Univ.-)

La mesure sur l'^{235}U qui avait été faite en 1967 a été renormalisée, grâce aux travaux exposés au paragraphe 3.1. De plus, les mesures elles-mêmes ont été reprises dans un domaine d'énergie allant de 40 KeV à 450 KeV, en visant une meilleure détermination du bruit de fond. Les résultats, qui vont être publiés incessamment, sont représentés par la figure 16. Une chambre de fission contenant 0,15 mg de ^{239}Pu a été construite avec le concours du B.C.M.N. qui a réalisé et calibré le dépôt de plutonium. Les mesures sont actuellement en cours.

3.3. Mesures de la distribution angulaire des neutrons diffusés élastiquement par le calcium (D. Abramson, C. Le Rigoleur, J.C. Bluet, A. Arnaud)

Le spectromètre à temps de vol à cinq compteurs, déjà décrit ailleurs [22], a été utilisé pour mesurer la distribution angulaire des neutrons diffusés par le calcium entre 1,2 MeV et 2,4 MeV, avec un pas en énergie de 100 KeV. La valeur absolue de la section efficace a été obtenue directement à partir des rapports des flux incidents et diffusés, des paramètres géométriques de l'expérience et du nombre d'atomes de l'échantillon. La correction tenant compte de la variation d'efficacité des compteurs en fonction de l'énergie des neutrons diffusés, a été déterminée par comparaison avec le compteur directionnel dont il est question au paragraphe 3.1. La correction la plus importante (10 à 20 %) provient de l'effet d'atténuation du flux incident à travers l'échantillon. Ce problème ainsi que celui de la diffusion multiple qui s'y rattache a été traité au moyen d'un calcul de Monte-Carlo. Les résultats sont donnés par la figure 17.

4. GROUPE EVALUATION (P. RIBON)

Cette année a été caractérisée par une augmentation des effectifs qui s'évaluent maintenant à cinq physiciens (MM. Ribon, Krebs, Le Coq, l'Hériteau, Mezza), et par un passage progressif d'une phase de démarrage (mise au point de méthodes et de programmes), à une phase d'études proprement dites.

4.1. Traitement de l'information

4.1.1. Mise au point d'un programme d'analyse des résonances pour un noyau fissile : destiné à l'étude du ^{235}U, ce programme devrait permettre la détermination, par moindres carrés, des paramètres de résonances d'après l'analyse de forme simultanée des différentes sections efficaces expérimentales. Les interférences sont traitées comme des termes correctifs et n'interviennent pas dans les moindres carrés.

4.1.2. Transformation dans le format UKAEA des données présentées dans le format KEDAK La mise au point d'un programme FORTRAN assurant automatiquement cette transcription a été entreprise en liaison avec le Département de Calcul Electronique de Saclay ; ce programme devrait être disponible vers mai 1970.

4.2. Etudes effectuées

4.2.1. ^{240}Pu [23] : nous avons remis à jour les évaluations de Yiftah et Pitterle en tenant compte des résultats récents et en essayant de préciser les incertitudes sur les valeurs numériques. Ces deux évaluations présentent un désaccord au sujet de $\nu(E$

la loi de variation que nous avons été amenés à proposer est :

$$\nu(E) = (2,95 \pm 0,1) + (0,15 \pm 0,01)\ E$$

4.2.1. ^{241}Pu : nous avons été amenés à recommander l'évaluation de Yiftah avec quelques réserves concernant notamment les largeurs moyennes de fission et ν (E). Avant d'entreprendre un travail plus approfondi, il paraît raisonnable d'attendre l'achèvement de diverses expériences en cours et des précisions sur l'existence éventuelle d'un état métastable ainsi que d'un isomère de fission du ^{241}Pu.

4.2.3. L'examen des sections efficaces de capture de ^{78}Kr, ^{80}Kr, ^{124}Xe, ^{126}Xe, ^{128}Xe et ^{129}Xe a été effectué [24] ainsi que celui des données relatives à la réaction Rh (n, n') Rh^m [25].

4.3. Etudes en cours

4.3.1. ^{241}Am (à paraître sous forme de rapport EANDC) : les données expérimentales sont limitées (domaine thermique et premières résonances) et souvent discordantes. L'existence de deux modes de désexcitation (vers les états fondamental τ = 16 ans et métastable τ=152 ans de ^{242}Am) constitue une difficulté supplémentaire [26].

4.3.2. ^{235}U : l'étude générale de cet élément a débuté par le domaine des résonances où un programme d'analyse a été mis au point (voir 4.1.1.) et les données expérimentales ont été comparées. Pour les sections efficaces de fission, les interférences supposées entre niveaux dépendent très fortement de la section efficace résiduelle entre les résonances ; or celle-ci varie considérablement d'une expérience à l'autre et apparaît d'autant plus faible que l'expérience est "propre" (par exemple à 29,2 eV, $\sigma_f \sim 2,4$ b. pour les expériences de Geel et $\sigma_f < 1$ b. pour celles de Los Alamos). Nous avons essayé d'interpréter ces désaccords par l'effet de la diffusion des neutrons incidents par le détecteur [27] : la correction en résultant -qui n'a jamais été effectuée par les expérimentateurs sauf pour l'expérience de ORNL-RPI- ne dépasse jamais 0,4 b. et apparaît donc insuffisante pour rendre compte de la totalité des désaccords ; d'autres diffusions parasites (par les collimations par exemple) sont difficiles à évaluer. Ces incertitudes rendent difficile l'étude des structures intermédiaires de fission et leur interprétation par des résonances larges superposées aux résonances étroites.

5. GROUPE DES REACTIONS PHOTONUCLEAIRES (R. BERGERE)

Ce groupe comprend les physiciens suivants : R. Abdon, H. Beil, R. Bergère, P.J. Carlos, A. Leprêtre, A. Veyssière, J.A. Bayart .

5.1. Dispositifs expérimentaux : en 1969, l'adjonction d'une 4ème section au guide accélérateur a permis d'accroître le flux γ monochromatique dans la plage d'énergie

jusqu'ici accessible (5 à 35 MeV) et d'étendre cette plage jusque vers 60 MeV. De plus, une deuxième optique magnétique a été installée.

5.1.1. La première optique est spécialisée dans l'étude des réactions photonucléaires à l'aide d'un scintillateur liquide d'efficacité ≈ 60 %. Ce dispositif permet la détection simultanée et l'enregistrement individuel des sections efficaces partielles (γ, 1n), (γ, 2n), (γ, 3n) et (γ, 4n) en fonction de l'énergie des photons incidents [28].

Il est en outre possible d'effectuer des mesures de sections photonucléaires totales par transmission en utilisant comme détecteur γ un cristal I Na (Tl) 8"x8".

5.1.2. La deuxième optique est destinée à l'étude des spectres de photoneutrons : les photoneutrons sont détectés par des scintillateurs à protons de recul et les spectres d'impulsions obtenus sont traités par une méthode de déconvolution mathématique mise au point à Oak Ridge par W.R. Burrus et V.V. Verbinski. Ce procédé a été testé avec des neutrons de 9 MeV et apparaît prometteur. La figure 18 représente le spectre d'impulsions expérimental et le spectre de neutrons correspondant.

5.2. Système d'acquisition de données

En vue d'augmenter la précision, la "fiabilité" et la vitesse d'acquisition de nos données expérimentales, nous avons installé un processeur PDP/8/I en ligne couplé au dispositif de mesures par une interface STDAN mise au point à Saclay par le Département d'Electronique. Ainsi les mesures peuvent être fragmentées, analysées, conservées ou rejetées selon qu'elles répondent ou non aux conditions statistiques imposées, ce qui permet d'éliminer les erreurs systématiques.

5.3. Etudes et résultats expérimentaux

5.3.1. Sections efficaces photoneutroniques totales et partielles

Faisant suite à l'étude du noyau sphérique ^{139}La et des noyaux déformés ^{181}Ta, ^{165}Ho, ^{159}Tb [29] [30] nous avons poursuivi nos investigations tant sur les noyaux sphériques que sur les noyaux déformés :

- noyaux déformés. Nous avons étudié en particulier les noyaux ^{127}I [31], Sm Er et ^{175}Lu [32] et déterminé les sections efficaces photoneutroniques partielles et totales, les règles de sommes et les moments quadrupolaires électriques dans le formalisme du modèle hydrodynamique de M. Danos. En particulier grâce à une analyse fine de la section efficace photoneutronique totale de l'^{127}I il a été possible de mettre en évidence son faible moment quadrupolaire négatif (fig.19).

- noyaux sphériques . Dans cette catégorie de noyaux, nous avons étudié les noyaux suivants : Ce [32], ^{208}Pb [33] [34] et ^{89}Y [35]. En particulier, nous nous sommes attachés à l'étude de structures observées dans la résonance géante du Pb et de l'Y.

Pour le ^{208}Pb (fig. 20), il apparaît très clairement des structures (à 7.59 MeV, 7.94 MeV, 9.25 MeV, 9.84 MeV et 11.2 MeV) qui ont pu être observées grâce à l'amélioration de la résolution en énergie de notre faisceau de gammas.

Cette structure pourrait être due à l'existence d'états à grand nombre de quasi-particules liés et non-liés [36] .

Pour ^{89}Y il apparaît (fig.21) un très net dédoublement de la résonance géante bien que le noyau soit sphérique en neutrons. Cette structure a été prédite par B. Goulard et S. Fallieros dans le cas du dédoublement isobarique de la résonance géante des noyaux voisins de la couche magique à 50 nucléons.

Le tableau I donne quelques résultats sur les corps étudiés.

5.3.2. Calibration du flux γ "monochromatique". Une analyse théorique a permis de prédire la forme et l'intensité de la raie de photons obtenue par annihilation en vol de positons [37] . Les résultats de ce calcul ont été comparés aux résultats expérimentaux et on a pu noter une très bonne concordance entre les deux.

5.3.3. Etude de la résolution du faisceau de γ. L'étude du transport de faisceau de positons [38] a conduit à améliorer notablement la résolution en énergie du faisceau de γ, en modifiant certains paramètres du système magnétique. L'étude de la réaction ^{28}Si (γ, P_0) ^{27}Al a permis de mesurer la résolution vraie $\Delta E\gamma$ de la raie et de confirmer aussi les résultats théoriques ; par exemple, pour $E\gamma = 10$ MeV on a $\Delta E\gamma = 140$ keV.

5.4. Etudes en cours

Les sections efficaces photoneutroniques de ^{197}Au, ^{103}Rh, Sr et ^{93}Nb sont en cours de dépouillement.

BIBLIOGRAPHIE

[1] C. Carles, M. Asghar, T. Doan, R.Chastel, C. Signarbieux Phys. and Chem. of Fission - Vienne 1969 - SM 122/80

[2] M. Asghar, C. Carles, R. Chastel, T. Doan, M.Ribrag, C. Signarbieux Nucl. Phys. à paraître

[3] J. Poitou, H. Nifenecker, C. Signarbieux - Note C.E.A. à paraître.

[4] H. Nifenecker - Nucl. Inst. and Meth. à paraître.

[5] H. Nifenecker, M. Ribrag, J.Fréhaut, J.Gauriau - Nucl. Phys. A131, 261, 1969

[6] H. Nifenecker, J. Fréhaut, M. Soleilhac, - Phys. and Chem. of Fission Vienne 1969 -SM 122/78

[7] J. Irigaray - Thèse, Bordeaux 1969

[8] R.Samama,P.Carlos,J.Girard,B.Maier,G.Perrin - CR Ac. Sc. B267,424,1969

[9] R.Samama,J.Girard,R.Babinet,A.Audias,J.Gardien - Neutron Capture γ ray Spectroscopy - Studsvik 1969.

[10] H. Tellier, M. Alix, J. Dabbs - C.R. Ac. Sc. 269, 266, 1969

[11] H. Tellier, J. Dabbs - Note C.E.A. n° 1 268

[12] C. Newstead, B. Cauvin, A. Katsanos, H. Tellier - BAPS 14, 1 236, 1969

[12 bis] H. Tellier, M. Alix, - Note C.E.A. n° 1 230

[13] D. Paya, J.Blons,H.Derrien,A.Michaudon - Phys. and Chem. of Fission - Vienne 1969 - SM 122/90

[14] A.Michaudon - Fast neutrons and the study of nuclear structure, Duilo'o 1969.

[15] J.Dabbs,C.Eggermann,B.Cauvin,A.Michaudon,M.Sanche - Phys. and Chem. of fission - Vienne 1969 - SM 122/123.

[16] D. Paya, A. Lottin - Neutron Capture γ Spectroscopy - Studsvik 1969.

[17] E A N D C (E) 89, 191, 1968

[18] J.L.Leroy,J.Huet,I.Szabo,C.Le Rigoleur,D.Abramson-Rev.Phys.Appl.4,251,1969

[19] E. Fort, J.L. Leroy - à paraître.

[20] E. Fort - à paraître.

[21] J.L. Leroy - à paraître.

[22] C. Le Rigoleur, D. Abramson - Rev. Phys. Appl. 4, 253, 1969.

[23] J.P. L'Hériteau, P. Ribon - rapport EANDC (E) 126, 1970.

[24] G. Le Coq - rapport SMPNF 802, 1970.

[25] P. Ribon - rapport SMPNF 714, 1969.

[26] M. Mezza - rapport SMPNF - à paraître -

[27] G. Le Coq - rapport SMPNF 735, 1969.

[28] H. Beil et al. Rev. Phys.Appl. 4, 294,1969 et Nucl.Inst.Meth.67,293,1969.

[29] A. Veyssière et al. - C.R. Ac. Sc. 267 B, 234, 1968.

[30] R. Bergère et al. - Nucl. Phys. A 121, 463. 1968.

[31] A. Veyssière - C.R. Ac. Sc. 268B, 981, 1969.

[32] R. Bergère et al. - Nucl. Phys. A 133, 417, 1969.

[33] H. Beil et al. - C.R. Ac. Sc. 269B, 216, 1969.

[34] R. Bergère et al. - Nucl. Phys. - à paraître.

[35] R. Bergère et al - Conf. on properties of nuclear states, Montréal, 1969

[36] V. Gilet - Conf. on properties of nuclear states, Montréal 1969.

[37] H. Beil, G. Audit et al. - Nucl. Inst. and Meth. - à paraître.

[38] J. Bayart - Thèse 3ème cycle - Orsay 1969

LEGENDES DES TABLEAUX ET FIGURES

TABLEAU I : Emission neutronique des fragments de fission du ^{252}Cf

- $\sigma^2(\nu_1 : E_T, Z)$ et $C(\nu_1 \nu_2 : E_T, Z)$ valeurs moyennées sur E_T de la variance et de la covariance de l'émission neutronique à Z et E_T fixes.
- $\sigma^2(E_1 : E_T, Z)$ valeur moyennée sur E_T de l'énergie cinétique d'un fragment à Z et E_T fixes.

TABLEAU II : Rayons γ émis par absorption de neutrons dans ^{239}Pu.
A/ γ observés lors de l'absorption de neutrons thermiques par ^{239}Pu (R. Greenwood et als IITRI 1193, 53 Vol. 1, 1965)
B/ γ observés lors de l'absorption de neutrons résonants par ^{235}U (H. Weigmann et als, Nucl. Phys. 535, A 134, 1969)
C/ γ observés lors de l'absorption de neutrons résonants par ^{239}Pu (ce travail)
D/ Origine des rayons γ (capture ou fission) déduite de A, B et C.

TABLEAU III : Résultats des études photoneutroniques.

Figure 1 : variance de la distribution de l'énergie cinétique totale E_K en fonction de la masse des fragments de fission

Figure 2 : probabilité de la tripartition P_α (en fonction du rapport R des masses des fragments.

Figure 3 : fluorescence nucléaire : dispositif expérimental et spectre γ "monochromatique" donné par une cible de titane.

Figure 4 : fluorescence nucléaire : spectre de fluorescence donné par le niveau à 3,560 MeV du ^6Li.

Figure 5 : histogrammes $\sum_0^{E_n} \Gamma n°$ pour les niveaux J = 3 et J = 4 de Ho.

Figures 6, 7 et 8 : multiplicité des rayons γ de capture radiative pour les résonances de ^{127}I, ^{147}Sm et ^{149}Sm.

Figures 9 et 10 : distributions des largeurs de fission pour ^{239}Pu dans les gammes d'énergie 110-220 eV (fig. 9) et 350-660 eV (fig. 10).

Figure 11 : σ_T et σ_f pour ^{239}Pu

Figure 12 : efficacité en % du scintillateur NE 905

Figures 13 et 14 : méthode du bain de sulfate de manganèse pour les mesures absolues de flux neutroniques.

Figure 15 : efficacités mesurées (traits pleins) et calculées (points individuels) de deux versions du long compteur directionnel.

Figure 16 : σ_f pour ^{235}U

Figure 17 : diffusion élastique des neutrons sur ^{40}Ca (cœfficients polynômes de Legendre).

Figure 18 : déconvolution du spectre d'un scintillateur liquide par la méthode de Burrus et Verbinski (E_n = 9 MeV).

Figures 19, 20 et 21 : section efficace photoneutronique de ^{127}I, ^{208}Pb, ^{89}Y.

TABLEAU II

E_γ kev	A	B	C	D
457		×		
476	×	×	×	Fission
483		×		
495		×		
554	×		×	Capture
571		×	×	Fission 2 ou 3 raies
586		×	×	Fission 2 raies
596	×		×	Fission
(603)			×	
615		×	×	Fission
693	×	×	×	Fission
706		×	×	Fission
728		×	×	Fission
767		×	×	Fission
814	×	×	×	Fission
835		×	×	Fission
843			×	Fission
896			×	Fission
912			×	Fission
936			×	
951		×	×	
960	×	×	×	Fission
972			×	
987			×	
1010			×	
(1045)			×	
1089	×		×	
1109			×	
1131			×	
1180		×	×	Fission
(1189)			×	
1211	×		×	
1219		×	×	Fission
1278		×	×	Fission
(1308)			×	
(1325)			×	
5835			×	Capture

TABLEAU I

Z	$\Gamma^2(\nu_1:Z)$	$C(\nu_1\nu_2:Z)$	$(\langle d\nu/dE\rangle_Z)^{-1}$	$\Gamma^2(\nu_1:E_T,Z)$	$C(\nu_1\nu_2:E_T,Z)$	$\Gamma^2(E_1:E_T,Z)$	$\langle dE_1/dE_T\rangle_Z$	$\langle dE_1/d\nu_1\rangle_Z$
40	1.33±0.223	-0.72±0.148	13.51 ± 0.94	0.78±0.236	-1.05±0.154	66.828±14.961	0.690±0.1296	9.318±0.9608
41	1.42±0.164	-0.61±0.106	11.38 ± 0.52	0.65±0.179	-1.01±0.113	52.180± 8.547	0.716±0.0962	8.142±0.6174
42	1.34±0.099	-0.83±0.084	12.67 ± 0.30	0.71±0.103	-1.14±0.090	67.782± 9.203	0.753±0.0805	9.546±0.5616
43	1.02±0.045	-0.41±0.046	12.80 ± 0.24	0.41±0.051	-0.87±0.053	43.252± 3.883	0.653±0.0488	8.358±0.2938
44	1.29±0.073	-0.69±0.119	17.57 ± 1.48	0.97±0.091	-0.99±0.124	81.365±14.559	0.571±0.0918	10.034±0.8405
45	1.17±0.210	-0.75±0.135	16.02 ± 1.68	0.78±0.226	-1.09±0.147	75.321±17.702	0.621±0.1269	9.946±0.9867
46	0.94±0.194	-0.50±0.196	23.64 ± 4.84	0.76±0.207	-0.68±0.201	89.738±44.392	0.620±0.2822	14.657±1.9755
52	1.61±0.298	-0.50±0.196	23.80 ± 3.35	1.44±0.302	-0.68±0.201	89.738±44.392	0.380±0.1177	9.044±1.2191
53	1.88±0.125	-0.75±0.135	18.31 ± 2.39	1.58±0.148	-1.09±0.147	75.321±17.702	0.379±0.0708	6.942±0.6886
54	1.64±0.202	-0.69±0.119	19.17 ± 1.61	1.36±0.207	-0.99±0.124	81.365±14.559	0.429±0.0605	8.223±0.6887
55	1.35±0.068	-0.41±0.046	17.17 ± 0.98	1.01±0.079	-0.87±0.053	43.252±3.883	0.347±0.0271	5.958±0.2093
56	1.86±0.112	-0.83±0.084	25.33 ± 2.66	1.71±0.117	-1.14±0.090	67.782±9.203	0.247±0.0319	5.245±0.3674
57	1.36±0.093	-0.61±0.106	22.34 ± 1.94	1.16±0.099	-1.01±0.113	52.180±8.547	0.284±0.0378	6.356±0.4819
58	1.66±0.137	-0.72±0.148	21.94 ± 2.45	1.45±0.145	-1.05±0.154	66.828±14.961	0.310±0.0538	6.809±0.7020
				VALEURS MOYENNES				
FRAGMENT LOURD (52 à 58)								
	1.57±0.045	-0.62 ±0.031		1.33±0.048	-1.00±0.048	60.659 ±4.464	0.321±0.0175	6.601±0.2010
FRAGMENT LEGER (40 à 46)								
	1.18±0.039	-0.62 ±0.031		0.66±0.043	-0.95±0.043	62.633±5.288	0.653±0.0388	9.522±0.2876
FRAGMENTS PAIRS								
	1.56±0.056	-0.72±0.051		1.29±0.058	-1.02±0.058	73.285±6.332	0.426±0.0292	8.228±0.2860
FRAGMENTS IMPAIRS								
	1.35±0.039	-0.53±0.038		0.97±0.044	-0.95±0.044	64.664±3.583	0.428±0.0200	6.958±0.1899

TABLEAU III

	Paramètres des raies de Lorentz						Moments quad.	Règles de somme de 0 à 28 MeV		
	MeV E_1	mb σ_1	MeV Γ_1	MeV E_2	mb σ_2	MeV Γ_2	Intr. barn Q_o	σ_o MeV barn	σ_{-1} mb	σ_2 mb MeV^{-1}
La	15.12	365	4.45					2.32 ± 0.25	146 ± 10	9.6 ± 0.6
Ce	15.05	370	4.35					2.13 ± 0.15	140 ± 12	9.5 ± 0.6
Pb	13.42	640	4.05							
Y	16.57	215	4.25	20.87	45	2.87		1.41 ± 0.1	76 ± 5	4 ± 0.5
Ta	12.35	270	2.57	15.30	330	4.47	7 ± 0.6	2.90 ± 0.3	206 ± 15	15 ± 1
Ho	12.07	250	2.7	15.62	285	4.8	7.1 ± 0.6	2.79 ± 0.3	194 ± 14	14 ± 1
Tb	12.12	205	3.25	15.97	240	4.87	8 ± 0.6	2.5 ± 0.3	172 ± 12	12 ± 0.8
I	14.5	255	3.78	16.8	130	3.87	- 2.3 ± 0.4	2.02 ± 0.14	129 ± 10	8.6 ± 0.6
Sm	12.77	155	4.25	15.46	260	4.6	4.5 ± 0.4	2.48 ± 0.17	167 ± 14	12 ± 1
Er	12.0	225	2.9	15.45	260	5.0	7 ± 0.4	2.70 ± 0.19	186 ± 15	14 ± 1
Lu	12.35	230	2.7	15.52	280	4.5	7 ± 0.3	2.65 ± 0.18	182 ± 15	13 ± 1

FIGURE 1

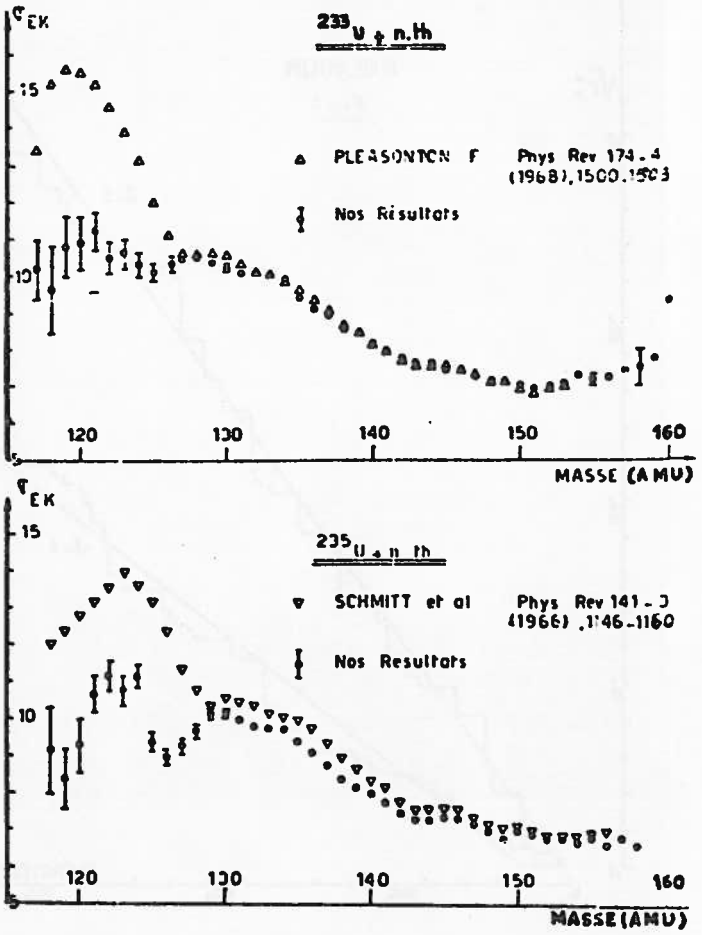

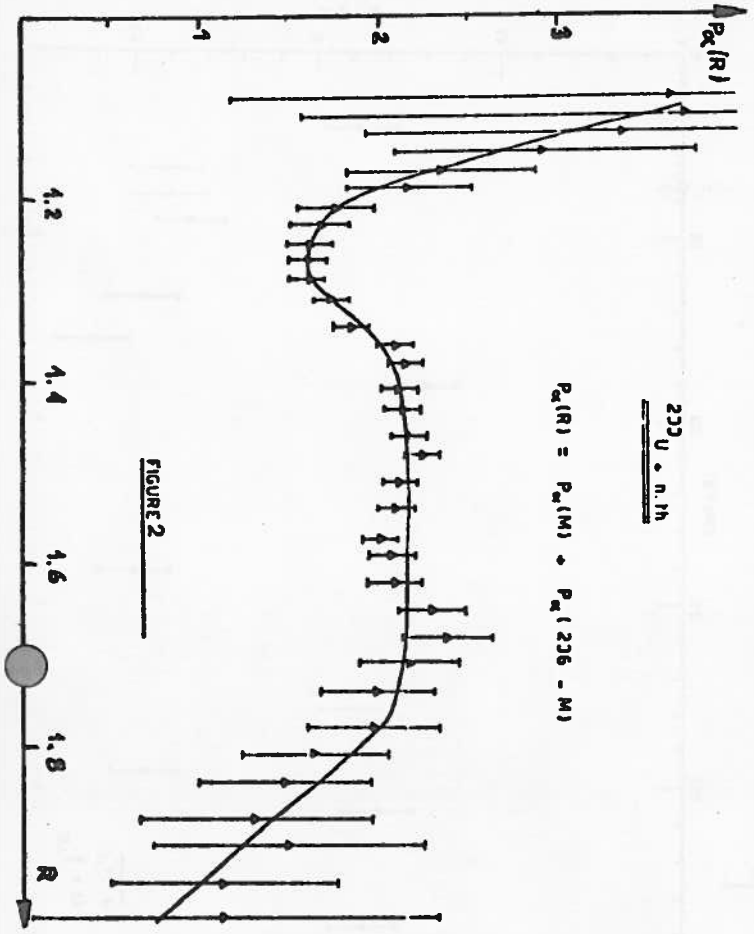

FIGURE 2

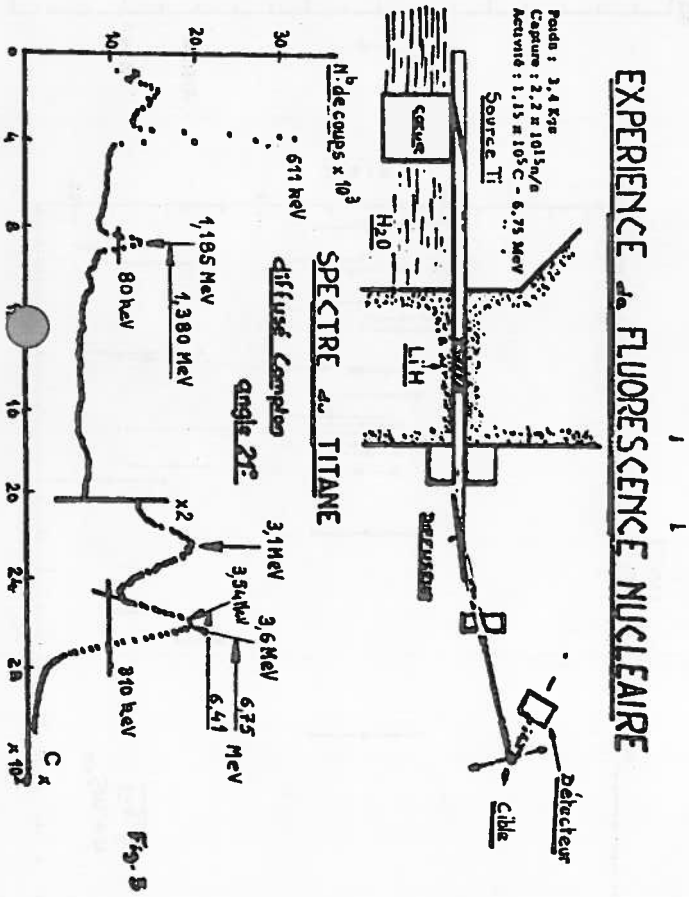

Fig. 5

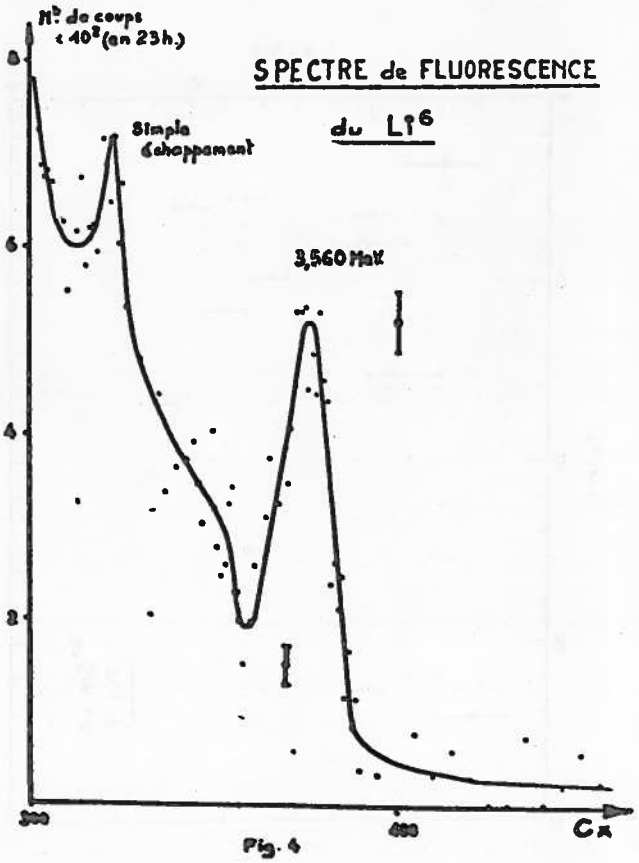

Fig. 4

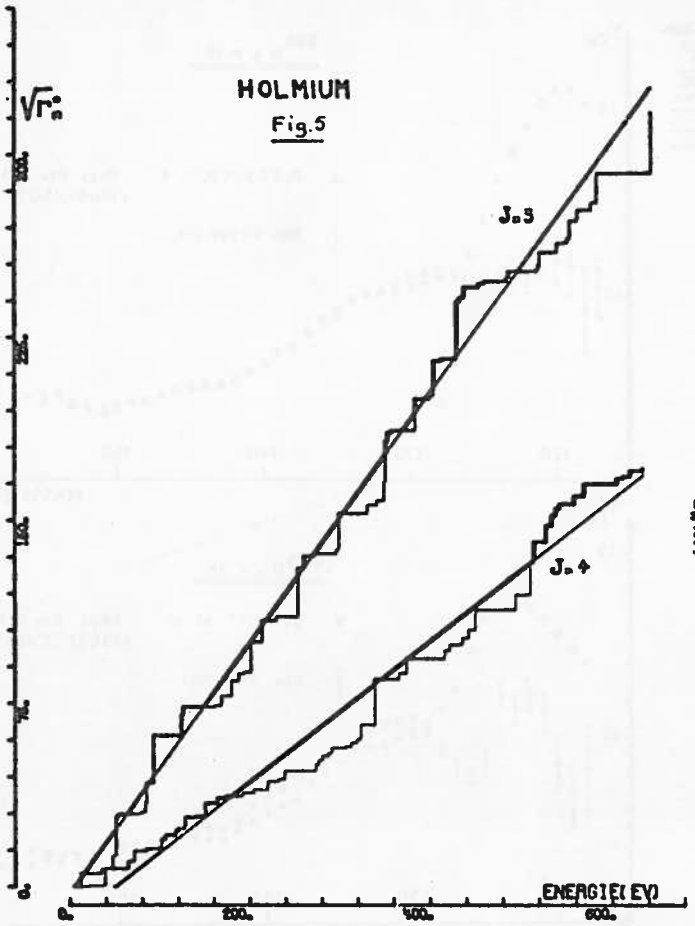
HOLMIUM
Fig.5
$\sqrt{\Gamma_n^0}$
J=5
J=4
ENERGIE(EV)
0
200
400
600

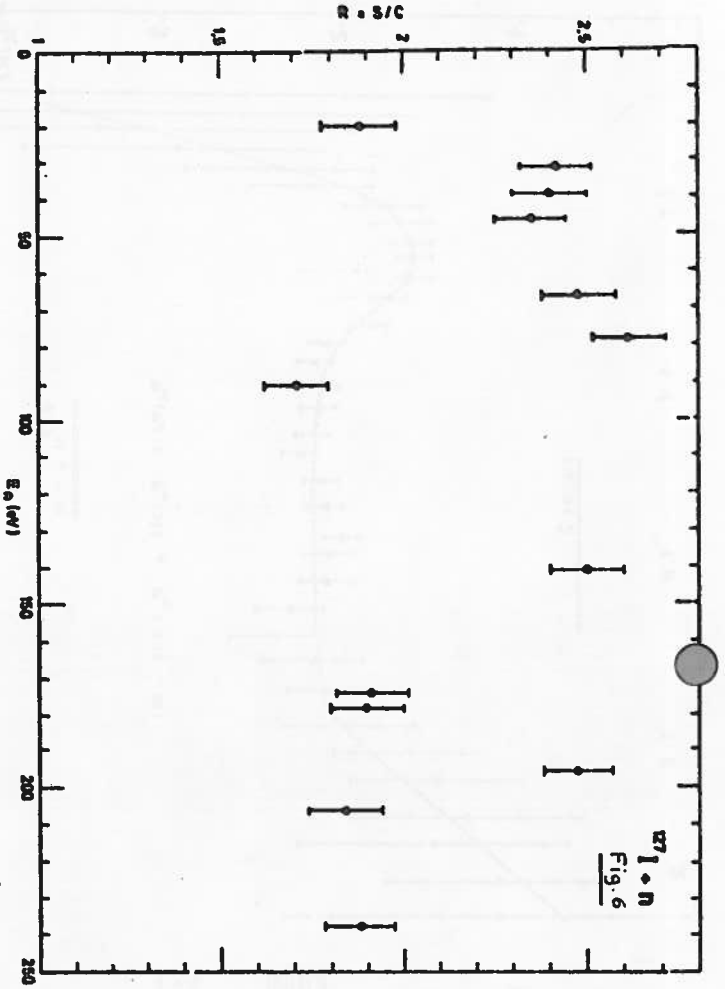
R = S/C
E_n (eV)
$^{127}I + n$
Fig.6

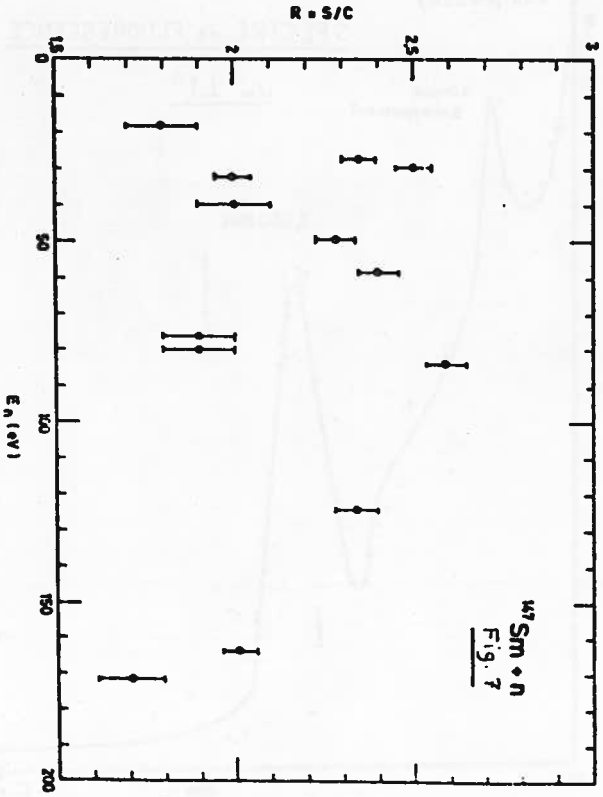
R = S/C
E_n (eV)
$^{147}Sm + n$
Fig.7

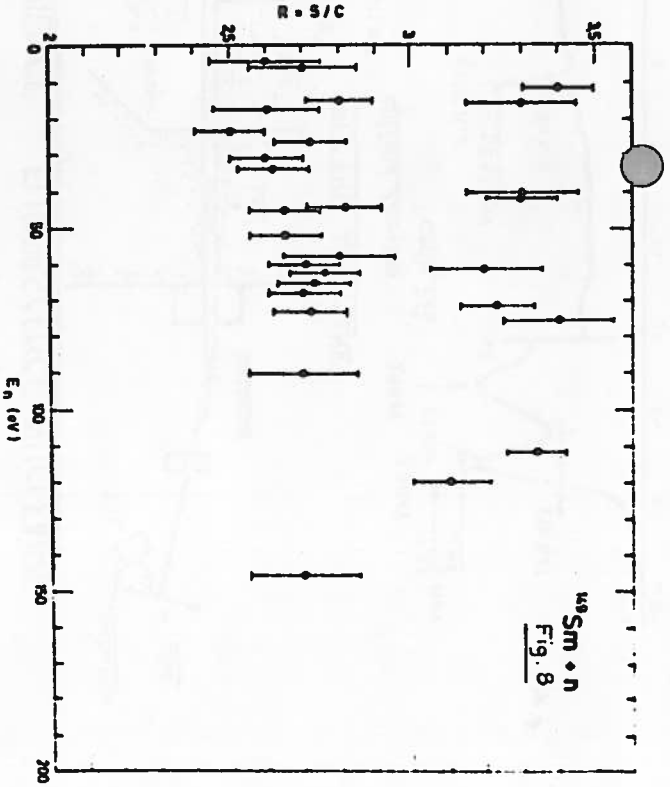
R = S/C
E_n (eV)
$^{149}Sm + n$
Fig.8

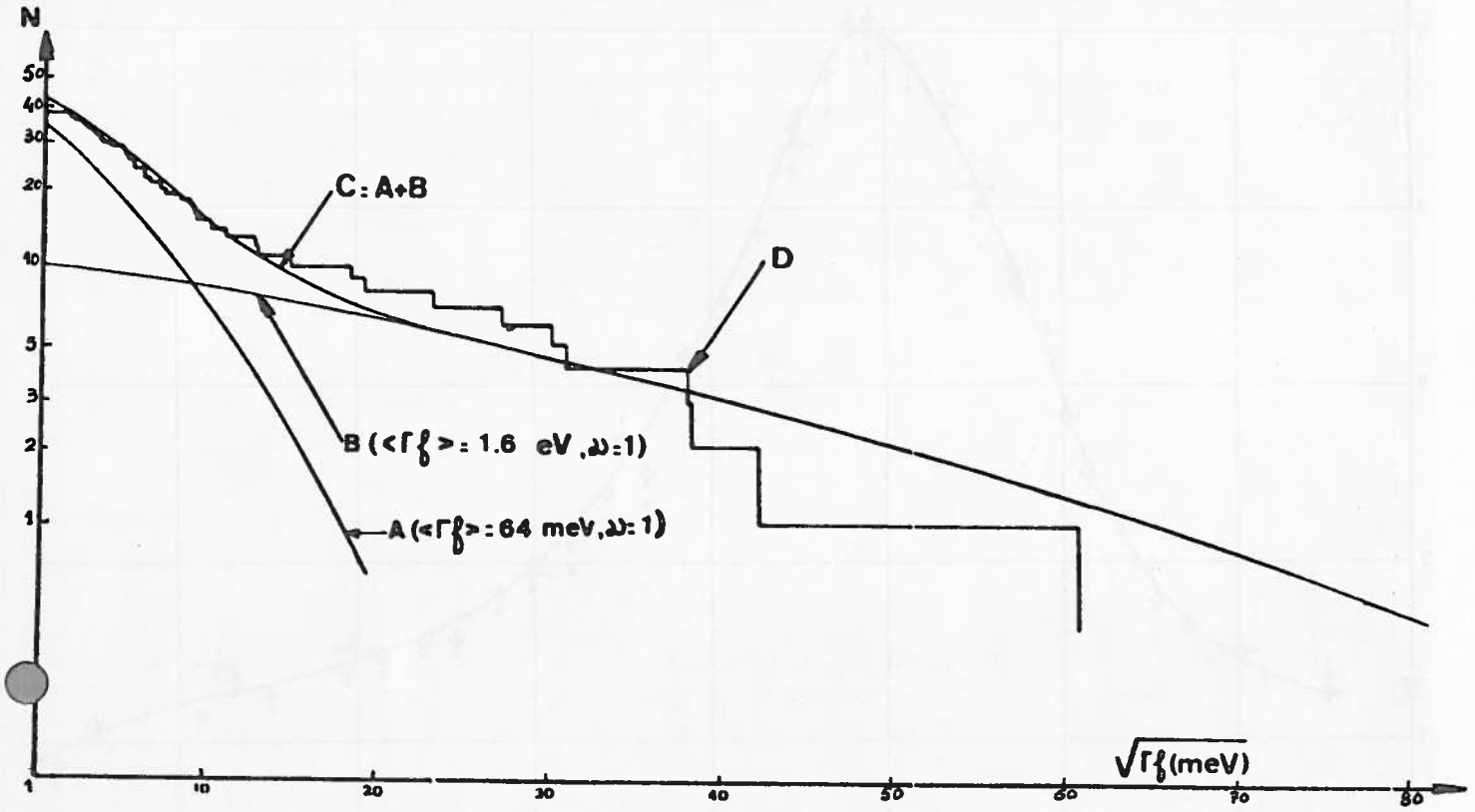
N
C: A+B
D
B (<Γf> = 1.6 eV, ν = 1)
A (<Γf> = 64 meV, ν = 1)
√Γf (meV)

Fig. 9

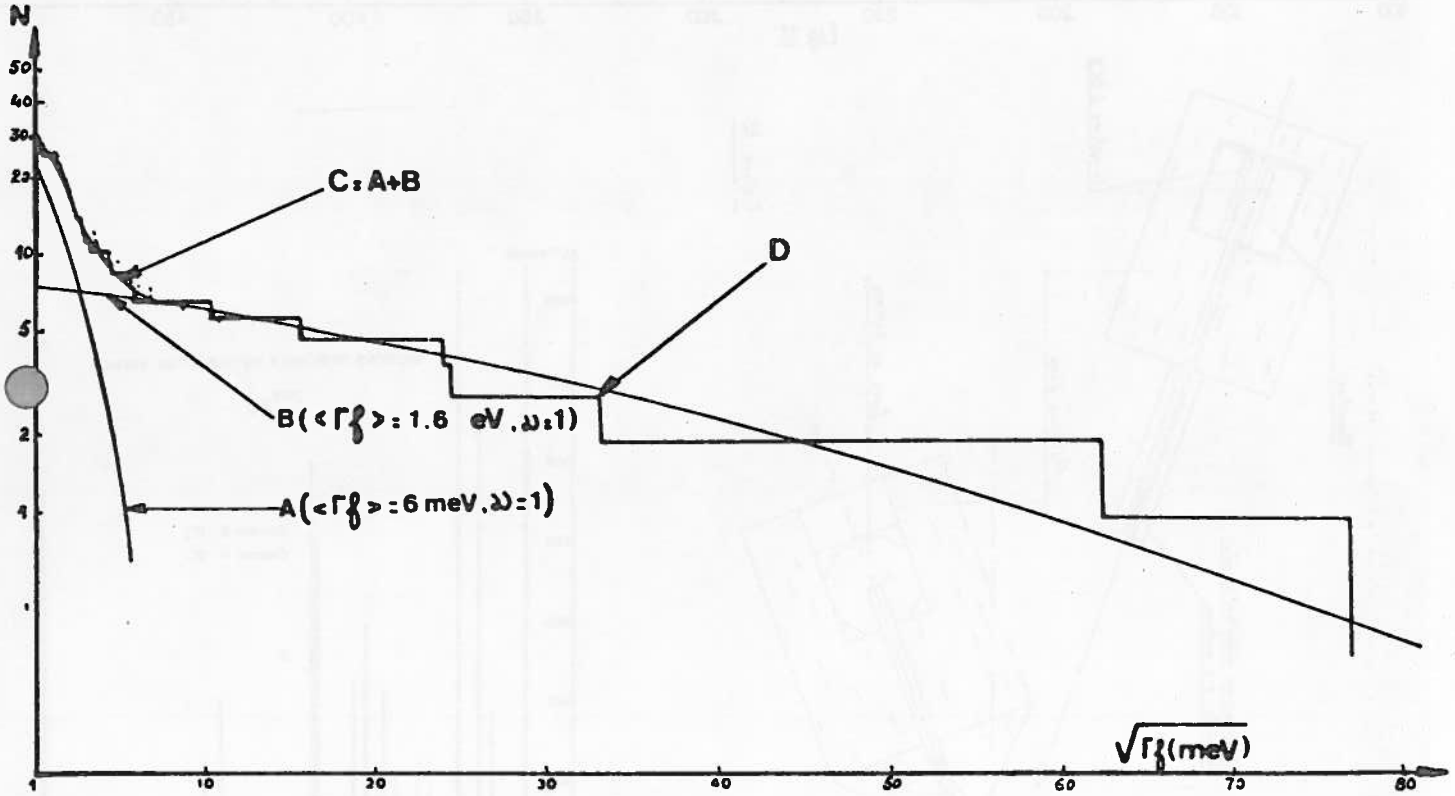
N
C: A+B
D
B (<Γf> = 1.6 eV, ν = 1)
A (<Γf> = 6 meV, ν = 1)
√Γf (meV)

Fig 10

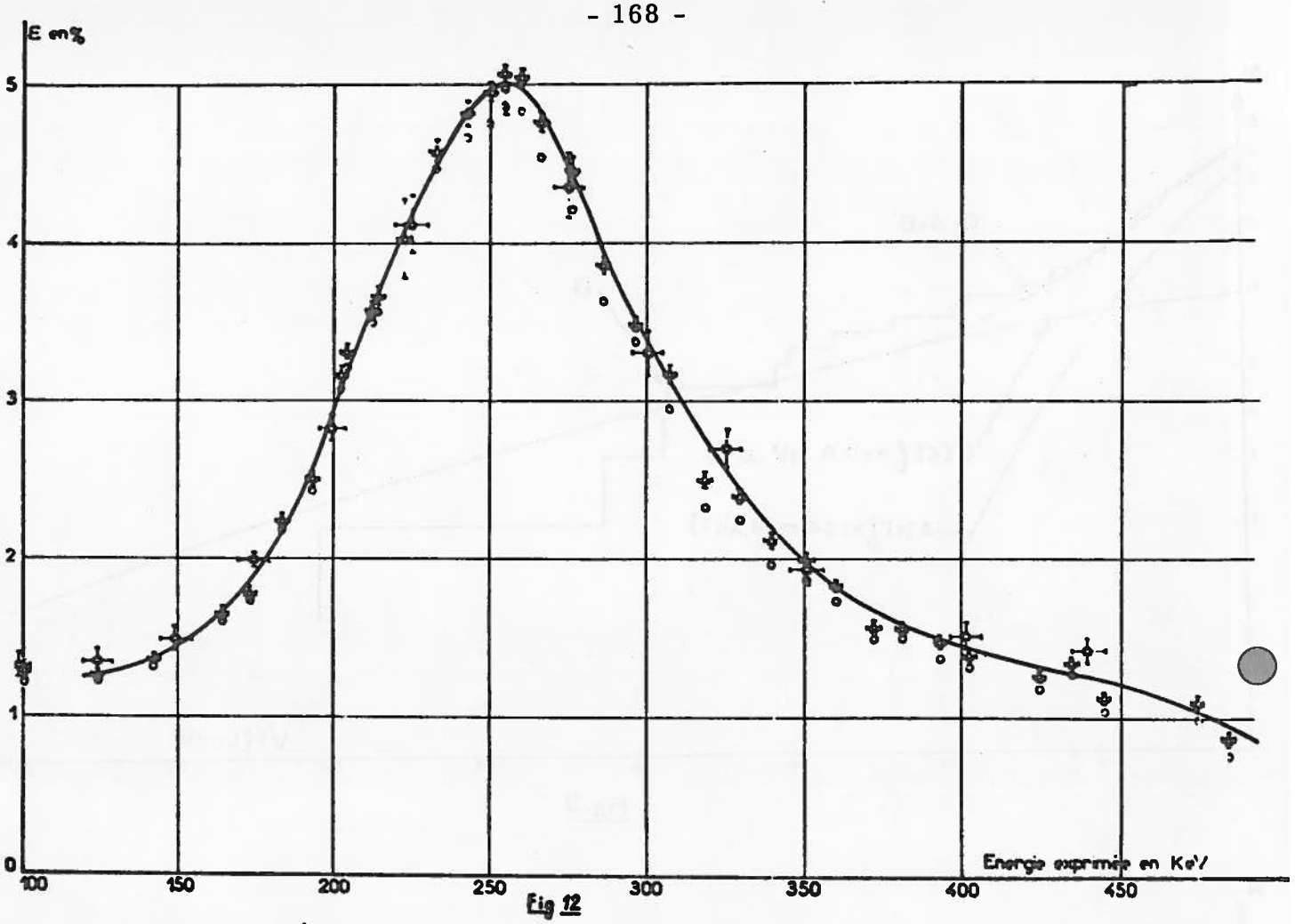

Fig 12

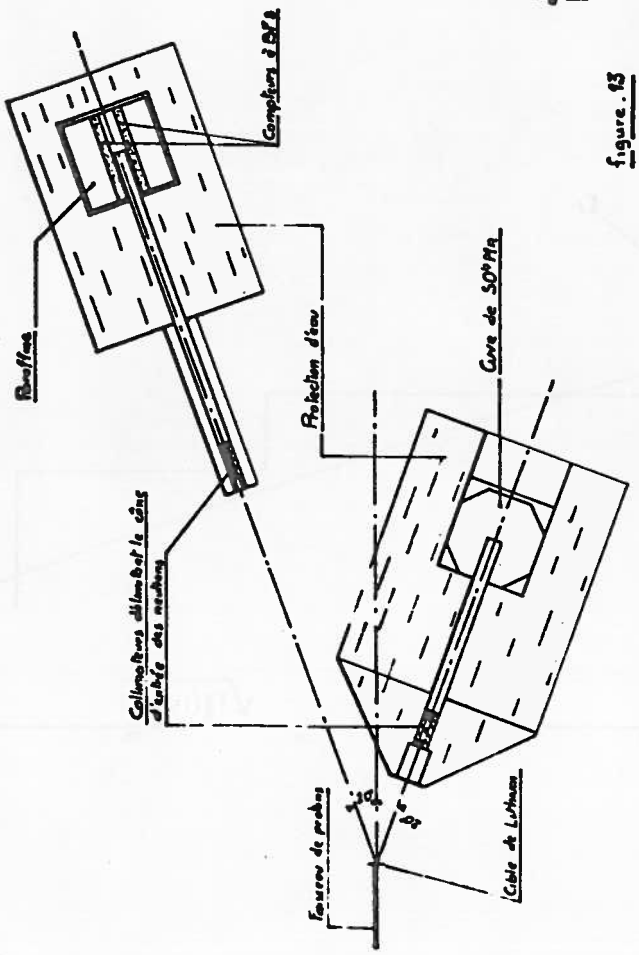

figure. 13

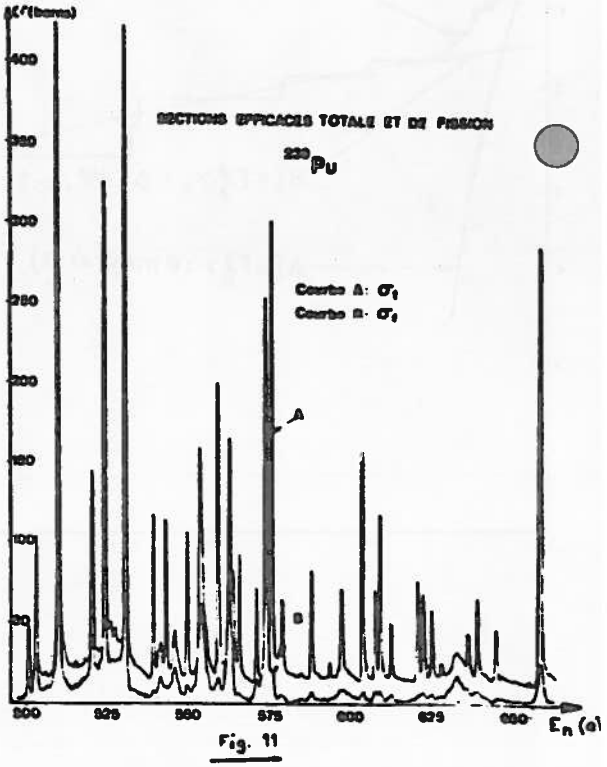

Fig. 11

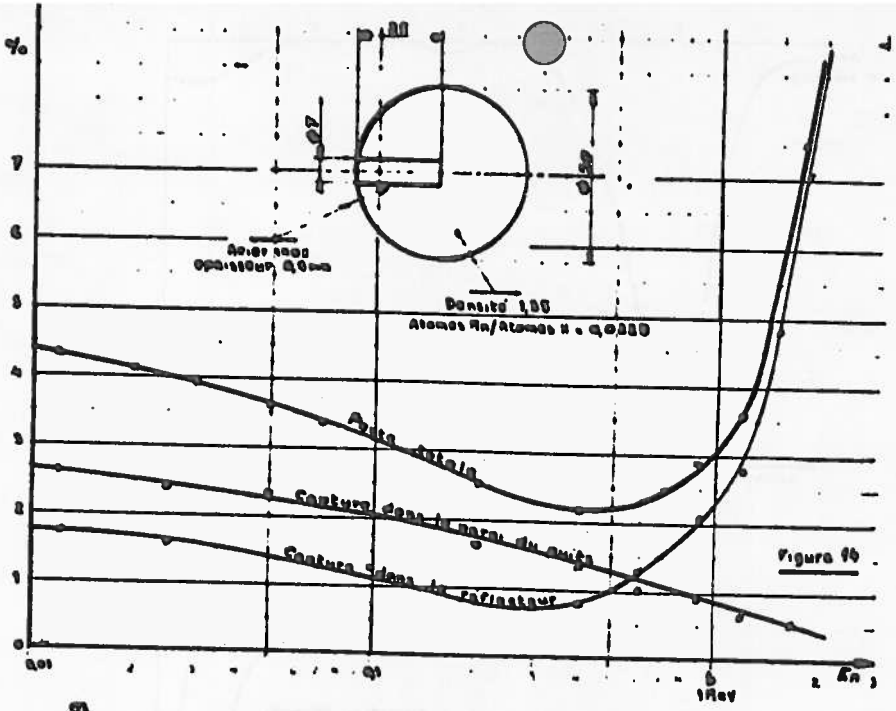

Figure 14

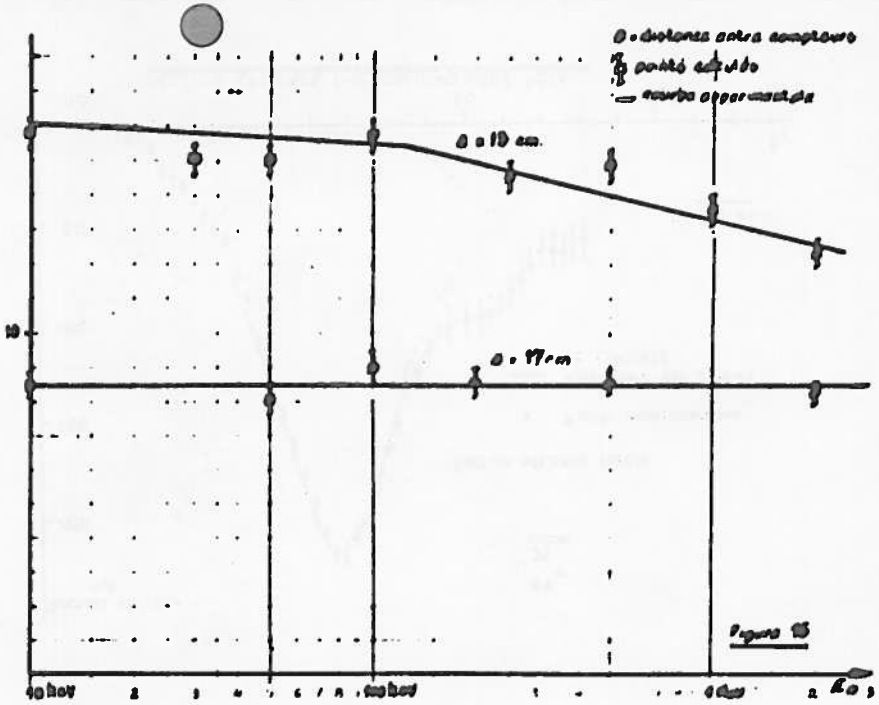

Figure 15

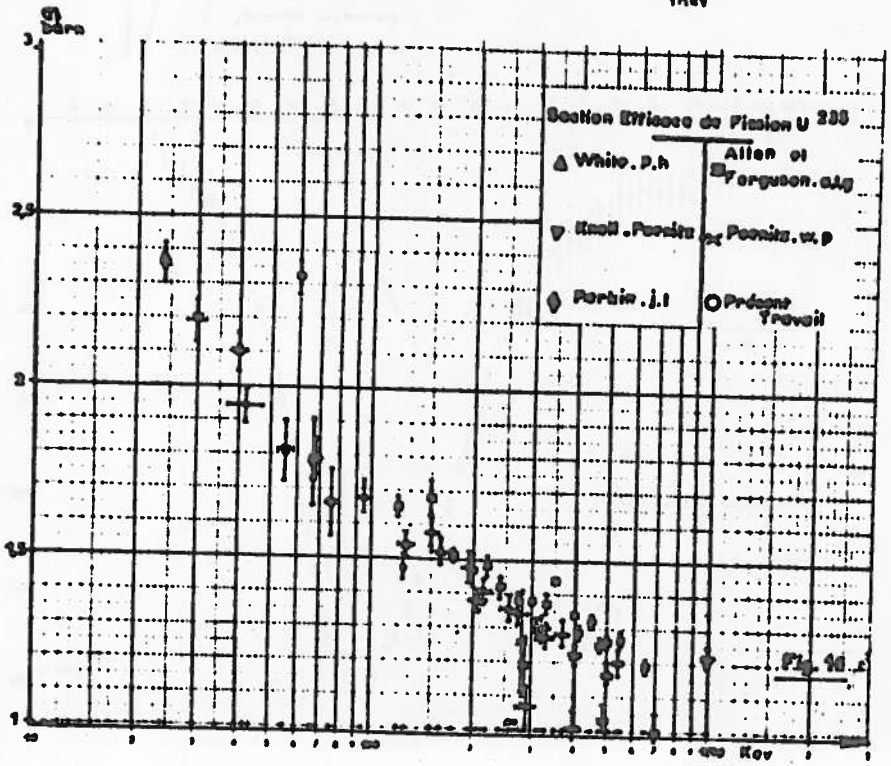

Fig. 16

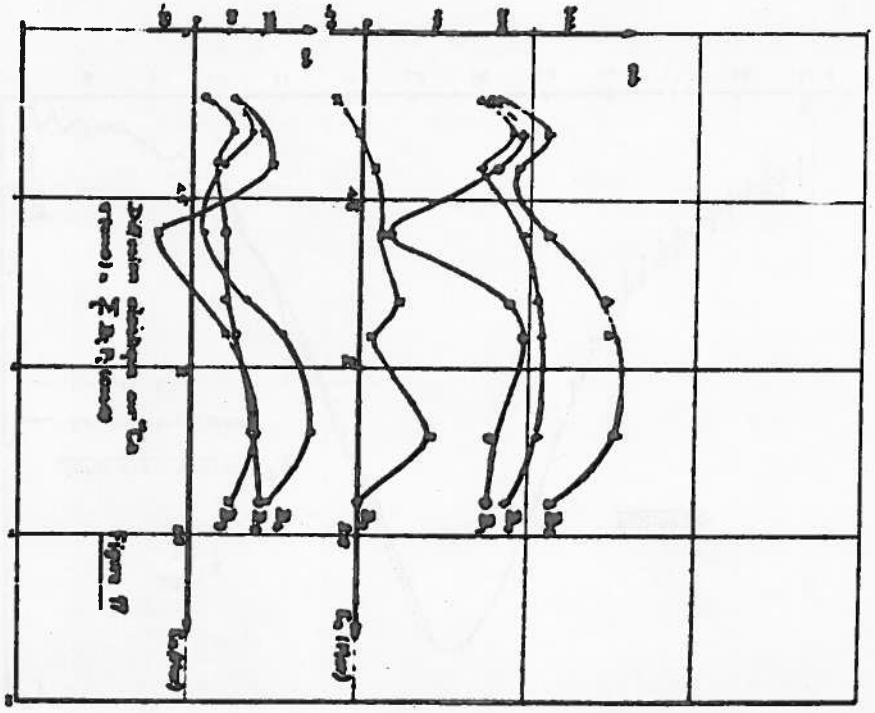

Figure 17

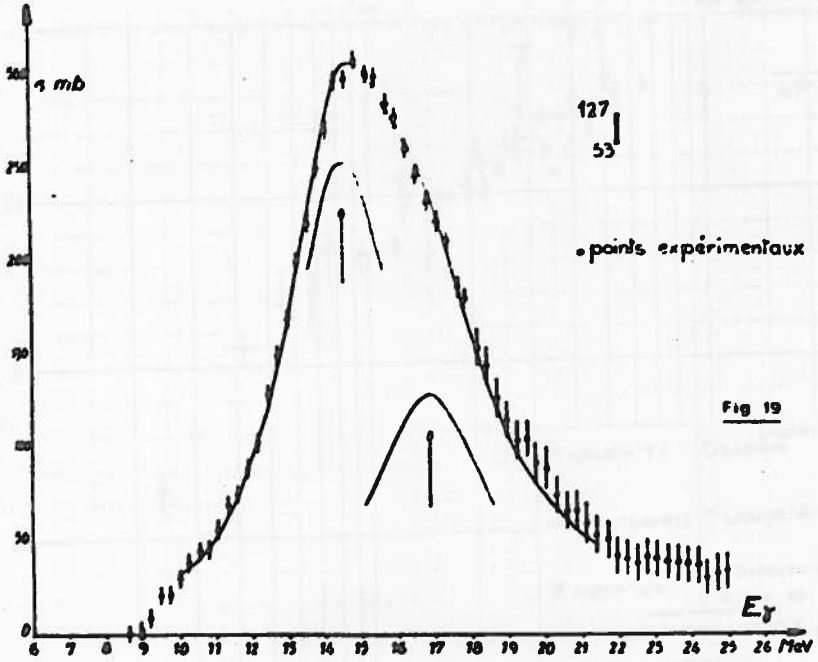

Fig 19

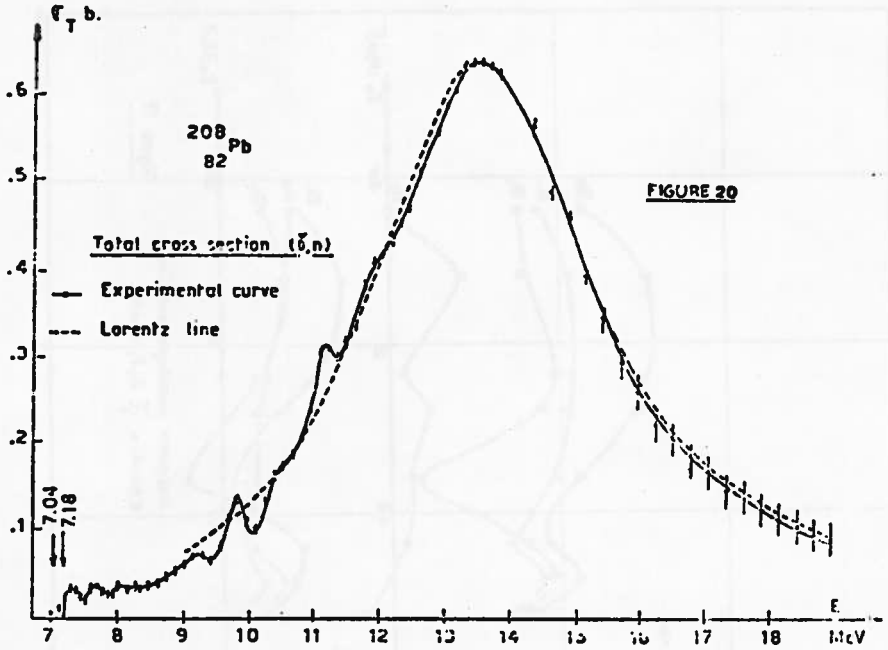

FIGURE 20

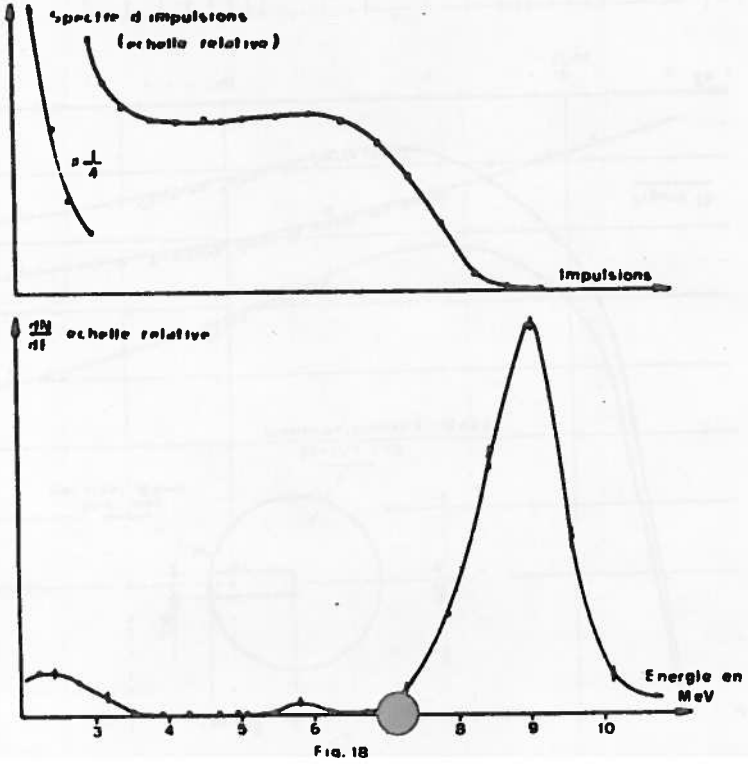

Fig. 18

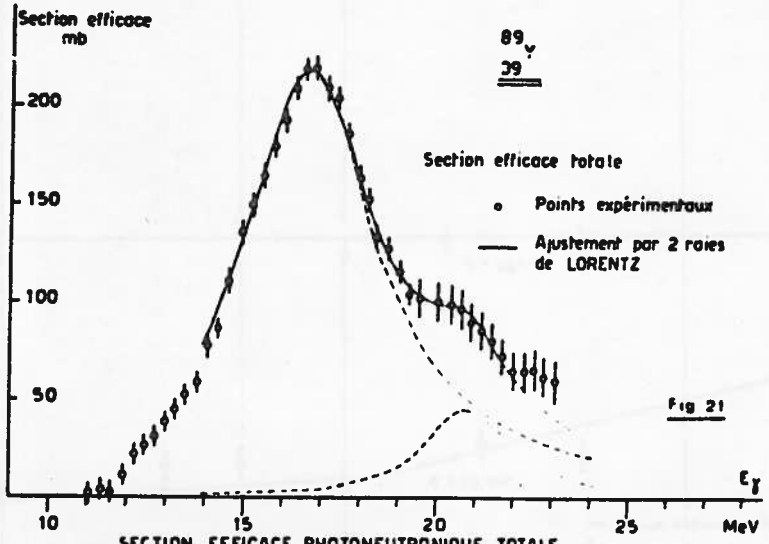

Fig 21

SECTION EFFICACE PHOTONEUTRONIQUE TOTALE

XXII. SERVICE DE PHYSIQUE EXPERIMENTALE - C.E.A. - BRUYERES-le-CHATEL -

P. LEUBA, D. DIDIER

1. APPAREILLAGE

1.1. Accélérateurs (A. Dandine, J.C. Ciret, L. Degueurce)

Une source à extraction directe destinée à équiper l'accélérateur Van de Graaff tandem de 12 MeV, est en cours de réalisation. Une salle de cibles de grandes dimensions et à parois légères spécialement conçue pour l'étude des spectres de neutrons par la méthode du temps de vol, est en construction à proximité de ce même accélérateur. L'équipement complet pour les études de temps de vol sera mis en place au cours de l'année 1970.

1.2. Acquisition et traitement des données (P. Fernier, J. Labbé, J.P. Laget, G. Marin, M. Renaud)

La livraison des trois ordinateurs 10020, éléments de base du système d'ordinateurs hiérarchisés, a été effectuée fin 1969.

- une période de mise au point, estimée à 6 mois, sera nécessaire pour l'essai des matériels connectés aux postes d'acquisition.
- un délai comparable sera utilisé à la mise au point des programmes système et à la constitution d'un software d'application.
- un langage conversationnel de création et de manipulation d'images graphiques à destination d'unité de visualisation SINTRA VU 2000 sera développé courant 1970.
- la liaison avec un ordinateur 10 070 sera également mise en service en 1970.
- l'ensemble des programmes de calcul d'exploitation des données a été augmenté de nombreux programmes nouveaux.

2. ETUDES DES REACTIONS NUCLEAIRES ENTRE ELEMENTS LEGERS -

2.1. Diffusion élastique des deutérons sur les noyaux légers entre 2 et 12 MeV (G. Bruno, M. Le Bars, Y. Decharge, G. Surget)

Des mesures préliminaires ont été effectuées à divers angles et diverses énergies incidentes. Dans le cas de diffusion sur ^{6}Li et ^{7}Li, des réactions parasites sur l'oxygène et sur le support de cible en carbone donnent, dans certaines conditions cinématiques rencontrées ici, des particules de même énergie que les deutérons diffusés. Il est alors indispensable de discriminer les particules diffusées.

Nous avons donc été amenés à essayer un système de discrimination de particules utilisant simultanément la méthode de Goulding et le temps de vol, afin de pouvoir couvrir une gamme totale d'énergie comprise entre 1 et 10 MeV. Les informations E, Δ E et t sont envoyées dans la mémoire d'un calculateur fonctinnant

en ligne. Le calculateur effectue un classement des particules en fonction d'une part de la différence $\left[(E + \Delta E)^{1,73} - E^{1,73}\right]$ qui est caractéristique du type de particule, et d'autre part de Et^2 qui est proportionnel à la masse de la particule. Ces opérations permettent un contrôle continu du fonctionnement de l'expérience. Les résultats obtenus jusqu'ici sont en cours de dépouillement.

2.2. Réaction ^{6}Li (d,n) ^{7}Be mesures à basse énergie (G. Bruno, M. Le Bars, M.Y. Decharge, G. Surget)

La section efficace résulte du comptage des noyaux de ^{7}Be formés (comptage des γ de désexcitation de ^{7}Li * 0,478 MeV).

La section efficace en valeur absolue a été déterminée par deux méthodes :
- comparaison avec la section efficace de la réaction ^{6}Li (d,p_1) ^{7}Li*(0,478)
- estimation du produit (efficacité) x (angle solide) du détecteur pour les γ de 478 keV de désexcitation du ^{7}Li* 0,478 MeV.

Les résultats obtenus par ces deux méthodes entre 80 et 250 keV, sont en bon accord entre eux (fig. 1), dans la limite des erreurs (35 %). Des mesures identiques ont été effectuées pour la gamme d'énergie du Van de Graaff de 2 MeV (0,5 à 2 MeV). Les résultats sont en cours d'exploitation.

2.3. Etude de la réaction ^{6}Li (d,n) ^{7}Be (A. Adam, J. Cabé, M. Cance, M. Labat, M. Laurat, M. Beaufour)

On a mesuré par temps de vol, auprès du Van de Graaff 12 MeV pulsé, les distributions angulaires entre 15° et 135° des neutrons produits par la réaction ^{6}Li (d,n) ^{7}Be, pour E_d compris entre 1,8 MeV et 6 MeV par pas de 250 KeV. L'ensemble de détection, comportant une discrimination de forme neutron-gamma [1], permet une résolution en temps d'environ 1 ns pour toute la dynamique ; toutefois, les conditions actuelles de fonctionnement de l'accélérateur n'ont pas permis de séparer les neutrons provenant du niveau fondamental et du premier état excité du ^{7}Be (fig. 2). Les résultats (fig. 3) sont donc relatifs à l'ensemble de ces deux niveaux ils doivent être considérés comme préliminaires (précision 30 %) et seront améliorés par une meilleure détermination de l'efficacité du détecteur et par l'utilisation de cible de ^{6}Li sans support.

2.4. Etudes des réactions ^{6}Li + T (M. Cadeau, J.P. Laugier, F. Migeon, G. Mouilhayrat, F. Savioz)

Nous avons repris l'étude de la réaction ^{6}Li + T $\longrightarrow$ n + 2 α en accélérant comme cela avait été fait à Saclay (cf. M. Berrada et als. - J. de Phys. 28, 135, 1967) des ions lithium sur des cibles de tritium absorbé dans du titane. L'étude anté-

rieurement limitée à des énergies incidentes inférieures à 2 MeV, a été réalisée sur le Van de Graaff 12 MeV, les énergies incidentes étant comprises entre 3 et 6 MeV par pas de 250 ou 500 keV.

On a enregistré les spectres de particules α émises à 60°, 90°, 120° et 135° du faisceau incident. Les résultats pour le premier détecteur (60°) normalisés à un même angle solide et à une même charge recueillie sur la cible apparaissent sur la figure 4.

Parallèlement nous avons entrepris l'étude de la réaction miroir $^{6}Li + ^{3}He$ $p + 2\alpha$ en accélérant des ions ^{3}He sur une cible au lithium avec un Van de Graaff 2 MeV.

L'interprétation est en cours en relation avec celle des mesures antérieures [2] [3] [4] [5].

3. ETUDES SUR LES NEUTRONS RAPIDES

3.1. Sections efficaces totales (A. Adam, J. Cabé, M. Cance, M. Labat, M. Laurat, M. Beaufour)

3.1.1. Organisation des mesures : ces mesures font partie d'une série d'expériences ayant pour but soit de mettre en évidence des résonances isolées ou des structures d'une largeur de 100 à 300 keV du type état porte [6][7], soit de préciser des données mal connues (U 235 - U 2388). Les résultats ont été obtenus à l'aide de neutrons produits par la réaction T (p,n) ^{3}He, utilisant le Van de Graaff de 2 MeV. La définition en énergie des neutrons était de l'ordre de 4 keV dans les mesures fines et de l'ordre de 25 keV pour obtenir des valeurs moyennes. Les mesures s'étendent sur la plage d'énergie de neutrons comprise entre 100 keV et 1 200 keV. La précision absolue sur la section totale est de l'ordre de 3 %.

3.1.2. Résultats : Les mesures ont porté sur les noyaux ou éléments suivants : ^{9}Be, Ni, U naturel et ^{235}U (fig. 5, 6, 7, 8). Il est prévu de les étendre au ^{239}Pu et à la gamme d'énergie de neutrons incidents s'étendant de 1 200 keV à 6 MeV pour l'U naturel, ^{235}U et ^{239}Pu.

Les mesures sur le ^{9}Be paraissent cohérentes à l'exception d'une anomalie signalée aux environs de 200 keV [8] et qui n'est pas retrouvée. Les deux résonances observées correspondant aux états excités de ^{10}Be situés respectivement à 7,37 MeV et 7,54 MeV ; leurs largeurs (25 keV pour la première, $\sim$8 keV pour la seconde) correspondent respectivement à des états 3^- et 2^+ de $^{10}Be^*$.

La mesure faite sur le nickel est une reprise plus précise et sur une gamme d'énergie plus étendue d'une mesure antérieure [9].

3.2. Diffusion élastique de neutrons

3.2.1. Recherche d'une structure intermédiaire dans les sections efficaces totale et diffusion élastique de neutrons sur le titane. (A. Adam, J. Cabé, M. Cance, M. Labat, M. Laurat, M. Beaufour) [6] [7]

Ce travail fait suite à nos précédentes mesures de sections efficaces totale et de diffusion élastique, entre 150 keV et 1 200 keV [10] ; la section efficace totale convenablement moyennée présentait deux "bosses", l'une bien marquée à 700 keV l'autre moins nette vers 1 MeV. Pour déterminer si ces "bosses", caractérisaient des états de spin et parité définis, nous avons mesuré les distributions angulaires des neutrons diffusés élastiquement entre 580 keV et 1 200 keV avec une dispersion en énergie de l'ordre de 80 keV.

Après soustraction de la diffusion potentielle calculée σ_p, ces distributions ont été développées en série de polynômes de Legendre. Sur la figure 9, on a porté les points expérimentaux, les valeurs de σ_p calculées (courbes en pointillés marquées S.E. à 720 keV et 1 100 keV) ainsi que la somme de σ_p et du développement en polynômes de Legendre (courbes en trait plein). Au-dessous de 900 keV, seuls P_0 et P_1 contribuent à la section efficace ; au-dessus de 900 keV le meilleur lissage s'obtient avec une contribution de P_2 et P_3 qui n'est cependant pas vraiment significative en raison de la précision avec laquelle on connaît la section efficace due à l'état intermédiaire et l'interférence de celle-ci avec σ_p.

La variation en fonction de l'énergie de A_0 et A_1 est représentée sur la figure 10. On remarquera le comportement caractéristique d'une résonance de paramètres $E_o = 710$ keV $J = 1/2$ de A_0 et A_1 entre 580 keV et 820 keV ; au-delà de cette énergie, leur variation est peu nette et difficile à interpréter en terme de résonance . Avec les notations de Mahaux et Weidenmuller (Nucl. Phys. 91, 24, 1967) le lissage de la résonance donne les paramètres suivants :

largeur totale $\Gamma^{\uparrow} + \Gamma^{\downarrow} = (65 \text{ keV} \pm 7 \text{ keV})$ avec $\Gamma^{\uparrow} \sim 40$ keV et $\Gamma^{\downarrow} \sim 25$ keV.

Ces largeurs sont en bon accord avec les largeurs prévues par les théoriciens pou les structures intermédiaires. Par contre au-delà de 800 keV, les variations de P_0 et P_1 suggèrent la présence de parités opposées. Il semble que la "bosse" observée autour de 1 MeV ne puisse être attribuée à un moment angulaire et une parité définis, donc à la présence d'un état intermédiaire [11] .

3.2.2. Etude de la diffusion élastique des neutrons de 14 MeV (M. Cadeau, J.P. Laugier, F. Migeon, G. Mouilhayrat, F. Savioz)

Une étude de la diffusion élastique des neutrons de 14 MeV a été entreprise sur ^{238}U. On s'efforce de préciser en particulier la distribution angulaire des neutrons diffusés aux grands angles. Les données obtenues seront comparées aux résultats des calculs théoriques en tenant compte de l'excitation des premiers niveaux de ^{238}U.

4. ETUDES SUR LA FISSION (J. Fréhaut, J. Gauriau, G. Mosinski, M. Soleilhac)

4.1. Mesure du nombre moyen de neutrons prompts pour la fission de ^{235}U et ^{239}Pu induite par des neutrons d'énergie comprise entre 0,3 et 1,4 MeV

Cette mesure prolonge vers les basses énergies les résultats obtenus antérieurement de 1,3 à 15 MeV. Les neutrons incidents ont été produits par réaction ^{7}Li (p n) ^{7}Be avec l'accélérateur tandem Van de Graaff 12 MeV pulsé à la fréquence de 2,5 MHz. La cible de lithium métallique est suffisamment épaisse pour arrêter les protons. On produit ainsi tout un spectre de neutrons dont l'énergie est déterminée par temps de vol. Un tel procédé est à priori particulièrement bien adapté à la mise en évidence de structures éventuelles dans la loi $\nu_p = f(E)$. L'enregistrement des données s'effectue sur bande magnétique incrémentale. La mesure a été réalisée simultanément sur les deux matériaux fissiles placés dans la même chambre à fission qui contient également du ^{252}Cf pour étalonnage. Les résultats obtenus sont représentés sur les figure 11 et 12.

Pour ^{235}U ces résultats confirment l'ensemble des mesures effectuées précédemment dans ce domaine d'énergie : l'ouverture de nouvelles voies de fission se manifeste par une variation non linéaire de ν_p.

Pour ^{239}Pu nous avons porté la droite obtenue précédemment par la méthode des moindres carrés à partir de nos résultats obtenus entre 1,36 et 5,06 MeV d'une part et 12,41 et 14,85 MeV d'autre part. (Journal of Nuclear Energy vol. 23 p. 257). Une structure analogue à celle observée pour ^{235}U semble apparaître vers 400 keV mais avec une amplitude plus faible.

4.2. Mesure du rapport des sections efficaces de fission $\frac{\sigma_F\ ^{239}Pu}{\sigma_F\ ^{235}U}$ de 0,3 à 1,4 MeV

Du nombre de fissions de ^{239}Pu et ^{235}U détectées à une énergie donnée dans la mesure précédente et en tenant compte de la diffusion des neutrons incidents par la platine qui constitue le support de cible nous avons déduit les sections efficaces relatives de fission. Nos résultats normalisés sur le point à 0,6 MeV du KFK 750 sont représentés sur la figure 13.

4.3. Mesure de section efficace n - 2n sur matériaux fissiles . En utilisant la technique du gros scintillateur liquide nous avons mis au point une méthode permettant de réaliser la mesure des sections efficaces(n,2n) par rapport à la section efficace de fission sur matériau fissile. La première mesure réalisée de 6 à 10 MeV concerne ^{238}U, les résultats sont en cours d'exploitation.

5. ETUDE DU RAYONNEMENT GAMMA PRODUIT PAR LES NEUTRONS (J. Lachkar, G. Haouat, Y. Patin, J. Sigaud)

5.1. Réaction (n, x γ) sur ^{11}B : cette étude fait suite à celle précédemment effectuée sur ^{6}Li, ^{7}Li, ^{10}B et ^{12}C. Nous avons enregistré les fonctions d'excitation des photons émis par réaction (n, n'γ) dans la gamme d'énergie 5,3 MeV-9,8 MeV ainsi que les distributions angulaires des raies γ de 2,124 MeV ; 4,444 MeV ; 5,019 MeV ; 6,793 MeV ; 7,296 MeV pour des énergies neutroniques de (7,18 $\pm$ 0,1 MeV), (8,5 $\pm$ 0,1 MeV) et (9,72 $\pm$ 0,1 MeV) correspondant aux résonances à 9,95 MeV et 12,27 MeV du ^{12}B et à une région où ce noyau ne présente pas de résonance.

Les distributions angulaires sont isotropes à mieux que 10 % ; les fonctions d'excitation semblent peu sensibles aux résonances du ^{12}B ce qui laisse supposer qu'à ces énergies le mécanisme de réaction est un mélange complexe d'interaction directe et de noyau composé.

L'analyse théorique de ces résultats expérimentaux est en cours ainsi que l'étude expérimentale à E_n = 14,1 MeV.

Les sections efficaces absolues, obtenues par normalisation sur ^{12}C, ont pu être mesurées avec une précision de 15 %. La distribution angulaire est connue avec une précision meilleure que 10 %.

5.2. Etude des niveaux d'énergie du ^{56}Fe. Nous avons enregistré les rayonnements γ émis par la réaction : ^{56}Fe (n,n'γ) à l'énergie de neutrons incidents de 8,7 MeV et comparé au spectre de désexcitation radioactive du ^{56}Co.

La synthèse de nos résultats avec les données antérieures est rapportée dans le tableau et le schéma de désintégration de la figure 14.

Les principales conclusions sont les suivantes :

- les raies γ de 1038 keV et 2274 keV traduisent la mise en évidence d'un doublet : 3123 keV (3^+) et 3120 keV (0^+, 1^+).
- l'intensité relative de ces deux raies, et l'absence de détection de la transition 3120 keV, paraissent exclure l'attribution du spin 3^-, proposée par Benjamin et al (Nucl. Phys. 79, 241, 1966).

- le spin du niveau 3445 keV semble être 3^+ et non 1^+ comme l'avait suggéré Ferguson et al (AERE, 14, 32, 1968). Le spin 3^+ est en accord avec le peuplement important de ce niveau par le C_o^{56}, dont le niveau fondamental a le spin 4^+ ; par ailleurs les rapports d'embranchement expérimentaux (0,765 et 0,234) sont voisins de ceux qui ont été calculés, dans l'hypothèse du spin 3^+ (0,71 et 0,34).
- la mise en évidence d'un photon de 3598 keV confirme le niveau 4445 keV ($4^{\pm}$, $3^{\pm}$) proposé par Sher et al (Nucl. Phys. A 112, 85, 1968) se désexcitant sur le niveau 847 keV.
- les huit niveaux dont les énergies d'excitation sont supérieures à 4445 keV, avaient été précédemment observés par réactions (p, p') et (p,α) mais ces mesures ne permettaient pas de définir d'une manière unique les spins de ces niveaux. Le schéma de niveaux que nous proposons en précisant spins et parités est en excellent accord avec celui qui résulte du calcul théorique de Mac Grovy (Phys. Rev. 160, 160, 1967).
- l'ensemble des données figurant dans le schéma a été utilisé dans un calcul théorique de la fonction d'excitation du niveau 847 keV jusqu'à E_n = 8,7 MeV. Il était indispensable d'y faire intervenir toutes les données car ce calcul basé sur l'hypothèse du noyau statistique tient compte des principales voies de sortie de la diffusion inélastique et des contributions des principales cascades aboutissant à ces niveaux.

5.3. Analyse des spectres nn'γ déformés par effet Doppler

La durée de vie de nombreux niveaux isomériques a été mesurée à partir de l'effet Doppler par des méthodes ne nécessitant pas la connaissance de la fonction de corrélation entre le noyau de recul et le photon diffusé. Nous avons dans une démarche inverse tenté de tirer de l'analyse des spectres nn'γ sur les noyaux légers une connaissance au moins qualitative de cette fonction de corrélation. Quel que soit le mécanisme de la réaction, la fonction de corrélation $W(\hat{k}, \hat{k}_n, \hat{k}_\gamma)$ entre le neutron diffusé dans la direction $\vec{k}_n$ par rapport au neutron incident $\vec{k}_o$ et le photon de désexcitation émis dans la direction $\vec{k}_\gamma$ (par rapport à $\vec{k}_o$) s'écrit (Bredenharn et al, Rev. of Mod. Phys. 25, 729, 1953) :

$$W(\hat{k}_o, \hat{k}_n, \hat{k}_\gamma) = \sim \sum_{\mu\nu\lambda} B_{\mu\nu\lambda} \; S_{\mu\nu\lambda} \; (\hat{k}_o, \hat{k}_n, \hat{k}_\gamma)$$

Dans le cas où la durée de vie du noyau est infiniment brève, et en considérant la formule bien connue de l'effet Doppler, la densité de probabilité pour qu'un

photon soit enregistré à l'angle θ_γ avec l'énergie E se met sout la forme :

$$P(E,\theta_\gamma) \sim \sum_{\lambda\mu\nu} B_{\lambda\mu\nu} \; A_o(\lambda\mu\nu) \; P_\mu(\cos\theta_\gamma) \; P_\nu\left[\frac{c}{v}\left(1 - \frac{E}{E} + \frac{v_a}{c}\cos\theta_\gamma\right)\right]$$

$P(E,\theta_\gamma)$ est exprimé dans le laboratoire, v est la vitesse du noyau de recul exprimé dans le centre de masse, v_a est la vitesse du centre de masse.

Dans le cas où l'on doit tenir compte de la durée de vie et du ralentissement du noyau de recul dans le diffuseur, la fonction $P(E,\theta_\gamma)$ est modifiée mais peut être calculée analytiquement.

Ces méthodes sont actuellement utilisées pour retrouver soit dans le cas du mécanisme du noyau composé statistique, soit dans le cas du mécanisme d'interaction directe sous sa forme simplifiée, la forme expérimentale des raies γ suivantes, produites par diffusion inélastique de neutrons : 0,478 MeV de ^{6}Li ; 0,717 MeV, 2,15 MeV, 3,58 MeV, 5,16 MeV de ^{10}B ; 2,13 MeV, 4,46 MeV, 5,03 MeV de ^{11}B ; 4,43 MeV de ^{12}C ; 1,346 MeV, 1,459 MeV, 1,554 MeV, 2,780 MeV de ^{19}F.

6. EVALUATION DE CONSTANTES NUCLEAIRES - THEORIE -

6.1. Calculs de niveaux d'énergie (B. Duchemin, J.C. Rolard)

Le calcul des niveaux d'énergie des noyaux pair-pair dans l'approximation de B.C.S. a nécessité de notre part une étude complète de cette approximation dans le cas où les neutrons et les protons remplissent les mêmes couches. Nous avons en outre mis au point un programme de modèle en couches que nous comptons utiliser comme calcul exact, pour tester nos hypothèses de calcul. Nous envisageons pour débuter d'effectuer des calculs sur les noyaux de la couche $1f^{7/2}$.

6.2. Calculs de sections efficaces

6.2.1. Diffusion élastique et inélastique - Noyau composé (J.C. Rolard, G. Lagrange, B. Duchemin) :

dans l'hypothèse du noyau composé statistique, un ensemble de programmes de calcul a été mis au point en vue de l'étude des sections efficaces et des distributions angulaires des neutrons diffusés élastiquement et inélastiquement ainsi que des gammas de désexcitation des niveaux excités finals. Ces programmes dans lesquels les fluctuations du type Moldauer sont incluses sont destinés aussi bien à l'exploitation d'expériences qu'à l'évaluation. A titre de test nous avons étudié le cas des neutrons de 2,5 MeV diffusés inélastiquement sur le ^{209}Bi et des gammas de désexcitation de la réaction $^{89}Y(n,n')^{89}Y^*$ formée par des neutrons de 4 MeV. Une étude sur le ^{56}Fe est actuellement en cours.

6.2.2. Diffusion inélastique - Interaction directe - (G. Lagrange) : dans l'hypothèse de l'interaction directe, un programme de calcul des sections efficaces et des distributions angulaires des nucléons diffusés inélastiquement, utilisant la méthode D.W.B.A. a été mis au point avec un facteur de forme collectif ; il a été appliqué à la réaction $^{63}Cu\ (n,n')\ ^{63}Cu^{*}$ [12].

6.3. Transfert d'une particule (L. Faugère) : nous avons adapté sur notre calculateur le programme de transfert de un nucléon, suivant la méthode D.W.B.A. (rapport TID 24 250) et le programme de modèle optique de Smith (rapport USC 136 119). Une étude de l'importance des corrections de portée finie (1er et 2ème ordre) en fonction de la masse du noyau cible est actuellement en cours.

BIBLIOGRAPHIE

[1] A. Adam, J. Cabé, M. Cance, M. Laurat, J.C. Ponce
Rev. Phys. Appl. 4, 262, 1968

[2] L. Marquez, Thèse Orsay 1966

[3] J.P. Laugier, Thèse Orsay 1968 et Rapport C.E.A. - R.3670

[4] G. Gruber, E. Heinicke, B. Frois, L. Marquez, J. Québert, N. Schemer, J.P. Laugier - Etude sur la physique et la production d'ions lourds. La Plagne 1969.

[5] B. Frois, L. Marquez, J. Québert, N. Schemer, J.P. Laugier - Conf. sur les réactions nucléaires induites par ions lourds -Heidelberg 1969.

[6] J. Cabé - Thèse Paris 1967 et Rapport C.E.A. - R. 3279

[7] J. Cabé, M. Laurat, P. Yvon, G. Bardolle - Nucl. Phys. A102, 92, 1967

[8] A. Perrin, G. Surget, C. Thibault, A. Verrière- C.R. Ac. Sc. 255, 277,1962

[9] J. Cabé, M. Laurat, P. Yvon - EANDC (E) 49, 1963

[10] A. Adam, J. Cabé, M. Cance, M. Laurat, M.Longuève, EANDC(E) 115, 1968

[11] J. Cabé, Int. Summer Meeting of Physicists - Duilovo 1969

[12] C. Lagrange, Thèse 3ème cycle Orsay 1969

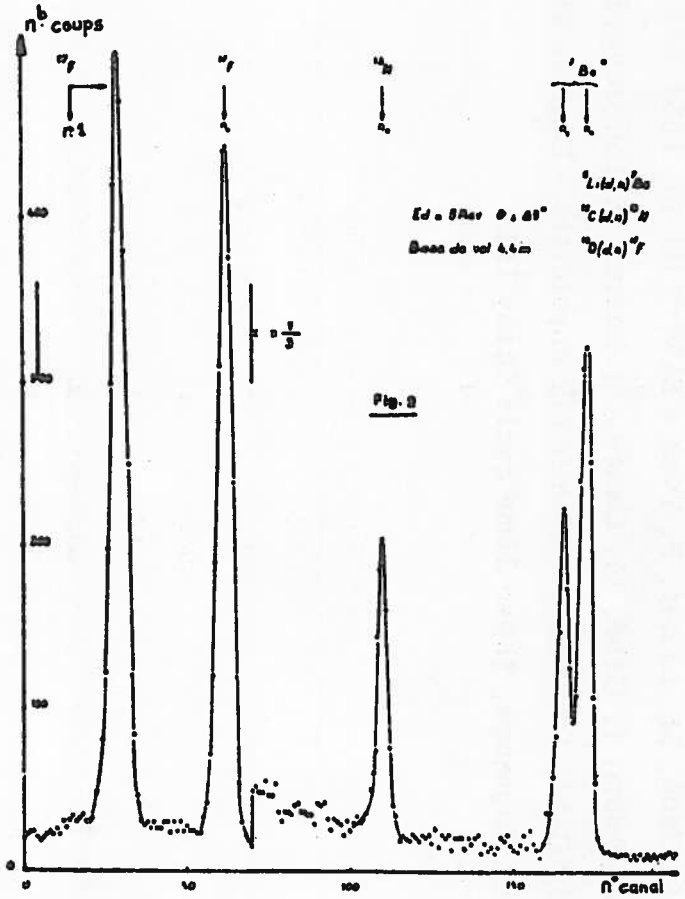

Fig. 2

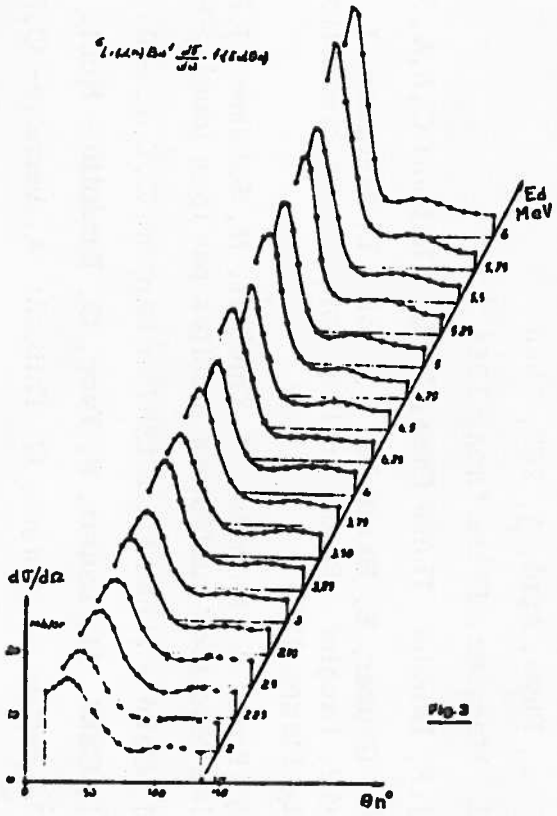

Fig. 3

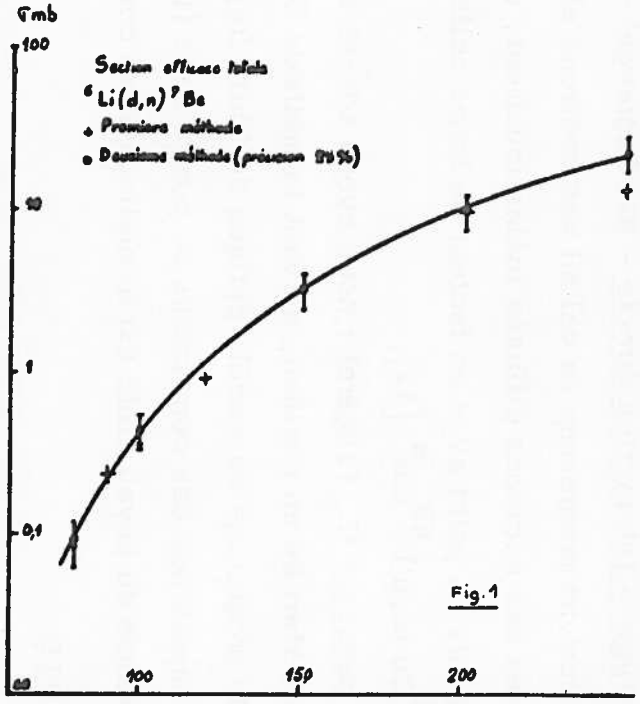

Fig. 1

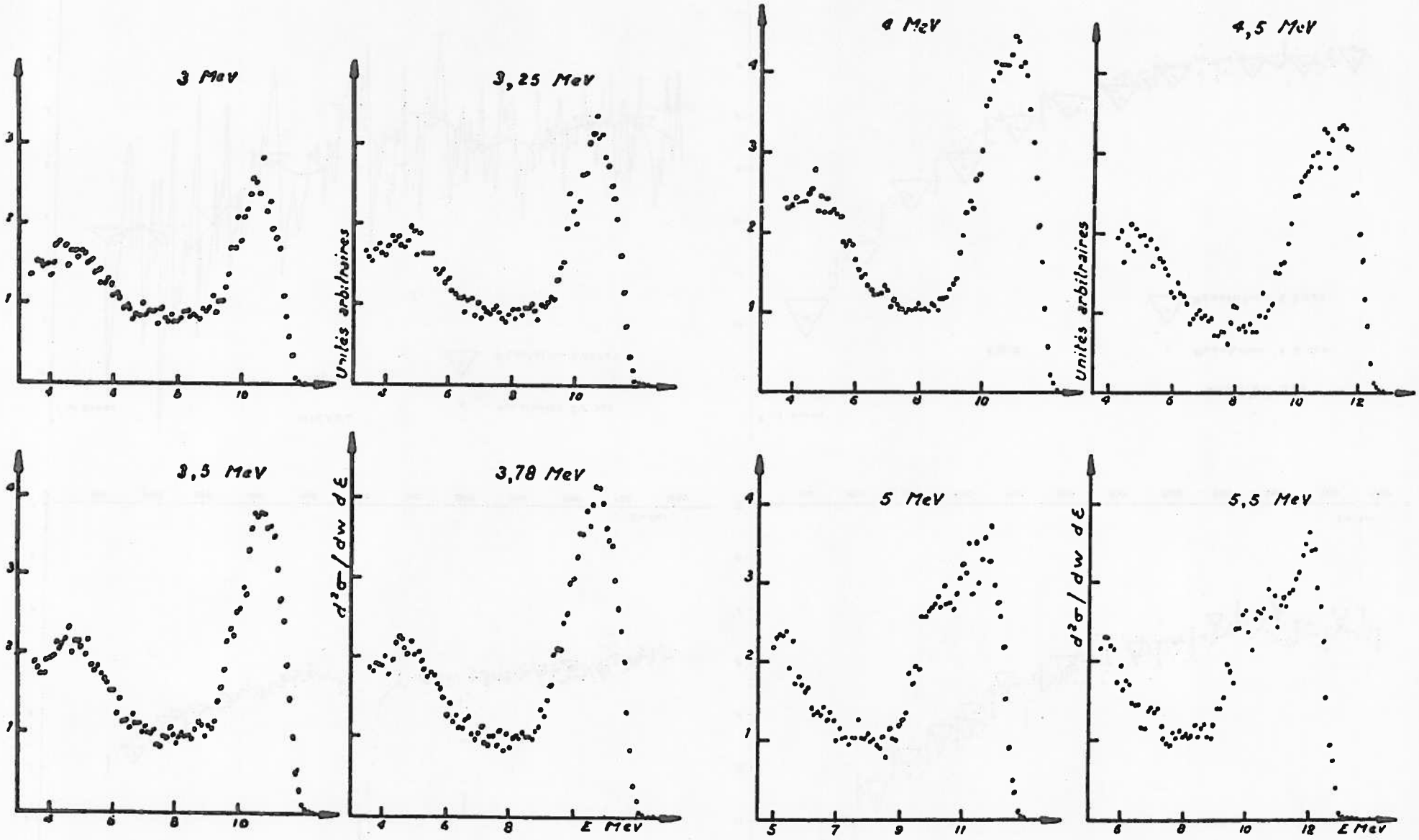

$^6Li + T$ à 60°

Fig.4

$^6Li + T$ à 60°

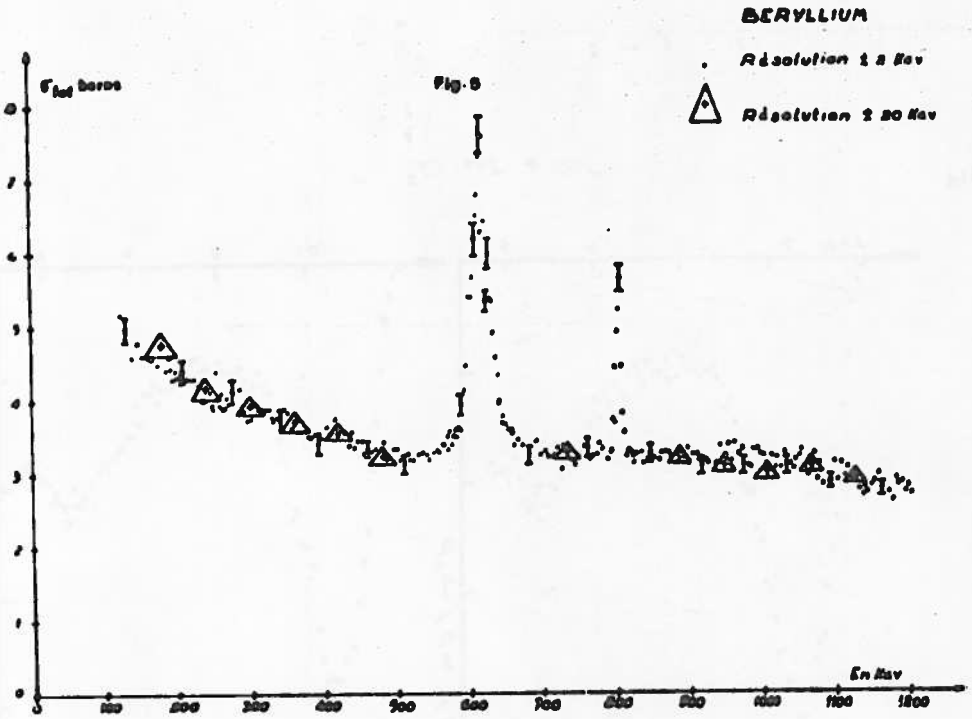
BERYLLIUM
Fig.5
Résolution ± 2 Kev
Résolution ± 20 Kev
σtot barns
En Kev

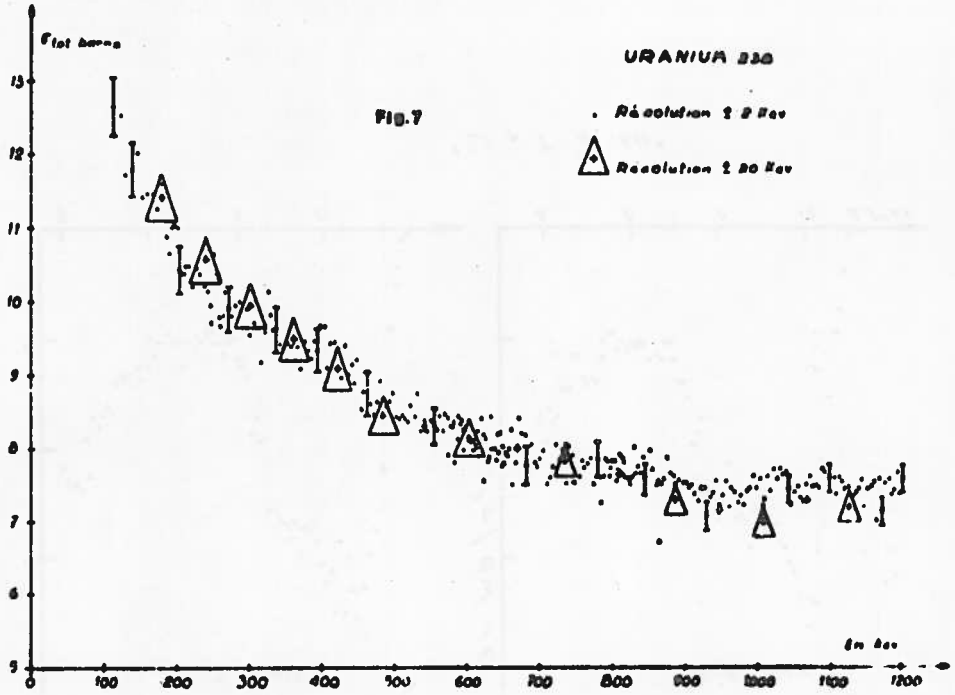
URANIUM 238
Fig.7
Résolution ± 2 Kev
Résolution ± 20 Kev
σtot barns
En Kev

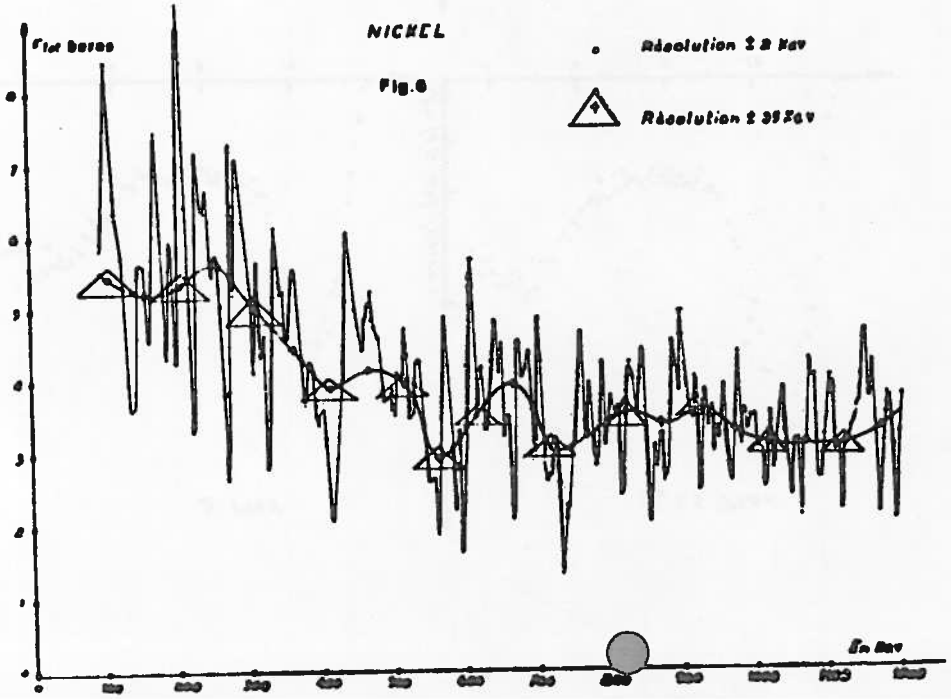
NICKEL
Fig.6
Résolution ± 2 Kev
Résolution ± 35 Kev
σtot barns
En Kev

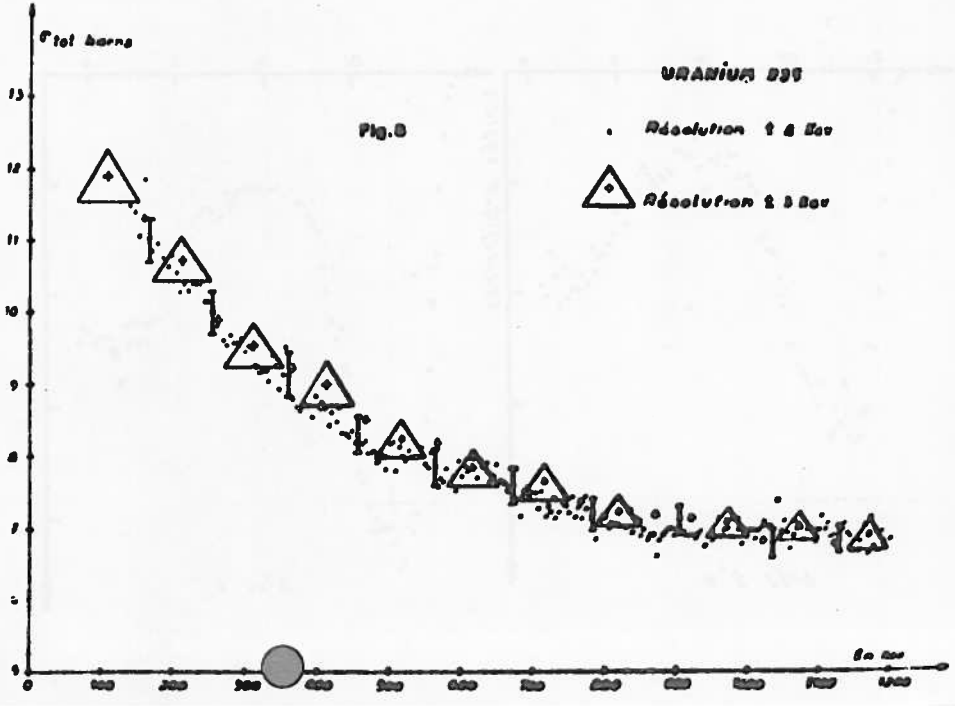
URANIUM 235
Fig.8
Résolution ± 6 Kev
Résolution ± 3 Kev
σtot barns
En Kev

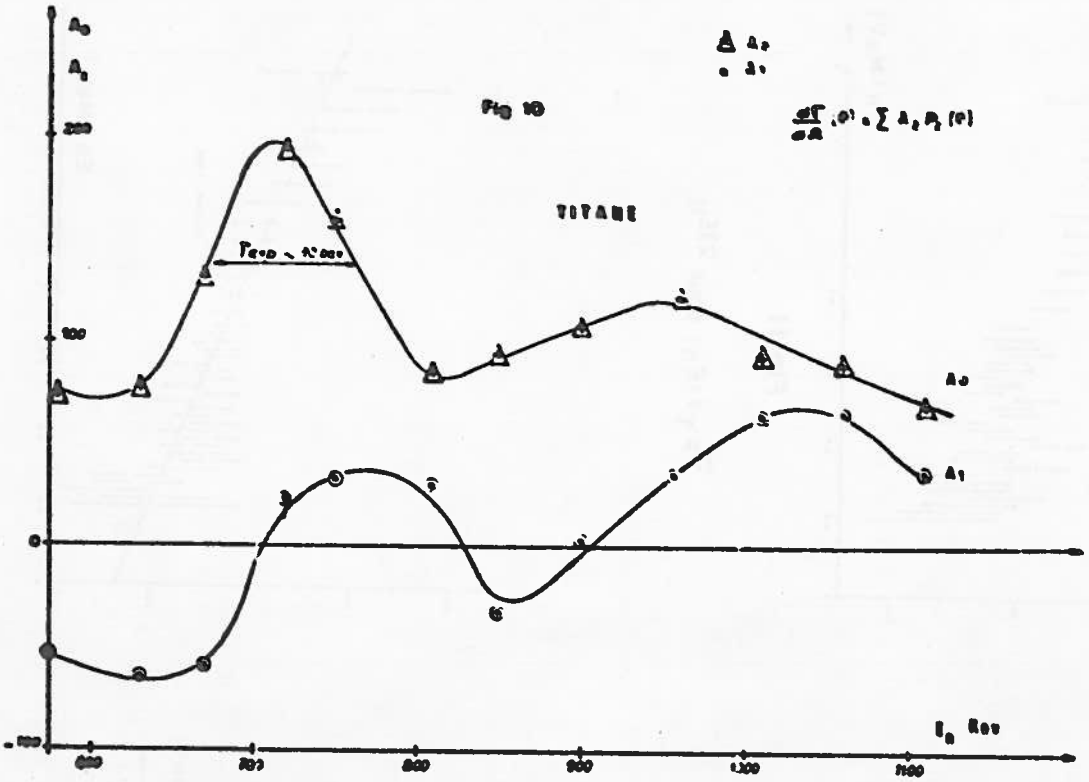
Fig 10
TITANE
A_0
A_1
E_n Kev

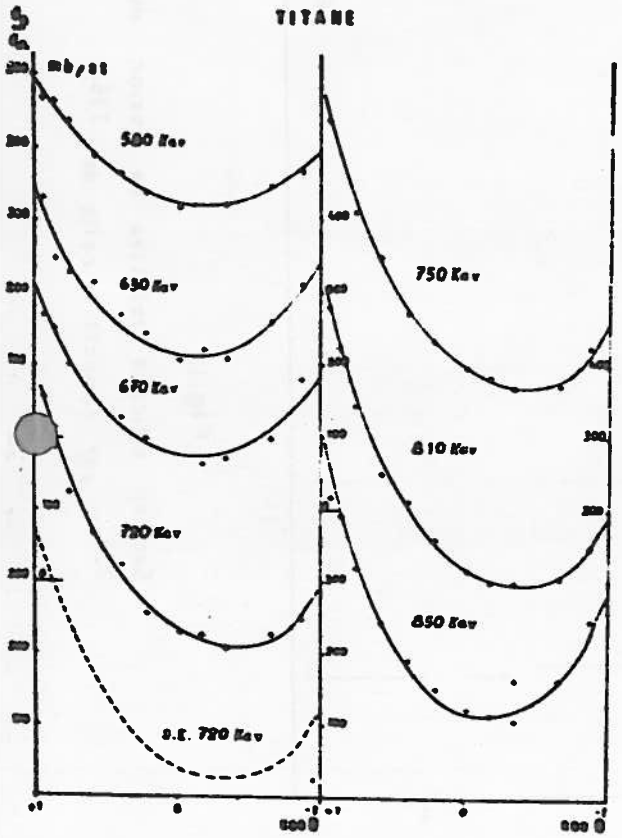
TITANE
mb/st
500 Kev
630 Kev
670 Kev
720 Kev
S.E. 720 Kev
750 Kev
810 Kev
850 Kev

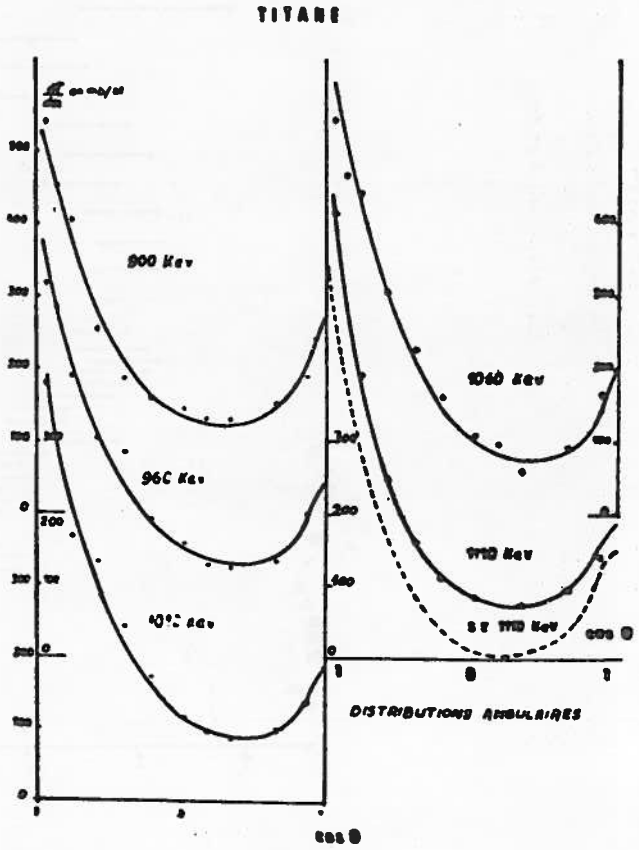
TITANE
900 Kev
960 Kev
1060 Kev
1110 Kev
S.E. 1110 Kev
DISTRIBUTIONS ANGULAIRES

Fig. 9

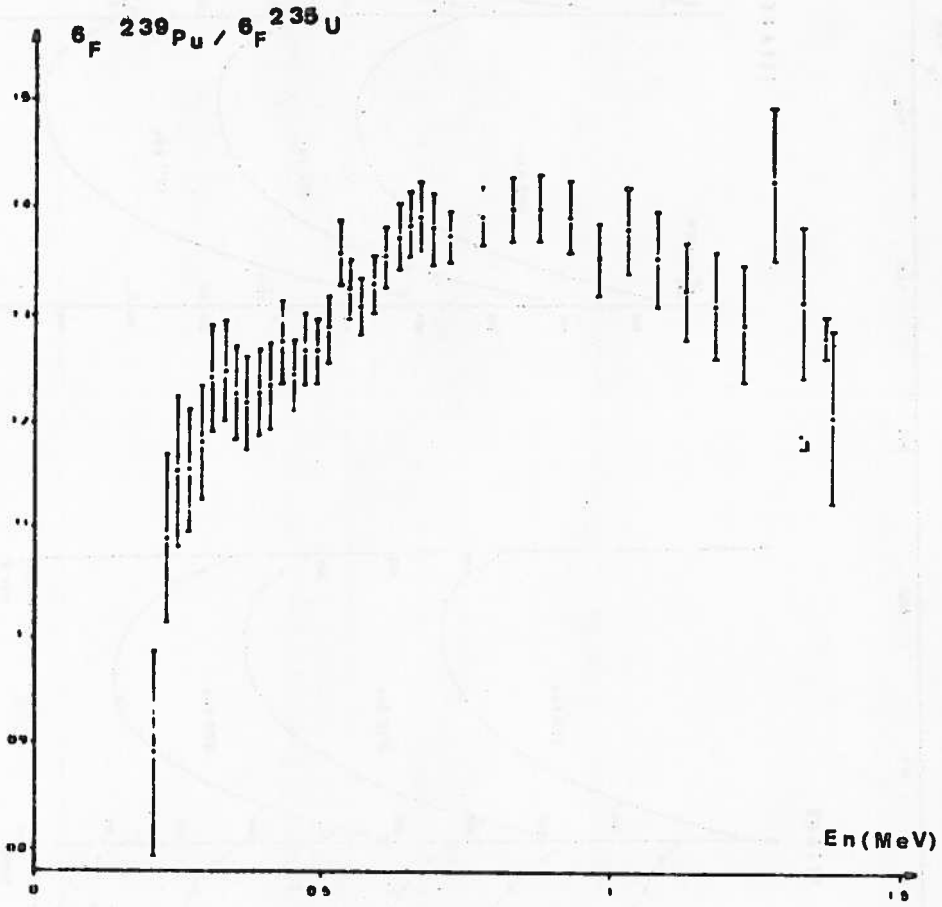

Fig.13

Section efficace relative de fission de ^{239}Pu par rapport a celle de ^{235}U

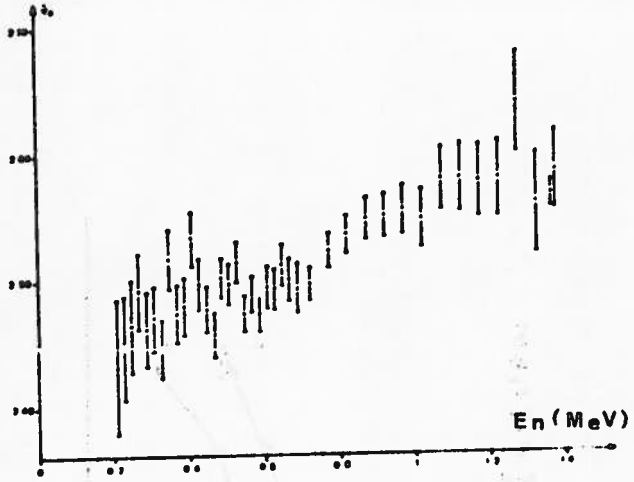

Fig.11

$\bar{\nu}_p = f(E_n)$ pour ^{235}U

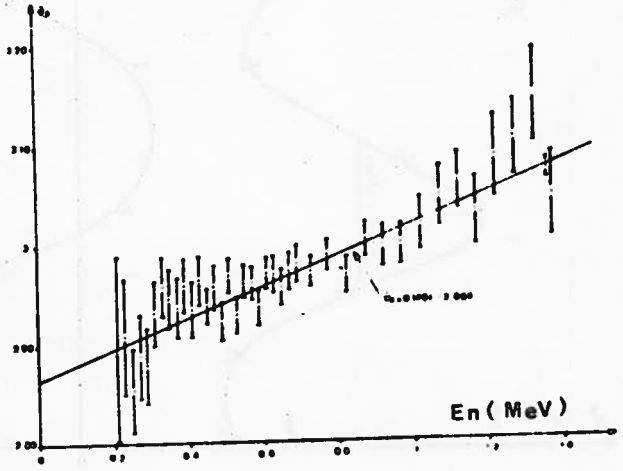

Fig. 12

$\bar{\nu}_p = f(E_n)$ pour ^{239}Pu

E_1 (initial)	E_γ transition	E_2 (final)	ΔJ	$\pi_i \pi_f$	$\frac{d\sigma}{d\Omega}$ mb	± erreur	Isotope réaction	Observations rapport d'embranchement
0,847	0,847	0	2 → 0	+	156	± 15%	F 56	100 %
2,085	1,240	0,847	4 → 2	+	45,2	± 15%	-	100 %
2,658	1,807	0,847	2 → 2	+	18,7	± 15%	-	
2,940	2,095	0,847	0 → 0	+	7,25	± 15%	-	
2,959	2,112	0,847	2 → 2	+	3,90	± 17%	-	100 %
3,120	2,274	0,847	0 → 2	+	4,7	± 17%	-	
3,123	1,038	2,085	4 → 4	+	14,25	± 15%	-	
3,370	2,522	0,847	2 → 2	+	6,47	± 17%	-	
3,447	2,600	0,847	3 → 2	+	12,25	± 16%	-	76,5 %
-	1,360	2,085	3 → 4	+	3,74	± 17%	-	23,4 %
3,388	1,302	2,085	4	+	4,6	± 17%	-	
3,830	1,178	2,657	0 → 2	+	4,5	± 17%	-	
3,856	1,760	2,085	4 → 4	+	3,52	± 17%	-	
4,120	2,035	2,085	3 → 4	+	5,1	± 17%	-	3,274 non observé
4,395	2,305	2,085	3 → 4	+	3	± 17%	-	
4,510	1,570	2,940			4,1	± 17%	-	
4,530	1,570	~~2,959~~						
-	1,870	2,658			4,2	± 17%	-	
4,653	1,533	3,120			3,2	± 17%	-	
-	1,530	3,123						
4,723	1,600	3,123			3,4	± 17%	-	
-	1,603	3,120						
4,804	1,682	3,120			4,4	± 17%	-	
-	1,682	3,123						
5,298	2,340	2,959			3,9	± 17%	-	
5,504	2,376	3,123			6,8	± 17%	-	
-	-	3,120						
5,769	2,376	3,388						

Diffuseur : Fe naturel (Ø 25 mm, h = 50 mm)

E_n = 0,72 MeV ; θ = 90°

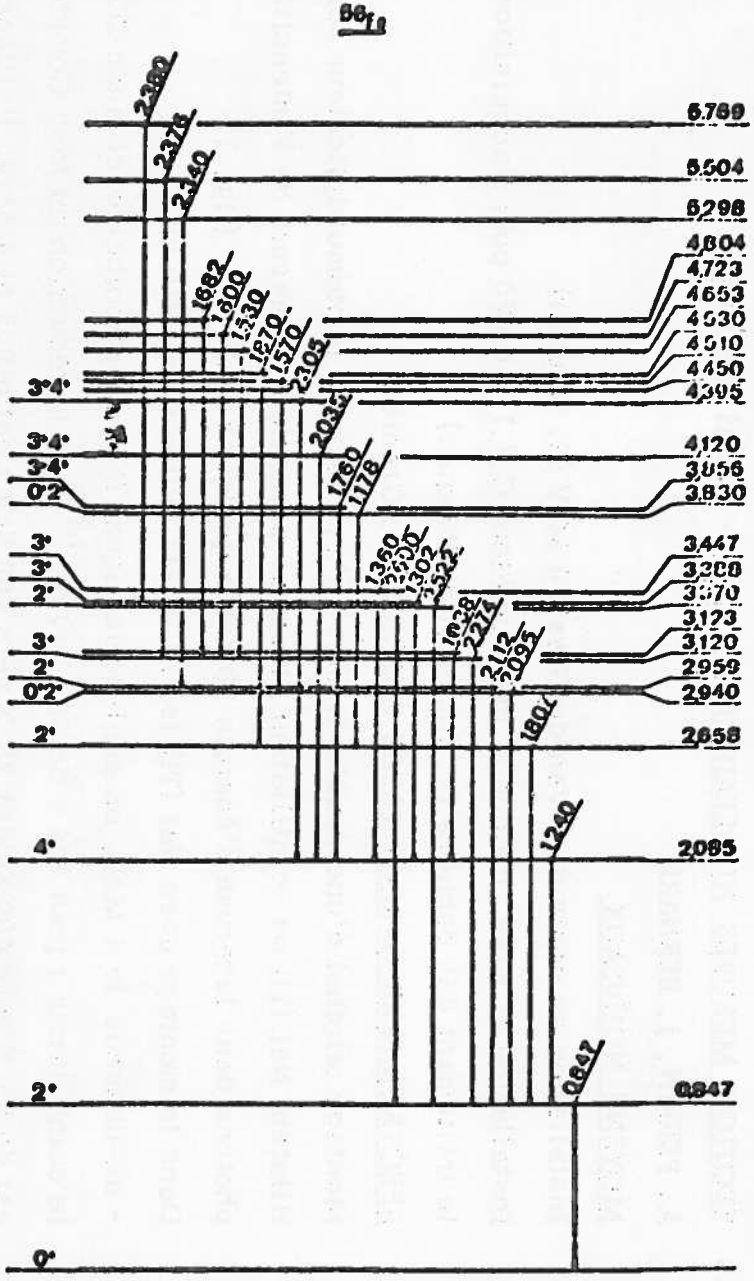

FIGURE 16

XXIII. SECTION MESURES NUCLEAIRES - C.E.A. - Limeil (FRANCE)

A. PERRIN, J. BERNARD

1. MOYENS NOUVEAUX

Installation en cours d'un Van de Graaff 4 MeV (S. Gautier)

Installation et mise en ligne d'un calculateur C.I.I. 10 020 pour l'acquisition et le traitement des données (Y. Jehannot de Penquer)

2. SPECTROMETRE GAMMA BASSE ENERGIE (G. Grenier)

Montage original d'une double diode et d'un ensemble photomultiplicateur scintillateur NaI (Tl) ou scintillateur plastique permettant la mesure de l'intensité des photons dans lagamme d'énergie 20 keV à quelques MeV [1] (fig. 1)

Dans le montage avec NaI (Tl) les résultats suivants ont été obtenus :

- au-dessous de 4 MeV, on analyse le signal D1 en anticoïncidence avec D2 et le scintillateur : pour les γ de 662 KeV du ^{137}Co, la réduction du fond Compton est de 85 % vers 400 KeV et 78 % vers 100 KeV ; entre 0,3 et 4 MeV, l'efficacité sous le pic photoélectrique se trouve toutefois réduite.
- au-dessus de 2 MeV, l'analyse du signal $D_1 + D_2$ associé au signal du scintillateur fournit un fonctionnement en spectromètre de paires classique.

3. ETUDE DES REACTIONS PRODUITES PAR IONS TRITIUM SUR DES NOYAUX LEGE

(F. Bertrand, J. Pornet, J.P. Ulpat)

Les courbes d'excitation ont été étudiées entre 0,300 MeV et 1 MeV ainsi que les distributions angulaires entre 40° et 170° à différentes énergies pour les réaction $^{9}Be\ (t, \alpha_0)\ ^{8}Li$, $^{9}Be\ (t, \alpha_1)\ ^{8}Li^*$ (fig. 2).

Des mesures semblables (fig. 3a et 3b) ont également été effectuées sur ^{12}C pour les réactions $^{12}C\ (t, \alpha_0)\ ^{11}B$, $^{12}C\ (t, \alpha_1)\ ^{11}B^*$, $^{12}C\ (t, p_0)\ ^{14}C$. Nos résultats sont en bon accord avec ceux de Sizov (Soviet Phys. JETP 17, 973, 1963) entre 0,750 et 1 MeV.

4. ETUDES DES REACTIONS $^{6}Li + ^{6}Li \longrightarrow p + ^{11}B$ (F. Bertrand. J. Pornet, P.J. Ulpa

Nous avons effectué sur l'accélérateur Van de Graaff 2 MeV de l'Institut de Physique Nucléaire de Lyon une étude de la distribution angulaire à 2 MeV et une court d'excitation par pas de 100 keV entre 1,5 et 2 MeV (fig.4). L'exploitation des résultats est en cours.

5. ETUDE DES SPECTRES DE RENVOI DE RAYONNEMENT γ

5.1. Mesures effectuées auprès de l'accélérateur linéaire ALE 30 (A. Bertin, G. Lucas)

La source de neutrons est la cible en uranium de l'ALE 30 (spectre s'étendant de 0,5 à quelques MeV avec un pic vers 1 MeV) et les γ produits sont détectés à 90°

du faisceau de neutrons par un scintillateur NaI (Tl) de 4" x 4". On enregistre en biparamétrique ($E\gamma$, E_n), l'énergie des neutrons E_n étant obtenu par temps de vol. L'analyse des premières mesures (Fe, Al, U) est en cours.

5.2. Mesures effectuées à une énergie E_n déterminée

La détection des γ utilise une jonction Ge (Li) placée à 90 ° du faisceau de neutrons.

5.2.1. Etude des éléments Mg, Ca, Sc, Ni à 14,1 MeV (G. Clayeux, G. Grenier) : le tableau 1 donne les sections efficaces différentielles des raies les plus intenses.

5.2.2. Etude du C à 14,1 MeV (G. Clayeux, G. Grenier, M. Martinot) : un dédoublement des pics correspondant au niveau 4,43 MeV du carbone a été observé : il est produit par effet Doppler (fig. 5).

5.2.3. Etude des éléments N, O, Mg, Sc, Ni de 5 à 9 MeV (G. Clayeux, G. Grenier) : l'analyse des mesures, effectuées avec un pas de 1 MeV, est en cours.

5.2.4. Evaluation des spectres de renvoi (M. Martinot, F. Ouvry) : nous avons mis au point un programme permettant de calculer le spectre gammas émis dans une réaction induite par neutrons et procédant par noyau composé. Seules les voies neutrons, gammas et fission sont prises en considération, le spectre de fission étant pris dans son ensemble.

6. POSSIBILITES DE MESURES (n, 2n) PAR DOUBLE TEMPS DE VOL [2] (G. Clayeux, J.J. Voignier)

Des mesures préliminaires ont été effectuées avec des neutrons de 14,1 MeV sur le plomb avec deux mesures de temps de vol par la méthode de la particule associée. De ce fait, l'efficacité de comptage est faible et entraîne des temps de mesures assez longs.

Des résultats satisfaisants sont obtenus malgré la faible résolution due à la faible longueur des bases de vol. Une analyse rapide des résultats semble montrer une anisotropie importante dans la distribution angulaire relative des deux neutrons.

7. MESURE PAR TEMPS DE VOL DU SPECTRE DE NEUTRONS DE FUITE D'UN MILIEU MULTIPLICATEUR RAPIDE (A. Bertin, G. Lucas)

Ces mesures doivent être réalisées à l'aide de l'accélérateur linéaire ALE 30 du centre en collaboration avec une équipe de Cadarache. La mise sur pied de l'expérience a commencé en septembre et les mesures sont prévues pour le premier semestre 1970.

8. CHAMBRE A FISSION POUR L'ETUDE DU SPECTRE DE NEUTRONS DE FISSIONS PRODUITS PAR NEUTRONS RAPIDES (A. Bertin)

Cette étude se fait en liaison avec les mesures de M. Soleilhac du Centre d'Etudes de Bruyères-le-Châtel. La chambre contient 14 g d'uranium répartis en une centaine de plaques en dépôt de 1,5 mg/cm^2 d'épaisseur. Ces plaques distantes entre elles de 1 mm sont groupées par vingt. Les impulsions obtenues ont un temps de montée de 10 n/s. permettant des mesures de temps. L'efficacité calculée de cette chambre est 10^{-3} pour des neutrons de 14 MeV.

BIBLIOGRAPHIE

[1] G. GRENIER - C. POUSSIER : rapport C.E.A. à paraître

[2] G. CLAYEUX - J.J. VOIGNIER : rapport C.E.A. à paraître

SECTIONS EFFICACES DIFFERENTIELLES A 90° POUR DES NEUTRONS DE 14,1 MeV

E_γ (MeV)	Réaction probable	Transition	$\frac{d\sigma}{d\Omega}$ mb/sr	Autres résultats
Magnésium				
0,58	$^{25}Mg(n,n')^{25}Mg^*$	0,58 → 0	Présent	
0,88	$^{24}Mg(n,p)\ ^{24}Na^*$	1,35 → 0,47	3,2±0,5	2,5±0,8 2/
0,98	$^{25}Mg(n,n')^{25}Mg^*$	0,98 → 0	Présent	
1,13	$^{26}Mg(n,n')^{26}Mg^*$	2,94 → 1,81	3,6±0,6	3 ±1 2/
1,37	$^{24}Mg(n,n')^{24}Mg^*$	1,368 → 0	31,4±1,9	{31,5±3,6 1/ {30,9±3,1
1,61	$^{25}Mg(n,n')^{25}Mg^*$	1,61 → 0	Présent	
1,81	$^{26}Mg(n,n')^{26}Mg^*$	1,81 → 0	4,4±0,7	5,7±0,6 2/
2,75	$^{24}Mg(n,n')^{24}Mg^*$	4,12 → 1,37	3,9±0,7	4,1±0,8 2/
Calcium				
0,75	$^{40}Ca(n,n')^{40}Ca^*$	4,48 → 3,73	Présent	
0,77	$^{40}Ca(n,p)\ ^{40}K^*$	0,800 → 0,030	2,0±0,6	5,6±1,2 2/
0,89	$^{40}Ca(n,p)\ ^{40}K^*$	0,89 → 0	2,5±0,6	4,8±1,0 2/
1,15	$^{44}Ca(n,n')^{44}Ca^*$	1,15 → 0	2,4±0,7	2,2±0,3 2/
1,40	$^{40}Ca(n,\alpha)\ ^{37}Ar^*$	1,40 → 0	2,5±0,7	
1,60	$^{40}Ca(n,\alpha)\ ^{37}Ar^*$	1,60 → 0	2,3±0,7	5,4±0,6 2/
2,00	$^{40}Ca(n,\alpha)\ ^{37}Ar^*$	2,00 → 0	Présent	{2,7±0,5 pour $^{40}Ca(n,d)^{39}K^*$ 2,82
3,73	$^{40}Ca(n,n')^{40}Ca^*$	3,73 → 0	8,8±1,7	9,0±1,8 2/
3,9	$^{40}Ca(n,n')^{40}Ca^*$	3,90 → 0	Présent	3,8±1,3 2/

E_γ (MeV)	Réaction probable	Transition	$\frac{d\sigma}{d\Omega}$ mb/sr
Scandium			
0,55	$^{45}Cc(n,n')^{45}Sc^*$	0,54 → 0	Présent
0,718	$^{45}Cc(n,n')^{45}Sc^*$	0,718 → 0	4,5
0,895	$^{45}Cc(n,n')^{45}Sc^*$	1,493 → 0,53	Présent
0,97	$^{45}Cc(n,n')^{45}Sc^*$	0,97 → 0	3,0±0,4
1,06	$^{45}Sc(n,n')^{45}Sc^*$	1,06 → 0	4,2±0,6
1,12	{$^{45}Sc(n,n')^{45}Sc^*$	1,66 → 0,54	11,3±0,7
	{$^{45}Sc(n,d)\ ^{44}Ca^*$	2,28 → 1,16	
1,15	$^{45}Sc(n,d)\ ^{44}Ca^*$	1,15 → 0	29,1±1,6
1,238	$^{45}Sc(n,n')^{45}Sc^*$	1,238 → 0	12,9±0,8
1,408	$^{45}Sc(n,n')^{45}Sc^*$	1,408 → 0	1,3±0,3
1,43	$^{45}Sc(n,n')^{45}Sc^*$	1,43 → 0	Présent
1,50	$^{45}Sc(n,d)\ ^{44}Ca^*$	2,66 → 1,16	1,3±0,3
1,55	$^{45}Sc(n,n')^{45}Sc^*$	1,55 → 0	1,9±0,4
1,66	$^{45}Sc(n,n')^{45}Sc$	1,66 → 0	2,7±0,4
2,05	$^{45}Sc(n,d)\ ^{40}Ca^*$	5,40 → 3,35	Présent
2,08	{$^{45}Sc(n,d)\ ^{40}Ca^*$	2,25 → 0,176	Présent
	{$^{45}Sc(n,n')^{45}Sc^*$	2,08 → 0	
2,106	$^{45}Sc(n,n')^{45}Sc^*$	2,106 → 0	Présent
2,28	$^{45}Sc(n,n')^{45}Sc^*$	2,28 → 0	1,6±0,4
2,35	{$^{45}Sc(n,p)\ ^{44}Ca^*$	2,35 → 0	1,3±0,3
	{$^{45}Sc(n,n')^{45}Sc^*$		

E_γ (MeV)	Réaction probable	Transition	$\frac{d\sigma}{d\Omega}$ mb/sr
Nickel			
0,83	$^{60}Ni(n,n')^{60}Ni^*$	2,158 → 1,33	1,6±0,6
0,93	$^{58}Ni(n,\alpha)\ ^{55}Fe^*$	0,93 → 0	Présent
1,0	$^{58}Ni(n,n')^{58}Ni^*$	2,45 → 1,45	6,7±0,6
1,17	{$^{58}Ni(n,n')^{58}Ni^*$	2,50 → 1,33	10,1±0,8
	{$^{62}Ni(n,n')^{62}Ni^*$	1,17 → 0	
		2,34 → 1,17	
1,21	{$^{61}Ni(n,n')^{61}Ni^*$	1,21 → 0	9,3±0,8
	{$^{58}Ni(n,\alpha)\ ^{55}Fe^*$	2,15 → 0,93	
1,33	{$^{60}Ni\ (n,n')^{60}Ni^*$	1,33 → 0	19,6±1,2
	{$^{58}Ni(n,n')^{58}Ni^*$	2,78 → 1,45	
1,45	$^{58}Ni(n,n')^{58}Ni^*$	{1,45 → 0	18,6±1,1
		{2,90 → 1,45	
1,75	$^{58}Ni(n,d)\ ^{57}Co^*$	1,75 → 0	1,4±0,4
1,79	$^{60}Ni(n,n')^{60}Ni^*$	3,12 → 1,33	Présent
2,06	{$^{58}Ni(n,n')^{58}Ni^*$	3,52 → 1,45	Présent
	{$^{60}Ni(n,n')^{60}Ni^*$	3,39 → 1,33	
2,16	$^{60}Ni(n,n')^{60}Ni^*$	2,16 → 0	0,8±0,3

1/ P.W. Martin et D.T. Stewart (13,1 MeV, 90°) - Canadian Journal of Physics 46 (1968) 1657

2/ F.C. Engesser et W.E. Thompson (14,7 MeV, 90°) - Journal of Nuclear Energy 21 (1967) p. 487 à 507

SCHEMA du DISPOSITIF

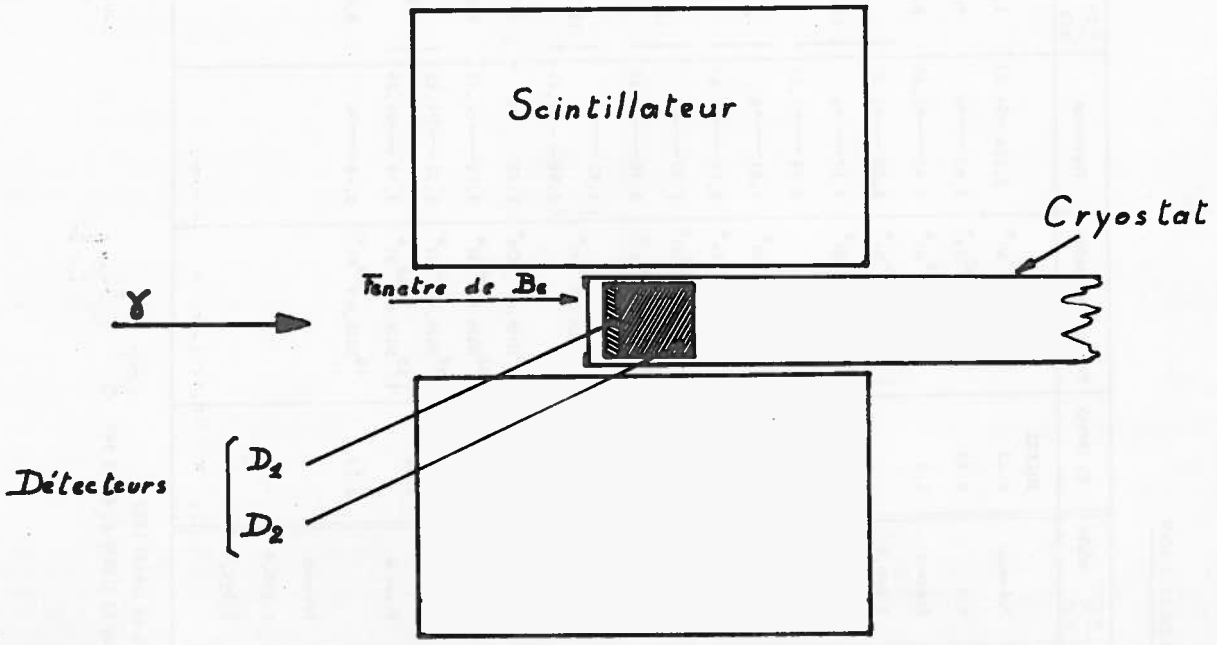

ANALYSE DES GAMMAS DE BASSE ENERGIE D'UNE SOURCE DE ^{226}RA
EN PRESENCE D'UNE SOURCE DE ^{60}Co

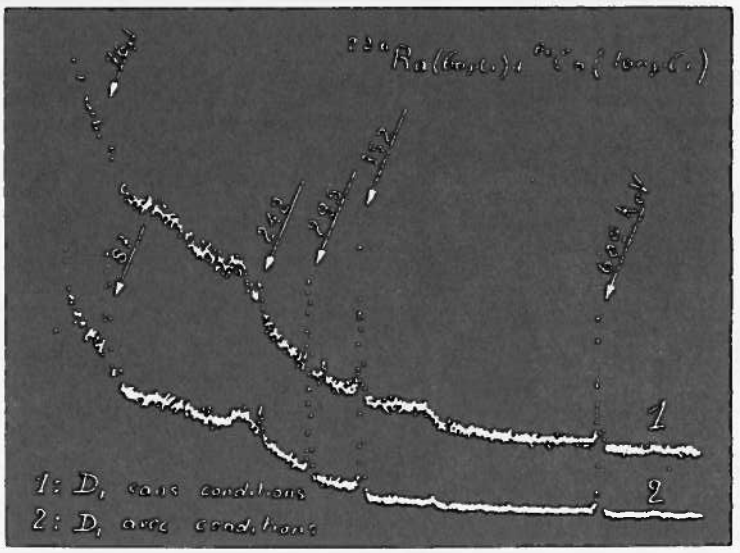

FIG. 1

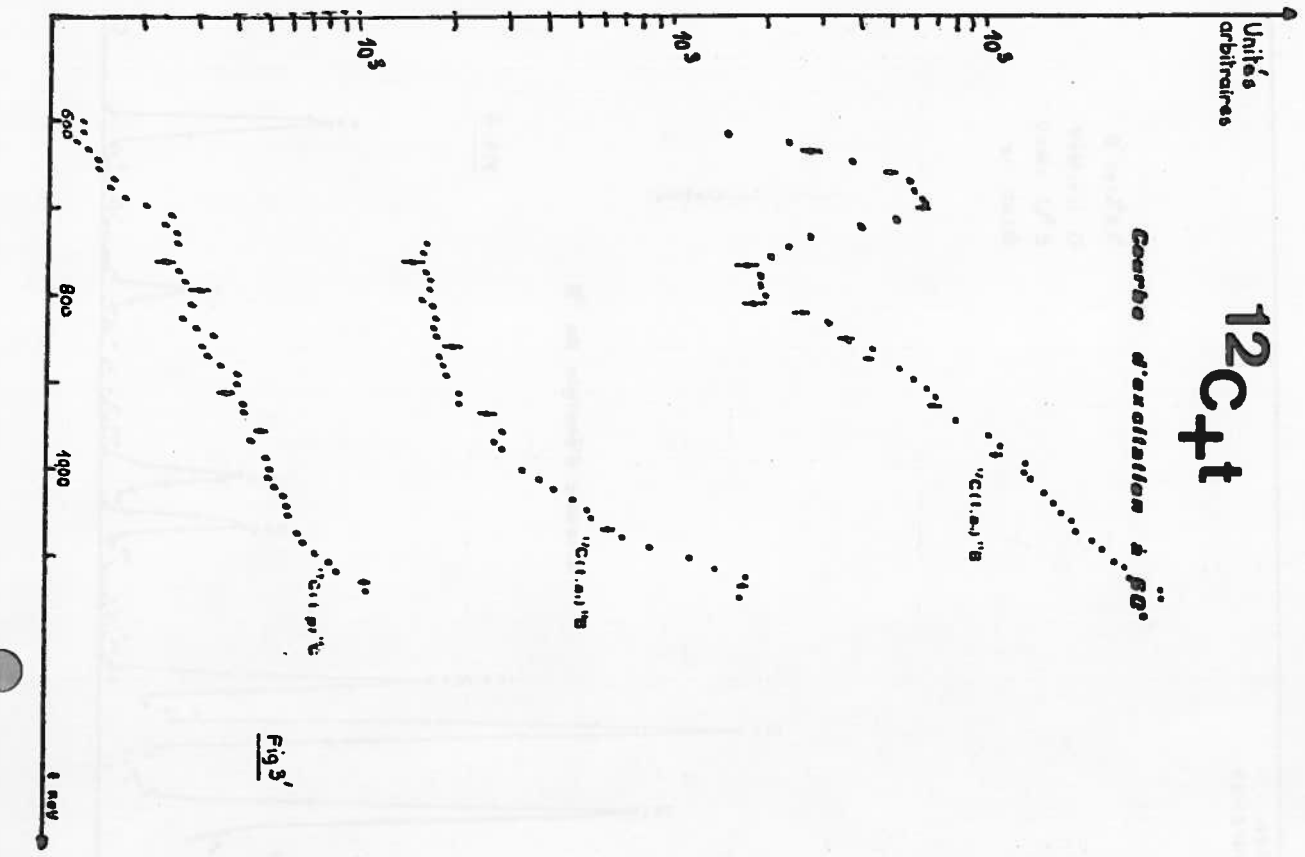

Fig 3'

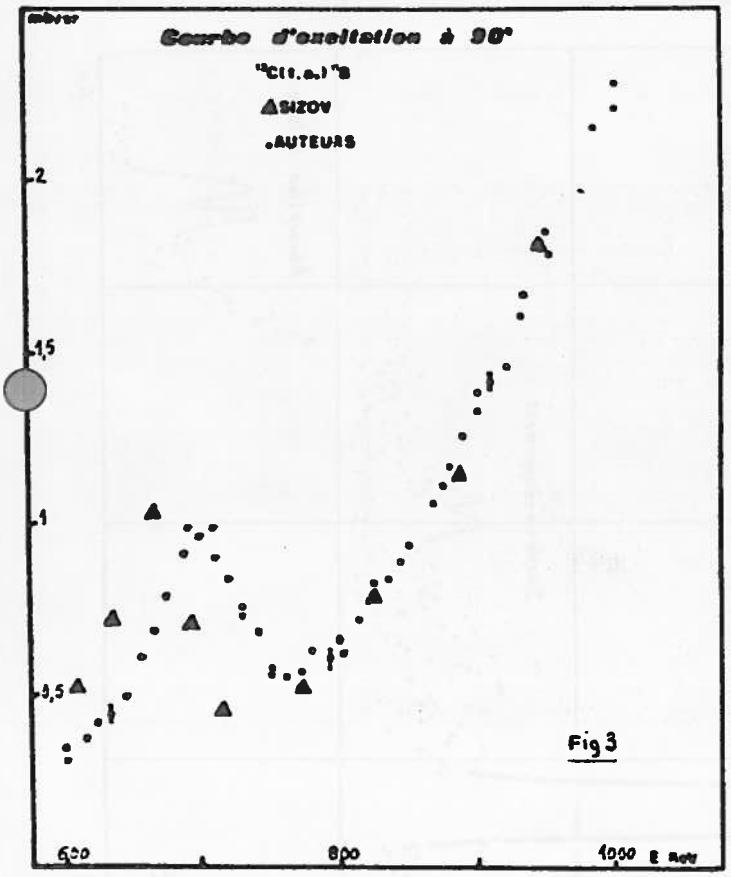

Fig 3

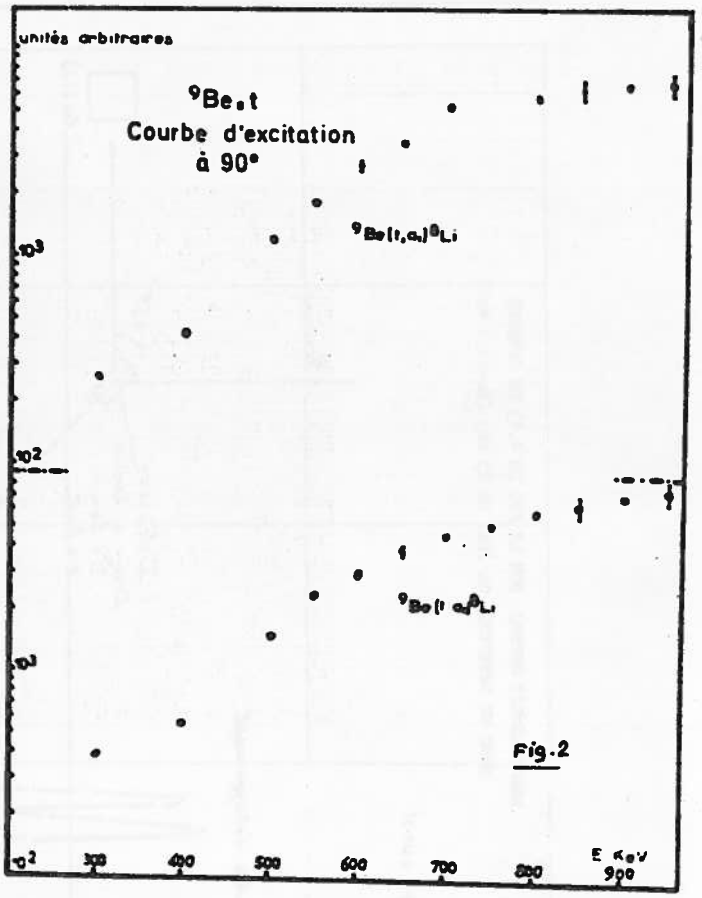

Fig.2

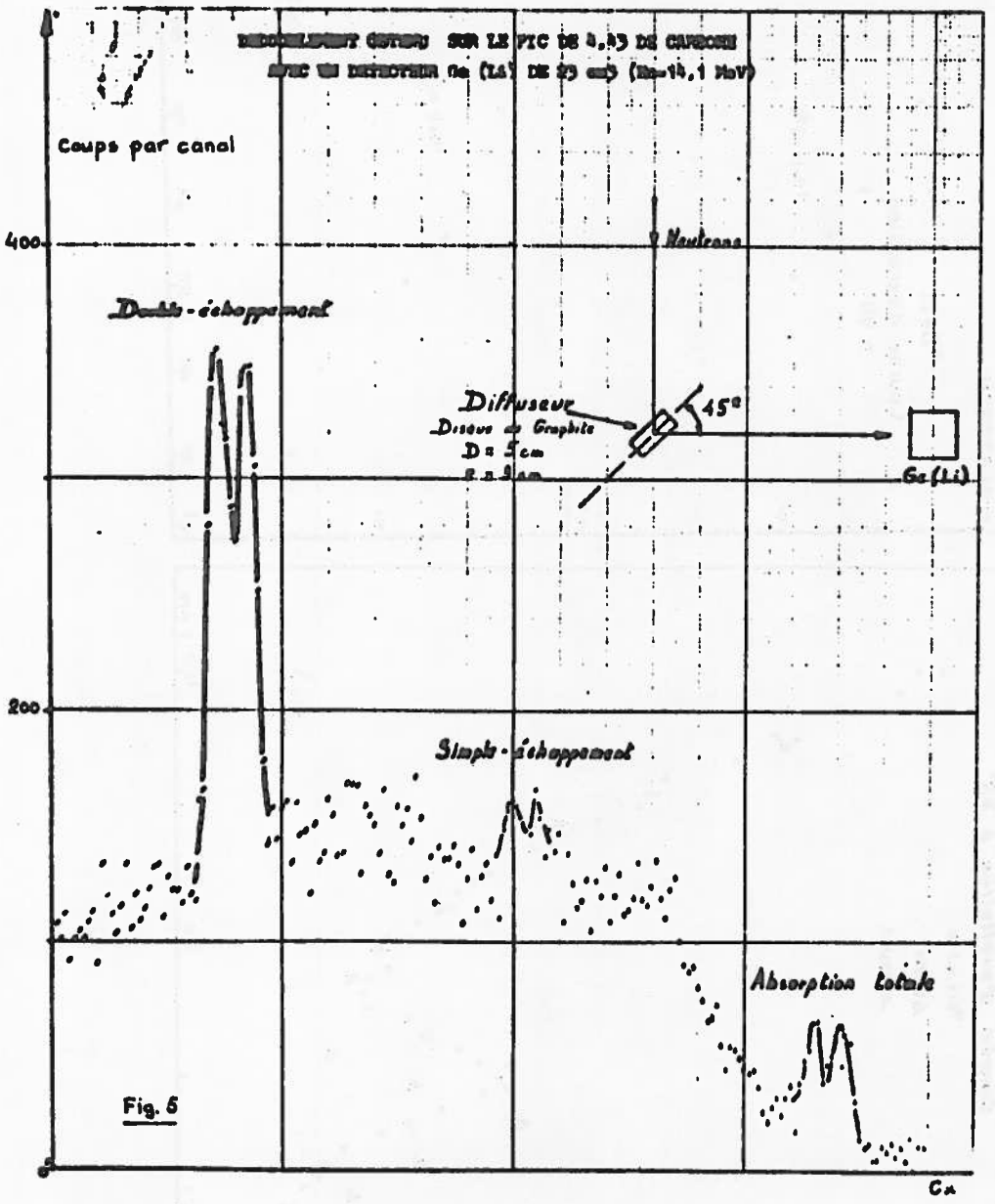
Coups par canal
400
200
Neutrons
Double-échappement
Diffuseur
45°
Ge(Li)
Simple-échappement
Absorption totale
Cx

Fig. 5

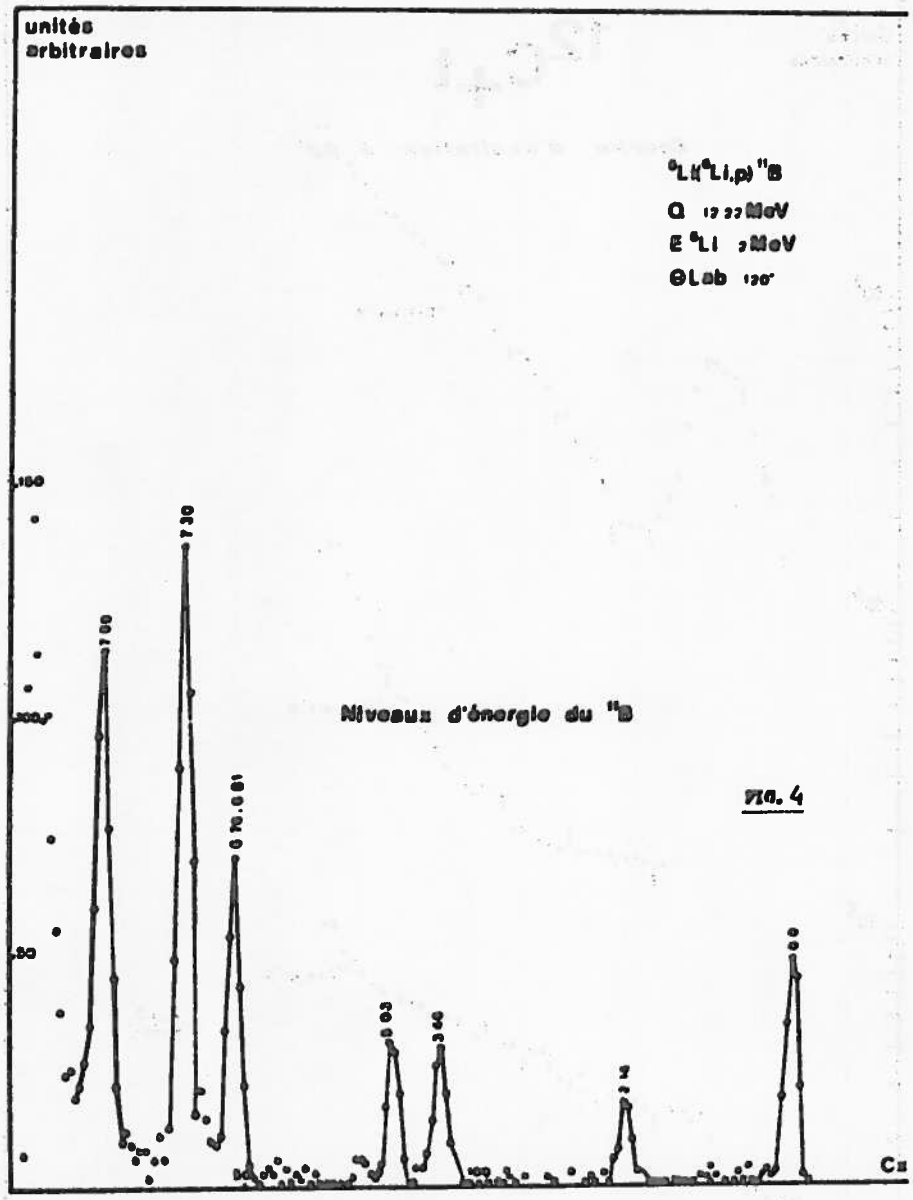
unités
arbitraires
Niveaux d'énergie du ¹¹B
Cx

FIG. 4

XXIV. DEPARTEMENT DES ETUDES DE PILES - GROUPE DES EXPERIENCES NEUTRONIQUES
C.E.A. - Fontenay-aux-Roses - (FRANCE)

R. VIDAL

1. MESURES DES SECTIONS EFFICACES THERMIQUES D'ABSORPTION DU LITHIUM 6 ET DU LITHIUM 7 :

Des expériences sont en cours pour mesurer les sections efficaces d'absorption du ^{6}Li et du ^{7}Li en neutrons thermiques. Les échantillons fabriqués par le BCMN de Geel sont des solutions de Li (OD) dans l'eau lourde. Deux séries d'expériences ont été effectuées, l'une avec du Lithium enrichi à 99,1 % en ^{6}Li, l'autre avec du Lithium naturel. Des échantillons de Lithium enrichi à 99 % en ^{7}Li sont en cours de préparation pour une troisième série d'expériences.

2. MESURE DES SECTIONS EFFICACES THERMIQUES DE l'^{233}U :

La section efficace de fission et le η de l'^{233}U pour des neutrons de 2 200 m/s, en prenant l'^{235}U comme étalon, ont été déterminés à partir de mesures intégrales faites dans un spectre de neutrons thermiques :

2.1. Mesure des sections de fissions à l'aide de chambres à fission :

Le rapport des sections efficaces de fission de l'^{233}U et de l'^{235}U est déterminé en irradiant dans un spectre maxwellien des chambres à fission contenant de l'^{238}U allié à de l'^{233}U ou de l'^{235}U. L'originalité de la méthode réside dans l'étalonnage des chambres qui est effectué dans un spectre de neutrons rapides en mettant à profit les fissions qui se produisent dans l'^{238}U. Ainsi la seule connaissance des teneurs isotopiques des dépôts permet un étalonnage relatif très précis. On a obtenu $\sigma_f(U^{233}) = 526 \pm 3$ b. à 2 200 m/s.

Les mêmes expériences sont prévues pour mesurer la section efficace de fission du ^{239}Pu.

2.2. Mesure du η par la méthode d'oscillation :

Le rapport (η 3/η 5) est déterminé en mesurant les variations de réactivité produites dans un réseau à uranium naturel et eau lourde par l'oscillation d'échantillons d'uranium contenant quelques grammes d'^{233}U ou d'^{235}U. En pondérant les sections efficaces différentielles de l'^{233}U et de l'^{235}U sur le spectre neutronique où ont été faites les mesures, on rapporte les valeurs intégrales de η mesurées aux valeurs correspondantes à 2 200 m/s.

On a obtenu : $(\eta\ 233)_{2200\ m/s} = 2,245 \pm 0,013$

ce qui permet de déduire : $\sigma_a(^{233}U) = (584 \pm 5)$ barns à 2 200 m/s.

3. MESURES INTEGRALES DE ALPHA POUR LE PLUTONIUM 239 ET L'URANIUM 235

La dispersion des résultats de mesures différentielles concernant le α du ^{239}Pu dans les énergies intermédiaires a conduit à effectuer des mesures intégrales de ce paramètre . Deux catégories d'expériences ont été réalisées :

3.1. Mesures de réactivité et de taux de réaction dans l'assemblage ERMINE :

Une méthode originale basée sur l'utilisation d'une chambre locale à dépôt d'^{238}U a été développée pour séparer les termes de capture et de fission. Moins sensible à l'imprécision sur ν et sur les rapports d'importance que la méthode d'étalonnage par le bore utilisée précédemment, elle permet de plus d'obtenir α pour la dilution réelle de l'échantillon sans nécessiter une extrapolation à la dilution infinie. La méthode du bore a également été utilisée et la comparaison des résultats traduit un bon accord.

Les valeurs de α du ^{239}Pu obtenues à partir de ces mesures sont très voisines des valeurs calculées avec la version II du jeu de Cadarache établi à partir des résultats des plus récentes mesures différentielles.

3.2. Irradiations dans une capsule de bore au centre de la pile piscine OSIRIS de 70 MeV :

Différents échantillons d'^{235}U et de ^{239}Pu et d'^{238}U ont été irradiés au cours de deux campagnes, les flux intégrés étant pour l'une de 5.10^{21} n/cm^2 environ et pour l'autre voisine de 10^{22} n/cm^2 ; ces échantillons étaient placés dans une capsule de carbure de bore de façon à donner un taux de capture élevé dans le domaine 1 KeV-20 KeV.

Trois déterminations de α sont effecutées en utilisant respectivement la formation du ^{148}Nd, la disparition de l'^{235}U et le taux de capture dans l'^{238}U. Les deux dernières qui n'utilisent pas le rendement du ^{148}Nd ont été rendues possibles grâce aux mesures effectuées sur le réacteur ISIS, maquette à faible puissance d'OSIRIS, dans lequel on a pu reconstituer les conditions réelles de l'irradiation et mesurer les indices de spectre indispensables pour l'interprétation. Cette utilisation d'ISIS a également permis un certain nombre de vérifications expérimentales du spectre au centre de la capsule.

Les échantillons de la première campagne sont actuellement en cours d'analyse, ceux de la deuxième campagne seront analysés au cours du 2ème trimestre 1970. La même série d'échantillons est en cours d'irradiation dans RAPSODIE et permettra d'atteindre $\bar{\alpha}_9$ et $\bar{\alpha}_5$ dans une gamme d'énergie plus élevée.

XV. LABORATOIRE DE PHYSIQUE NUCLEAIRE - C.E.A. - Grenoble (FRANCE)

Pr. R. BOUCHEZ

1. COMPARAISON DE L'INTERACTION NEUTRON-NEUTRON et NEUTRON-PROTON DE L'ETAT FINAL DANS LA REACTION D(n,nnp) A 14,55 MeV (C. Perrin*, J.C. Gondrand*, Mme M. Durand*, P. Perrin, S. Desreumaux, A. Kossentini, R. Bouchez)

La mesure de la section efficace à 14,55 MeV des interactions n-n et n-p a été effectuée par réaction D (n,nnp) avec détection des deux neutrons à (+ 30°, + 30°) et (+ 30°, - 80°) dans un spectromètre à double temps de vol (fig. 1). Les valeurs de sections efficaces suivantes sont été obtenues : pour l'interaction n-n(+ 30°, + 30°) $d^4\sigma/d\omega_1 . d\omega_2 \approx 26,8$ mb/sr^2 ; pour l'interaction n-p (+ 30°, - 80°) $d^4/d\omega_1 . d\omega_2 \approx 5,5$ mb/sr^2. Ces valeurs ont été déterminées par simulation à l'aide d'une méthode de Monte-Carlo et seront comparées aux valeurs fournies par la théorie utilisant les équations intégrales couplées de Faddeev [1] [2].

On a aussi évalué pour ces deux géométries, les sections efficaces différentielles en fonction de l'énergie d'un des deux neutrons émis [3] [4] par une méthode de déconvolution permettant de s'affranchir de la résolution en énergie du spectromètre-neutron.

2. REACTION (n,γ) et (n,n'γ) (C. Sonrel, P.Perrin, R. Bouchez)

L' analyseur multiparamétrique comprenant un spectromètre à double temps de vol, associé à un spectromètre γ utilise un détecteur Ge (≈20 à 120 cm^3) ayant une résolution en temps ≈5 ns. L'efficacité et la résolution en énergie de la voie γ ont été mesurées entre 2 et 17 MeV (fig. 2) [5] [6]. Ce dispositif a été étalonné avec les réactions ^{7}Li(n,n'γ) et ^{12}C(n,n'γ) à 14 MeV (fig. 3). Les applications sont notamment les réactions (n,n'γ).

BIBLIOGRAPHIE

[1] S. DESREUMAUX, thèse Docteur 3è cycle, Grenoble n° 1110, 1969.

[2] C. PERRIN et al., "International Conference on the Three Body Problem in Nuclear and Particule Physics", Birmingham (England), 8-10 July 1969.

[3] J.C. GONDRAND, thèse Docteur ès Sciences Physiques, Grenoble (à paraître)

[4] A. KOSSENTI, thèse Docteur 3è cycle, Grenoble (à paraître)

[5] C. SONREL et al., "14th International Summer Meeting of Physicists" Duilovo (Yougsolavie) 8-20 septembre 1969

[6] C. SONREL, thèse Docteur-Ingénieur, Grenoble, n° 1210, 1969

---

* Institut des Sciences Nucléaires - Université de Grenoble (FRANCE)

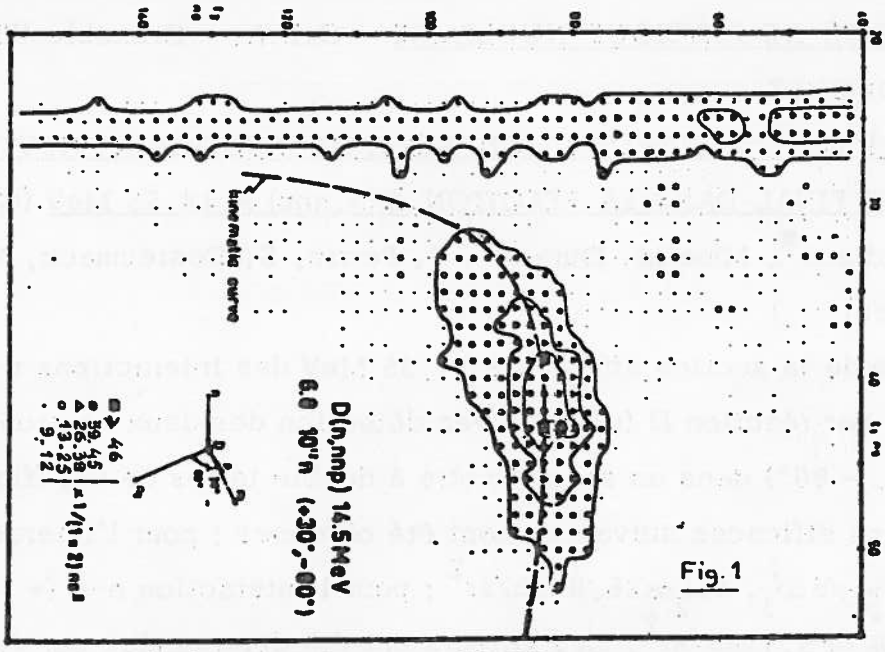
D(n,nnp) 14.5MeV
6.8 10⁻⁶n (+30°,-80°)
Fig. 1

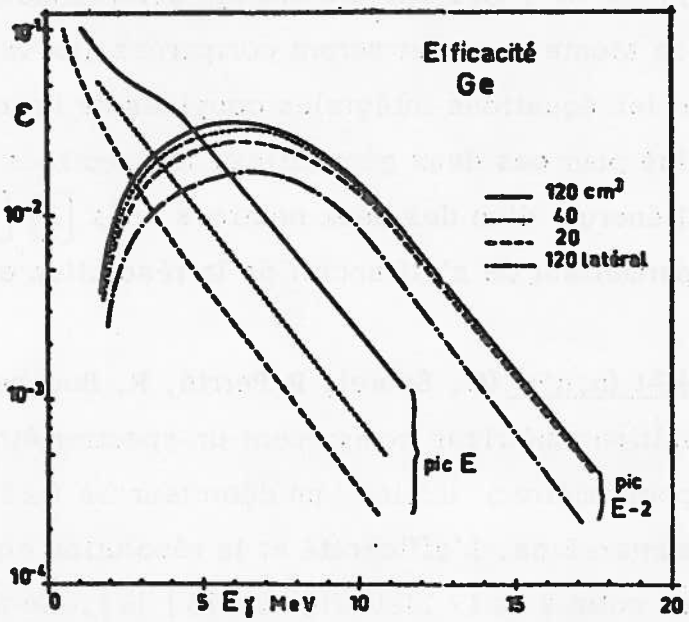
Efficacité
Ge
ε
120 cm³
40
20
120 latéral
pic E
pic
E-2
Eγ MeV

Fig. 2

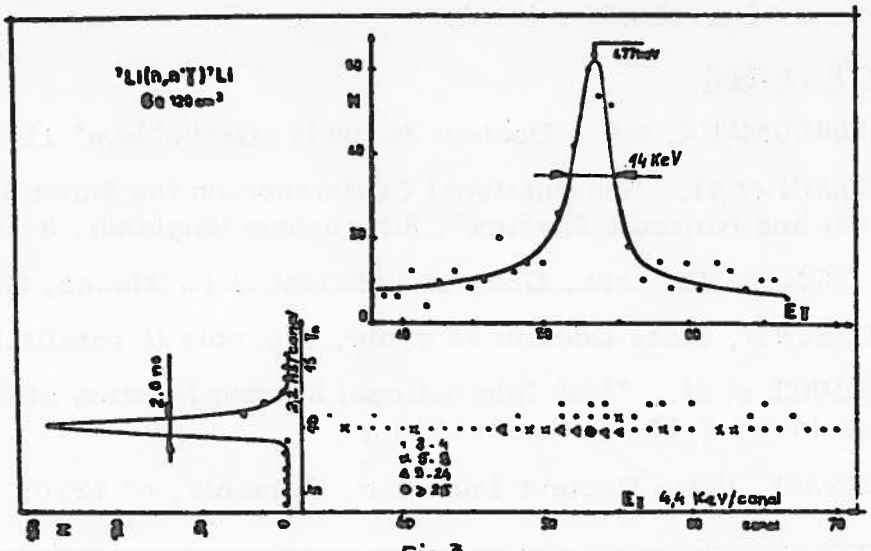
⁷Li(n,n'γ)⁷Li
Ge 120 cm³
477 keV
14 KeV
Eγ 4,4 KeV/canal
canal

Fig. 3

XXVI. INSTITUT DES SCIENCES NUCLEAIRES - Université de Grenoble (FRANCE)

Pr. R. BOUCHEZ

Etude expérimentale ^{6}Li (n,p) à 14 MeV et comparaison des transitions Δ T = 1 pour A = 6 (F. Merchez, J. Pouxe, M. Tournier, R. Bouchez)

L'étude expérimentale de la transition Δ T = 1 ^{6}Li(n,p)^{6}He pour En = 14 MeV a été effectuée avec un télescope à 3 détecteurs silicium. La mesure de sections efficaces faibles ($\simeq$ 0,5 mb/sr) a pu être obtenue malgré un bruit de fond important. L'identification des particules chargées (protons, deutons, tritons) et le contrôle permanent de l'expérience ont été réalisés à l'aide d'un petit calculateur (CAB 500) mis en ligne avec le dispositif expérimental. (Fig; 3)

Les sections efficaces des réactions ^{6}Li(n,t)^{4}He [1] [2] et ^{6}Li(n,d)^{5}He [1] ont été trouvées en accord avec les valeurs précédentes. Les distributions angulaires des réactions ^{6}Li(n,p)^{6}He (fig. 1) et ^{6}Li (n,p)^{6}He*(2+) (fig. 2) vers le premier niveau (T = 1, 2+) de ^{6}He ont été mesurées et correspondent à des sections efficaces totales respectives de 7,5 et 5 mb. Les sections efficaces différentielles (fig. 1) pour ^{6}Li (p,p'),(p,n) et (n,p) à la même énergie sont analogues mais ne s'interprètent pas par un mécanisme simple (knock-on, stripping...) même en utilisant les corrections DWBA.

La mesure de la section efficace différentielle de la réaction ^{14}N (n,p)^{14}C correspondant au premier niveau excité (0+ ; T = 1) de ^{14}N est en cours avec le même dispositif.

BIBLIOGRAPHIE

[1] G.M. FRYE Jr - Phys. Rev. 93, 1086, 1954

[2] V. VALKOVIC et al. - Nucl. Phys. A 98, 305, 1967

Fig. 3 : Spectres à 10° à $E_n = 14$ MeV

-en haut : spectres de d et de t provenant de $^6Li(n,d)$ et $^6Li(n,t)$

-en bas : spectres des p provenant de $^6Li(n,p_0)$ $He(0^+)$ et $^6Li(n,p_1)$ $He(2^+)$

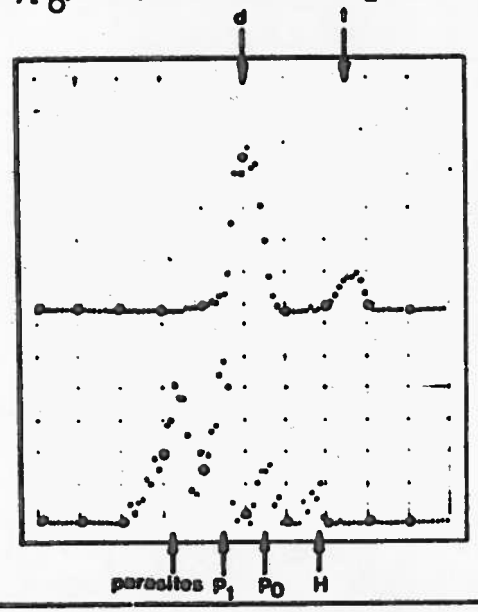

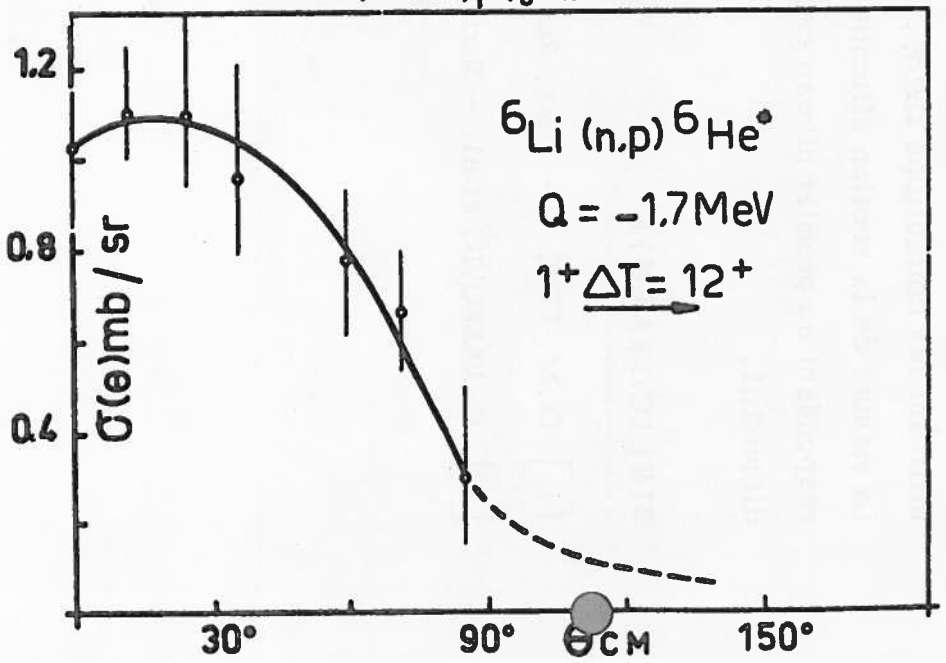

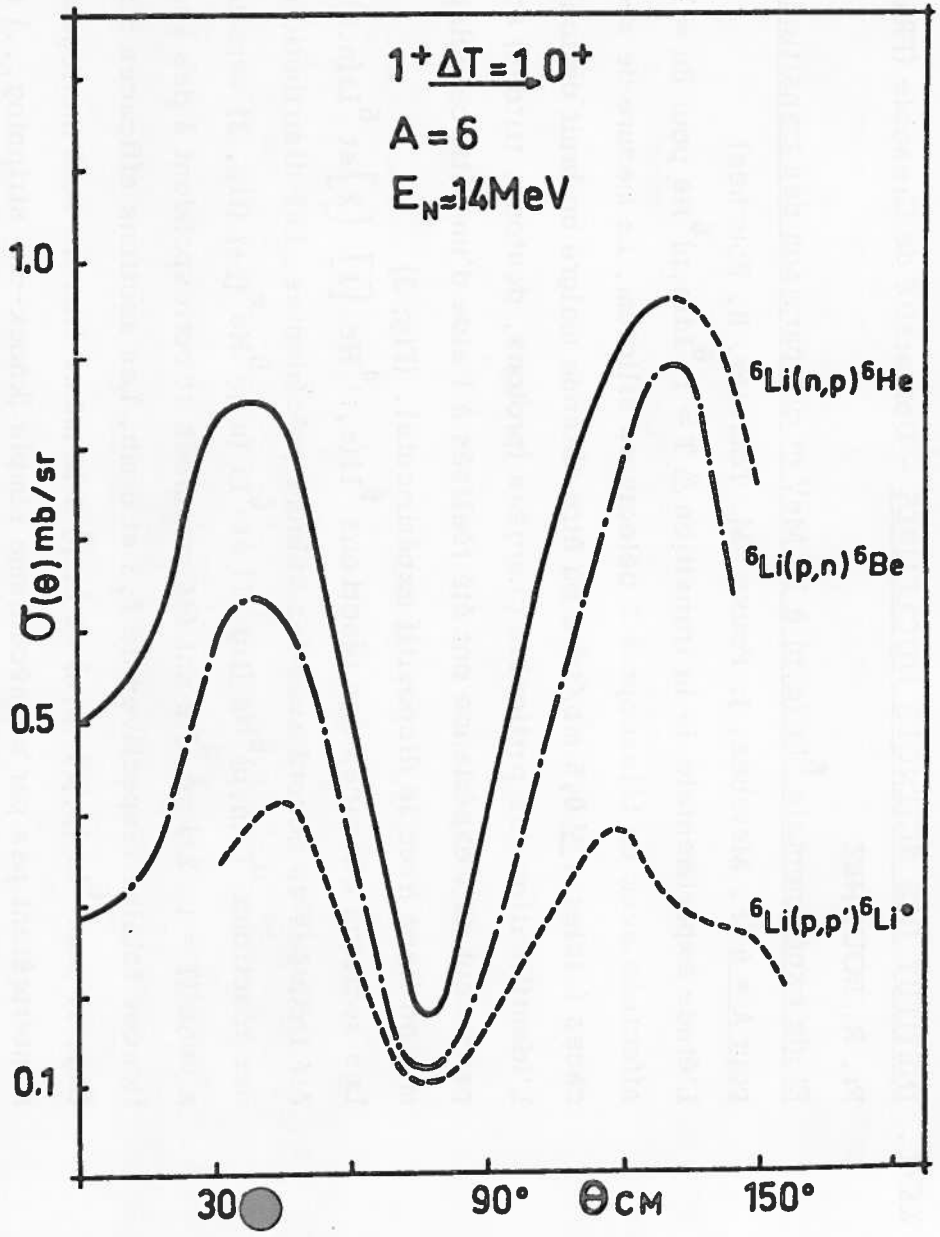

XXVII. CENTRE DE PHYSIQUE NUCLEAIRE DE L'UNIVERSITE DE LOUVAIN (Belgium)

1. Réactions (p,n) sur le Be^9

F. BODART, G. DECONNINCK

En vue de préciser la structure en (2α + 1n) fortement liée du Be^9, nous avons détecté les neutrons issus du bombardement du Be^9 par des protons d'énergies comprises entre 2.9 et 4 MeV au moyen de la méthode du temps de vol. Les neutrons émis dans les réactions suivantes ont fait l'objet de mesures de distributions angulaires à différentes énergies :

Be^9 (p,n) B^9, Be^9 (p,pn) Be^8, Be^9 (p,pn) 2α.

Afin de compléter les informations ainsi recueillies, la réaction séquentielle Be^9 (p,p') Be^9 (2.43 MeV) (n') Be^8 a été observée en détectant le neutron en coïncidence avec le proton diffusé inélastiquement par le Be^9 à une énergie incidente du proton de 4 MeV. Les résultats obtenus ne montrent aucune composante f 5/2 dans ce niveau du Be^9.

2. Etude spectroscopique du Cu^{66} et du Zn^{65} à l'aide de la réaction Cu^{65} (p,nγ) Zn^{65}

J. DAS, G. DECONNINCK, J-P. MEULDERS

La réaction Cu^{65} (p,nγ) Zn^{65} a été entreprise afin de déterminer le moment angulaire total et la parité des niveaux du Cu^{66} par la corrélation (n,γ) des neutrons émis par leurs analogues isobariques dans le Zn^{66} et des γ émis par les niveaux excités du noyau résiduel Zn^{65}. L'expérience comprend 2 parties :

(a) La voie de sortie γ

Une courbe d'excitation a été mesurée de 2.8 à 3.0 MeV à l'aide d'une cible fine (4.5 keV) de Cu naturel. Un détecteur Ge-Li a permis la mesure simultanée des γ de 0.115, 0.155 et 0.210 MeV, correspondant à la désexcitation des niveaux de 0.115 et 0.210 MeV vers le fondamental et du niveau de 0.210 MeV vers celui de 0.054 MeV dans le Zn^{66}. Deux résonances ont été mises en évidence à E_p = 2.874 MeV et 2.959 MeV. La distribution angulaire des γ de 0.118 et 0.155 MeV a été mesurée. Il est possible d'en déduire le spin et la parité des niveaux dans le Cu^{66}. Un résultat préliminaire assigne un spin 2^+ au niveau de 0.462 MeV. Ces mesures vont être complétées à l'aide d'une cible de Cu^{65} isotopiquement pure et auto-portante.

(b) Voie de sortie du neutron

Les distributions angulaires des neutrons émis aux énergies de protons correspondant au sommet et autour de la résonance à 2.959 MeV ont été mesurées par la méthode de temps de vol. Une piste de 1.80 m permet de séparer les groupes de neutrons correspondant au noyau final, Zn^{65}, dans son état fondamental et dans ses états excités à 0.054, 0.115 et 0.210 MeV.

Le dépouillement des mesures s'effectue sur les ordinateurs PDP-9 et I.B.M. 360/44. Le premier permet la soustraction du bruit de fond d'un spectre de temps de vol à l'aide d'un crayon lumineux et par calcul d'une courbe du 2nd degré. Le second permet de calculer une courbe, somme incohérente de gaussiennes, à travers les pics du spectre de temps de vol. Une analyse préliminaire confirme les expériences de la première partie.

3. Résonances analogues isobariques

3.1. Cr^{52} ; Réaction V^{51} (p,n) Cr^{51}

G. DECONNINCK, J. ROYEN

Les résonances analogues isobariques constituent un outil récent des plus précieux pour la spectroscopie nucléaire. Dans le cas du Cr^{52}, elles ont été étudiées en premier lieu par la réaction (p,n) sur V^{51} (cible auto-portante de 5 keV). La courbe d'excitation de cette réaction a permis de confirmer l'existence d'un niveau particulièrement intense à E_p = 2.334 MeV, ce qui correspond au niveau 1.557 MeV du V^{52}.

Des distributions angulaires ont été mesurées sur la résonance et autour de la résonance à E_p = 2.334 MeV; l'analyse de ces distributions est effectuée avec l'hypthèse de "random phase approximation"; la distribution obtenue est isotrope. Nous en concluons que le niveau de 1.557 MeV du V^{52} est formé par $j_n = 1/2^+$ dans une réaction de stripping du deuton. La courbe d'excitation par la réaction V^{51} (p,γ) a montré un comportement similaire de la résonance à E_p = 2.334 MeV.

3.2. Nb^{92} ; Réaction Zr^{91} (p,n) Nb^{91}

G. DECONNINCK, J-P. MEULDERS, J. ROYEN

La courbe d'excitation de la réaction Zn^{91} (p,n) a été mesurée pour des énergies de protons incidents comprises entre 2.9 MeV et 3.9 MeV. Il n'a pas été observé de résonance, vers E_p= 3.18 MeV, analogue au niveau fondamental du Zr^{92}. Par contre, une forte résonance se manifeste à E_p = 3.96 MeV.

Des distributions angulaires au sommet de la résonance et à côté de celle-ci, sont entreprises à l'aide de la méthode de temps de vol sur une piste de 2 m ; cette longueur permet de séparer les neutrons quittant le noyau final dans son état fondamental de ceux qui le quittent dans son premier état excité (Q = - 0.104 MeV). La distribution mesurée est isotrope comme il se doit si le niveau observé est l'analogue du Zr^{92} (g.s) qui est de spin 0^+.

4. Production de neutrons mono-énergétiques par la réaction V^{51} (p,n) Cr^{51}

G. DECONNINCK, J. ROYEN

La fonction d'excitation des neutrons quittant le noyau résiduel dans son niveau fondamental et dans ses trois premiers niveaux excités a été mesurée entre E_p = 2 MeV et E_p = 4 MeV à l'aide d'une cible épaisse (1 mg/cm^2) par la méthode du temps de vol. Dix neuf distributions angulaires ont été mesurées ainsi que les sections efficaces absolues n_0, n_1, n_2 et n_3. Ces mesures ont montré que la réaction fournissait une source de neutrons parfaitement isotrope. Ces résultats ont été publiés dans Nucléar Instruments and Methods, 75 (1969) p. 266.

5. Etude expérimentale temps-énergie des milieux non-multipliants par des neutrons pulsés

G. DECONNINCK, Ph. MONSEU

L'étude des spectres de neutrons rapides dans les milieux non-multipliants se fait essentiellement selon deux méthodes expérimentales. La première est celle du temps de vol, utilisant des sources de neutrons pulsés. La seconde analyse un état stationnaire à l'aide d'un détecteur sensible à l'énergie.

Nous avons développé une méthode qui permet l'analyse, simultanément en énergie et en temps de vol, du comportement des neutrons pulsés dans un milieu non-multipliant; l'étude de massifs de plomb et de carbone a été réalisée dans des géométries diverses : sphérique, cubique, "mur infini". La géométrie sphérique utilise une source de neutrons centrale et isotrope à partir de la réaction V^{51} (p,n) Cr^{51}, les autres géométries utilisent la réaction T (pn,) He^3 comme source de neutrons.
L'analyse des temps de vie des groupes de neutrons de différentes énergies s'effectue par méthode graphique sur l'ordinateur PDP9.
Cette étude sera complétée par d'autres éléments (Fe et Al) afin de déterminer l'influence de niveaux inélastiques importants dans ces noyaux sur le comportement des groupes de neutrons.

XXVIII. CENTRE D'ETUDE DE L'ENERGIE NUCLEAIRE (C.E.N.-S.C.K.) Mol, Belgium

1. NEUTRON SPECTROMETRY

Low energy scattering cross section of ^{235}U and ^{239}Pu

F. POORTMANS, H. CEULEMANS

This research is performed under contract with IAEA, Vienna. It involves the accurate measurement of the scattering cross-section of ^{235}U and ^{239}Pu in the region between 1 eV and 0.025 eV, using the BR2 crystal spectrometer as neutron source. The aim is to obtain scattering cross sections to better than 0.5 barn, which will consequently improve the precision on the absorption cross section.

Systematic errors are kept small by using metal samples of high purity and high neutron transmission. The correction for fission neutrons is based on a simultaneous counting of scattered and fast neutrons in separate channels in the ^{3}He detector. Relevant figures for the uranium sample are : purity 93.1 % ^{235}U (the remainder being essentially ^{238}U), thickness 332 mg/cm^2, giving a transmission at thermal energy of about 50 %; with this thickness the background contribution is about 3 % at thermal energy and the fast-neutron induced background about 20 %. The sample was obtained from CBNM. The plutonium was made at Oak-Ridge and contains 99.34 % ^{239}Pu with a thickness of 24 mg/cm^2, giving a transmission of 90 % at thermal energy.

The measurements on ^{235}U are finished and the analysis of the results is in progress. The ^{239}Pu measurements are scheduled for the first quarter of 1970.

Total cross section of ^{226}Ra and ^{227}Ac

H. CEULEMANS, H. CHRISTIAEN +, F. POORTMANS

The large discrepancies existing between the values quoted for the total and absorption cross-sections of ^{226}Ra and ^{227}Ac and their importance in the calculation of the yields of ^{227}Ac and ^{228}Th after irradiation of ^{226}Ra in an intense neutron flux, with a reactor spectrum, have created an urgent need to measure these cross-sections with good precision. The problems in the case of ^{226}Ra are the availability of a chemically pure sample and the handling of high specific activities and in the case of ^{227}Ac this is compounded with the problem of disposing only of milligram quantities. Up to now, the construction of the Ra target and its encapsulation have been studied together with the shielding and the safety procedures.

Resonance scattering cross section of ^{235}U

F. POORTMANS, H. CEULEMANS, J. THEOBALD ¤, E. MIGNECO ¤

This research is conducted in co-operation with CBNM, Euratom, Geel, under the terms of contract EUR/C/4146/67 f. The detector system described in the Annual Report for 1968 (EANDC-E-115-U) has been used succesfully for the measurement of ^{235}U scattering cross section in the region between 1 eV and 100 eV neutron energy. The Geel Linac was used as neutron source. This measurement is very important as it helps to increase the precision on the other cross-sections and allows to deduce spins in a direct way.

+ IWONL fellow, Association S.C.K./C.E.N. - Univ. Leuven

¤ C.B.N.M., Euratom, Geel

This last point is important as there are several phenomena in fission (average number of neutrons emitted, mass distribution, etc...) which are believed to be spin-dependent. The measurement is however very complicated as it involves low counting rates and elaborate corrections for multiple interactions and fission neutrons. Using parameters obtained from transmission experiments it has been possible to determine unambiguously the spin of about fourteen resonances. A paper with the details of the results will be presented at the IAEA Conference on Nuclear Data for Reactors, to be held in Helsinki, July 1970.

Scattering and total cross section of ^{181}Ta and ^{237}Np

F. POORTMANS, H. CEULEMANS, J. THEOBALD [x], E. MIGNECO [x]

This research is conducted in co-operation with CBNM, Euratom, Geel under the terms of contract EUR/C/4146/67f. The aim of the ^{181}Ta experiments is to satisfy the request for better values of the resonance parameters for this material which is quite important in the construction of fast reactors (control rods, canning materials). Preliminary measurements have been made to check the minimum sample thickness and the importance of multiple interaction corrections. It will probably be necessary to develop Monte Carlo type codes for solving this problem satisfactorily. Contacts have been established with an outside scientist who has already worked in this field.

The ^{237}Np experiment was started recently. Its purpose is to find evidence for the hypothesis that the group of near-barrier fission resonances occuring around 35 eV neutron energy, all have

---

x CBNM, Euratom, Geel.

the same spin. A first attempt had been unsuccesful due to a deficient sample. The new sample preparation containing 9 g of Np_2O_3 is giving satisfactory results.

Capture Cross Section of ^{238}U

H. CEULEMANS, F. POORTMANS, G. VANPRAET +

The U^{238} capture cross-section is one of the most important quantities influencing the economics of fast breeder reactors. At the same time the accurate knowledge of this quantity and its behaviour as a function of energy may give new details important to a better understanding of the compound state. During the past year preliminary experiments have been performed to demonstrate the feasibility of scattering experiments on very thin samples of U^{238}. In this special case scattering experiments could provide a better alternative to measure the capture cross-section, at least in the region below 1 keV. New gas scintillation detectors have been tested, which have given poor results up to now. At the same time the response function of liquid, hydrogen-free scintillaters is being investigated in order to use also the direct approach. With this method the gamma-ray yield after neutron capture is measured, taking into account the dependence of the detector efficiency on the gamma-ray energy. A data-acquisition system for multi-dimensional time-of-flight experiments has been set up and is nearly operational, although with limited capacity. A 800,000 word disk store will be added later.

+ R.U.C. Antwerpen

Total Cross Section of Nd isotopes

H. CEULEMANS

These results were obtained in 1968 during a stay at Columbia University, N.Y., where a series of transmission and self-indication measurements were performed. The analysis of such a large amount of experimental data requires the extensive use of computers and an appropriate technical support, and the rate at which it can be analysed depends strongly on the situation in this respect.

In the energy region below 1700 eV, 40 levels have been found in ^{143}Nd and 71 in ^{145}Nd. Several of these resonances have been assigned previously (Kharzavina et al., Yad. Fiz. 8, 1968, 639) but only up to about 1000 eV. Furthermore in ^{145}Nd, which has the highest level density, several levels have been missed in the quoted article, due to insufficient resolution. In Table I are listed the ^{143}Nd resonances above 1000 eV and the ^{145}Nd resonances above 750 eV. The analysis of the transmission data of isotopically enriched samples is in progress, but has met with certain difficulties mentioned above.

2. FISSION PHYSICS AND CHEMISTRY

Short lived Fission Isotopes and Delayed Neutron Precursors

P. del MARMOL, D.C. PERRICOS [m]

^{87}Se and ^{88}Se were separated as the hydrides at short time intervals from the fission products of ^{235}U irradiated with thermal

---

m IAEA fellow, on leave from Demokritos Centre, Athens

neutrons (P. Del Marmol and H. Van Tigchelt, Radiochem. Acta, 12, 57, 1969). Their half-lives were measured through the neutron activities of their bromine daughters as 5.9 ± 0.2 sec for ^{87}Se and 1.3 ± 0.3 sec for ^{88}Se ; the ^{87}Se fission yield was 0.65 ± 0.13 per cent.

From a delayed neutron activity consistent with the ^{87}Se half-life and in constant ratio with the ^{87}Br activity, a P_n value of 0.23 ± 0.07 per cent was evaluated for ^{87}Se. Evidence was not conclusive as regards delayed neutron emission from ^{88}Se for which an upper limit of $P_n \ll 1$ per cent was estimated (Physics a. Chemistry of Fission, IAEA, Vienna 1969, p. 898 and J. Inorg. Nucl. Chem., in press).

The delayed neutron emission from ^{137}I is being remeasured with respect to that of ^{87}Br in thermal neutron fission of ^{235}U. ^{137}I was separated chemically while the 55 sec delayed neutron activity was measured from unseparated irradiated ^{235}U samples. From these measurements a more precise measurement for the ^{137}I half-life is also expected.

TABLE I

^{143}Nd resonances above 1000 eV (energies in eV)

1028 ± 1	1433 ± 2
1082 ± 1	1463 ± 2
1125 ± 1	1472 ± 3
1167 ± 2	1512 ± 3
1205 ± 1	1558 ± 3
1211 ± 1	1584 ± 3
1264 ± 2	1653 ± 3
1276 ± 2	1667 ± 3
1307 ± 2	

^{145}Nd resonances above 750 eV (energies in eV)

756.0 ± 0.5	938.3 ± 0.7	1195 ± 2	1448 ± 2
761.8 ± 0.5	946.2 ± 0.7	1237 ± 2	1491 ± 3
787.4 ± 0.5	972.8 ± 1	1267 ± 2	1524 ± 3
820.9 ± 0.5	978.0 ± 1	1287 ± 2	1553 ± 3
828.0 ± 0.5	1007.5 ± 1	1303 ± 2	1562 ± 3
848.1 ± 0.5	1054 ± 1	1313 ± 2	1576 ± 3
880.8 ± 0.5	1093 ± 1	1379 ± 2	1612 ± 3
885.4 ± 0.5	1117 ± 1	1397 ± 2	1650 ± 3
902.1 ± 0.5	1140 ± 1	1402 ± 2	1658 ± 3
913.9 ± 0.5	1163 ± 1	1429 ± 2	1663 ± 3
920.2 ± 0.7			

Joint S.C.K./C.E.N. - C.B.N.M. (Euratom) Studies on Fission

A. DERUYTTER [x], C. WAGEMANS [xx], G. PENNING [xxx]

Some fission studies related to reactor requests for fission cross-sections were pursued under the terms of contract EUR/C/4146/67f. The measurements were made on a short neutron flight path at the Geel Linear accelerator.

Ratio of the binary-to-ternary fission cross-section of U^{235}

The ratios of the areas in counting-rate versus neutron time-of-flight spectra for binary and ternary fission in the strongest well-isolated resonances (8.78 eV, 12.39 eV, 19.3 eV and 21.1 eV) were calculated. In Table II the obtained T/B-ratios are compared with the spin assignments of Poortmans et al. (cf. supra), and with measurements of the 0°/90°-angular anisotropy measurements for oriented ^{235}U-nuclei of Dabbs et al. (Physics and Chemistry of Fission, IAEA, Vienna 1969, p. 321) and Pattenden et al. (Physics and Chemistry of Fission, IAEA, Vienna 1969, p. 330). A strong correlation between these results seems to be present.

Normalisation of ^{235}U fission cross-sections in the resonance region

The analysis of the data has been considerably improved especially concerning the shape of the neutron spectrum in the low energy region, and the analysis is now considered as final. A thorough analysis of the published σ_f-data in the resonance region allows to conclude that a large part of the differences in published resonance integrals

---

x C.B.N.M., Euratom Geel

xx N.F.W.O. bursar, University of Gent and SCK/CEN

xxx IWONL bursar, University of Gent and SCK/CEN

TABLE II

Energy (eV)	T/B normalized at 8.79 eV	Spins Assignment by Poortmans et al.	Dabbs et al. * (0°/90°)	Pattenden et al. * (0°/90°)
21.1	120 ± 5	no result	no result	1.345
19.3	115 ± 3	4^-	1.124 ± 0.004	1.361
12.39	102 ± 3.5	3^-	1.042 ± 0.005	1.163
8.79	100 ± 2.5	3^-	1.041 ± 0.008	1.298

* The absolute values of Dabbs and Pattenden cannot be compared directly.

are due to different ways of normalization of the relative cross-sections. For this reason a further normalization of fission cross-sections of ^{235}U is proposed, based on the fission integral $\int_{7.8eV}^{11eV} \sigma_f(E)dE$ obtained by the present normalization at thermal energy.

Normalization of the ^{239}Pu fission cross-section in the resonance region

Accurately normalized fission cross-sections for ^{239}Pu were demanded at the IAEA-Meeting on Alpha of ^{239}Pu, held at Winfrith (UK) in July 1969.

The induced reaction-rates of a back-to-back ^{239}Pu- and ^{10}B-foil were registered simultaneously in two halves of a 4096 channel time-of-flight analyser. The measurements are performed at a short-flight path of the CBNM-Linac (8 meters)with two surface-barrier detectors. Relative cross-sections will be normalized to the 2200 m/s reference fission cross-section.

Comparison of the spontaneous fission of ^{240}Pu and thermal neutron induced fission of ^{239}Pu

Bidimensional measurements were performed with surface-barrier detectors on both sides of a 4π -source of 60 $\mu g/cm^2$ Pu (90.44 % ^{240}Pu and 8.06 % ^{239}Pu) at the BR1-reactor. With the reactor stopped (i.e. no neutrons) the characteristics of the spontaneous fission of ^{240}Pu were measured; with the reactor in operation, the thermal neutron induced fission of ^{239}Pu was studied in the same geometrical conditions and with the same source. From a registration on tape, event by event, of both

pulse-heights, the distribution of the sum of the kinetic energies of the fragments, their difference, the ratio of the masses and the mass-distribution were calculated (program written by L. De Corte). A surprisingly large difference of 6.6 ± 1.0 MeV was found between the average kinetic energies of the two systems.

3. INELASTIC SCATTERING OF SLOW NEUTRONS

Phonon dispersion relation of zinc oxide

S. HAUTECLER, W. WEGENER[x]

An experimental study of the lattice dynamics of ZnO was undertaken by means of coherent inelastic scattering of neutrons using the BR2 time-of-flight spectrometer. Neutrons of 4.16 meV energy were selected from a reactor beam by Bragg reflection on a lead single crystal. Their energies after scattering were analyzed in flight paths of 4 m length under 7 angles between 45.8° and 106.5° and for 21 different orientations of the sample (a single crystal of 3 x 2 x 0.3 cm^3) relative to the incident monochromatic beam. The plane containing the points A, Γ, M of the first Brillouin zone of ZnO was used as scattering plane. The analysis of the time-of-flight spectra yielded the scattering surfaces and the phonon dispersion relation for waves propagating along the symmetry directions. A comparison between the measured branches of the dispersion relation and the results of lattice dynamics model calculations was started. A short article on the preliminary results has been written.(to appear in Physics Letters).

---

x Kernforschungsanlage Jülich

Molecular motions in plastic-crystalline neopentane

S. HAUTECLER, L. DE GRAAF [***]

Neopentane, $C(CH_3)_4$, belongs to the class of globular molecular crystals which show a phase transition in the solid state from a low-temperature crystalline phase with low symmetry to a high-temperature plastic-crystalline phase with high symmetry. In plastic crystals the entropy change at the phase transition is comparable to or greater than that at the melting point, and is an indication that there is orientational disorder in the plastic phase. The rotational motions of the neopentane molecules in the plastic phase have been investigated by incoherent neutron scattering. The broadening of the quasi-elastic peak was observed at 110°, 150°, 175° and 200°K, for 7 scattering angles and for incident neutron wavelength of 4.17 Å (with a t.o.f. resolution of 2 %) and 1.86 Å (t.o.f. resolution 3 %). A comparison of the shape of the measured quasi-elastic peaks with calculations for simple models for molecular reorientations is in progress.

Dynamical properties of polymers

H. BERGHMANS [*], G. GROENINCKX [*], N. OVERBERGH [*], S. HAUTECLER

The intra- and intermolecular vibrations have been localised in polyethylene terephtalate by incoherent neutron scattering. From the results obtained for different samples, it is hoped to get useful information on the effects of temperature, crystallinity, branching and cross-linking.

*** Reactor Instituut Delft
* Laboratorium voor Makromolekulaire Scheikunde, K.U. Leuven

4. INTEGRAL CROSS SECTION MEASUREMENTS AND NUCLEAR DATA RELATED TO REACTORS

4.1. Standard neutron spectra

A. FABRY, M. DE COSTER, G. and S. DE LEEUW, J.C. SCHEPERS, P.VANDEPLAS

The aim of this work has been outlined in previous progress reports EANDC 89 "U" p 124 and EANDC 115 "U" p 198 and is described in more details elsewhere (Fast reactor physics, IAEA, Vienna 1968 vol.I p 389 and EACRP - A - 97).

A few data already obtained are summarized here but must be considered still as of a preliminary nature :

1.1. Spherical shell transmission measurements have been performed by means of the threshold reactions $^{115}In(n,n')$ and $^{238}U(n,f)$; the shells were 2 and 4 cm thick depleted uranium. The detailed analysis of these measurements implicates that the inelastic scattering data for uranium-238 in the evaluated files ENDF/B (WITTKOPF et al - ENDF - 103), KEDAK (SCHMIDT - KFK 120) and DFN (VASTEL - HX - 1/1375 Electricité de France), essentially based on the high resolution time-of-flight measurements of BARNARD (BARNARD et al - Nucl. Phys. 80, 46), lead to an overestimate of the proportion of neutrons downscattered from high energies down to below 1 MeV; the downscattering matrix as derived (SMITH et al - AEEW - R 491) from the oldier DFN set (PARKER - AWRE O-79/63) is found reasonably correct, while the total inelastic scattering cross sections as suggested by BARRE (PWR/SETR 69.031) , by BERLIJN (LA 3527) and by

RAKAVY (Fast reactor physics, IAEA, Vienna 1968 vol.I p 255) seem seriously too low, especially below 2 MeV : this might be related to undue allowance for uncertainties in fission neutron spectra when performing the generalized perturbation and least squares analysis of combined differential and integral measurements and it is believed that this illustrates the possible ambiguity of such methods if all degrees of freedom and their correlations are not accounted for.

1.2. New precise absolute average cross sections have been measured in the uranium-235 thermal fission neutron spectrum and confirm within uncertainties the previously reported results (Nukleonik 10, 5, 280 and NBS. special public. 299 p 1263). The major improvement lies in the method used for experimental correction of wall return epithermal backgrounds (details and all results to be presented at HELSINKI conference on Nuclear Data for Reactors, July 1970).
Furthermore, the techniques for determination of absolute reaction rates have also been systematically ameliorated, for instance the registration of fission fragments by means of track recorders; a recent intercomparison with standards of the IAEA has shown an agreement within 1 % in the case of the $^{32}S(n,p)^{32}P$ threshold reaction.
A re-evaluation of all differential energy cross sections involved in this work has also been undertaken and in the present stage of this effort, a best representation for the uranium-235

thermal fission neutron spectrum has been tentatively deduced using the semi-empirical function

$$\chi_5(E) = [\, e^{-E_f/T} / (\pi E_f T)^{1/2} \,]\; e^{-E/T} \sinh[2(E\,E_f)^{1/2} / T\,]$$

giving the parameter T as equal to 0.952 MeV while the average fragment kinetic energy per nucleon E_f amounted to 0.684 MeV only. This is illustrated on the accompanying figure, which shows that such a representation is not strictly incompatible with differential photoplate/time-of-flight/cloud chamber measurements based on (n,p) scattering; however, the obtained average fission neutron spectrum energy of 2.11 MeV is considerably higher than the 1.93 MeV value of the conventional maxwellian representation, as accepted for instance in ENDF/B, but is lower than suggested by GRUNDL (Nucl.Sci.Eng. 31, 191) and by Mc. ELROY (Nucl.Sci.Eng. 36, 109). Other theoretical suggestions are presently investigated in order to express and possibly understand the results in the light of more recent concepts.

1.3. As a consequence of 1.1. and 1.2., the underestimation of k_{eff} and of uranium-238 fission rates relative to uranium-235 in dilute fast assemblies as generally found with ENDF/B for instance should be entirely removed; however, the measurements referred to in 1.2. also implicate surprisingly large values

for the uranium-235 fission cross section between about 300 keV and 5 MeV, i.e. values close to a curve suggested by RAKAVY et al (Fast reactor physics, IAEA, Vienna 1968 vol.I p 255); therefore the uranium-238 and other fission cross sections must also be increased according to the present data and very over-reactive fast systems would result if uranium-238 capture and other absorption processes are not to be modified either; further measurements and re-evaluations on such cross sections are consequently pursued in order to understand the situation.

4.2. Track recorders

M. DE COSTER, P. POPA*, P. VAN ASSCHE, D. LANGELA

The precision of absolute fission rates measurements for uranium-235, 238, plutonium-239 and thorium-232 foils has been continuously improved, as well as the method for the determination of fine structures of the absolute fission rates within reactor fuel pins. On another hand, a paper has been sent for publication in Nucl.Sci.Eng. and the abstract follows;

" The absolute ratio of fission densities due to thermal- and epi- "
"cadmium-neutron fluxes has been measured by solid-state track detectors"
"A systematic deviation from this absolute ratio is observed when "
"measuring gamma activities of fission products. From a careful analysis"
"of the gamma spectra with a Ge(Li)detector, it was concluded that this "
"systematic deviation is due to impertant changes in the mass distribu- "
"tion of fission products produced by epicadmium neutrons, with res- "
"pect to the well-known mass distribution for thermal neutrons. "

---

* On leave from the Institute of Atomic Physics
BUCAREST, ROUMANIA

4.3. Evaluation of nuclear data for threshold detectors

A. FABRY, J.C. SCHEPERS

A thorough re-evaluation has been undertaken for a number of threshold reactions relevant to neutron dosimetry.
Final results (to be presented at the 27th meeting of the EURATOM WORKING GROUP FOR REACTOR DOSIMETRY, Ispra, 19.2.70) are available for the four fluence monitors $^{58}Ni(n,p)^{58}Co$, $^{54}Fe(n,p)^{54}Mn$, $^{46}Ti(n,p)^{46}Sc$ and $^{63}Cu(n,\alpha)^{60}Co$, both in graphical form as well as in a fifty-group structure, including always an appraisal of the confidence interval of the data.

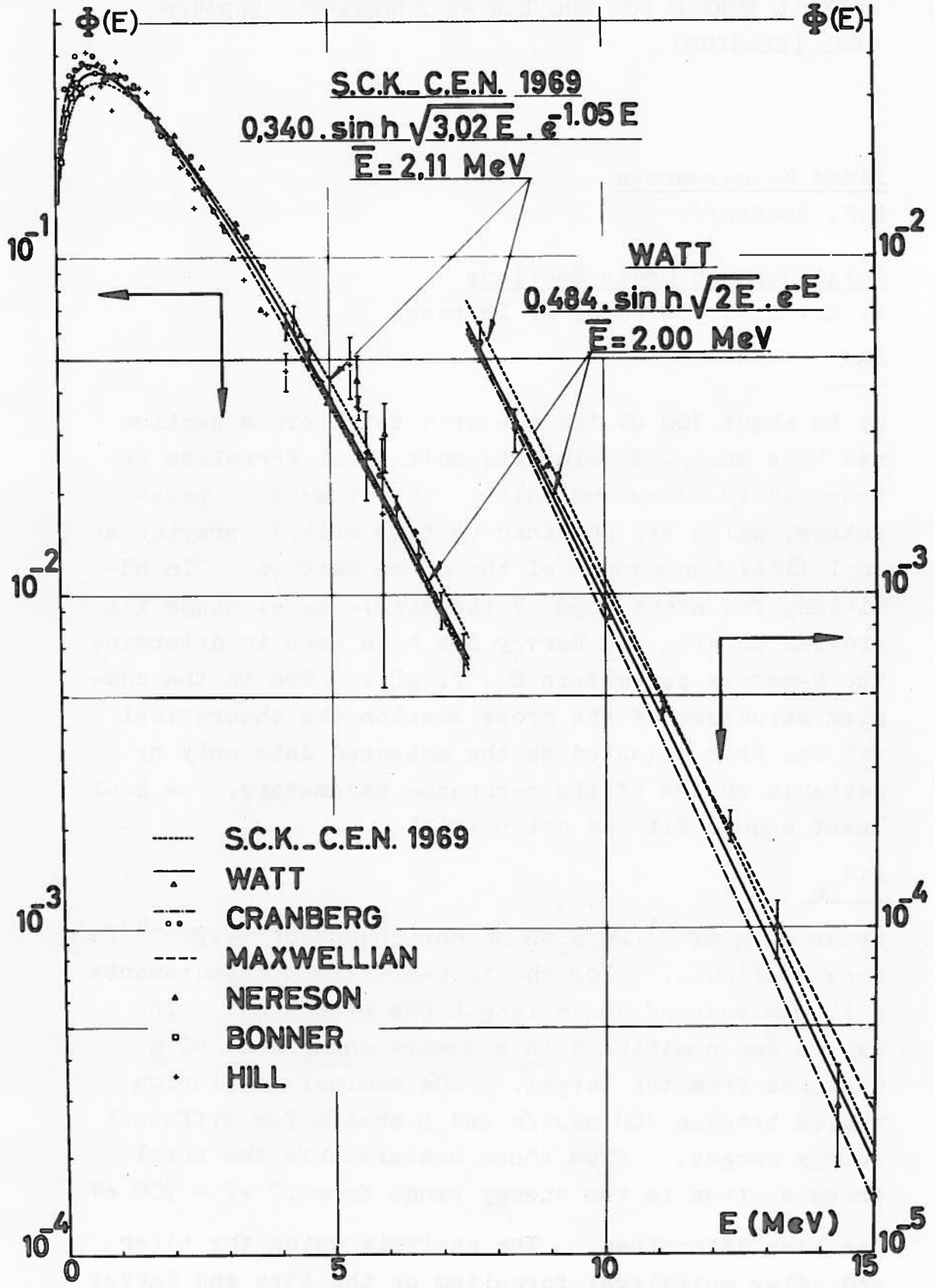

URANIUM 235 THERMAL FISSION SPECTRUM

XXIX. CENTRAL BUREAU FOR NUCLEAR MEASUREMENTS, EURATOM, GEEL (BELGIUM)

1. Linac Measurements

K.H. Böckhoff

1.1. Total Neutron Cross Sections

W. Kolar, G. Carraro, A. Dufrasne

^{233}U

Up to about 100 eV the measured total cross section has been analysed using the multilevel formalism as proposed by Adler and Adler. The resonance parameters, which are obtained by this method, provide an analytical description of the cross section. In addition, for about 3-50 eV the single level shape fit program of Atta and Harvey has been used to determine the R-matrix parameters E_o, Γ, $g\Gamma_n^o$. Due to the complex structure of the cross section the theoretical fit has been adjusted to the measured data only by suitable choice of the resonance parameters. A real least square fit was not possible.

^{241}Pu

About 20 g of ^{241}Pu with an enrichment of 94.7% ^{241}Pu were available. For the time-of-flight measurements a flight path of 100 m length has been used. The sample was positioned in a sample changer at 50 m distance from the target. The nominal resolution varied between 100 nsec/m and 3 nsec/m for different energy ranges. From these measurements the total cross section in the energy range from .7 eV - 700 eV has been determined. The analysis using the Adler and Adler multilevel formalism or the Atta and Harvey single level shape fit program is in progress.

^{238}U

The neutron total cross section of ^{238}U has been measured

from 60 eV to 14 keV, analysis of the data has been performed up to 6 keV. The thickness of the sample was 110 atoms/b, the resolution varied between 0.8 and 0.2 nsec/m at the highest energy.

About 270 resonances were observed and the corresponding parameters have been calculated using the Atta-Harvey area analysis program. The values of energies and Γ_n^o observed are in good agreement with those of Garg and al.

The evaluation of the statistical properties of the resonance parameters, and the S-wave strength function are in progress.

1.2. Fission Measurements

E. Migneco, J. Theobald, J.A. Wartena, M. Merla

Fission Cross Section of ^{233}U

The fission cross section of ^{233}U, measured with a spark chamber fission fragment detector from thermal energies up to 80 eV and with a liquid scintillator neutron detector between 10 eV and 2 keV, has been analysed with a modified multilevel program "Codilli" of Adler and Adler. Parameters for the resonances up to 65 eV have been determined, and an autocorrelation analysis, introduced by Egelstaff, has been applied to this cross section to search for quasiperiodical intermediate structures. The results are described in a paper accepted for publication [1].

Fission Cross Section of ^{241}Pu

The neutron induced fission cross section of ^{241}Pu has been measured between 2 eV and 2 keV. The fission neutron liquid scintillator has been used as detector. The resulting fission yield curve has been reduced and the fission cross section as well as resonance integrals have been determined (Fig. 1 shows a cross section display from 2 eV up to 53 eV).

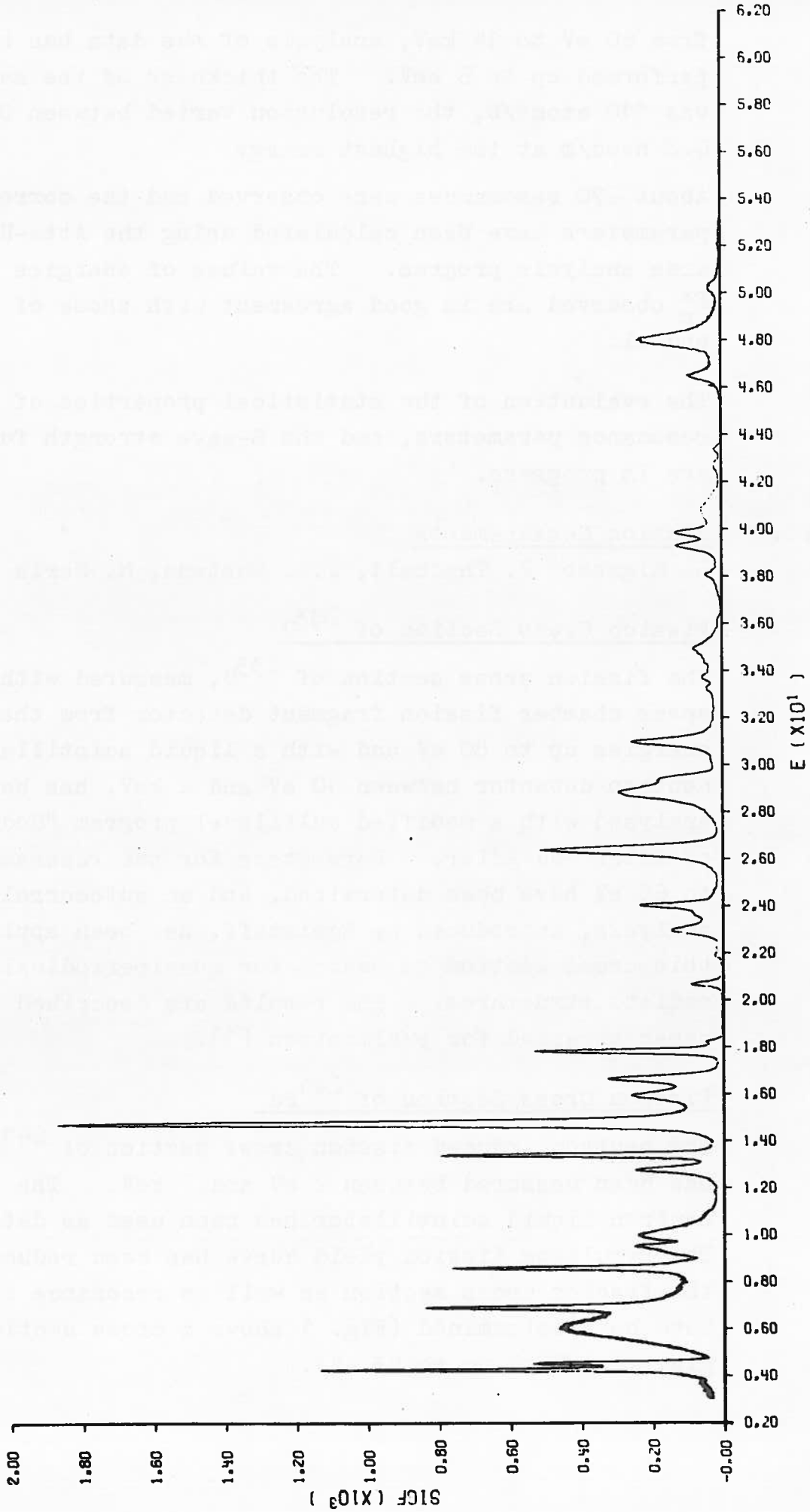

Fig. 1 PU 241 FISSION CROSS SECTION

Subthreshold Fission of ^{241}Am

In two experiments with time-of-flight resolutions of 20 nsec/m and 2 nsec/m it has been tried to confirm the spikes indicated in the Petrol cross section display of the $^{241}Am(n,f)$ of the $^{241}Am(n,f)$ reaction at about 1.6, 2.3 and 2.8 keV and to identify them as resonance groups of the type found in ^{237}Np, ^{234}U and ^{240}Pu. The result of this investigation is, that in spite of a 10 times higher resolution no structure of more than 1 barn could be confirmed, although the subthreshold fission resonances at energies lower than 100 eV, which have already been observed by Bowman et al., are clearly pronounced in our cross section. A discussion of this experiment has been published at the Vienna Conference on Fission [2].

1.3. Scattering Data

E. Migneco, J. Theobald, J.A. Wartena, M. Merla

Resonance Parameters of Nd

The scattering cross section measurement on natural Nd has been analysed together with capture data (see 1.2.4.). The results have been published [3].

Parity Assignment of ^{98}Mo Resonances

An experiment of ^{98}Mo is running for a parity assignment of the 429 eV, 612 eV and 818 eV resonances using the technique of Asami et al.*) The experiment is performed in order to clarify a preliminary parity assignment proposed by Rohr et al. (see 1.4.) as a result of capture γ-spectroscopical work. In this measurement boron-10-loaded liquid scintillation counters with pulse shape discriminators against γ and fast neutron radiation are used as detectors for the scattered neutrons. The differential cross section with interference has been calculated for $\Theta = 35°$. For this calculation the theory of Blatt and Biedenharn has been applied with the computer program "Blatt 4" by M.G. Czo (report EUR 3744 f.). The experiment seems to be feasible, although it presents a hard problem in background reduction.

*) A. ASAMI, M.C. Moxon, W.E. Stein, Phys.Lett. 28B, 656 (1969)

Resonance Scattering Cross Section of ^{235}U

F. Poortmans*, H. Ceulemans*, J. Theobald, E. Migneco

This work is conducted in co-operation with S.C.K.-C.E.N., Mol. The detector system described in the Annual Report for 1968 has been used successfully for the measurement of ^{235}U scattering cross section in the region between 1 eV and 100 eV neutron energy. This measurement helps to increase the precision of other cross sections and allows to deduce spins in a direct way.

This last point is important as there are several phenomena in fission (average number of neutrons emitted, mass distribution, etc..) which are believed to be spin-dependent. The measurement is however very complicated as it involves low counting rates and elaborate corrections for multiple interactions and fission neutrons. Using parameters obtained from transmission experiments it has been possible to determine unambiguously the spin of about fourteen resonances. A paper with the details of the results is being prepared.

Scattering and Total Cross Section of ^{181}Ta and ^{237}Np

F. Poortmans*, H. Ceulemans*, J. Theobald, E. Migneco

The aim of the ^{181}Ta experiments, also a cooperation with S.C.K.-C.E.N., Mol, is to satisfy the request for better values of the resonance parameters for this material, which is quite important in the construction of fast reactors (control rods, canning materials). Preliminary measurements have been made to check the minimum sample thickness and the importance of multiple interaction corrections. It will probably be necessary to develop Monte Carlo type codes for solving this problem satisfactorily.

The ^{237}Np experiment was started recently. Its purpose is to find evidence for the hypothesis that all of near-barrier fission resonances occurring around 35 eV neutron energy have the same spin. A first at-

---

*) S.C.K.-C.E.N., Mol, Belgium

tempt had been unsuccessful due to a deficient sample. A new sample containing 9 g of Np_2O_3 seems to give satisfactory results.

1.4. . Capture Measurements

G. Rohr, H. Weigmann, J. Winter, M. Heske

Capture Cross Sections of Nd

The capture data on natural Nd have been analysed together with scattering data (see 1.2.3.). The results have been published [3].

Capture Cross Section of ^{238}U

Resonance analysis of the ^{238}U data in the neutron energy range from 20 eV to 1.05 keV is almost complete. A preliminary value of the average radiative width is $\langle\Gamma_\gamma\rangle = (24.1 \pm 1.1)$ meV, which is in good agreement with the value given by Asghar et al.* No evidence for a nonstatistical variation of the radiative widths with neutron energy has been found.

Capture Cross Section of Mo-Isotopes

Neutron radiative capture in separated Mo-isotopes has been measured in the neutron energy range from 10 eV to 10 keV. The measurements were performed at a 60 m flight path station. The nominal resolution varied between 1.5 nsec/m and 3 nsec/m for different energy ranges. A resonance analysis of these data is in progress.

Instrumentation for Gamma-Ray Spectra from Resonance Capture

The electronic system has been completed by a "condition control unit", which controls the fast linear gate: Pulses are accepted only if their amplitude and time of arrival are inside preselected limits and if they are not disturbed by pile-up. As this preselection is done in the fast pulse domain, it is possible to measure samples of high natural activity without severe losses of useful events.

---

*) M. Ashgar et al., Nucl. Phys. 85, 305 (1966).

Gamma-Ray Spectra from Resonance Capture in ^{237}Np

Gamma-ray spectra from neutron capture in (^{237}Np+n) resonances between 30 eV and 50 eV neutron energy have been measured with a 30 cm^3 Ge(Li) detector as well as with a 4"x3" NaI(Tl) crystal. From the observed spectra it is concluded that the intermediate structure in sub-barrier fission of ^{237}Np is an example of the case $\Gamma^{\downarrow} << \Gamma^{\uparrow}$, which means that the maximum of the second potential barrier is approximately equal to the neutron binding energy. A more detailed discussion of the measurements has been published [6].

Gamma-Ray Spectra from Resonance Capture in ^{98}Mo

Measurements of γ-ray spectra from neutron capture in (^{98}Mo + n) resonances have been completed. A paper on this subject is in preparation. A preliminary abstract is given below:

Neutron capture γ-ray spectra from individual ^{98}Mo+n resonances have been measured with a Ge(Li) detector. From the observation of very intense high energy γ-rays it is concluded that several of the resonances are extraordinarily strong p-wave resonances with very large E1 strengths for decay into low lying positive parity states in ^{99}Mo. Inspection of the ^{98}Mo γ-ray spectra themselves as well as a comparison with similar data for other nuclei in this mass region lead to results which are in contradiction to a statistical decay of the compound nucleus and suggest that nuclear structure effects like valency nucleon transitions or two particle one hole doorway states play an important role in the decay of these resonances. Moreover, the extremely high value for the p-wave strength function computed from the ^{98}Mo resonances assigned as p-wave can only be interpreted in terms of a strong energy dependence of the strength function due to the excitation of two particle one hole doorway states.

1.5. Capture Resonance Parameters and Gamma-Ray Spectra (Joint Program CNEN-CBNM)

C. Coceva[+], F. Corvi[+], P. Giacobbe[+], M. Stefano[+], G. Carraro

Neutron Energy Dependence of Capture Gamma Spectra in ^{115}In

Several measurements in different experimental conditions were performed in order to confirm and extend the evidence of the observed (see BCMN Annual Progress Report 1968, 1.2.6.4.) systematic behaviour of the sum of partial radiation widths over final states with low excitation energy. The relative intensity of this sum shows a fluctuation as a function of neutron resonance energy which cannot be explained in terms of the statistical model of the gamma decay. This effect suggests the influence of simple nuclear configurations in the gamma decay of compound nucleus states.

Resonance Neutron Capture Gamma-Ray Spectra

The measurement of the high-energy capture gamma-rays of 15 resonances of ^{105}Pd was completed. The intensities of the primary transitions to final states having an excitation energy lower than 3.16 MeV were determined. As spin and parity of all capture states and of several final states were known from previous work, it was possible to assign the multipolarity character of the measured transitions. The results were consistent with the assumption that the average reduced M1 and E1 strengths do not depend on the particular final states concerned. Average values of reduced M1 and E1 transition strengths were determined. Spin assignments were deduced for several low-lying excited states of ^{106}Pd.

Data analysis is under way for a determination of the statistical distribution of partial E1 and M1 reduced radiation widths. First results for M1 widths indicate

[+]CNEN, Italy

a X^2-distribution with one degree of freedom.

The detection equipment was improved: a 50 cm^3 Ge(Li)-crystal was installed, together with a bidimensional 4096 x 4096 time-amplitude analyser and magnetic tape recorder.

Resonance Parameters of Zirconium

Several transmission measurements with different sample thicknesses of Zr were performed of a 50 m flight-path. Data were recorded up to 10 keV neutron energy. Calculations are in preparation.

1.6. Standard Cross Sections in the Resonance Region Normalization of the ^{235}U Fission Cross Section

A.J. Deruytter, C. Wagemans[+]

The analysis of the data has been considerably improved especially concerning the shape of the neutron spectrum in the low energy region, and the analysis is now considered as final.

A thorough analysis of the published σ_f-data in the resonance region allows us to conclude that a large part of the differences in published resonance integrals are due to different ways of normalisation of the relative cross sections. For this reason we propose to base all further normalisation of fission cross section of ^{235}U on the integral

$$\int_{7.8eV}^{11eV} \sigma_f(E)dE$$

obtained by our normalisation at thermal energy.
The absolute value of this integral will be given when the more precise CBNM-value of the ^{234}U-half life is known.

[+] NFWO-Research Fellow

Normalization of the ^{239}Pu Fission Cross Section

A.J. Deruytter, C. Wagemans[+], G. Penning[++]

The induced reaction-rates in a back-to-back ^{239}Pu- and ^{10}B-foil are compared with two surface barrier detectors and registered simultaneously in two halves of a 4096 channels time-of-flight analyser. The measurements are performed at a short (8m) flight path of the CBNM Linac. Relative cross sections will be normalised to our reference cross section at 2200 m/s neutron-velocity.

The aim again is to be able to give an absolute fission integral for further normalisation of $\sigma_f(^{239}Pu)$. Accurately normalised fission cross sections for ^{239}Pu were demanded at the IAEA Meeting on Alpha of ^{239}Pu, held in Winfrith (U.K.), July 1969, and discussed at the EANDC Meeting at Bournemouth (U.K.), October 1969.

Variation of the Binary-to-Ternary Fission Ratio for ^{235}U

A.J. Deruytter, C. Wagemans[+]

The ratios of the areas in the counting-rate versus neutron time-of-flight spectra for binary and ternary fission in the strongest well-isolated resonances (8.78 eV, 12.39 eV, 19.3 eV and 21.1 eV) were calculated and compared with previously published contradictory data (Table 1). Our data were obtained with a ternary α detection level of about 10 MeV as were the results of Saclay.

We repeated these ratio measurements with a detection level of 15 MeV α-energy and the effect was considerably reduced. We therefore intend to repeat the measurements with an α detection window between 10 and 15 MeV.

[+] NFWO-Research Fellow

[++] IWONL-Research Fellow

Table 1: Comparison of ternary/binary values

E(eV)	Mehta et al.(+)	Michaudon et al.(++)		These measurements		
		I	II	I	II	Average
21.1	96 ± 5	92.5 ± 5	105.5 ± 3.5	122 ± 6	118 ± 8	120 ± 5
19.3	97.5 ± 3	90 ± 2.5	105 ± 2	114 ± 3.5	116 ± 5	115 ± 3
12.39	" 99 ± 3	92.5 ± 2.5	100 ± 2	105.5 ± 4	99 ± 6	102 ± 3.5
8.78*	100 ± 2	100 ± 1.5	100 ± 1.5	100 ± 3	100 ± 4	100 ± 2.5
Detection level	9 MeV	7.3 MeV	10.9 MeV	10 MeV		
Detector	Si(Au)	ionisation chamber		Si(Au)		

* All the ratios are normalized at this energy

(+) E. Melkonian and G. Mehta: "Physics and Chemistry of Fission", Vol.II, IAEA (1965).

(++) A. Michaudon et al., Nucl.Phys. 69, 573 (1965).

There seems to be a strong correlation between measurements of the fission fragment angular anisotropy for oriented ^{235}U-nuclei (Dabbs et al, Pattenden et al)* and our values for the T/B ratios in the resonances.

Branching-Ratio in the ^{235}U α-Decay

A.J. Deruytter, G. Penning

A few α-spectra of highly enriched ^{235}U sources were recorded (isotopic composition: 99.999% ^{235}U, ^{234}U<0.0002%) with a high resolution surface-barrier detector.
A preliminary calculation of the branching-ratio in the ^{235}U α-decay was made in view of the determination of the half life value.

The $^{6}Li/^{10}B(n,\alpha)$Cross Section Ratio

J.A. Wartena, J. Theobald

A mock up of two back-to-back gridded ionization chambers was built and tested. The γ-flash signal under typical machine parameters had an amplitude of 150 MeV α-equivalent and a width of 15 MeV F.W.H.M.. The subtraction of the signals of the two chambers resulted in a rest signal of 0 ± 8 MeV when the linear accelerator is running with 50 Hz (synchronized with the line). The tail of the γ-flash signal is similar to that observed with the surface barrier detectors. Like the surface barrier detectors, the two gridded ionization chambers turned out to be not suited for the measurement of the $^{6}Li/^{10}B$ (nα) cross section ratio.

An agreement was found with the AERE Harwell to test there the possibility of using surface barrier detectors together with the booster target.

---

* Conference on Physics and Chemistry of Fission, Vienna, 1969

1.7. Thermal Neutron Standard Data

A.J. Deruytter

Fission Cross Section of ^{235}U at 2200 m/s and in the Subthermal Region

A.J. Deruytter

The analysis of the two series of measurements with the slow chopper at BR2 (runs at 92 and 40 rps rotor resolution speed) yield 4 independent values of σ_f^o, which are in good agreement. We further conclude that σ_f behaves as 1/v above 700 us/m (or below 0.01 eV neutron energy).

The absolute values of σ_f and especially the 2200 m/s-value will be communicated in a definite publication, when the α half-life of ^{234}U (needed for the determination of the amount of ^{235}U in the foils) is known with a better accuracy (CBNM project). When the trend to a lower value of this α half life is confirmed in the CBNM measurements the obtained σ_f^o-value will be higher than the recommended IAEA-value. Some trends in other 2200 m/s fission parameters seem to confirm this higher σ_f^o-value.

The shape of the cross section curve in the thermal and subthermal region can be used for the calculation of g-factors for reactor spectra and yields more information on the negative energy levels (below the neutron binding-energy).

Fission Cross Section of ^{239}Pu at 2200 m/s and in the Subthermal Region

A.J. Deruytter, W. Becker[+]

Two well-defined layers of ^{239}Pu-acetate have been compared with two standard boron layers in order to determine the ^{239}Pu fission cross section relative to $^{10}B(n,\alpha)$ as absolute standard. These measurements

[+] Euratom Research Fellow

were performed with the slow chopper at BR2 (revolution speed 40 rps) in the energy region 0.1 eV to 0.002 eV.

An analysis was made for a first group of measurements and the very preliminary result obtained was 745 ± 6 barns at 2200 m/s. The agreement with the IAEA-review of 2200 m/s-constants is very satisfactory.

$\sigma_f(^{239}Pu)$ approaches a 1/v behaviour at energies below 10 meV (700 µs/m) and the shape of the cross section at thermal energy is already strongly influenced by the huge resonance at 0.3 eV. The curvature of the σ_f/E-curve above thermal energy is opposite to that of the σ_f/E-curve for ^{235}U. These data can also serve to calculate g-factors and to obtain information on negative energy resonances.

Comparison of the Spontaneous Fission of ^{240}Pu and Thermal Neutron Induced Fission of ^{239}Pu

A.J.Deruytter, G. Penning[+]

Two-dimensional measurements were made with surface-barrier detectors on both sides of a 4π-source of 60µg/cm^2 Pu (90.44% ^{240}Pu; and 8.06% ^{239}Pu). With the reactor stopped (no neutrons) the characteristics of the spontaneous fission of ^{240}Pu were measured, with neutrons the characteristics of the thermal neutron-induced fission of ^{239}Pu were studied with the same source in identical geometrical conditions. From a registration on tape, event by event, of both pulse-heights, the distribution of the sum of the kinetic energies of the fragments, their difference, the ratio of the masses and the mass-distribution were calculated. A surprisingly large difference in the average total kinetic energy for both systems was found:

[+] IWONL-Research Fellow

(177.91 ± 0.56)MeV for thermal neutron fission and only (171.25 ± 0.85)MeV for spontaneous fission of ^{240}Pu. This would mean that all binding energy of the neutron is converted in kinetic energy of the fragments.

2. Van de Graaff Accelerator

K.H. Böckhoff

2.1. Precise Determination of Neutron Fluxes

H. Liskien, A. Paulsen, R. Widera

A preliminary comparison between associated ^{3}He particle counting and the recoil proton counter with collimator was successful using the T(p,n) reaction with 0.5 MeV neutrons at 110° (associated ^{3}He particles at 20°). With the new T-Ti targets with 0.2 mg/cm^2 Al backings the ^{3}He peak is very well resolved in the charged particle spectrum by using the same technique as used for the comparison at E_n = 1 MeV. For reliable background measurements the collimator counter had to be equipped with a shutter with which the collimator could be closed from outside for all recoil protons. The definite comparison will be carried out in the near future. The results will be published with a special description of the collimator counter. The computer program CALCOLEFF which is used for the efficiency determination of the collimator counter was described in a report EUR-4117.e (1969).

In cooperation with the C.E.N. Cadarache the response of a calibrated ^{6}Li-glass scintillator from the C.E.N. was checked in the 0.1 to 0.4 MeV neutron energy region against a hydrogen filled proportional counter from the C.B.N.M. The final results agree within ± 4%.

Initiated by a publication of Hrehuss and Czibok (Phys. Letters 28B, 585, (1969)) a check was performed on the angular distribution of the scattered protons as a function of neutron energy. The abovementioned

authors indicate that a ± 5% variation of the total n-p scattering cross section may be due to a considerable fluctuating anisotropy at proton scattering angles near 0°. The recoil protons were observed in a telescope counter which has in 0° position an observation angle of about 5° (corresponding to 10° in the c.m. system). This measurement was then compared with one at 22.5° (corresponding to 45° in the c.m. system) relative to the incoming neutrons. This comparison was carried out in steps of 100 keV neutron energy between 1.2 and 2.2 and between 3.8 and 6.2 MeV. The results did not indicate any fluctuating anisotropy [11].

Cross Sections for Neutron Induced Threshold Reactions

H. Liskien, A. Paulsen, R. Widera

The excitation functions for the neutron-induced threshold reactions $^{93}Nb(n,2n)^{92}Nb$ and $^{103}Rh(n,2n)^{102}Rh$ were determined by the activation technique. The results were compared with the theory of compound nuclear reactions with special respect to the isomeric states in ^{92}Nb and ^{102}Rh.

Threshold reaction cross sections were printed as the 1968 supplement sheets for EUR 119.e Vol.1. In cooperation with international institutions 368 CINDA entries were transmitted to the Neutron Data Compilation Centre at Saclay.

2.2. Neutron Scattering Measurements

N. Ahmed+, M. Coppola, H.-H. Knitter

^{239}Pu (energy range between 190 and 380 keV)

In this primary neutron energy range elastic scattering cross sections were calculated for comparison with angular distribution measurements which had been performed earlier. This was done on the base of a spherical optical model, using the parameter sets of Cossola and Koshel, of Agee and Rosen and of Witmore and Hodgson. A paper about the results of the measurements and the calculations was published [14].

+Guest from Pakistan A.E.C.

^{239}Pu (energy range 1.5 to 5.5 MeV)

Neutron scattering measurements on ^{239}Pu were extended to this interval, using the multicounter system already described elsewhere. Neutron scattering angular distribution have been measured at 1.5, 1.9, 2.3, 4.0, 4.5, 5.0 and 5.5 MeV. Neutrons up to 2.3 MeV were produced through the T(p,n)^{3}He-reaction, using a solid Ti-T target. From 4.0 to 5.5 MeV the neutrons from the D(d,n)^{3}He reaction were used and a deuterium gas target was employed in order to increase the primary neutron flux. The extensive calculations for the corrections due to finite size of the scattering samples have been made and applied to the raw experimental data in order to get the final differential elastic neutron scattering cross sections.

For comparison with our experimental data, neutron differential scattering cross sections of ^{239}Pu were calculated on the base of the spherical nuclear optical model, partly in collaboration with the data handling team of CBNM (M.G. Cao), using the parameter set of Cossola and Koshel. Some examples of the experimental results and the results of the calculations are shown in fig. 2. A paper on this work has been accepted for publication. [15]

Carbon (energy range between 0.5 and 2.0 MeV)

Since the total cross section of carbon is a smooth monotonic function of the neutron energy below 2.0 MeV and since neutrons are only elastically scattered from carbon in the same energy range, the differential neutron scattering cross section of carbon is very well suited as standard cross section in this region. Therefore an accurate determination of the differential elastic scattering cross sections of carbon from a few hundreds keV up to 2 MeV was desired. So far, all neutron angular distributions have been measured, in steps of 50 keV, in the energy interval from 0.5 to

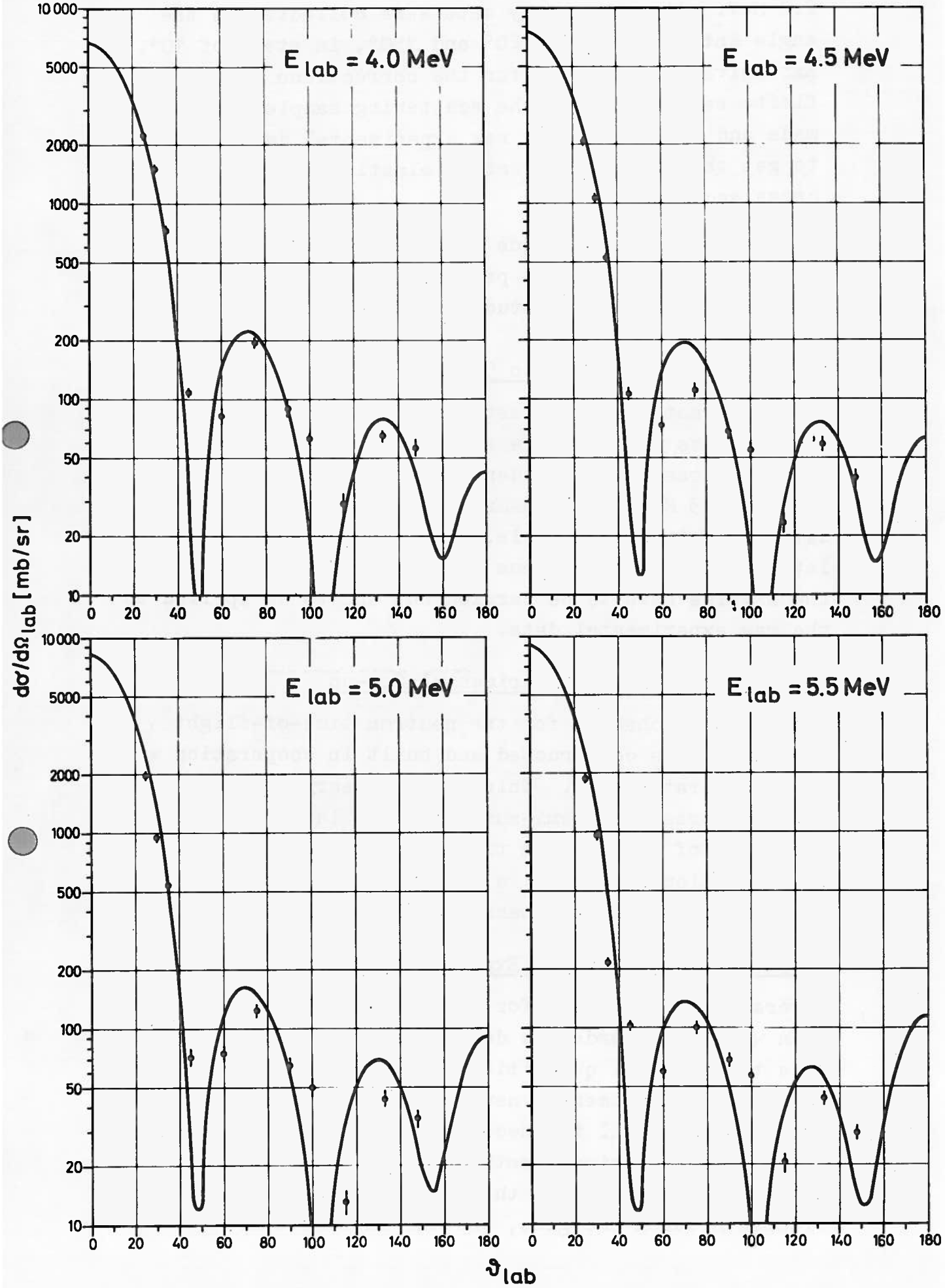

Fig. 2. Neutron differential elastic scattering cross sections of ^{239}Pu in the Lab - system

2.0 MeV. At each energy data were collected in the angle interval between 20° and 150°, in steps of 10°. Extensive calculations for the corrections due to the finite sample size of the scattering samples have been made and applied to the raw experimental data, in order to get the final differential elastic neutron scattering cross sections.

Cross section calculations using a spherical real nuclear potential are in progress. A phase shift analysis is also under study.

^{238}U (energy range 1.5 to 5.5 MeV)

Neutron elastic and inelastic scattering cross section measurements on ^{238}U were started. Three angular distributions at an incident neutron energy of 1.5, 1.9 and 2.3 MeV were measured. Final cross section data are not yet available, since the extensive calculations of the corrections due to the finite sizes of the samples have to be carried out and to be applied to the raw experimental data.

Improvements of the Experimental Set-up

A new sample changer for the neutron time-of-flight experiment was constructed and built in cooperation with the accelerator team. This was necessary in order to allow at present a semi-automatic and later an automatic operation of the neutron time-of-flight experiment. In connection with this, a steering unit for the sample changer and the multi-channel analyser was installed.

Computer Evaluations of Experimental Data

Several small programs for the IBM 1800 computer have been written in order to derive from the experimental data the physical quantities. The program KACO applies to the raw experimental neutron differential scattering cross sections all the necessary corrections received by other calculational methods. The programs TEMP, INEL and INFIS were made for the evaluation of the average fission neutron energies, and the inelastic neutron

evaporation temperatures from the neutron time-of-flight spectra which were taken during the above mentioned ^{239}Pu-experiment.

3. Data Handling

K.H. Böckhoff, H. Horstmann

Data Processing Equipment

A. De Keyser, H. Horstmann

The IBM 1800 data acquisition and control system has been used for on-line data reduction and off-line data analysis. Complicated analysis problems have been solved on the computers of CETIS via the tele-processing system or by direct access. The source of most of the data to be processed were neutron cross section measurements.

The equipment for multi-parameter experiments is being modernized by the installation of a small on-line computer which is planned to be operated as satellite of the IBM 1800.

The functional characteristics of the computer analyser interface units have been improved with regard to greater flexibility.

Data Analysis and Programming

M.G. Cao, C. Cervini, H. Horstmann, W. Kolar, G. Nastri

Reduction and Analysis of Fission Cross Section Data

M.G. Cao

Data reduction for fission cross sections of ^{241}Pu(3eV-4keV), ^{241}Am(0.7-3keV) and ^{237}Np(20eV-5 keV) has been performed. A multilevel analysis with an improved version of the program of Adler and Adler has been made for ^{233}U in the energy range 1-67eV. For the analysis of ^{241}Am data the single-level program 032S of Saclay has been used.

Analysis of Resonance Parameters for Total Cross Section Data

W. Kolar

In order to translate the single-level resonance analysis program of Atta and Harvey from FORTRAN II to FORTRAN IV work has been started to rewrite machine language subroutines (IBM 7090) in FORTRAN IV.

Reduction of Total Cross Section Data

G. Nastri

The efficiency of the IBM 1800 programs for reduction of total cross section data has been considerably increased. The improved programs have been used to reduce total cross section data of ^{233}U, ^{238}U, and ^{241}Pu.

Three-Dimensional Plotting Programs

C. Cervini, G. Nastri

A FORTRAN-IV-IBM 1800 program for three-dimensional plots has been developed, which projects a surface on a plane from a given observation point and plots the projected surface without hidden points.

Programming Assistance

C. Cervini, H. Horstmann, G. Nastri

Programming assistance for various data processing problems (chemistry, radioisotopes, mass spectrometry) has been given. Several programs for miscellaneous data analysis problems, mainly least squares fit procedures, have been written.

System Analysis and Programming

F. Colling, H. Horstmann

IBM 1800 Software Modifications

F. Colling

System modifications for the attachment of a fourth disk drive 1810 which is not supported by IBM soft-

ware have been studied and prepared. Standard data handling subroutines affected by this system modification have been changed.

Test and Verify Programs for Analyser-Computer Interface Units

F. Colling, H. Horstmann

The functional characteristics of an improved analyser-computer interface unit have been thoroughly tested by a set of ASSEMBLER routines. These routines can also be used by technicians to isolate the source of malfunctions.

Programs for On-Line Data Acquisition and Reduction

H. Horstmann

The system of programs for on-line data acquisition and reduction has been extended with regard to additional data acquisition stations. A set of programs for interactive data reduction problems via the analyser-computer interface units is being developed.

4. RADIONUCLIDES

A. Spernol

4.1. Standardization

W. Bambynek

In collaboration with the NPL in England the ^{252}Cf has been standardized in order to determine the number of fissions with the highest possible accuracy. This measurement is important for the planned determination of the mean number of neutrons per fission ($\bar{\nu}$) (E. De Roost, O. Lerch, A. Spernol).

A new version of the recommendation of the EURATOM working group on neutron dosimetry concerning the measure of fluences of thermal neutrons has been elaborated in cooperation with the IAEA and the CNEN (R. Vaninbroukx).

A systematic examination of the published values concerning the K-shell fluorescence yields (ω_k) has been made. It comprehends also a comparison of the reported ω_k-values on an unitary basis and the determination of "best" values of ω_k for all Z-values. The results of this examination will be part of a report to be published in Rev. Mod. Physics written in collaboration with some american physicists (W. Bambynek).

An extended program for the preparation of 0.2-0.5 % accurate γ-ray standards covering the energy interval between a few keV and a few hundred keV has been continued. The necessary accurate redeterminations of the decay schemes involved are under performance (see 2.4). The investigations on ^{241}Am, ^{203}Hg, ^{170}Tm, ^{139}Ce, and ^{44}Ti did not yet yield the required accuracies of a few tenths of a percent (W. Bambynek, E. De Roost, H.H. Hansen, A. Spernol, W. van der Eijk, R. Vaninbroukx).

4.2. Assistance to Other Laboratories

W. van der Eijk

About 15 % of the total radionuclides group activity have been spent for the assistance to other laboratories. Most services involved the high precision measurements of α-particles (B. Denecke, O. Lerch, W. van der Eijk, W. Zehner) or of γ-rays (B. Denecke, G. Grosse, W. van der Eijk, R. Vaninbroukx).

In 1969 about 100 special standard sources have been prepared and distributed on request (CCR Ispra, CCR Karlsruhe, GEX Mol, GfK Karlsruhe, ANL Argonne, SCK Mol, Philips Eindhoven, Universities of Bologna, Brussels, München, Göttingen, Delft, and others). About 40 of these standards have been distributed to 12 reactor institutes for an intercomparison of flux measurements of fast neutrons with threshold detectors (G. Grosse, R. Vaninbroukx).

4.3. Improvement and Development of Counting Methods

R. Vaninbroukx

A new 4π pressure counter has been constructed. Its main feature is the pulse-energy proportionality even for rather high primary energies. It can be fitted by a standardized flange coupling also to other experimental equipments and can be used for different coincidence measurements. Further it will be suitable for the accurate determination of absorption- and scattering-corrections in 2π α-measurements (B. Denecke, W. van der Eijk, W. Zehner).

A sensitive anti-Compton spectrometer with a central Ge(Li) detector surrounded by two specially shaped 6"x6" NaI(Tl) crystals has been designed and is under construction. It will be used for the determination of impurities and for the investigations of low intense γ-rays (A. Spernol, R. Vaninbroukx).

The studies concerning a measuring system with a ionization chamber which will be used for relative measurements with 0.01 % precision have been continued. The first tests with the adjacent electronical equipment have been performed and give satisfying results (G. Bortels).

Concerning the magnetic β-spectrometer an electronically supplied reference voltage for the stabilization is in preparation and the mounting of a detector for low energy electrons (Channeltron) has been designed (H.H. Hansen, D. Mouchel).

A new application of the 4π coincidence method has been studied for the determination of the number of fissions by f-γ coincidence counting (E. De Roost, O. Lerch, A. Spernol).

The efforts to enhance the precision of the 4πβ-coincidence method till about 0.02 % have been continued. The efficiency of the β-counter to γ-rays has been investigated as well as the influence of secondary effects in the radioactive decay. It has been found that these studies were affected seriously by perturbations due to the network and due to the environmental radiation produced by the accelerators (especially the Van de Graaff machine) (E. De Roost, E. Funck+, A. Spernol) [22].

4.4. Determination of Nuclear and Atomic Constants

H.H. Hansen

Several investigations on different radionuclides have been performed and partly published. The half-lives of ^{204}Tl (G. Bortels) [23], of ^{113m}In (E. De Roost, R. Vaninbroukx), and ^{234}U (O. Lerch, A. Spernol, W. van der Eijk, R. Vaninbroukx, in collaboration with other CBNM-groups) have been determined. The half-life of ^{234}U, $(2.43 \pm 0.01)\cdot 10^5$ y, has been found to be in disagreement

+) EURATOM Research Fellow

with the generally adopted value. The study on the decay scheme of ^{137}Cs has been published [24]. In the decay of ^{170}Tm a low intense EC-branch has been measured (H.H. Hansen, S. Hellström+) [26]. The investigations on the K-shell fluorescence yield of Rb using the decay of ^{85}Sr (W. Bambynek, D. Reher) have been finished as well as those on the K-shell conversion coefficient of the 279 keV γ-ray in ^{203}Tl by the e-X coincidence method (H.H. Hansen, D. Mouchel).

The studies on the decay of ^{7}Be (M. Mutterer+) and on the EC/β^+ ratios (E. De Roost, E. Funck+) have been continued. It has been shown that the results of $4\pi\beta$-γ coincidence measurements of the ^{7}Be decay depend on the cut-off energy in the β-channel. This seems to be due to second order effects which are under investigation. Measurements for the determination of the conversion coefficients in the decays of ^{87m}Sr, ^{113m}In, ^{119m}Sn, ^{139}Ce, ^{170}Tm, and ^{203}Hg using different methods are in progress or in preparation (E. De Roost, H.H. Hansen, S. Hellström+, G. Maillé++). Absolute and relative methods have been used for the determination of the 59.6 keV γ-ray intensity in the ^{241}Am decay (E. De Roost, R. Vaninbroukx).

+) EURATOM Research Fellow

++) Visitor from the University of Montreal

5. MASS SPECTROMETRY

G.H. Debus

5.1. Mass Spectrometry of Solids

P.J. De Bièvre

The results of the mass-spectrometric analyses have been used in industry (transfer of nuclear materials), in research (determination of half-lives and standard samples) and for fissile material control in the community (Contrôle de Sécurité). An umpire measurement has been performed on request of CEA and Eurochemic (OECD). Isotopic and quantitative definitions of standard and reference samples prepared at CBNM were an important part of the work.

Application of the isotope dilution technique allowed quantitative determination of small samples, e.g. 1 mg uranium total with an accuracy of 0.4% and better, 8 µg Pu/ml with an accuracy of 1.5%, and low concentrations of Eu (1%, 20 ppm and 2 ppm) in aluminium with an accuracy of 1.5 to 4% [27].

The precision of the measurements of the $^{10}B/^{11}B$ ratio has been improved (now 0.02%) and a second mass spectrometer has been calibrated by means of 18 synthetic isotope blends. This tedious experimental work made it possible to improve the accuracy on the $^{10}B/^{11}B$ ratio of the CBNM standard (now 0.05%) and to analyse elemental natural boron with an accuracy $\leq$ 0.1%.

The isotopic analyses of uranium, obtained in the framework of the USAEC Umpire Qualification Programme, are achieved. The results for uranium^{233} have been examined in the USA and the USAEC informed the CBNM that the laboratory is qualified for a period of two years for this material.

5.2. Mass Spectrometer of Gases

T. Babeliowsky

The reproducibility of the measurements of the D/H

ratio (in heavy water) is increased with a factor 15 (now 0.0002% mol % for heavy water containing 99.8 D_2O.) Four D_2O reference samples of UKAEA (Winfrith) have been analysed. On request of P.T.B. (Germany) the D_2O content and the density (of metrology) of a 300 ml heavy water sample has been determined.

A number of studies have been made on the normalisation of the oxygen isotopes in heavy water and on the memory effects in gas mass spectrometers.

A program has been written for the calculation of ion paths in a mass spectrometer in order to permit the construction of a double collection system.
A Fortran program for matrix universion was elaborated in order to replace a former part of a "least square fit" program. The possibilities for absolute determination of C^{14} were examined. The analytical chemical studies [28] for the Lithium Isotope Standard Project have been performed.

6. SAMPLE PREPARATION AND ASSAYING

For many nuclear measurements an accurate knowledge of the absolute number of atoms of each nuclide in a target used for the experiments is essential. It is an important part of the task of the laboratories for chemistry, mass spectrometry, metallurgy, metrology and radionuclides to aid in the preparation and definition of this kind of targets. The respective activities of each of these laboratories in this field are described in the corresponding chapters of this report.

In 1969, 943 samples have been delivered corresponding to 106 requests coming from outside or from inside of the CBNM.
Table 2 shows how many samples were distributed.

Table 2

Samples delivered in 1969								
	Number of requests				Number of samples			
Requestor	Metallurgy	Chemistry	Metrology	Mass Spectrometry	Metallurgy	Chemistry	Metrology	Mass Spectrometry
CCR Ispra	2	--	-	-	65	-	-	-
CCR BCMN	9	23	4	-	117	92	25	-
Germany	8	6	2	-	15	35	7	-
Belgium	21	--	9	-	72	-	127	-
France	-	3	2	-	-	34	34	-
Italy	2	3	-	1	3	3	-	1
The Netherlands	1	-	-	-	1	-	-	-
U.S.A.	-	1	-	-	-	3	-	-
Great Britain	-	-	-	3	-	-	-	3
Austria	-	1	-	-	-	1	-	-
Danemark	-	-	-	1	-	-	-	1
Canada	1	1	-	1	1	2	-	1
IAEA Vienna	1	-	-	-	300	-	-	-
Total	45	38	17	6	574	170	193	6
	106				943			

6.1. METALLURGY

J. Van Audenhove

Certified Metallurgical Samples [29]

45 requests covering 574 samples were satisfied in 1969 (see Table 3). 28 of those requests consisted of different non commercial available certified alloys needed by European laboratories for accurate neutron flux measurements or calibration of analytical techniques.

Applied Metallurgical Research

Spark Erosion Machining

Spark erosion conditions, electrode materials and shapes have been determined for the machining and finishing of UC, UC + V and UC + Cr disks into close tolerances and without oxygen contamination. This project is made on request of the S.C.K. - MOL for irradiation experiments in BR 2 with the POM - irradiation equipment.

Purification and Crystallization of Amorphous ^{10}B - Powder

A total amount of 35 g of purified crystalline ^{10}B obtained by repeated electron beam melting of isostatic pressed and sintered powder compacts is available.

The vertical electron bombardment zone refining method was time consuming and unsuccessfull. The vertical H.F. zone refining method has not yet been tried.

Levitation Techniques [30]

There seems to be a constant ratio between the mass of an U-layer on a disc and on a witness-ring evaporated in a same cycle. 3 quantitative determinations of 3 pairs disk - ring by isotope dilution (M.S. solids) spread within $\pm$ 0.25 %. Further measurements are still proceeding. This method has the advantage, that it allows the accurate quantitative determination of the disk by analyzing the ring, thus leaving the disk undestructed, and it allows quick preparation (4 or more layers/day) in a simple vacuum equipment.

Pu-Metallurgy

The installation of several glove-boxes needed for melting, thermal treatment, cleaning and rolling of Al-Pu alloys has been finished and is used for the preparation of Pu fissile detectors.

Preparation of Small Quantities of Metallic Isotopes by Reduction of their Fluorides

V. Camurri*

The necessary equipment has been developed. A serie of experiments on 1.5 g amounts of CeF_4 permitted to determine parameters as : influence of the atmosphere in the bomb, heating cycle, the presence of a booster, the use of Mg or/and Ca as reducing agent, the granulometry of this agent, the preparation of the charge.

The experience with CeF_4 as a "stand in" permitted to start work on UF_4. Reduction yields of about 80 % have been obtained for UF_4 quantities of 1 down to 0.5 g.

6.2. Analytical and Preparative Chemical Methods

Ch. Berthelot, G. Del Bino, K.F. Lauer, Y. Le Duigou, V. Verdingh

An important effort was spent on the treatment of 4000 Curies of ^{241}Pu (about 35 g), this in connection with the program of total and fission cross section measurement of ^{241}Pu.
This included, the installation of glove boxes for weighings, purifications, oxyde preparations, sampling for analyses, sample preparations (vacuum canning assembly), analyses, decontaminations, mounting of the samples and quantitative recuperation of the plutonium after the experiments. Five samples were prepared and used in Linac experiments. In the following table the characteristics of these samples are given:

Type of sample	Quantity of Pu in the sample g	Pu content of the sample g	Specific thickness mg Pu/cm^2
T1	25.291	22.056	701.5
T2	24.277	21.217	674.8
T3	9.535	8.333	265.2
f1	9.158	8.044	96.11
f2	2.077	1.815	21.79

A quantitative recovery of the oxyde was done after the neutron experiments were finished. For a series of five purifications, preparations and recoveries the total loss on a quantity of 35 g of plutonium was of the order of 0.25 g.

One ^{241}Am sample of high γ activity (16 Curies) was prepared and canned under vacuum. Special effort was made for the decontamination of the sample. As in the case of the ^{241}Pu a quantitative recovery of the americium followed the neutron measurements.

Two ^{237}Np samples (about 8 g) were prepared and canned under vacuum. Here also decontamination of the samples and quantitative recovery of the material were necessary.

A series of 10 samples of highly enriched Mo isotopes was prepared by a sedimentation technique and vacuum canning. Minimal loss occurred during the recovering of the isotopes. A gravimetric analysis of Mo was done.

Thick and large samples (1 - 3 g/cm^2) of rare earth oxydes and other compounds were prepared by powder compression and subsequent canning in appropriate containers.

For the half-live measurement program, two standard solutions of ^{233}U and ^{234}U and approximately twenty ^{235}U acetate layers were prepared.

To fulfill the demands of the CBNM and of other laboratories for californium sources, a study was made

on the preparation of these sources. The self-transfer method enables the preparation of sources of good quality (about 15 keV α resolution).

Important analytical work including major constituents determinations and trace analyses has been performed in parallel for these programs.

6.3. Metrology

H. Moret, H.L. Eschbach, G. Müschenborn

Measurements on thin layers and foils

Extended use of x-rays was made to define the dimensions, the uniformity and in a few cases also the composition and the structure of evaporated or electrosprayed layers and of thin foils. Thickness measurements of thin layers (e.g. UF_4, stainless steel, Au) were usually done by x-ray fluorescence. The uniformity of thin pressed powder samples and of thin rolled foils is detected by x-ray absorption. The composition of evaporated tungsten oxide and stainless steel layers was studied for different evaporation parameters by x-ray diffraction.

The optical density of thin transparent Au, Al and Co-layers was measured. A photometer has been constructed and is being tested which will trace automatically lines of equal optical density.

Multiple beam interferometry has been applied to measure the surface roughness of polished aluminium and stainless steels disks. A small unit has been developed to test the mechanical strength of thin self-supporting foils.

As a further application of the miniature source the fabrication of ^{86}SrO layers on C-foils has been carried out.

Boron reference samples

In order to improve the evaporation conditions an uhv-evaporation unit fitted with two ion getter pumps, a Ti-evaporator and a liquid nitrogen cool trap is under construction. The stainless steel vessel has been tested

and accepted. Bake-out ovens, vacuum balance, evaporation crucible and shieldings are nearly finished and will be tested in the near future.

Uranium reference samples

After changing of the uhv evaporation unit for the fabrication of metallic uranium layers by high frequency evaporation, a series of residual gas analyses were carried out [33] to investigate the influence of different heating cycles. In collaboration with the metallurgy group a first successful evaporation of metallic ^{235}U could be made. The metal was condensed on a quartz disk (40 mm in diameter and 0.65 mm thick). In total four preliminary samples could be fabricated, three of which were covered with a thin Al-layer after U deposition in the same vacuum cycle. First checks made by counting show a very good reproducibility ($\leq$ 0.2%) of the weighing by the vacuum microbalance. The fabrication of 5 definite uranium reference samples has been started.

7. LIST OF PUBLICATIONS

1. CAO,M.G., E. MIGNECO, J.P. THEOBALD, and M. MERLA, Fission Cross Sections Measurement on ^{233}U, to be published in Journal of Nuclear Energy.

2. MIGNECO,E., J.P. THEOBALD, and J.A. WARTENA, Subthreshold Fission of ^{241}Am, Conference on Physics and Chemistry of fission, Vienna, July 1969, paper SM-122/140.

3. MIGNECO,E., J.P. THEOBALD, and H. WEIGMANN, Analysis of Nd Neutron Resonances, Journal of Nuclear Energy 23, 369 (1969).

4. POORTMANS, F., H. CEULEMANS, E. MIGNECO, and J.P. THEOBALD Spin Determination of ^{235}U Resonances below 100 eV, Conference on Physics and Chemistry of Fission, Vienna, July 1969, paper SM-122/70.

5. WEIGMANN,H., J. WINTER, and M. HESKE, Prompt γ-Rays from Neutron Interaction in ^{235}U and Resonance Spin Assignments, Nuclear Physics A 134, 535 (1969).

6. WEIGMANN,H., G. ROHR, and J. WINTER, A study of Coupling Conditions in Subthreshold Fission of ^{237}Np by Means of γ-Ray Spectra, Physics Letters 30B, 9 (1969).

7. DERUYTTER, A.J., Charactéristiques de la fission dans les résonances neutroniques, presented to "Journées d'Etudes sur la Fission", Brussels, January 1969.

8. PENNING, G., Vergelijking van de thermische splitsing van ^{239}Pu en de spontane splitsing van ^{240}Pu, Thesis, University of Gent (June 1969).

9. WAGEMANS, C., Onderzoek van enkele aspecten van de door resonantie-neutronen in ^{235}U geïnduceerde fissie, Thesis, University of Gent (June 1969).

10. DERUYTTER, A.J., and C. WAGEMANS, Variation of the Binary-to-Ternary Fission Ratio for ^{235}U in the Resonance Region, presented to the conference "Physics and Chemistry of fission", Vienna, July 1969 and EANDC(E) "AL".

11. PAULSEN, A., and H. LISKIEN, Search for Fluctuating Anisotropy in the n-p Scattering Process at a Few MeV Neutron Energies, Physics Letters 29 B, 562 '1969).

12; LISKIEN, H., G. NASTRI, and A. PAULSEN, Efficiency Calculations for a Recoil Proton Counter with Collimator, Nucl. Instr. and Meth. 67, 133 (1969).

13. LISKIEN, H., G. NASTRI, and A. PAULSEN, The Computer Program CALCOLEFF, Rapport EUR. 4117. e (1969).

14. KNITTER, H.H., and M. COPPOLA, Elastic Neutron Scattering Measurements on ^{239}Pu in the Energy Range Between 0.19 and 0.38 MeV, Z. Physik 228, 286 (1969).

15. COPPOLA, M., and H.H. KNITTER, Interactions of Neutrons with ^{239}Pu in the Energy Range between 1.5 and 5.5 MeV, Z. Physik, to be published.

16. HORSTMANN, H., Radiation Shielding for the Electron Linear Accelerator of the Central Bureau for Nuclear Measurements, Kerntechnik, 11, 212 (1969).

17. HORSTMANN, H., A. DE KEYSER, and H. SCHMID, Use of a Process Control Computer System in Analysis of Neutron Cross Section Data and the Control of Neutron Data Acquisition Facilities around a Van de Graaff and an Electron Linear Accelerator, Proceeding of the Conference on the Effective Use of Computers in the Nuclear Industry. Knoxville, Conf-690401, p. 143 (1969).

18. SCHMID, H., An IBM 1800 Program Package for On-Line and Off-Line Operation of a CALCOMP Digital Incremental Plotter, EUR-4225e (1969).

19. SCHMID, H., and H. CLAESSENS, IBM 1800 Utility Programs for Magnetic Tapes and Tele-Processing Input/Output. EUR-4263e (1969).

20. SCHMID, H., H. HORSTMANN, and H. CLAESSENS, IBM 1800 Programs for Data Processing at the Accelerators of the Central Bureau for Nuclear Measurements, Part 1, Off-Line Programs for Data Handling and Reduction. EUR-report in press.

21. NASTRI, G., and H. SCHMID, Data Reduction Programs for Total Cross Section Experiments, EUR-report in press.

22. DE ROOST, E., E. FUNCK, and A. SPERNOL, Improvements in 4πβ-Coincidence Counting, Int. J. appl. Rad. Isotopes 20, 387 (1969).

23. BORTELS, G., The Half-Life of ^{204}Tl, Int. J. appl. Rad. Isotopes 20, (1969).

24. HANSEN, H.H., G. LOWENTHAL, A. SPERNOL, W. VAN DER EIJK, and R. VANINBROUKX, The Beta Branching Ratio and Conversion Coefficients in the ^{137}Cs Decay, Z. Physik 218, 25 (1969).

25. HANSEN, H.H., and A. SPERNOL, The e-(X,A)-Coincidence Method for the Accurate Determination of Internal Conversion Coefficients, Proc. Int. Conf. on Radioactivity in Nuclear Spectroscopy, Nashville, August 11-15, 1969 (in press).

26. HANSEN, H.H., and S. HELLSTRÖM, The EC-Decay of ^{170}Tm, Z. Physik 223, 139 (1969).

27. DE BIEVRE, P.J., G.I. DEL BINO, Accurate Quantitative Determination of Trace Ampunts of Europium in Aluminium, to be published on Analytica Chimica Acta.

28. PAUWELS, J., Het bereiden van accurate Lithium isotopenmengsels, Thesis, University of Gent (December 1968).

29. SPAEPEN, J., Euratom Reference Materials, Proc. International Standard Reference Materials Symposium, Washington (1969).

30. VAN AUDENHOVE, J., Levitation Melting, a Preparation Technique for Reference Samples, Euro Spectra 8, 46 (1969).

31. BERTHELOT, Ch., G. DI BRANCO, Analyse isotopique du Lithium par interférométrie. EUR-4116 f., 1969.

32. ESCHBACH, H., and A. GRILLOT, Constructions et caractéristiques de sources miniatures d'évaporation, Le Vide 24, 97 (1969).

33. MÜSCHENBORN, G., Onderzoek van de ontgassingsverschijnselen in een UHV-apparatuur, submitted to Nederlands Tijdschrift voor Vacuumtechniek.